SANDIA REPORT

SAND2014-9040
Unlimited Release
Printed March 2014

Methodology for Design and Economic Analysis of Marine Energy Conversion (MEC) Technologies

Vincent S. Neary[1], Mirko Previsic[2], Richard A. Jepsen[1], Michael J. Lawson[3], Yi-Hsiang Yu[3], Andrea E. Copping[4], Arnold A. Fontaine[5], Kathleen C. Hallett[3], Dianne K. Murray[1]

[1]Sandia National Laboratories
Water Power Technologies Department
P.O. Box 5800
Albuquerque, New Mexico 87185-1124

[2]Re Vision Consulting, LLC

[3]National Renewable Energy Laboratory

[4]Pacific Northwest National Laboratory

[5]Pennsylvania State University, Applied Research Laboratory

Prepared by
Sandia National Laboratories
Albuquerque, New Mexico 87185 and Livermore, California 94550

Sandia National Laboratories is a multi-program laboratory managed and operated by Sandia Corporation, a wholly owned subsidiary of Lockheed Martin Corporation, for the U.S. Department of Energy's National Nuclear Security Administration under contract DE-AC04-94AL85000.

Sandia National Laboratories

Issued by Sandia National Laboratories, operated for the United States Department of Energy by Sandia Corporation.

Available to DOE and DOE contractors from
U.S. Department of Energy
Office of Scientific and Technical Information
P.O. Box 62
Oak Ridge, TN 37831

Telephone: (865) 576-8401
Facsimile: (865) 576-5728
E-Mail: reports@adonis.osti.gov
Online ordering: http://www.osti.gov/bridge

Available to the public from
U.S. Department of Commerce
National Technical Information Service
5285 Port Royal Rd.
Springfield, VA 22161

Telephone: (800) 553-6847
Facsimile: (703) 605-6900
E-Mail: orders@ntis.fedworld.gov
Online order: http://www.ntis.gov/help/ordermethods.asp?loc=7-4-0#online

SAND2014-9040
Unlimited Release
Printed March 2014

Methodology for Design and Economic Analysis of Marine Energy Conversion (MEC) Technologies

Vincent S. Neary[1], Mirko Previsic[2], Richard. A. Jepsen[1], Michael J. Lawson[3], Yi-Hsiang Yu[3], Andrea E. Copping[4], Arnold A. Fontaine[5], Kathleen C. Hallett[3], Dianne K. Murray[1]

----

[1]Sandia National Laboratories
Water Power Technologies Department
P.O. Box 5800
Albuquerque, New Mexico 87185-1124

[2]Re Vision Consulting, LLC
1100 Corporate Way
Sacramento, CA 95831

[3]National Renewable Energy Laboratory
Wind and Water Power Program
15013 Denver West Parkway
Golden, CO 80401

[4]Pacific Northwest National Laboratory
P.O. Box 999
Richland, WA 99352

[5]Pennsylvania State University,
Applied Research Laboratory
P.O. Box 3-0
State College, PA 16804-0030

Abstract

This report describes the development of four Marine Energy Conversion (MEC) technology Reference Models for producing renewable electricity from water currents (tidal, open-ocean, and river) and waves. Each Reference Model is a "point design," a term used to emphasize that it is a unique device designed for a reference resource site modeled after an actual site in the United States. The Reference Models served as non-proprietary open-source study objects for technical and economic evaluation; specifically, they allowed the benchmarking of technical and economic performance, the collection of experimental data sets for validating open-source design tools, and the identification of cost reduction pathways and research priorities for improving performance and reducing costs. The levelized cost of energy (LCOE), in dollars per kilowatt-hour ($/kWh), was estimated for each Reference Model, including LCOE for a single device and arrays of 10, 50, and 100 units in order to quantify cost reductions associated with economies of scale. The Reference Models also facilitated the development of an open-source methodology for the design, analysis, and economic evaluation of MEC technologies.

This project is sponsored by the U.S. Department of Energy's (DOE) Wind and Water Power Technologies Program, within the Office of Energy Efficiency & Renewable Energy (EERE). Sandia National Laboratories, the lead in this effort, collaborated with partners from National Laboratories, industry, and universities to design the four open-source MEC Reference Models (RM1–RM4). The methodology was applied to identify key cost drivers and to estimate LCOE. Many costs are difficult to estimate at this time due to the lack of operational experience, particularly for the RM3 wave energy conversion (WEC) device.

Acknowledgements

The following people provided a broad range of subject matter expertise in developing this report. All contributors also provided general review of the report and made many invaluable suggestions. The work on this project has spanned from 2010 to this 2014 publication.

Sandia National Laboratories

- **Vincent Neary, Ph.D., P.E., F.ASCE, Sandia National Laboratories (SNL).** Project manager and lead author for this report (March 2013 to present). Previous to March 2013, contributed to this effort under Oak Ridge National Laboratory (ORNL).
- **Richard Jepsen, Ph.D., SNL.** Project manager for the RM1–RM4 development effort from June 2010 to December 2012.
- **Jesse Roberts, SNL.** Supported resource (reference site) characterization for RM2.
- **Matthew Barone, Ph.D., Aerosciences Department, SNL.** Lead engineer for the RM2 design.
- **Ann R. Dallman, Ph.D., SNL.** Provided input for Environmental Compliance (EC), O&M Strategy, and M&D Strategy Modules, and LCOE discussions including the revision of all figures and charts for these modules.
- **Budi Gunawan, Ph.D., SNL.** Provided technical review for the design and analysis of all reference models (RM–RM4).
- **Dianne Murray, SNL.** Provided technical writing/editing and illustrating and supported environmental compliance.

Re Vision Consulting, LLC

- **Mirko Previsic, Re Vision Consulting, LLC.** Led the cost and economic analysis for RM1–RM4, supported the concept development for RM1–RM4, developed the installation and operational strategies, led the wave tank testing of RM3, led the performance and extreme loads analysis on RM3, led the structural design efforts and design for manufacturability, and developed a concept 100 kW hydraulic powertrain design for RM3.
- **Jeffrey Epler, Re Vision Consulting, LLC.** Developed CAD design for RM1–RM4, structural design for RM2 and RM3, and assisted with wave tank testing on RM3.
- **Kourosh Shoele, Re Vision Consulting, LLC.** Conducted performance modeling for RM3, structural design of RM4, and assisted with wave tank testing on RM3.

National Renewable Energy Laboratory (NREL)

- **Michael Lawson, Ph.D., NREL.** Lead engineer on design development for RM1 and RM4.
- **Yi-Hsiang Yu, Ph.D., NREL.** Lead engineer on the performance modeling for RM3 and supported the development of the RM3 design.
- **Kathleen C. Hallett, NREL.** Led review and integration of the economic analysis.
- **Ye Li, Ph.D., NREL.** Supported the RM1 design effort and initial development of the overall methodology approach.
- **Robert Thresher, Ph.D., NREL.** Technical support for RM1, RM3, and RM4 designs.

Pacific Northwest National Laboratory (PNNL)

- **Andrea Copping, Ph.D., PNNL.** Developed pathways to evaluate potential environmental effects on marine animals and habitats for each reference model. Developed the cost analysis input associated with the environmental permitting and regulatory concerns for each resource
- **Simon Geerlofs, PNNL.** Developed pathways to evaluate potential environmental effects on marine animals and habitats for each reference model, and developed the cost analysis input for the environmental permitting and regulatory concerns for each resource.

Oak Ridge National Laboratory (ORNL)

- **Glenn Cada, Ph.D., ORNL.** Supported the development of the marine habitat definitions for each of the RM1 and RM2 resource models.

Universities

- **Arnold Fontaine, Ph.D., Pennsylvania State University, Applied Research Laboratory.** Coordinated the power conversion chain (PCC) designs for all current energy conversion (CEC) technology devices.
- **Brian Polagye, Ph.D., University of Washington.** Developed inflow characterization model for the tidal energy resource.
- **Michael Beam, Pennsylvania State University, Applied Research Laboratory.** Supported design of power conversion chains (PCC) for RM1, RM2 and RM4.
- **Brian L. Kline, Pennsylvania State University, Applied Research Laboratory.** Designed power electronics for the power conversion chain (PCC) designs.

Other Industry Partners

- **Roger Bagbey, Cardinal Engineering, LLC.** Served as DOE Headquarters Technical Lead for the project for year one.
- **Jeffrey Rieks, Cardinal Engineering, LLC.** Served as DOE Headquarters Technical Lead for the project for years two and three.

Contents

Figures

Tables

Nomenclature

AC	alternating current
ADCP	acoustic Doppler current profiler
AEP	annual energy production
AISC	American Institute of Steel Construction
API	American Petroleum Institute
ARL	Applied Research Laboratory
ADV	acoustic Doppler velocimeter
BACI	Before-After Control-Impact
BEM	boundary element method
BEMT	Blade Element Momentum Theory
BOS	balance of system
CACTUS	Code for Axial and Cross-flow TUrbine Simulation
CAD	computer aided design
CapEx	capital expenditure
CBS	cost breakdown structure
CEC	Current Energy Conversion
CFD	computational fluid dynamics
CI	confidence interval
COTS	commercial off-the-shelf
CREW	Continuous Reliability Enhancement for Wind
D&A	design & analysis
DEA	drag embedment anchor
DNV	Det Norske Veritas
DO	dissolved oxygen
DOE	U.S. Department of Energy
DoF	dimensions of freedom
DP	dynamic positioning
EC	environmental compliance
ECA	energy capture area
EERE	Energy Efficiency & Renewable Energy
EIS	Environmental Impact Statement
EMF	electromagnetic field
EPRI	Electric Power Research Institute
FAU	Florida Atlantic University
FCR	fixed charge rate
FEA	finite element analysis
FERC	Federal Energy Regulatory Commission

FOS	factor-of-safety
FPA	floating point absorber
HAWT	horizontal axis wind turbines
HMRC	Hydraulics and Maritime Research Center
IEC	International Electrotechnical Commission
IRR	Internal Rate of Return
IRS	Internal Revenue Service
ITC	Investment Tax Credit
JPD	joint probability distribution
LCOE	levelized cost of energy
M&D	manufacturing and deployment
MACRS	Modified Accelerated Cost Recovery System
MEC	Marine Energy Conversion
MHK	Marine Hydrokinetic
MIT	Massachusetts Institute of Technology
MMH	maximum measured height (of wave)
MMPA	Marine Mammal Protection Act
NACA	National Advisory Committee for Aeronautics
NDBC	National Data Buoy Center
NEPA	National Environmental Policy Act
NREL	National Renewable Energy Laboratory
NMREC	National Marine Renewable Energy Centers
NOAA	National Oceanic and Atmospheric Administration
OD	outside diameter
OEM	original equipment manufacturer
O&M	operations and maintenance
OCT	Ocean Current Turbine
OD	outside diameter
OpEx	operations and maintenance expenditure
ORNL	Oak Ridge National Laboratory
PCC	power conversion chain
PM	permanent magnet
PNNL	Pacific Northwest National Laboratory
PTC	Production Tax Credit
R&D	research and development
RM	Reference Model
RMP	Reference Model Project
ROV	remotely operated vehicle
SAFL	St. Anthony Falls Laboratory

SCADA	supervisory control and data acquisition
SEPLA	Suction Embedment Plate Anchor
SNL	Sandia National Laboratories
SNL-EFDC	Environmental Fluid Dynamics Code (EFDC) and SNL enhancements (SNL-EFDC)
TSR	tip-speed-ratio
TRL	Technology Readiness Level
UCC	University College of Cork
UCSD	University of California San Diego
UNH	University of New Hampshire
USFWS	U.S. Fish and Wildlife Service
USGS	U.S. Geological Survey
VAWT	vertical-axis wind turbine
VSVP	variable-speed variable-pitch
WACC	Weighted Average Cost of Capital
WEC	Wave Energy Conversion
WindPACT	Wind Partnerships for Advanced Component Technology

Units

$K	dollars in thousands	m	meter
$M	dollars in millions	m^2	square meter
in	inch	mm	millimeter
ft ft-lbf	foot foot-pound force	Mg	Megagram 1Mg = 1 metric tonne = 1.102 tons 1 short ton = 2,000 lb = 0.907 Mg
HP	horse power		
Hz	Hertz (cycles per second)	m/s	meters per second
kg	kilogram	MPa	megapascal
km	kilometer	MW	megawatt
kN	kilonewtons	MWh	megawatt-hours
kNs/m	kilonewton • second/meter	psi	pounds per square inch
ksi	1000 psi	s	second
kV	kilovolt	TWh	Terawatt-hours 1 TWh = 10^6 MWh = 10^9 kWh
kW	kilowatt		
kWh	kilowatt-hours		
lbs	pounds		
lbf	pound force		

Executive Summary

The Reference Model Project (RMP), sponsored by the U.S. Department of Energy's (DOE) Wind and Water Power Technologies Program within the Office of Energy Efficiency & Renewable Energy (EERE), is a partnered effort to develop robust Marine Hydrokinetic (MHK) reference models for wave energy converters (WECs) and ocean and river current energy converters (CECs). In this report we use the term Marine Energy Conversion (MEC) in place of MHK; both terms are equivalent and inclusive of energy conversion within rivers.

The RMP team includes a partnership between DOE, four national laboratories—Sandia National Laboratories (SNL), the National Renewable Energy Laboratory (NREL), Pacific Northwest National Laboratory (PNNL), and Oak Ridge National Laboratory (ORNL); two consulting firms—Re Vision Consulting, LLC and Cardinal Engineering; and the University of Washington and Pennsylvania State University. The team is led by SNL. This report is the outcome of several years of collaborated effort by the RMP team which was initiated to:

- Develop and illustrate a methodology for 1) the design and economic analysis of MEC technologies—including a methodology for estimating annual energy production (AEP) for single devices and arrays with 10, 50, and 100 units, 2) determining annualized capital and operational expenditures, and 3) estimating the levelized cost of energy (LCOE) in $/kWh.
- Design four MEC technology Reference Models. Each Reference Model is a "point design," a term used to emphasize that it is a unique device designed for a reference resource site modeled after an actual site in the United States; it is not intended to be a device that is a general representation of a specific MEC technology archetype.
- Demonstrate the application of this methodology for the four MEC technology Reference Models, referred to herein as Reference Models (RM) 1, 2, 3, and 4.

  * NOTE: The term array refers to multiple connected MEC/MHK devices in a configuration for generating renewable electrical energy. For commercial scale projects, we assume 10 connected devices for a small commercial scale array and 50 or more connected devices for a large commercial scale array. These array numbers are somewhat arbitrary from an economic standpoint since similarly sized arrays are not comparative in their actual electrical generating capacity. The intention of specifying a range based on the number of units was to evaluate the economy of scales for each Reference Model.

We encourage MEC developers to apply our methodology, with the appropriate reference resource sites, to design and estimate LCOEs for their technologies. Of course, such a comparison is only possible if developers use the same methodology, reference resource sites, and assumptions and approximations, which we attempt to clearly articulate in this report. Alternatively, MEC developers can adjust assumed costs based on their judgment and experience and as operational experience with these nascent technologies improves. For this purpose, we have archived supporting documentation on the Sandia National Laboratories' Energy, Climate, and Infrastructure Security website:

http://energy.sandia.gov/rmp

Sandia's website contains reports detailing the design and analysis of each RM, model validation studies, reference resource site development, as well as Excel spread sheets that detail the cost breakdown structure (CBS) and calculate the annual energy production (AEP) in kilowatt-hours (kWh), capital expenditure (CapEx) costs, operations and maintenance expenditure (OpEx) costs, and LCOE ($/kWh). All calculations are general estimates since these cost determinations have a wide range of uncertainty depending on each device and many factors affecting its deployment costs at the reference site. The level of uncertainty is discussed under each RM section.

The methodology centers on four core modules, which are applied to each Reference Model to design and analyze devices and arrays and determine their LCOEs:

1. The **Design & Analysis (D&A) Module** applies engineering models to design, analyze, and optimize power and structural performance for a given MEC device paired with a reference site resource. Output from this module determines the feasibility of the device/array and the potential AEP. The final design specifications provide the data needed to determine materials and manufacturing costs in the Manufacturing & Deployment (M&D) Strategy Module.

2. The **Manufacturing & Deployment (M&D) Strategy Module** delineates the materials and manufacturing processes and deployment strategies that are adopted in order to determine CapEx associated with manufacturing the device and deploying it at different array scales. This includes CapEx for subcomponent materials based on structural analysis of extreme loadings, subsystem requirements to reduce O&M costs, and deployment (installation) costs. Deployment strategies include service vessel requirements and other considerations for the installation of the MEC devices and their associated infrastructure, referred to as balance of system (BOS) components—an example would be the transmission cables connecting the device/array to the substation for grid connection.

3. The **Operations & Maintenance (O&M) Strategy Module** delineates an O&M strategy and identifies costs based on estimates of subcomponent and subsystem failure rates and service requirements for operations and other OpEx categories. O&M strategies include service vessel requirements to maintain the MEC devices and the array infrastructure. This module also accounts for expected operational availability—this is based on land-based wind plant/farm data—which determines the actual AEP considered in the LCOE estimate.

4. The **Environmental Compliance (EC) Module** details the site studies and environmental monitoring needs and estimates the costs for assessing environmental impacts and meeting compliance with the many requirements necessary for deploying the Reference Model array at a particular reference site. EC costs are mainly CapEx because many monitoring activities, site studies, and related research work are critical for compliance with environmental regulations and permitting requirements (e.g., the National Environmental Policy Act [NEPA]), addressing stakeholder input, and determining the overall feasibility of deploying the MEC device/array given all discovered factors. Both pre-installation studies and—if deployment at the selected site is found acceptable—post-installation studies will be conducted as well as recurring

environmental monitoring that will take place during the lifecycle of the device/array. Recurring routine environmental monitoring costs are treated as OpEx.

These four modules include sub-modules for analysis, design iteration, and optimization to meet structural and environmental constraints.

We applied our methodology to the four RMs described below. Each RM is paired with, and designed for, a reference resource site that is modeled after an actual site in the United States. The RMs include three Current Energy Conversion (CEC) technologies—a tidal CEC turbine (RM1), a river CEC turbine (RM2), and an ocean CEC turbine (RM4)—and one Wave Energy Conversion (WEC) technology, a wave point absorber (RM3). As noted above, LCOE estimates for each RM device/array are subject to varying degrees of uncertainty, which are qualitatively assessed based on known knowledge gaps and modeling deficiencies.

Reference Models 1, 2, 3, and 4

The four RMs discussed in this report and their associated reference sites are as follows:

- **RM1,** Chapter 3. A dual-rotor axial-flow (horizontal-axis) tidal turbine designed for a reference tidal current energy resource modeled after the Tacoma Narrows in Puget Sound, Washington.
- **RM2,** Chapter 4. A dual-rotor vertical-axis cross-flow river turbine designed for a reference river current energy resource modeled after a reach in the lower Mississippi River near Baton Rouge, Louisiana.
- **RM3,** Chapter 5. A wave point absorber designed for a reference wave energy resource modeled after a wave site near Eureka, California, in Humboldt County.
- **RM4,** Chapter 6. A moored glider with four axial-flow ocean current turbines designed for a reference ocean current energy resource modeled after the Florida Strait ocean current site, within the Gulf Stream off the southeast coast of Florida near Boca Raton.

LCOE Estimates

LCOE estimates for 10- and 100-unit arrays for all four RMs are shown in Figure ES-1. Projects with 10 units are considered most likely in the early stages of commercialization. However, significant cost reductions can be gained with larger projects.

Installed capacity and the capacity factor were key drivers that affected the LCOE estimates. For 10-unit arrays, the low LCOE for the ocean current turbine, RM4 ($0.25/kWh), is due to the high installed capacity for each device (4 MW) and the high capacity factor (CF=0.7) due to the constancy of the Gulf Current in the Florida Strait. The capacity factors for all the other RMs were 0.3, less than half the value for RM4. The LCOE for the tidal current turbine, RM1 ($0.41/kWh), is slightly more than values reported for offshore wind turbines. For the river current turbine, RM2, the high LCOE ($0.80/kWh) is due to the low installed capacity and the spatial constraints inherent at a river site. The LCOE estimate for the WEC device, RM3 ($1.45/kWh), is comparatively much higher, but this largely reflects the lack of experience and tools available for designing this technology at the time of this study. Unlike the turbine-based Current Energy Conversion (CEC) RM designs, which benefited from decades of DOE laboratory R&D experience and investments in wind turbine technologies, there was relatively little design experience and developed tools that could be leveraged to design the RM3 device. Critical innovations to improve performance of RM3, such as advanced controls, were also not applied.

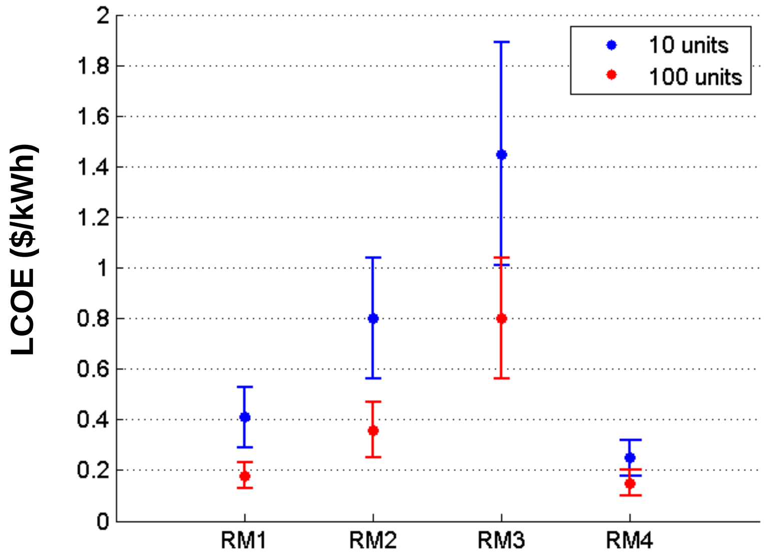

Figure ES-1. LCOE estimates ($/kWh) for four reference MEC technology point designs.

We advise caution when comparing the LCOEs among these four Reference Models for the following reasons:

1. The LCOE for each RM was estimated for a specific reference resource site. Therefore, the theoretical hydrokinetic power densities and environmental constraints varied considerably between sites.
2. Knowledge gaps and uncertainties are greater in some RMs as compared to others. WECs, for example, are more nascent technologies than CECs. Also, unlike CECs, WECs do not have analogue technologies such as wind turbine plants from which design, M&D, and O&M experience can be used to more accurately extrapolate the expected design, M&D, and O&M strategies and their costs.
3. Varying levels of design optimization were performed for the different RMs.

Key Cost Drivers for RM 1–4

One of the primary goals of this study was to identify key cost drivers and cost reduction pathways to direct future R&D efforts. For all CEC RMs (RM1, RM2, and RM4), CapEx contributions (development, M&D, subsystem integration, and profit margin, and contingency) are much greater than OpEx contributions—with M&D dominating the CapEx contributions to its LCOE. The cost for environmental studies and permitting activities, which are captured in the project development cost contributions to LCOE, are insignificant by comparison. Structural components and the power conversion chain (PCC) are clear cost drivers for all of the RMs and device components for which future R&D efforts should be methodically applied to reduce costs and LCOE. For the RM3, the WEC device, its mooring system and installation are also key cost drivers. Future R&D efforts should also focus on increasing performance and the AEP which will lower the LCOE, as well. There are clear R&D needs in advanced controls to increase WEC performance as discussed below.

Recommendations for Improvements

We fully recognize that the methodology we are presenting herein requires improvements and we encourage its further development. The following discussion summarizes the weaknesses identified in design, analysis, performance, and cost modeling and provides recommendations for: (1) closing knowledge gaps to reduce uncertainty bands on performance and costs, and (2) improving technology performance with improved design optimization modeling and refining advanced control systems.

1. Power Performance and AEP Estimates

Scaled model testing of MEC devices and arrays is critical to narrow the uncertainties and increase confidence levels in the power performance predictions and AEP estimates. These power estimates are derived from several hydrodynamic models that are commonly used for analyzing MEC devices. Scaled model testing is also a prerequisite for a device to advance, in DOE’s Technology Readiness Level (TRL) scale, to level 4 (TRL-4). At the TRL 4 stage, basic technological components of a sub-scale model have been integrated to validate design predictions and system level functionality; furthermore, the models and/or critical subsystems have been tested in a laboratory environment. Approximately half a dozen physical modeling experiments are completed, are underway, or are planned for scaled models of our RM devices or their rotors. These studies should provide more opportunities to validate the RM device designs and the models used for performance and AEP estimates. In order to facilitate further physical model testing and model validation, SolidWorks files (3D CAD software) of all RM device geometries are available for download from Sandia’s Energy, Climate, and Infrastructure Security website: http://energy.sandia.gov/rmp.

2. Operational Experience from Technology Analogues

Estimated CapEx and OpEx costs rely heavily on design, M&D, and O&M experience and actual data from land-based wind plants. To estimate RM device and array availability, and to calculate the AEP used in the LCOE estimate, we applied an operational availability level of 95% (the percentage of the time the device is actively producing electricity). This percentage is equal to the 2011 operational availability benchmark reported for land-based wind plants surveyed in the United States by the Continuous Reliability Enhancement for Wind (CREW) database, a DOE-funded national reliability database; this is 2% less than the 2012 benchmark for wind plants, which had operational availability levels of 97% (Peters et al. 2012). Uncertainties in CapEx and OpEx costs can be narrowed further by incorporating empirical data from other, more mature, renewable energy technology analogues used to delineate M&D and O&M strategies and costs. Operational data from offshore wind plants would be particularly valuable because it would help quantify the additional costs associated with the challenges of marine operations. In the end, however, these costs can only be assessed accurately with actual operational experience of MEC technologies at commercial scales.

3. Operations Modeling

As demonstrated by Teillant et al. (2012), estimates for operational costs and device availability can be improved by applying more rigorous operational models (based on O&M experience with wind plants as well as oil and gas exploration). For example, Teillant et al. (2012) apply weather windows to determine when conditions are suitable for operation of vessels and equipment required for preventative and corrective O&M tasks, such as installation, repair, inspection, and removal. Weather windows, which vary among the different resource types (e.g., wave environments compared to tidal current environments) and specific sites, were not considered in our O&M Strategy Module.

4. Design Optimization

Our RM device designs were developed primarily to calculate LCOE estimates. They are simple, robust, preliminary designs. Optimization of the performance of the RM devices was minimal and also varied among the four different RMs. For CEC RM devices, this can be improved using well developed optimization methods used for wind turbines. For WEC RM devices, however, more fundamental R&D is needed in the area of real-time-forecasting and improving advanced control systems. Recent research shows that advanced controls can provide substantial improvements to energy capture efficiency. Finally, until array optimization models are further developed, there remains large uncertainty in array costs covered under the M&D, O&M, and EC modules described above.

5. Environmental Compliance Costs

We assigned no OpEx costs for ongoing mitigation activities that will be required for managing environmental risks. Until knowledge gaps can be closed—including knowing the potential impacts of MEC devices and projects on the physical and biological environment (e.g., animal strike, noise levels, and electromagnetic fields [EMF]), it will not be possible to determine mitigation requirements and their costs.

1 Introduction

Recent estimates indicate the maximum theoretical AEP that could be produced from waves and tidal currents is approximately 1,420 TWh per year, approximately one-third of the nation's total annual electricity usage (Hagerman et al. 2011, Haas et al. 2011). This finding has renewed commercial and government interest in Marine Energy Conversion (MEC)[1] technologies and indicates that wave and tidal energy could play a significant role in the U.S. renewable energy portfolio in the years to come. However, MEC technologies are at a nascent stage of development and require significant research and development (R&D) before becoming cost-competitive with other energy generation technologies on a commercial scale. In response to this need, the U.S. Department of Energy (DOE) initiated the Reference Model Project (RMP) with three objectives:

1) Develop and illustrate a methodology for 1) the design and economic analysis of MEC technologies—including a methodology for estimating their annual energy production (AEP) for single devices and arrays with 10, 50 and 100 units, 2) determining annualized capital and operational expenditures, and 3) estimating levelized cost of energy (LCOE) in $/kWh;

2) Design four MEC technology Reference Models. Each Reference Model is a “point design,” a term used to emphasize that it is a unique device designed for a reference resource site modeled after an actual site in the United States; it is not intended to be a device that is a general representation of a specific MEC technology archetype; and

3) Demonstrate the application of this methodology for the four MEC technology Reference Models, referred to herein as Reference Models (RM) 1, 2, 3, and 4, and identify the cost drivers and calculate LCOE estimates (in $/kWh) for each RM device and for 10-, 50- and 100-unit arrays.

Figure 1-1 shows the four RM devices discussed in this report.

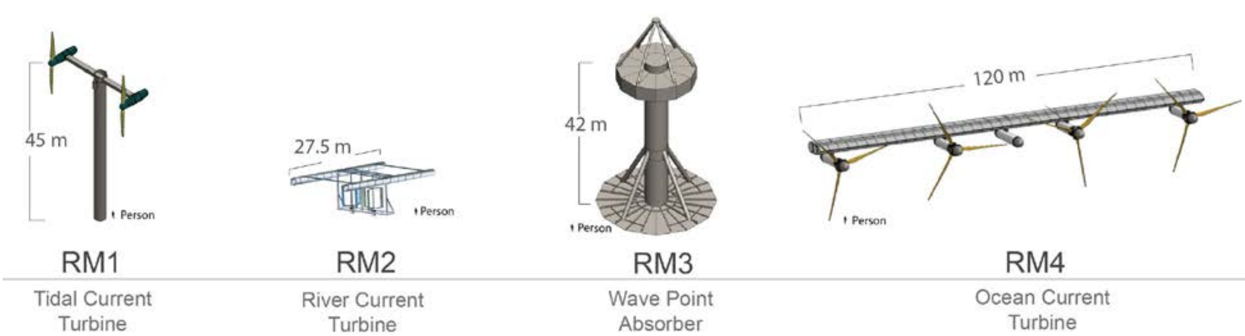

Figure 1-1. RMs 1, 2, 3, and 4 shown in approximate scale.

[1] We adopt the term Marine Energy Conversion (MEC) throughout this document in place of Marine Hydrokinetic (MHK).

1.1 Background

The RMP team responsible for the development of this report includes participants from four different national laboratories, two universities, and two private consulting firms as described under Acknowledgements. Working closely with DOE, our sponsor on this RMP, we developed this report through a nationwide collaboration of expertise in MEC technologies, wind plant technologies, environmental compliance, reference site resource characterization, project planning and cost estimating, operational project management, and various other areas of subject matter knowledge. The input for this report has been compiled, updated, and refined starting with early draft reports compiled by Re Vision LLC (unpublished); the content has since been substantially revised to include a methodology for the design and analysis of MEC technology devices/arrays and LCOE estimation. These revisions helped make the discussions for each RM chapter as consistent as possible and improved transparency to the design process and the analysis and LCOE estimation, including supporting documentation and the rationale used for our assumptions.

1.2 Report Organization

Chapter 2 of this report describes the design, analysis, and LCOE estimation methodology, which is centered on four core modules. This methodology accounts for all aspects of: device design and analysis (**D&A Module**), manufacturing and deployment (**M&D Strategy Module**), operation and maintenance (**O&M Strategy Module**), and environmental compliance (**EC Module**).

Following the methodology description outlined in Chapter 2, the Reference Model Chapters—3, 4, 5, and 6—provide examples of the application of this methodology to designing the four RM devices and arrays. The four RM devices include three Current Energy Conversion (CEC) technologies—a tidal current turbine (RM1), a river current turbine (RM2), and an ocean current turbine (RM4), and one Wave Energy Conversion (WEC) technology (RM3), a wave point absorber.

In Chapter 7, we present the results of our qualitative assessment of uncertainty, including the uncertainty in analyzing each device's performance, structural design, power conversion chain (PCC) design, site resource (physical and environmental), and economics, as well as our assessment of uncertainty estimating capital expenditure (CapEx) and operational expenditure (OpEx) costs used to derive the LCOE estimate.

In the last chapter, Chapter 8, we summarize key cost drivers for each RM where future R&D efforts can be focused. We also identify remaining weaknesses in the design, analysis, performance, and cost modeling and provide recommendations to improve these areas by closing knowledge gaps with better empirical information from technology analogues, as well as the application of new or improved modeling tools.

1.3 Levelized Cost of Energy

We calculate LCOE estimates (in $/kWh) for each RM over a range of installed capacities based on 1-, 10-, 50- and 100-units. These estimates are subject to varying degrees of uncertainty, which are qualitatively assessed based on known knowledge gaps as well as known modeling deficiencies, which are common to nascent technologies not yet commercialized. For example, the uncertainties of the hydrodynamic (power) performance predictions and the annual energy production (AEP) (in kWh), as estimated for a single MEC device (unit), are generally assumed to be low when performance models have been validated against data collected in physical model experiments. Comparatively, since modeling data on arrays have yet to be well developed or validated, AEP estimates for RM arrays have high uncertainty, which are also biased high based on simplifying assumptions discussed herein.

Since knowledge gaps and uncertainties are greater for some RMs as compared to others, it is not appropriate to compare their LCOEs. Instead, we place more emphasis on developing a consistent and well-documented methodology that identified key cost drivers to address with future R&D efforts.

For those in the MEC industry or R&D community who are interested in developing LCOE estimates for their technologies, they can adopt this study's methodology, and if they are using similar site resource information, assumptions, and approximations, then compare their LCOEs against those estimated here. We recognize that some of the costs used in the LCOE estimates, for example, deployment costs, may be overly optimistic, representing a mature industry. However, industry and the research community can adjust these costs based on their judgment and experience and as operational experience with these nascent technologies improves. Although not explicitly delineated as part of our methodology for designing MEC devices, we maintain that physical model testing for device design and model validation is an essential part of the design and analysis process.

1.4 High-Level Goals

The design methodology and the RM devices and arrays developed through the Reference Model Project are intended to support DOE's MEC technology development and market acceleration efforts. This specifically includes advancing the R&D efforts of participating National Laboratories and research universities and meeting the needs of MEC industry partners and investors in the following ways:

- Provide a documented methodology for MEC device/array design and LCOE estimation.
- Provide Reference Models paired with reference resource sites that can be used as study objects for open-source research and development (R&D).
- Provide reference MEC resource sites (modeled on actual MEC sites) to allow developers to assess their device's performance. These sites have considerable data on the hydrokinetic energy resource, site attributes (not inclusive of seabed conditions [for mooring] for all sites), and characterization of potential environmental risks. These sites are also generally prototypical of locations that are likely candidates for utility-scale MEC development, thus, providing a reference from which developers can assess technology competitiveness in the U.S. market.

- Identify key cost drivers and cost reduction pathways for MEC technology point designs.
- Provide benchmark technical performance and LCOE estimates for these point designs.
- Provide numerical and experimental data sets that can be used to verify and validate open-source MEC design tools and methods.
- Identify known gaps in modeling and design tools needed to advance MEC technology. Each stage of advancement is assessed against DOE's Technology Readiness Levels (TRLs) from one to nine, with nine being a design that is commercially ready for production. As the technology is studied and tested, it is expected that future entrepreneurs and researchers will develop the next generation of MEC devices.
- Provide guidance for the National Environmental Policy Act (NEPA) compliance process. Environmental compliance efforts will include extensive siting characterization and permitting and conducting pre-installation studies required to meet acceptance by regulators and stakeholders. If the project meets environmental, operational, and other criteria and achieves all necessary regulatory permitting, then post-installation studies and environmental monitoring will be required for the life of the project.

2 Methodology for Design, Analysis, and LCOE

An idealized methodology for designing, analyzing, and estimating levelized cost of energy (LCOE) for MEC Reference Model (RM) devices and arrays is illustrated schematically in Figure 2-1. Table 2-1 summarizes the primary cost categories captured in Figure 2-1 (the costs listed in the figure and the table are high-level costs only). This chapter provides a general overview of our methodology including the four key modules listed in Table 2-1. These modules drive the estimates for capital expenditure (CapEx) costs, operational expenditure (OpEx) costs, and annual energy production (AEP). CapEx are those costs associated with activities prior starting MEC energy operations, and OpEx are those costs associated with operating and maintaining the MEC array. The methodology outlined in this chapter was then generally applied to the four RMs, which are discussed in Chapters 3, 4, 5, and 6.

Table 2-1. Typical CapEx and OpEx costs under the four modules.

Module	CapEx Costs ($) *Prior to MEC operations*	OpEx Costs ($) *Post MEC Operations*
Design & Analysis (D&A)	- Design & Development	None
Manufacturing & Deployment (M&D) Strategy	- Device structure - PCC system - Infrastructure (e.g., cable layout) - Assembly - Foundation Mooring - Deployment (device Installation) - Decommissioning (retrieval)	None
Environmental Compliance (EC)	- Environmental Siting Studies - Environmental Analysis - NEPA compliance process - Local permitting process - Stakeholder Meetings - Mitigation Studies - Addressing potential showstoppers	- Environmental Monitoring - Renewing permits
Operations & Maintenance (O&M) Strategy		- Marine Ops - Shoreline Ops - Replacement Parts - Consumables - Insurance - Downtime

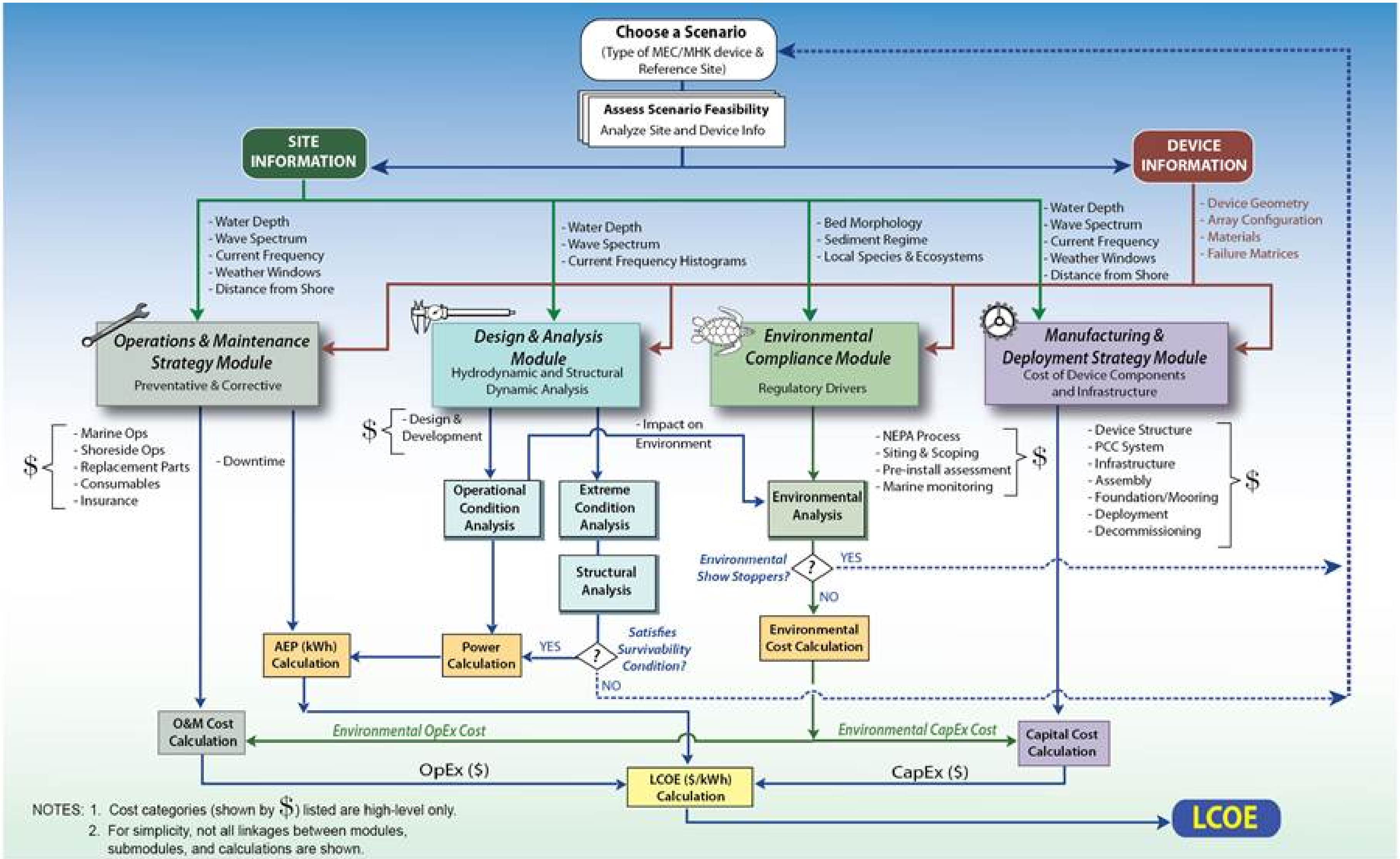

Figure 2-1. Methodology for design, analysis, and LCOE estimation for MEC technologies.

NOTE: This figure is intended to be illustrative and does not capture all details and items covered in the methodology.

RM devices are only conceptual designs at DOE Technology Readiness Levels TRL 3 to 4[2]. The four designs were purposefully made simple and robust in order to calculate approximate LCOE estimates, rather than pursuing the design iterations necessary to optimize energy output and LCOE.

Although not shown in Figure 2-1, physical model testing is an essential part of the methodology for designing MEC technologies at TRLs 3 and 4. Highlights on the scale model testing conducted on our RM devices are discussed in the shaded boxes below.

Scale Model Testing of MEC Devices

RM1 Testing

Performance measurements for a single 1:25 scale RM1 rotor were collected at the **U.S. Naval Academy** tow tank (Luznik et al. 2012) and were used to validate the numerical model employed to predict the rotor performance for RM1.

Performance measurements for a single 1:45 scale RM1 rotor were collected by the University of Washington in an open channel flume at the **Bamfield Marine Sciences Center** (Javaherchi et al. 2013); however, their results had problems due to testing at a low Reynolds number and their method of controlling the rotational speed of the rotor with a magnetic brake. In July 2013, the Bamfield Marine Sciences Center addressed these limitations by conducting new experiments using a three-turbine array; the results have yet to be published.

The demonstrated power performance results of Bamfield's second round of testing on RM1 were in agreement with the U.S. Naval Academy's earlier results. RM1 results are described in Chapter 3.

(continued)

[2]DOE (Reed et al. 2010) defines nine Technology Readiness Levels from conceptual level to commercial readiness. The RM 3-4 level is defined as follows: At the **TRL 3** stage, active research is initiated, including engineering studies and laboratory studies to physically validate analytical predictions of separate elements of the technology. At the **TRL 4** stage, basic technological components of a sub-scale model are integrated to validate design predictions and system level functionality. The models, or critical subsystems, are tested in a laboratory environment. For further reading, refer to *U.S. Department of Energy Technology Readiness Assessment Guide*, DOE G 413.3-4 (Oct 12, 2009), at https://www.directives.doe.gov/directives/0413.3-EGuide-04/view

Scale Model Testing of MEC Devices *(Continued)*

RM2 Testing

For RM2, performance tests on scaled model rotors, similar but not identical to the RM2 design, were conducted. Performance measurements were collected for a 1:6 scale model rotor with NACA 0020 foils in a tow tank at the Center for Ocean Renewable Energy (CORE) located at the **University of New Hampshire** (UNH) (Bachant and Wosnik 2013). However, model simulations of this experiment using CACTUS (Code for Axial and Cross-flow TUrbine Simulation), the same code used to design the RM2 rotor, predicted significantly higher performance than that observed in the experiments (Michelen et al. 2013). The likely cause for the discrepancy appears to be a limitation in the CACTUS model to account for the higher chord-to-radius (c/R) ratio of the CORE turbine. In comparing the results for the CORE and RM2 turbines, the CORE turbine ratio is higher (c/R=0.28) along the entire span of the foil, while the ratio for the RM2 design, is less than half the value at the root and transitions (c/R=0.124) and even less to the blade tip (c/R=0.074). RM2 results are described in Chapter 4.

RM3 Testing

For RM3, measurements for a 1:33 scale RM3 device were collected at the **Scripps Institution of Oceanography** wave tank (Yu et al. 2013, in preparation) and applied to validate the numerical model used to predict the performance of the RM3 device. RM3 results are described in Chapter 5.

RM4 Testing

The RM4 design, discussed in Chapter 6, is based on the RM1 design. Specifically, because the RM4 rotor and hydrofoil designs are similar to those for RM1, the **U.S. Naval Academy's** tow tank experiment also supports model validation for the RM4 power performance predictions; and since the blade structural design was scaled up from the RM1 blade design, the blade's structural design is not described in Chapter 6.

Scaled model testing is planned in 2014 for a 1:40 scale model of the RM1 device and a 1:10 scale model of the RM2 device at **St. Anthony Falls Laboratory (SAFL)** located at the University of Minnesota. The measurements from the RM2 scale model test will be particularly useful because, unlike the UNH experiments, it is an exact geometric representation of the RM2 turbine with the same chord-to-radius ratios. We will use the measurements collected in the RM2 model performance tests to validate the CACTUS model.

We generally employed minimal design optimization for the four RM devices, and the amount of design optimization varied between the RMs as well. We are also still developing far-field numerical modeling that accounts for device interactions (turbulent wake effects within an array). Therefore, we also did not conduct optimization for array designs. However, our four

RM designs do consider the necessary trade-offs between maximizing energy production and minimizing the costs for fabrication, deployment, and operations and maintenance.

Figure 2-1 illustrates the design iterations needed to meet key constraints imposed for structural design and for environmental compliance (dashed lines from the decision boxes below the blue and green module boxes shown in the center of the flowchart). The methodology used for the reference models deviate in varying degrees from the idealized methodology presented in this chapter—areas of difference are noted in this chapter and the deviations particular to a given RM are discussed in each RM chapter. These deviations were due mainly to the limitations on resources available for this study. For example, weather windows were not calculated for the four reference model sites. Where applicable, we reference work done by others who have performed higher order analyses.

We are careful to identify key knowledge gaps and qualitatively assess the uncertainty in our analyses. This uncertainty is greater at lower TRLs and is largely due to the lack of operational experience with commercial MEC projects and the absence of validated modeling tools for designing and analyzing current and wave device (CEC and WEC) arrays. At this time, there are no operating commercial scale MEC projects[3] for any WEC or CEC technologies in the world.

2.1 The Design Methodology

2.1.1 Design Methodology for a Single Device

The MEC Reference Model (RM) design methodology can involve multiple design iterations until constraints are satisfied, depending on the level of design optimization desired. The design process starts by selecting an initial scenario that pairs initial reference model device specification information (e.g., device geometry and size, power performance expectations, subcomponent reliability, etc.) to a reference hydrokinetic energy resource site (e.g., water depth, hydrokinetic resource characteristics such as wave spectra, distance to shore, and environmental concerns such as the local species and habitats present). Although not done in this study, the weather window is an important site characteristic that can be included in this methodology.

Device (and array) design specifications are initially determined using engineering judgment based on subjective and qualitative assessment of the reference site characteristics and consideration of the costs associated with manufacturing and deployment (M&D), operations and maintenance (O&M), device survivability, and environmental constraints. For example, because repair of the power conversion chain[4] (PCC) requires complete recovery (which is costly), redundant subsystems (e.g., cooling system pumps, control systems, and sensors) are included in the design to reduce the service frequency. CEC RMs are designed with dual or multiple rotors

[3] We define commercial MEC projects as those consisting of 50 or more devices.

[4] The power conversion chain definitions have been adapted from Hydraulics and Maritime Research Center (HMRC) University College of Cork (UCC) in which the definition's applicability has been broadened to other renewable technology definitions that the DOE uses when assessing cost (O'Sullivan et al. 2010). The PCC is composed of the following components: 1) a drivetrain that converts the device motions into the final form of mechanical power needed to drive the generator (e.g., hydraulics, shafts, bearings, gearboxes); 2) a generator that converts mechanical power into electrical power; 3) short term storage, which may be used to either affect power quality or other aspects of the PCC; and 4) power electronics that enable power quality requirements to be met (the supervisory control and data acquisition [SCADA] is part of the power electronics).

mounted on a single deployment structure (e.g., tri-frame, piling, pontoon, or wing) to reduce M&D and O&M costs. Considerations for transporting system components and subcomponents on land and on water can also influence the design of MEC devices.

As illustrated in Figure 2-1, the process begins with the input of specific **device information** and reference **site information** variables into the four modules described in detail below. The D&A Module predicts the hydrodynamic (power) and structural performance of the device, which allows calculation of the annual energy production (AEP). The design outputs of this module also influence the cost of materials and system components input to the M&D Strategy Module because material and component specifications have to satisfy survivability constraints. Capital costs (CapEx) for manufacturing, deployment, balance of system (BOS), and decommissioning are estimated in the M&D Strategy Module. Operations and maintenance (OpEx) costs are estimated using the O&M Strategy Module. The EC Module estimates the CapEx for environmental studies, implementation of mitigation strategies (e.g., sound attenuation technology during pile driving), and permitting for environmental compliance. The EC Module also determines post-installation environmental monitoring needs and their associated OpEx over the life of the project.

Water depth and hydrokinetic resource characteristics (wave spectra or current frequency histograms) are inputs to the D&A Module to determine the power output and the AEP (kWh) prior to applying an operational availability factor. The D&A Module also performs structural analysis to determine required material specifications (e.g., type of materials, plate thicknesses, dimensions of structural members, etc.), which affects manufacturing costs. The D&A Module includes hydrodynamic modeling to determine potential environmental impacts (e.g., redistribution of currents, tidal flushing effects, sediment transport, and scour) that affect OpEx for environmental monitoring and CapEx for environmental impact studies and mitigation measures (such as sound attenuation technology during installation and adding marine mammal warning devices (Wilson and Carter 2013). Once the device design satisfies survivability constraints (based on structural analysis under extreme loading conditions) and environmental constraints (based on regulatory requirements for minimal impacts on physical processes as well as conservation and protection of local species and habitat at the site), the total cost ($) for a given RM device is calculated to reflect the annualized OpEx and CapEx costs. The O&M Strategy Module also predicts device downtime from which an AEP (kWh) that accounts for non-operational periods can be predicted. LCOE is then calculated as the total annualized costs divided by the AEP (kWh).

2.1.2 Design Methodology for Arrays

After determining the LCOE for an individual device, the same methodology is applied for the design and analysis of a commercial array (farm) consisting of multiple devices. The array-scale LCOE estimate is intended to reflect economy-of-scale reductions in manufacturing and fabrication costs, as well as installation. Further, O&M cost savings can be realized when multiple devices are deployed at a single site. The array is characterized by the number of devices, the specific layout (e.g., linear, staggered, or random pattern) and density (longitudinal and lateral spacing between the devices).

The LCOE of a commercial array is expected to be lower than that of a single device since the deployment of multiple devices at a site reduces M&D and O&M unit costs. Naturally, the total

AEP of a commercial array (defined as equal to or greater than 10 devices) will be greater than that of an individual device, albeit at the cost of reduced power produced by each device within the array due to wake, blockage, and other effects (Garrett and Cummins 2007). These effects are ideally addressed in the D&A Module using far-field hydrodynamic models that account for momentum and power extraction effects on flow recovery in the wakes of individual devices. These models can also assess the environmental impacts of the array, including its effect on tidal flushing (tidal replacement of salt water/nutrients in an estuary), as well as its effect on the sediment transport regime and fish migration.

Design analysis for MEC arrays (to determine optimum configuration and number of devices) using models such as far-field hydrodynamic models was not conducted in this study. We assumed that a maximum of 100 units could be deployed at a reference site to achieve reductions in costs from the economy of scale, which would lower LCOE estimates. However, we emphasize LCOE estimates based on 10-unit MEC arrays because MEC plants with this number of units seem most likely based on the wind turbine plant experience..

The development of array optimization models will be needed to design and analyze future MEC arrays. Presently, modeling tools for the design and optimization of CEC and WEC arrays are under development (Hassan 2013, Weywada et al. 2012). For this project, we simplified the AEP calculations by assuming that inflow conditions (and available power density) for all devices in the array were the same as for a single device—therefore, the AEP estimate for an array was the AEP for a single device multiplied by the number of devices in the array. This would obviously overestimate the AEP for an array, resulting in an underestimation of the LCOE. The application of more advanced modeling tools for higher-level array designs (at TRLs 4-7) would ideally be applied to reduce the uncertainty in the AEP estimate for an array. These models would also account for feedback and optimization between the environmental analysis and operational conditions analysis and array design specifications (e.g., number of devices, location, and spacing).

2.2 Module Inputs

2.2.1 Site Information

Reference resource sites were modeled after actual sites selected for their potential viability as commercial-scale hydrokinetic energy sites as well as the availability of data at the site to accurately characterize the hydrokinetic energy resource and its environmental conditions. For example, the Reference Model 1 **(RM1)** technology, a dual-rotor, axial-flow tidal turbine, was designed for a reference resource site modeled after the Tacoma Narrows in Puget Sound, Washington. The site has been extensively studied and a wealth of data is available to fully characterize its physical and biological features, including water depth, current frequency histogram, weather windows, distance-to-shore, sea bed morphology, sediment regime, and local species present (Polagye 2011b). For similar reasons, the reference resource site for the **RM2** technology, a vertical-axis, dual-rotor, cross-flow river turbine, was modeled after a reach in the lower Mississippi River near Baton Rouge, Louisiana; the reference resource site for the **RM3** technology, a wave point absorber, was modeled after a wave site near Eureka, Humboldt County, California; and the reference resource site for the **RM4** technology, a moored glider with four axial-flow turbines, was modeled after the Florida Strait ocean current site near Boca Raton, Florida.

Site information, including water depth, adjacent port facilities and grid options (proximity to service port and stations for grid connection), extreme event conditions for structural design, and weather windows, ideally, are inputs to both the O&M and M&D Strategy Modules. This information is needed to develop O&M strategies and to predict O&M costs (OpEx). Additionally, the M&D Strategy Module needs this information to develop deployment strategies and to determine the costs of deployment and BOS infrastructure. Although we were not able to include weather windows for any of the RMs in our study, weather windows are also used to predict the device and array downtime, which affects the annual energy production (AEP).

The D&A Module requires site water depth and hydrokinetic power characteristics derived from current frequency histograms, in the case of CECs, or wave time series (or wave spectra) for WECs. These inputs limit the size of the device and array, and are used to predict the potential AEP based on a device and array performance (CEC power curve or WEC power matrix). The current frequency histograms and wave spectra are also used to estimate extreme hydrodynamic conditions needed for worst case structural analyses to ensure survival of the device over its design life. The reference site's sea bed morphology and sediment regime (e.g., sediment type, cohesiveness, and grain size distribution) are important features that influence the selection and design of foundations and moorings as well as the design of the buried electric cable infrastructure. With the exception of RM3, this type of geologic information was not available for the other RMs to factor into such designs.

The EC Module requires similar information to the D&A Module on the bed morphology and sediment regime, the tidal flushing regime (specific to tidal energy sites), and local species that may be impacted by the MEC device/array.

2.2.2 Device/Array Information

The device information includes its basic design concept, geometry, and size, as well as the material, mechanical and electrical properties of the device's subsystem components and subcomponents, including:

- Turbine rotor (rotor diameter, number of blades, blade geometry);
- Power conversion chain (PCC), which includes components defined in Section 2.1.1.
- Controls;
- Foundation/mooring system (e.g., monopiles, tower, pontoon, anchors, and mooring cables);
- Support Balance of System (BOS) infrastructure (e.g., transmission cables, cable landing, dockside improvements and, if needed, a dedicated service vessel); and
- Transmission efficiencies and device and array availability.

The materials and components for each RM device are specific to the environment at the selected site. For example, the strength of materials required for the hull of a WEC device or the blades for a CEC turbine are selected to withstand extreme hydrodynamic loads estimated for their reference resource sites. Further, the harsh marine environment also requires additional measures to prevent water and salt damage, corrosion, and biofouling such as special coatings. Other information that goes into the design process includes consideration of the reliability of system components (failure matrices) and BOS infrastructure. All of this information is also needed to determine the O&M costs. As discussed above, the number of devices in an array, the array layout (linear, staggered, or random), and its density (the longitudinal and lateral spacing between devices) are inputs that influence BOS infrastructure requirements and expenditures. An example would be the required length and cost of subsea cables.

2.3 Design, Analysis, and Cost Modules

Figure 2-1 centers on four core modules that process site and device/array design inputs to determine RM designs (the D&A module), strategies for manufacturing and device installation (the M&D Module), operational and maintenance strategies (the O&M Module), and efforts required to ensure environmental compliance (the EC Module). Outputs from these modules are used to estimate annual energy production (AEP) in kilowatts per hour (kWh), and annualized costs for OpEx and CapEx—the ratio provides the LCOE ($/kWh).

The four main module outputs, detailed in the sections below, include variables that drive various analytical sub-modules such as for determining device/array power and structural and environmental performance. The methodology illustrated in Figure 2-1 shows the interrelationships between the modules and *sub-modules*. For example, information from the D&A sub-module (*Operational Condition Analysis*) is input to the EC sub-module (*Environmental Analysis*) to determine the impact on the environment. The resulting environmental costs for monitoring, studies, permitting, and mitigations required prior to operations and monitoring and mitigations required post-operations will affect both the CapEx and OpEx calculations. Unit costs of materials and labor that affect CapEx and OpEx costs are primarily derived from the M&D and O&M Strategy Modules, respectively. These inputs can be traced in Figure 2-1 by the lines leading to the *O&M Cost Calculation* and the *Capital Cost Calculation* sub-modules. In some cases, a sub-module, such as for the *AEP (kWh) Calculation* requires input from two modules—the O&M Strategy and D&A Modules. Sub-module outputs may or may not satisfy constraints on power, structural, or environmental performance, thus requiring adjustments (design iterations) such as improving the robustness and longevity of a device by substituting stronger materials or increasing the material thicknesses. The decision box under the D&A sub-module *Structural Analysis* illustrates how a “No” answer reiterates the design process back to the beginning.

The following four subsections detail the calculations and inputs required for the four main modules:

- Design & Analysis (D&A) Module, Section 2.3.1
- Manufacturing & Deployment (M&D) Strategy Module, Section 2.3.2
- Operations & Maintenance (O&M) Strategy Module, Section 2.3.3

- Economic Compliance (EC) Module, Section 2.3.4

2.3.1 Design & Analysis (D&A) Module

The Design & Analysis Module uses numerical hydrodynamic models that simulate the hydrodynamic (power) performance of the prospective device or array, which can then be combined with the given reference site's hydrokinetic resource characteristics to calculate the AEP.

2.3.1.1 Performance Analysis and AEP Estimation

AEP Calculation for CEC Devices

For current energy conversion (CEC) devices (RM1, RM2, and RM4), the AEP for each rotor is calculated by combining the predicted mechanical power performance characteristics $P_m = 1/2 \cdot \rho \cdot A \cdot C_p(u_i) \cdot u_i^3$ in kW with the current frequency histogram $p(u_i)$ using the equation:

$$AEP = 0.95\left(\frac{8766}{1000}\right)\eta_1\eta_2\eta_3\frac{1}{2}\rho A\sum_{i=1}^{n}C_p(u_i)\cdot u_i^3\cdot p(u_i)\ \text{[kWh]}$$

where $C_p(u_i)$ is the power coefficient that accounts for the conversion of hydrokinetic power in the resource (tidal, river, or ocean current) to mechanical power, $p(u_i)$ is the probability of a given current speed occurring during the year for the reference resource (obtained from the current speed frequency histogram) and u_i is a given current speed in m/s, A is the rotor energy capture area (ECA) in square meters, ρ is the density of water in kg/m^3, 8766 is the number of hours in a Julian year (365.25 days), and 1000 is the number of Watts (W) per kW. The assumed operational availability is 95%. AEP is expressed in units of kilowatt-hours (kWh).

Specific values for gearbox and generator efficiencies, η_1 and η_2, were based on data supplied by manufacturers. Values for η_1 ranged from 0.92 (92%) to 0.96 (96%). Values of 0.96 (96%) are typical for wind turbine gearboxes (McGuinn 2011). Values for η_2, ranged from 0.90 (90%) for the small generators used in the RM2 device to 0.98 (98%) for the large permanent magnet generators used in RM1 and RM4 devices (ABB 2013, TECO Westinghouse 2013, TM4 Electrodynamic Systems 2013). We applied a value for transmission efficiency, η_3, of 0.98 (98%), which accounts for the heat loss in the conductor (*Joule effect*) of about 2.5% (IEC 2013).

In this study, we simplified the operational availability calculation. Rather than determine the downtime by predicting weather windows and component reliability, we assumed an operational availability of 95% based on land-based wind plant operation studies (Graves et al. 2008, Peters et al. 2012). Recognizing that the land-based wind plant analogue does not reflect the added cost of working in the marine environment, our reference model device designs incorporate redundancy for components with high-failure rates in order to improve operational availability by reducing the number of service trips. In our O&M Strategy Module (Section 2.3.3), we also plan for one reserve device (an entire MEC unit), stored dockside, to reduce operational downtime for all array sizes. Finally, high operational availability is ensured by adopting design standards and insurance costs from offshore oil and gas exploration and shipping industries.

AEP Calculation for WEC Devices

For wave energy conversion (WEC) devices (e.g., RM3), the AEP is calculated by combining the predicted mechanical power matrix for the device $P_m(H_{s_i}, T_{e_i})$ with the joint probability distribution (JPD) that describes the reference resource site's sea state $p(H_{s_i}, T_{e_i})$ using the equation:

$$AEP = 0.95(8766)\eta_1\eta_2 \sum_{i=1}^{n} P_m(H_{s_i}, T_{e_i}) \cdot p(H_{s_i}, T_{e_i}) \text{ [kWh]}$$

where $P_m(H_{s_i}, T_{e_i})$ is the mechanical power absorbed by the device in kW that can be extracted from the resource for a given significant wave height H_{s_i} and peak wave period T_{e_i}. As with the CEC AEP calculation, 8766 is the number of hours in a Julian year. Again, 95% was used for the operational availability.

We assumed a coefficient η_1 = 0.80 (80%) for the PCC efficiency (which includes the generator efficiency) as reported by Cargo et al. (2011), η_2 is the transmission efficiency, which is also assumed to be 0.98 (98%) for RM3.

2.3.1.2 Materials Specification and Structural Analysis

The D&A Module tests device survivability by performing structural analysis of the rotor components to extreme hydrodynamic loadings. The type of hydrodynamic loadings considered were loadings due to extreme currents acting on a deployed device, loadings during deployment and retrieval, and loadings during towing the device to and from shore. We used a variety of modeling approaches, from simple beam models to finite element analysis (FEA) models, where higher-fidelity analysis was required. Design standards, for example, those for offshore steel structures (DNV 2011), were applied where applicable.

Based on the structural analysis results, material specifications are tested including:

- Material and yield strength (e.g., A36 Steel has a yield strength of 36 ksi [36,000 psi]),
- Dimensions,
- Plate thickness, and
- Tubular structure specifications.

We only calculated the material costs in the M&D Strategy Module (Section 2.3.2) for devices that were shown to be capable of surviving an extreme loading event; if not, the design was revised through material substitutions or other modifications until this constraint was satisfied.

In this study, we did not include dynamic loads, fatigue, buckling, and modal analysis in the structural analysis. However, doing so would have allowed for further structural optimization and, potentially, weight reductions of the RM designs; alternatively, such analysis could also point out areas where increased robustness and added weight was called for. Experience with wind turbine designs and platforms designed for offshore oil and gas operations have shown that dynamic loads, particularly for WECs, must be considered when assessing ultimate strength and structural fatigue.

2.3.1.3 Power Conversion Chain (PCC) Design

The PCC design for the CEC reference models (RM1, RM2, and RM4) leverages design experience from marine vehicle systems (e.g., submarine propellers). Emphasis was placed on developing a robust design using commercially available components, where possible, to preserve the low overall system cost and facilitate easier system maintainability. The initial device design estimates the performance characteristics (e.g., power coefficient, operating parameters, and predicted steady and unsteady operating loads based on the site characteristics), the operating environment, and the overall PCC system efficiency (Beam et al. 2012).

The PCC design for the WEC reference model (RM3) specified initial estimates of the PCC maximum hydraulic stroke, maximum power rating of electrical equipment, and minimum breaking loads of mooring lines (e.g., Teillant et al. 2012). Trade-offs on subcomponent reliability, service life, maintenance schedule, weight, and cost were all considered in the initial design. These were further refined in the D&A Module using feedback from other modules and sub-modules, with iterations, as needed.

2.3.1.4 Foundation and Mooring Design

The foundation and mooring designs depend on the type of MEC device (general design concept) and device (unit) deployment strategy, which is defined in the M&D Strategy Module. MEC devices can be surface-deployed from pontoons on the water surface or deployed from anchored or weighted support structures on the sea floor. In contrast, most WEC devices require mooring cables and anchoring systems that allow a limited range of movement for energy absorption, but maintain device placement at the site. For each RM device, we specified foundation and mooring system components, including their dimensions and material specifications to withstand structural loadings from extreme events occurring at the resource site. Site bed morphology and sediment properties are key inputs for foundation/mooring design; however, with the exception of the RM3 resource site, these parameters were based on assumptions for RM1 or RM4 designs as detailed in Chapters 3 and 6.

2.3.2 Manufacturing & Deployment (M&D) Strategy Module

Manufacturing and Deployment (M&D) Strategy Module costs include:

- Manufacturing of all subsystems and device assembly
- Device structural components
- PCC system
- Infrastructure (balance of system [BOS])
- Foundation/Mooring system
- Deployment (installation, including commissioning)
- Decommissioning

The M&D Strategy Module calculates the capital costs (CapEx) of manufacturing and assembling the device structure and system components (e.g., PCC components) and all balance of system (BOS) components (foundation, anchor and mooring, grid connector cables, etc.) based on unit costs of components and materials. It also calculates deployment (installation) and decommissioning costs. The distance to port, distance to substation for grid connection, and vessel speeds affect the transit time and cost of installation of the devices and the subsea cables, as well as the decommissioning operations. Installation costs estimated include transport to staging site, assembly and installation of cable-shore landing, mooring system, interconnecting cable system and device, and commissioning. Operational tasks (e.g., pile installation, transmission cable installation, and device installation) are delineated along with subtasks and their required service vessel needs. Decommissioning costs are not included in the LCOE estimates for RM1 through RM4 because the present value of the decommissioning cost, calculated using a discount rate of 7.25% (equal to the weighted average cost of capital), was negligible relative to total capital costs (CapEx) and had a negligible impact on LCOE[5].

2.3.2.1 Manufacturing Strategy and System Component Costs

The manufacturing strategy we adopt assumes the use of commercially available components (e.g., generators, transformers, bearings, and anchors) and conventional materials (A36 steel, standard fasteners, mooring cables, etc.), where possible. We also assume the application of conventional manufacturing processes (e.g., steel casting, welding, and fastening methods) rather than highly automated manufacturing processes (e.g., robotic welding), which could provide significant cost reductions in large productions scales. The strategy provides manufacturing costs of system components (e.g., PCC components, nacelles, support structures, mooring cables and anchors, floats) for different deployment scales (1, 10, 50 and 100 units). A steel manufacturing cost model, previously developed by Re Vision (Previsic et al. 2004) provides insight into the manufacturing cost drivers. This model was calibrated through discussions and data sharing with representatives of commercial manufacturing organizations.

For the PCC systems, learning curve progress ratios for the different subsystems are identified and applied to the cost breakdown structure to derive the PCC system cost at mature production scales. Supporting analysis investigated whether cost reductions are attainable through manufacturing process changes, such as going from machined parts to molded parts.

The number of cables and costs cannot be generalized for all RM devices; therefore, the layout and subsea cable sizing must be RM device-specific. Cable sizing and collector system layout was accomplished by sizing and optimizing subsea infrastructure components. We estimated the subsea electrical transmission cable costs for unit deployments of 1 to 100 based on vendor estimates. Because our RM designs are not yet sufficiently detailed, we did not calculate the cost of the terminations and the connectors and, therefore, these were estimated as a contingency cost[6], which was assumed to be 10% of the cable cost.

2.3.2.2 Deployment Strategy and Costs

All four RM devices require service vessel support for initial installation and for operations and maintenance. We assume a dedicated service vessel constructed through a ship conversion (including installation of a crane and winch) to install a MEC array and to decommission it. Custom O&M service vessels may also assist installation activities. In addition, a separate cable

[5] Including the present value of decommissioning did not change the LCOE of RM1, RM2 or RM4, but did increase the LCOE of RM3 by 2%.

[6] Contingency costs (contingencies) are traditionally calculated as an across-the-board percentage addition on the base estimate, typically derived from intuition, past project experience, and historical data. Ten percent is a common maximum value used for project contingency (Baccarini 2004).

installation vessel would be leased during the MEC array installation. The characteristics of leased and dedicated service vessels for deployment (installation) and decommissioning are required inputs for the M&D Strategy Module to determine CapEx. Unlike Teillant et al. (2012), we did not account for vessel speed under different sea states and loads in our M&D or O&M Strategy Modules. However, vessel costs were estimated based on the number of trips, their duration, and vessel day rates. For CapEx in the M&D Strategy Module, we assume that service vessels would be fabricated from existing ship conversions to reduce service vessel costs. Existing barges and cranes are identified in Asian markets and we determined the estimated costs for upgrading these vessels with dynamic positioning (DP) capabilities, thrusters, and mooring systems capable of holding position. The M&D Strategy Module is not sufficiently detailed for breaking out and estimating the cost of un-mating cable or handling slack cable during deployment and recovery.

The cost of dockside improvements are not addressed explicitly, but are included in the contingency cost, which is assumed to be 10% of the project cost.

2.3.3 Operations & Maintenance (O&M) Strategy Module

Operations and Maintenance (O&M) Strategy Module expenditures include costs for:

- Marine operations (e.g., the number and type of operational interventions)
- Shoreside operations
- Replacement parts
- Consumables
- Insurance
- Marine (post-installation) monitoring (from EC Module—see Section 2.3.4)

These costs were estimated based on data from the NREL WindPACT data (Poore and Lettenmaier, 2003) for a land-based wind plant with a similar installed capacity. Based on the number of interventions and replacement part values, the annual O&M cost was computed at different scales of deployment. However, due to lack of existing WEC operational data (and no commercial analogues), there are substantial uncertainties regarding actual maintenance costs (Telliant et al. 2012).

A shore-side crew of technicians and administrative personnel would be responsible for carrying out onshore repairs and supporting the repairs and maintenance activities that would take place offshore. Table 2-2 provides a summary of the assumed labor rates and average total staffing costs for shore-side operations over the expected 20-year operating life of the project.

Table 2-2. Shore-side operations: Annual staffing cost and requirements for a 100-unit project.

Staff Type	Salary ($/yr) or Wage (hr/yr)	# of Staff (varies per year of operating life)	Average Total Cost of Staff ($/yr) for a 100-unit project
Site Manager Salary	114,750	1	114,750
Admin. Asst. Salary	47,250	2	94,500
Sr. Tech Wage	24.30	1 to 4	126,360
Jr. Tech Wage	16.20	4 to 9	219,024

As pointed out by Teillant et al. (2012), O&M costs (and device reliability) are difficult to evaluate accurately due to the lack of O&M experience operating MEC arrays. To assess operational costs and device availability, they applied a much more rigorous operational model (based on O&M experience with wind energy plants and oil and gas exploration) than that applied in our study. In particular, Teillant et al. (2012) applied weather windows to determine when conditions are suitable for operation of vessels and use of equipment required for preventative and corrective O&M tasks—for example, installation, repair, inspection, and removal of MEC devices and infrastructure. While distance to shore and service vessel speeds affect the transit time for O&M, weather windows affect not only the timing of when O&M activities can be conducted, but also the period that vessels may have to “wait on weather” before completing a particular task. Again, weather windows were not considered in our O&M Strategy Module.

2.3.3.1 Service Vessel

In order to reduce costs, we assume that the dedicated service vessel described in Section 2.3.2.2 for deployment and decommissioning would serve O&M needs as well. The number of service vessel trips for O&M, the duration of these trips, and each vessel’s day rates were used to calculate service vessel contributions to OpEx.

2.3.3.2 Failure Rates

Our O&M Strategy Module includes a failure matrix (measure of reliability) for device and infrastructure (BOS) components, which accounts for the likelihood of failure of each component along with the requirements for the repair as well as the number and unit cost of service trips. These outputs are used to estimate O&M costs (OpEx). For failure rates, we used data from the Wind Partnerships for Advanced Component Technology (WindPACT) study (Poore and Lettenmaier 2003). While these data are for a land-based wind plants and are somewhat dated, they provide our best estimates on failure rate distributions for some of the components of a typical wind-power drivetrain. However, while the major components of wind-power drive trains (PCCs) are similar to CEC PCCs, they are not similar to WEC PCCs and the application of this data to PCC components for marine devices is less accurate.

Very little information is available on the reliability of WEC components. First-order estimates of failure rates are based on a review of limited manufacturer data (Previsic et al. 2012). The L-50 life[7] is assumed to be the mean-time period before the subsystem requires complete replacement. To simplify the analysis, the number of failures is averaged instead of following the more typical Weibull failure-rate distribution (Abernethy 2006) of many of the subsystems and components. This simplification likely over-predicts costs because failure rates tend to decrease over the lifetime of a project after an initial wear-in period (i.e., the failure distribution is a not a symmetrical distribution, such as the normal distribution). To compute the replacement part cost, we assume failures are evenly distributed over the 20-year project life and that the replacement part cost is equal to the value of the part/subsystem in the original device. To compute the number and type of interventions in the economic life of the MEC array, failures are divided into two types of repair activities: repairs that can be conducted on-site or onboard the device and repair activities that require recovery and repair of the device back on shore.

2.3.3.3 Annual Maintenance

Annual maintenance activities include the recovery of the power conversion system-to-shore, refurbishment of the PCC, replacement of hydraulic fluids, and replacement of filters. A one-year interval for maintenance requires a robust design of the hydraulic system. The same applies for the cooling system and filter design (which will need routine cleaning due to biofouling).

It is likely that the device will require periodic cleaning due to biofouling, which will typically require device and mooring system retrieval and re-deployment. Biofouling, the accumulation of microorganisms, plants, algae, or animals, is highly site-specific (depending on species, water temperatures, etc.) and is also dependent on the type of surface coating used on the device components. For the purpose of this costing exercise, we assume that visual inspection for biofouling and cleaning will occur every year. However, this is probably too infrequent based on empirical data on ship hull cleaning. The U.S. Navy performs hull inspections quarterly and surface ships receive five underwater hull cleanings every six years on average (EPA 1999).

Mooring chains will also require maintenance and replacement. The dip-section of the mooring chain typically starts to wear out its mooring links over time. This is especially true near the bed where sediments add to the abrasion of the steel links. With better understanding of the process, replacement cycles could be reduced by over-designing the mooring links. Adequate safety factors and frequent inspections of the mooring line links (every two to five years) were assumed to help identify failures early in the wear process. However, as stated above, biofouling rates (e.g., attached barnacles, mussels, sponges, algae, crabs) may require more frequent inspections of the mooring chain.

2.3.3.4 Insurance

Insurance costs are driven primarily by the perceived risk of a particular technology or plant operations. For one-off projects in the marine sector, rates are typically 2% of the capital cost. As a technology matures and risks are reduced, rates will also reduce. A typical land-based wind project has insurance costs at approximately 0.5% of capital cost. For all RM projects in this study, it was assumed that the single unit and 10-unit insurance rate is 2% of the device installed

[7] Here, L50 refers to the average (mean) life of a component in which 50% of the components will fail and 50% will remain reliable as described in http://www.weibull.com/hotwire/issue80/relbasics80.htm. The cost of replacement parts is computed by using the L50 life of the component as the replacement interval.

cost; at 50 units that would drop off to 1%, and at 100 units it would be at 0.5%. While scaling insurance cost to the number of units deployed is not the most accurate way of predicting the cost, it is still a valid representation. It is unlikely that a 100-unit project would be financed if a high level of technology-related risk is present.

2.3.4 Environmental Compliance (EC) Module

Responsible deployment of MEC devices in estuaries, coastal areas, and rivers requires that biological resources and ecosystems be protected through siting and permitting processes as described by Boehlert et al. 2008 and Dehlsen 2012. Scoping habitats and animal populations at likely MEC deployment locations, collecting baseline environmental data and post-installation monitoring information, and mitigating for impacts all add to the cost of developing each MEC array installation, and hence, adds to the LCOE.

Environmental Compliance (EC) Module expenditures include (at a minimum) costs for:

- Conducting the National Environmental Policy Act (NEPA) process to analyze and evaluate impacts and allow federal agencies to make informed decisions
- Siting and scoping studies
- Pre-installation assessment studies
- Post-installation environmental monitoring

The EC Module identifies environmental constraints related to the site including biological considerations, such as the population, health, and behavior of indigenous species; the quality of aquatic habitats; and the support of ecosystem functions. It also considers physical processes including water circulation, sediment transport, and maintenance of benthic habitats.

National Environmental Policy Act (NEPA)

NEPA (1970) established a national policy that calls for all federal agencies, when planning programs, projects, or issuing permits/grants, to conduct environmental analysis, evaluation, and public reviews prior to making a decision on how to proceed on a proposed action. In a new field such as marine energy development, meeting NEPA mandates and those of many supporting environmental statutes and regulations at the state and federal level will, in most cases, require extensive environmental studies for siting and scoping during the pre-installation decision-making phase (to establish an environmental baseline), and, if the federal action is approved, post-installation efforts that will include the development and application of mitigation strategies, as needed, as well as post-installation environmental monitoring for the project's design life. The extent and duration of each of these study phases will vary with the sensitivity of living resources and waterways at the project site.

Preparing an Environmental Assessment (EA) is a key first step in the NEPA process; large, complex projects (or those deemed to include new technologies) generally require that an Environmental Impact Statement (EIS) be prepared, and will require stakeholder input and multiple public reviews. The NEPA process allows all significant environmental impacts—including impacts to the human environment—to be identified, characterized, and evaluated. The NEPA process is a valuable planning tool that may take several years to complete, and it can be very costly. These NEPA analysis and documents may leverage information from similar, previous studies, where applicable. Initial study costs were calculated (as best estimates) and added to CapEx for NEPA compliance, siting and scoping, pre-installation, and first-year post-installation activities. Ongoing post-installation monitoring (through the design life) costs are added to OpEx.

Until sufficient data exist to anticipate interactions of MEC devices with marine animals and habitats, extensive monitoring is likely to be required during the initial years of deployment, resulting in front-loading of costs in the first five years (Copping and Geerlofs 2011). However, as additional understanding of potential effects is reached following this phase, it is likely that a reduced level of near-field monitoring will be needed for plants, animals, and habitats at risk, and costs are expected to reduce sharply. The goal of long-term monitoring is to determine not only effects on specific animals and habitats, but also to estimate ecosystem risk. Each phase requires individual environmental studies based on regulatory requirements, and the specific marine animals, habitats, and ecosystem processes found at the proposed development location. These studies use information gained from previous NEPA projects, research studies, and other sources of information.

Studying Potential Impacts on Marine Life from MEC Devices

There are concerns over the potential impacts on marine life from the installation of MEC technology and environmental studies are actively being conducted. Areas of interest specific to the introduction of marine energy devices into the environment include: **acoustic** characterization of marine energy devices (as underwater sound can disrupt marine animal communication and navigation [but may also serve to warn animals away from the devices]); measurement of **electromagnetic field** (EMF) output from power cables and rotating devices; **blade strike** of fish, marine mammals, sea turtles, and zooplankton; studies on **migration** patterns and potential disruptive factors of fish, sea turtles, and marine mammals; studies on changes to **habitat** quality and use patterns; **pollution** prevention; and many other issues. Recent studies in these and other areas include the following:

- **EMF:** Fisher (2010) noted that EMF in the marine environment can have both negative and positive effects, but overall, the potential for impact is highest for species that depend on electric cues to detect benthic prey. In his study, Fisher notes there is a significant lack of research into the potential impacts of EMF on sea turtles and marine mammals, although sea turtles do not appear to be as sensitive to EMF as marine mammals. Some Statistical evidence suggests that marine mammals are susceptible to stranding as a result of increased levels of EMF.
- **Habitat:** Inger et al. (2009) looked at the potential benefits of marine renewable energy studying various man-made installations that act as both artificial reefs and fish aggregation devices. Man-made installations have been successfully used to facilitate restoration of damaged marine ecosystems enhancing both biodiversity and fisheries. Currently, the University of Massachusetts is very active in researching the impacts from MEC technology and is working on several DOE-funded projects examining habitat impact. This includes an ongoing study to determine the impact of underwater turbines used for tidal energy production on zooplankton (University of Massachusetts 2013).

- **Accoustic Warning and Potential for Blade strike:** Through a Scottish Association of Marine Sciences study, Wilson and Carter (2013) conducted research on the use of acoustic devices to warn marine mammals of tidal-stream energy devices. As a related analogy, ship strikes of marine mammals are a problem worldwide and, unfortunately, strikes are not uncommon. As a point of reference, for marine mammal strikes from ship traffic (primarily from bows and propellers), Jensen and Silber (2003) compiled a NOAA database recording whale strikes worldwide, and, when reported, the type of vessel and the impact speed (most reported traveling between 13 and 15 knots). With the current lack of data for MEC technology, it is not known if *fixed* underwater turbines will cause injurious mammal-turbine collisions with significant frequency, or if marine mammals, sea turtles, and fish will be able to typically navigate around the devices. Wilson and Carter (2013), who are working on sonic warning devices for underwater turbines, acknowledge that strike scenarios are still conceivable with MEC devices. A team of researchers at Florida Atlantic University (Gerstein et al. 2009) found that acoustic shadowing by a ship's hull may be the primary cause of the numerous whale strikes. Using hydrophones, the team characterized the extent of the parametric acoustical shielded zone where the ship's propeller sounds are blocked. They also noted that a common denominator in whale strikes is that all strikes occur near the surface where the acoustical laws of reflection and propagation significantly limit the ability of marine mammals to hear and locate the sounds of approaching vessels. Further, the only sounds that can be heard in the shielded zone are very low frequency sounds with wavelengths larger than stern dimensions diffracting around the ship's hull to the bow. Gerstein's team noted that whales swimming outside this shadow zone can easily hear the ship's propeller and they swim to avoid it. Gerstein's late partner, Joe Blue, the former Director of the Underwater Sound Reference Detachment of the Naval Undersea Warfare Center and Navy Research Laboratory, conceived of a parametric acoustic alarm to mitigate these acoustic shadow affects. Gerstein et al. point out one thing is clear: marine mammals and other animals cannot react to sounds that become indiscernible from ambient background noise nor can they react to sounds that never reach their ears. While these acoustic shadowing issues are specific to ships and may not apply directly to underwater turbines, the data is still relevant; however, the data to ascertain the level of threat significance from underwater turbines is yet to be established. Wilson and Carter (2013) determined that a sonic warning device for MEC devices must have seven attributes: (1) the signal must elicit an appropriate response; (2) emission rates must suit approach velocities; (3) emission frequencies must be audible for target species; (4) amplitudes must be appropriate for detection ranges and sites; (5) signals must be directionally resolvable; (6) the warning should be coordinated with the threat; and (7) the location of the sound sources at a turbine or within an array must facilitate appropriate spatial responses.

No costs have been assigned for long-term mitigation activities for which environmental risks will be reduced through improved engineering, operations, or siting. If environmental concerns and/or regulatory constraints cannot be satisfied by mitigation strategies and post-monitoring, the device or array must be redesigned (requiring design iteration) or consideration of another device-energy resource site scenario. Environmental constraints may also affect the operational conditions analysis, reducing the potential AEP.

Environmental LCOE Estimates

The EC Module incorporates the methods developed by Copping and Geerlofs (2011) from Pacific Northwest National Laboratory (PNNL) to estimate the contribution of environmental siting and permitting requirements to the costs in LCOE estimates. Environmental studies contribute a significant component of overall LCOE for both pilot- and commercial-scale MEC projects (starting with 10 or more connected devices for a small commercial scale). In addition to the studies themselves, there is a need to account for the costs of data analysis and interpretation, outreach activities associated with engaging regulatory agencies and stakeholders, and the documentation associated with the regulatory processes. Additional costs are also derived from the collection of site-specific information that will assist MEC developers with choosing specific sites for development. Based on the need to account for these costs, Copping and Geerlofs (2011) developed a set of logic models that are driven by regulatory requirements, as well as processes for collecting data that support the regulatory processes and the needs of the project developer. These logic models describe the expected studies for siting and permitting MEC devices, driven by the siting and regulatory processes that require those studies. Each study and environmental permitting process has been assigned a cost derived from various data including: 1) existing and proposed MEC projects; 2) scaling factors that allow projections from single devices (pilot scale installations) to larger commercial arrays; 3) projections for future post-installation monitoring costs; and 4) expert opinion. Cost estimates for pilot-scale projects as well as small and large commercial-scale projects have been developed. A range of costs is presented for each type of study and regulatory requirement to reflect the significant uncertainty that results from the generic nature of the reference model site and MEC device. Cost estimates were reviewed by DOE's Wind and Water Power Technologies Program staff, researchers, and consultants familiar with MEC environmental permitting processes. Details of their methods can be found at http://energy.sandia.gov/rmp.

2.3.4.1 Logic Models for Assessment of Environmental Costs

The logic models[8] of Copping and Geerlofs (2011) are applied to determine the individual studies required during siting and permitting based on site characteristics and regulatory concerns.

The logic models and all environmental studies and related costing information are parsed into four stages:

1) NEPA and administrative process;

2) Siting and scoping;

3) Pre-installation assessment; and

4) Post-installation monitoring.

Each of these development stages has costs associated with it. While the specific technology and site will have a major influence on the costs for any project, there are many commonalities

[8] A logic model (also known as a logical framework, theory of change, or program matrix) is a tool used most often by managers and evaluators of programs to evaluate the effectiveness of a program. http://en.wikipedia.org/wiki/Logic_model

driven by regulatory requirements and information needs across the RM projects. Copping and Geerlofs (2011) derived cost ranges from the best available information on existing and planned MEC projects, consultation with developers and the consultants supporting them, and the best professional judgment of researchers and natural resource management agency staff. Costs for each of the RM1, RM2, and RM3 studies and processes were developed from pilot projects. However, for RM4 (Ocean Current Turbine), there are no projects in the water or in advanced stages of planning from which PNNL could begin the costing process, and, therefore, costs were extrapolated from the previous three models as will be described in Section 6.3.4. The environmental related costs for each of the RMs are then extrapolated for small (10 devices) and large (> 50 devices) commercial development arrays. While the size of a pilot project differs from one technology and location to another, in general, pilot projects are those in which the generation capacity totals less than 5 MW, and could be deployed for up to five years (FERC 2008). To date, there are only a small number of pilot projects under development in the U.S., and even fewer in the water. Copping and Geerlofs (2011) developed a set of scaling rules to extrapolate from pilot project costs to those of small commercial scale, and to large-scale commercial projects. Costing information, developed for the early stage of pilot projects, relies on information from on-going expenditures from U.S. projects. Post-installation monitoring costs are more speculative as no monitoring programs have been fully implemented to date.

The NEPA phases of the project, siting and scoping, pre-installation, and initial post-installation activities contribute to the capital cost (CapEx) of the project. Post-installation monitoring continues for the duration of the project and contributes to the annual operations and maintenance costs (OpEx); the first few years of post-installation are assumed to require an extensive set of studies, followed by a reduced level of near-field monitoring for animals and habitats at risk, and periodic special studies including those that examine far-field effects, to estimate the larger ecosystem risks.

2.3.4.2 NEPA and Administrative Process

Each stage of study development (scoping and siting; pre-installation assessment; post-installation monitoring) requires documentation and adherence to processes designed to meet regulatory requirements. These include conducting public/stakeholder meetings, filing necessary permitting paperwork, and performing periodic checks with government agencies. Each of these processes has a cost associated with it, and has been accounted for in our costing estimates. This category was developed with the understanding that NEPA acts as a broad regulatory umbrella; it was assumed that almost all of the siting and permitting processes that drive costs at the state and federal level are included under NEPA. However, there certainly may be other site-specific environmental permits, management plans, and regulations beyond the immediate purview of the NEPA permitting process that will be applicable to the project as it moves forward, and the cost of such additional requirements are not estimated in detail here.

2.3.4.3 Siting and Scoping

Once a potentially viable hydrokinetic site has been identified, a developer conducts feasibility investigations of the power resource potential and other information, such as bathymetry, slope and distance to port, to support siting devices in specific locations. A scoping process is undertaken to identify the environmental issues of concern including the presence of sensitive species and depleted populations and to determine if there are conflicting uses for the site. Necessary components of the scoping process include community outreach to ensure that stakeholders have a voice in determining environmental and competing use issues and to gain the trust of local leaders and the public through the open sharing of ideas. At the same time, project developers must work with regulatory agencies to determine what requirements they need to meet for pre-installation environmental assessment and post-installation monitoring. Each of these studies and processes has a cost associated with it that has been derived from the range of investments made by developers in the U.S.

2.3.4.4 Pre-installation Studies, Analysis and Documentation

After choosing a site, working with local stakeholders, and determining the requirements in conjunction with government agency staff, each developer must design and carry out the necessary site studies, analyze and interpret the data, and document the process under the existing regulatory authorities. Pre-installation studies (also frequently referred to as a baseline assessment) for hydrokinetic energy projects will differ from one another, and site-specific and technology-specific differences will have a major influence. Sample collection and analysis, data analysis and interpretation, quality assurance and quality control, and documentation for regulatory purposes are needed for each study. At this stage, developers must also carry out more detailed resource assessment studies and surveys to locate high-power density zones where individual devices should be deployed (micro-siting).

Closely associated with baseline assessment is the examination of potential conflicts with other resource users and/or concerned stakeholders that may include some of the following:

- Commercial fisheries (NOAA Fisheries)
- U.S. Military (impacts to marine installations, navigation, and operations)
- Commercial navigation
- Flood damage reduction
- Historic preservation
- Animal and ecosystem protection (NOAA, USFWS, and other agencies)
- Local community interests
- Recreational use assessment (required under Federal Energy Regulatory Commission [FERC])

The costs for investigations in these areas are included in the LCOE estimates.

In almost all cases, the environmental areas listed in Table 2-3 will be required by federal and state statutes. Environmental sample collection, observation, and analysis; data management and interpretation; quality assurance and quality control; and documentation for regulatory purposes, will be needed for each study.

Table 2-3. Pre-installation and environmental concerns that are likely to require studies and analysis to meet regulatory needs.

Environmental Concern	Elements of Concern/Studies Needed	U.S. Regulatory Driver
Species under special protection	Aquatic animals under threat of extinction	Endangered Species Act
Marine Mammals	Concern and special societal value afforded to specific groups of animals	Marine Mammal Protection Act
Migratory Birds	Birds that migrate across regions and continents and considered at risk	Migratory Bird Treaty Act (international treaty)
Important fish and shellfish populations	Fish populations of commercial, recreational, or cultural importance	Magnuson Stevens Fishery Conservation, Management Act (protects critical habitats and fish populations)
Habitats	Need to assess quantity and quality of habitat, due to important role in supporting marine species	Magnuson-Stevens Fishery Conservation and Management Act, and other federal and state regulations
Water Quality	Cumulative degradation of water quality (dissolved oxygen [DO], nutrients, human benefits), changes in sediment transport (affecting habitats and shore forms)	Clean Water Act and state equivalents

2.3.4.5 Post-installation Studies, Analysis and Documentation

Post-installation monitoring studies should be derived from the findings of pre-installation studies, existing baseline data, and other published information from relevant field and laboratory studies. For small (pilot) projects, most concerns are likely to focus close to the devices—wave energy converters or current turbines (nearfield); focusing on the potential for animals colliding with devices (e.g., blade strike) or becoming entangled in mooring lines; as well as potential effects of noise during construction (e.g., pile driving). Noise emitted from the devices during operation, and EMF emitted from cables and devices can be disorienting or cause physical harm. As the size of the array increases, regulations are likely to require that studies include those areas focused further from the devices (farfield), including assessments of biological processes such as food web effects, changes in water quality and sediment transport, and effects on marine populations and communities. While site- and technology-specific differences will drive the details of such studies, in general there is likely to be a common set of requirements (Table 2-4). As was done for pre-installation studies, sample collection and analysis, data analysis and interpretation, quality assurance and quality control, and documentation for regulatory purposes are costed for post-installation monitoring.

Table 2-4. Post-installation monitoring studies for ocean current project development

Target of Study	Project Scale	Type of Study	Reason for the Study
Marine Animals	Pilot and Commercial	Nearfield monitoring	Strike, entanglement, aggregation effects, avoidance effects
Fish, pelagic invertebrates	Pilot and Commercial	Nearfield monitoring	
Migratory birds, diving birds, seabirds	Pilot and Commercial	Nearfield monitoring	
Sea turtles	Pilot and Commercial	Nearfield monitoring	
Benthic invertebrates	Pilot and Commercial	Underwater survey	Periodic survey and sampling to determine effects
Acoustics of the device	Pilot and Commercial	Noise coming off ocean current turbines	Change in acoustics over time: damage, harassment of marine mammals, sea turtles, fish, diving birds
Seabirds	Commercial	Ecosystem effects	Changes to pre-installation population status, fitness, food availability and preference, reproductive success
Marine mammals	Commercial	Ecosystem effects	
Fish, pelagic invertebrates	Commercial	Ecosystem effects	
Sea turtles	Commercial	Ecosystem effects	

Post-installation environmental monitoring costs are assumed to be higher in the first few years (Copping and Geerlofs 2011), and therefore initial start-up costs for these studies are included in CapEx. Costs for further monitoring, which will be considered under OpEx, are expected to be at a lesser amount.

2.3.4.6 Scaling Pilot Project Costs to Commercial Scale

Cost estimates for permitting and siting at a small (10 devices) and large (greater than 50 devices) commercial-scale were extrapolated from costs determined for pilot-scale projects. Cost estimates assume that a pilot permitting process, associated studies, and short-term deployment have already taken place in the project area prior to development at the commercial scale. Cost estimates for commercial-scale are for additional costs beyond the pilot study. If a developer does not follow the pilot process but goes directly to a commercial scale project (which is allowed under the FERC process), an estimate of the commercial costs for environmental siting and permitting can be derived by summing the pilot and commercial estimates.

Translating costs from pilot- to commercial-scale followed a number of assumptions:

- Pre-installation environmental studies carried out at the pilot-scale focus on population and behavioral assessments to measure potential direct effects to species of concern (e.g., fish, seabirds, sea turtles, and marine mammals) in order to establish a baseline for post-installation monitoring. Information gathered from these pilot studies will inform the commercial-scale and, therefore, studies may not need to be repeated; however, supplemental baseline information may be required as the project footprint increases.
- At commercial-scale, additional pre-installation studies may focus on understanding ecosystem effects from arrays. These would be additional studies beyond those carried out at the pilot-scale.
- The threshold between a small and large commercial array cannot be viewed as absolute, and must be determined on a site-specific basis. We have chosen thresholds appropriate for the reference sites we are working at, based on the overall guidance generated by the DOE reference model team.

In addition to the assumptions that lead from pilot to commercial-scale cost estimates, PNNL developed a set of “scaling rules” shown in Table 2-5 to allow for consistent comparison between changes in study costs from pilot to commercial scale. This consistency allows for relative comparison, which is useful considering the uncertainty in cost estimates.

Table 2-5. PNNL's rules for scaling environmental study costs from pilot to commercial-scale projects.

Scaling Rules	Explanation	Example
Covered in pilot	Information need was covered under the pilot project licensing process. Additional funds are likely not needed for studies at the commercial scale.	Desktop studies for initial determination of economic and environmental feasibility. This information would carry over directly into commercial-scale.
Continuing costs	Recurring costs that continue from pilot into commercial-scale permitting processes.	Near-field monitoring studies may continue from pilot to commercial-scale, though the expectation is that pilot near-field monitoring studies may answer many of the questions required for commercial installation, so commercial costs may be at a lower level.
Incremental increase	Additional costs associated with larger footprint of a commercial-scale project. Cost increase likely to be marginal, incremental, and linear.	Resource assessment—larger project footprint may require procurement and deployment of additional acoustic Doppler current profilers (ADCPs), acoustic Doppler velocimeters (ADVs), or other instruments, incrementally higher equipment costs and additional ship days above what would be expected for a pilot-scale project.
Multiplicative cost increase	Significant study cost increases as scale of project goes from pilot to commercial, and regulators require greater understanding of system or basin effects. Cost increase likely to be more than double the cost at the pilot-scale and may increase in a non-linear fashion.	Habitat surveys and mapping may be expected to have a multiplicative cost increase if there is a large increase in footprint from pilot to commercial-scale, or if a far-field habitat baseline survey is required.
Additional study	Larger scale projects may require studies that are in addition to those required for a pilot project.	Far-field or ecosystem monitoring—pre-installation studies that characterize valued species (fish, birds, marine mammals, etc.) will be needed at up to the basin-scale. If effects of a commercial project are considered to extend beyond the near-field, or if regulators require "Before-After Control-Impact" (BACI)-style monitoring in the post-installation phase, completely new studies may be required.

Siting and scoping costs at commercial-scale will increase incrementally over pilot-scale costs, as the footprint of the MEC array increases. However, these costs will remain a relatively small fraction of total costs.

Pilot scale pre-installation studies may satisfy many of the regulatory needs at the commercial-scale; however, commercial scale projects may raise new questions about far-field or ecosystem effects, and, as a result, additive studies may be necessary to assess baseline health for species of concern. Detailed hydrodynamic modeling may also be needed to inform array siting and to understand potential water quality and sediment transport effects. Finally, habitat mapping costs could cause multiplicative cost increase when device numbers cross a threshold where far-field effects might be expected. This could lead to regulatory requirements for habitat mapping and assessment of a much larger area than that immediately adjacent to the array and associated infrastructure.

2.4 LCOE Calculation

The levelized cost of energy (LCOE) is a standard metric that can ideally be used to compare similar energy generation projects. It provides a uniform approach to assessing the diverse set of MEC technologies considered both in this RMP and throughout the industry. It reflects the expected AEP of the device and all costs that are expected to be incurred over its design life (from development through decommissioning), including capital costs, operations and maintenance costs, and financing costs (represented here by a fixed charge rate [FCR]).

The methodology presented in this report aims to facilitate a more transparent approach to calculating, presenting, and comparing LCOEs. There are a variety of assumptions embedded in the many costs for a MEC device or array, and the assumptions within a given LCOE estimate can vary significantly. Without adequate transparency into these assumptions, a uniform assessment across multiple MEC technologies (or even across multiple devices of the same device type) is difficult. Further complicating these comparisons, given the nascent stage of the industry and the varying levels of technological maturity, the amount of detailed cost data and numerical model validation is limited.

2.4.1 Cost Breakdown Structure (CBS)

To enable transparency in LCOE estimates, the U.S. DOE developed a standardized cost and performance data reporting process[9] (LaBonte et al. 2013). A key aspect of this reporting process is the use of a standardized cost breakdown structure (CBS) [10] to collect and organize all cost data, including both capital expenditures (CapEx) and annual operating and maintenance expenditures (OpEx).

[9] As of April 30, 2013, the draft LCOE reporting guidance is available for review and comment: http://en.openei.org/community/document/mhk-lcoe-reporting-guidance-draft

[10] As a functional tool for cost data collection and organization, the CBS was developed as an Excel spreadsheet and is designed to accommodate any level of data granularity. For any given device or array, all available cost data can be organized within the CBS, even though many of the cost items at the more detailed levels of the CBS might be blank until more detailed costs become available.

The CBS is a hierarchical system for categorizing and itemizing the costs associated with MEC project development. The scope of the CBS covers all project lifetime expenditures including project design, permitting, equipment purchases, O&M, and decommissioning of the installation. A CBS is not an exhaustive list of all project costs, but a comprehensive classification of majors cost categories.

The hierarchy in the CBS consists of six levels, where level zero is the main project from which all other cost levels stem. Level 1 is very general (in a MEC project: capital expenditures and operating expenditures) and each subsequent level in the hierarchy is increasingly specific. CapEx are those costs associated with activities prior starting MEC energy operations, and OpEx are those costs associated with operating and maintaining the MEC array including ongoing environmental monitoring.

The draft CBS published by DOE, from the work done by LaBonte et al. (2013) to standardize cost and performance reporting for MHK technologies, was developed to be sufficiently general to accommodate cost data from a variety of MHK (MEC) technologies, while still allowing for device customization at the detailed levels. As a result, the more detailed levels of the CBS (particularly levels 4 and 5) may contain elements that are device-specific. Figure 2-2 shows DOE's full CBS down to the third level, which will generally be applicable to any MEC technology.

LaBonte et al. (2013) provides a draft CBS with examples down to the fifth level for a specific MEC device; as an example, for structural costs (level 3), the level 4 costs include: air chamber, buoyancy plate, buoyancy tank, cross arm, cross bridge, device access, duct shell, fairing, flap, frame, nacelle or shell, pile, primary energy capture device, pontoon, powertrain enclosure/mounting frame, reaction plate, vertical column, and wing. For PCC costs (at level 3), level 4 costs include: generator, drivetrain, converter, gearbox and driveshaft, hydraulic system, step-up transformer, energy storage, riser cable, cylinder, accumulator, seals, control system, bearings and linear guides, mounting (machine/pipe foundations), filters, and PCC. At this level of detail, cost categories are expected to vary across technologies and even across devices within the same technology. The draft CBS is available via OpenEI.org [11].

The organization of relevant cost data and the LCOE analyses for our individual RM assessments (RM1 through RM4) were completed prior to the completion of DOE's draft CBS (LaBonte et al. 2013). Therefore, although we used a CBS to organize our relevant cost data for each RM, we did not use DOE's the exact CBS as described by LaBonte et al. (2013) above. The generic CBS used for RM1 through RM4 in our study is shown in Figure 2-3. A side-by-side comparison[12] of the DOE draft CBS and the CBS used for our RM assessments shows that the organization and specific terminology is somewhat different. However, these differences for how particular costs are categorized do not affect the types of cost data that are reported, nor do they affect the calculation of LCOE. For future RM assessments, we expect to adhere to DOE's proposed CBS for consistency, rather than the structure used herein for the first four RM assessments.

[11] As of April 30, 2013, the draft CBS spreadsheet is available for review and comment: http://en.openei.org/community/files/generalized.cbs_.draft_mhk_april.10.2013.xlsx
[12] A side-by-side comparison is available on OpenEI.org: http://en.openei.org/community/files/doe.draft_.cbs_comparison.to_.rm_.cbs_.xlsx

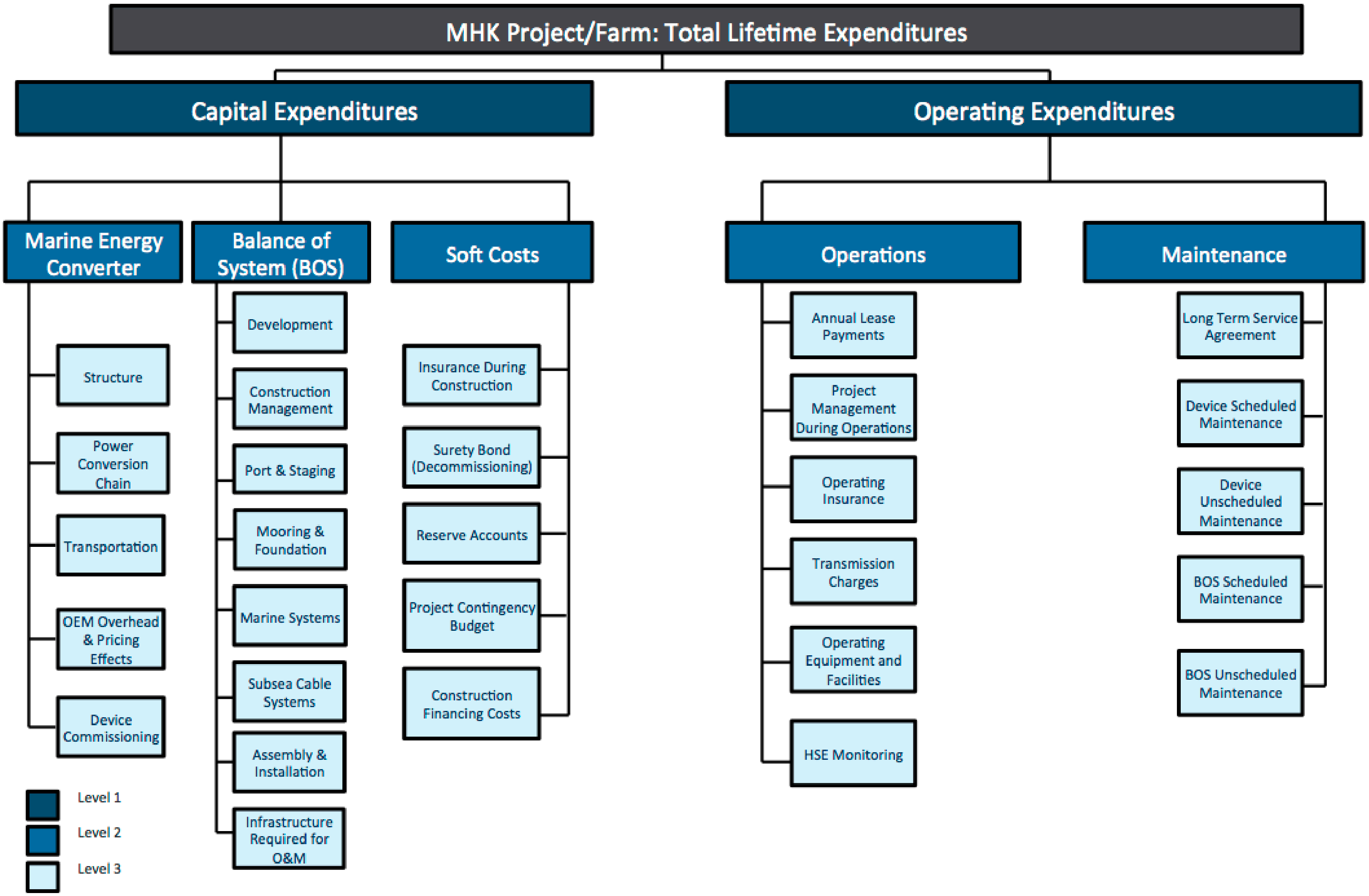

Figure 2-2. DOE's MHK Cost Breakdown Structure (CBS) for MHK technologies to Level 3.

NOTE: Chart from LaBonte et al. (2013). In this report, we adopt the terminology MEC which is equivalent to MHK (Marine Hydrokinetic) used in LaBonte et al. (2013).

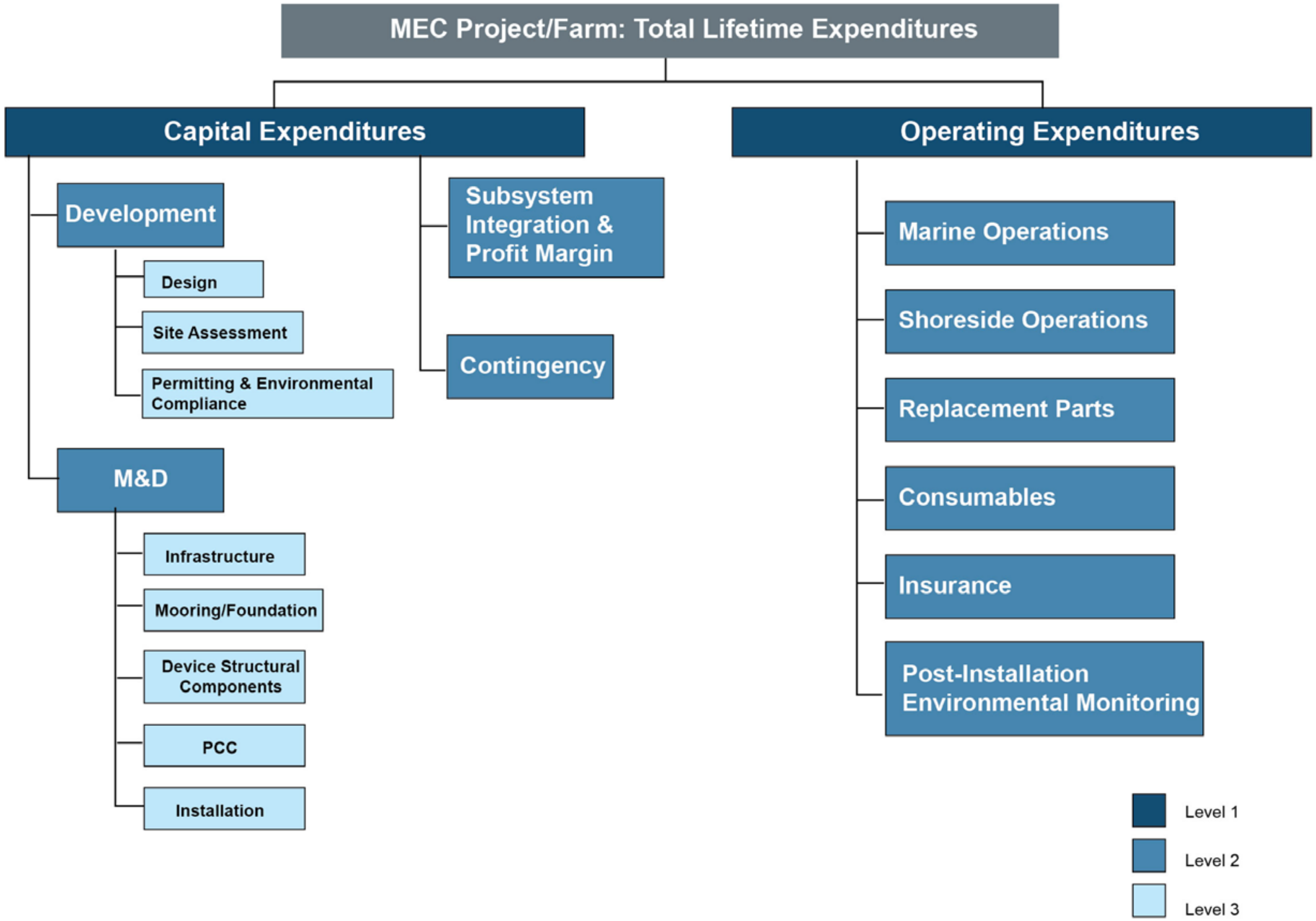

Figure 2-3. RMP team's Cost Breakdown Structure for RM1 through RM4 to Level 3.

As shown in Figure 2-3, the two major categories of the CBS, CapEx and OpEx, are two of the four key parameters used to calculate LCOE. The specific cost estimates for each cost category in the CBS were developed based on:

- Estimates generated by the team's subject matter experts using design metrics and engineering judgment;
- Vendor quotes for materials and components; and/or
- Public domain sources.

Notable costs captured in the D&A Module, M&D Strategy Module, EC Module and O&M Strategy Module are described in previous sections. Detailed cost estimates for all cost categories in the CBS are available within each RM's CBS spread sheet model on the Sandia National Laboratories Energy, Climate, and Infrastructure Security website: http://energy.sandia.gov/rmp

Our generic CBS (Figure 2-3) was applied to RM1 through RM4 for scales of 1, 10, 50, and 100 MEC units. These different scales capture the effects of multi-unit deployment and their related cost improvements, but they do not capture any potential improvements in the design itself that would likely occur as a developer gains experience. As such, it is simply captures the economies of scale of each reference design with respect to lifecycle cost and device performance.

2.4.2 LCOE Definition and Equation

The key parameters required to estimate LCOE are: CapEx, OpEx, fixed charge rate (FCR)[13], and AEP. As indicated in the methodology flow chart, Figure 2-1, CapEx is primarily an output of the M&D Strategy Module, OpEx is primarily an output of the O&M Strategy Module, and AEP is derived from output from both the O&M Strategy Module and the D&A Module. The Environmental Compliance (EC) Module also contributes both CapEx and OpEx costs.

It should be noted that although the financial parameters that make up the FCR (applicable to CapEx) are an important part of a final LCOE calculation, they reflect assumptions about the future market and the cost of capital, and therefore, introduce a higher level of cost uncertainty. Therefore, in order to focus on key technical cost *drivers*, our methodology emphasizes the *process* of calculating CapEx, OpEx, and AEP.

[13] FCR is the annual amount per dollar of initial capital cost required to cover the capital cost, a return on debt and equity, and various other fixed charges; the FCR calculation is based on the discount rate, the present value of depreciation, and the effective tax rate.

Per Short et al. (1995) LCOE is calculated as:

$$LCOE = \frac{CapEx * FCR + OpEx}{AEP} \tag{2-1}$$

Where,

- *LCOE* (\$/kWh), levelized cost of energy;
- *CapEx* (\$), installed capital costs, represents all capital expenditures associated with the planning (including environmental studies), design, manufacturing, deployment, and project management of a MEC array;
- *FCR* (%), fixed charge rate, is the annual return, represented as a fraction of installed capital costs needed to meet investor revenue requirements;
- *OpEx* (\$)**,** annual operations and maintenance (O&M) costs, includes all routine maintenance, operations, and routine post installation environmental monitoring activities (i.e., non-depreciable costs); and,
- *AEP* (kWh), annual energy production, describes the average annual energy generated (after accounting for device or array online availability) and delivered to the point of AC grid interconnection (i.e., the measurable basis for power purchase contracts).

As noted above, CapEx refers to all project expenses incurred prior to operation of the device or array, including hard costs (e.g., equipment, materials, installation, and salaries) as well as soft costs (e.g., contingency, reserve accounts, and other financial instruments). At this level, the details of the design heavily influence the corresponding estimate of CapEx. For example, the structural design influences the material and labor costs associated with manufacturing the device. Likewise, the structural design and site conditions affect the mooring design, which dictates the type(s) and length(s) (and therefore costs) of mooring lines and anchors required. Similarly, different power conversion chain (PCC) choices will have different cost implications.

OpEx refers to all annualized expenditures required to operate and maintain the system to ensure availability over the entire project life. The details of the design (and the characteristics of the deployment location) will heavily influence OpEx. Just as the different power conversion chain (PCC) technologies have different upfront costs, they also require different operations and maintenance strategies. Different device structural designs will also require different operations and maintenance strategies; some designs allow for all maintenance to be conducted in situ, yet other designs could require the entire device (or a specific section of the device) be disconnected and towed back to shore (or a maintenance port) for repairs. These types of differences, which distinguish one device design from another, affect the overall annualized OpEx estimate for a particular device.

Generally, OpEx costs are comprised of operation-related costs such as facility management and insurance and maintenance-related costs, which will include both scheduled and unscheduled repairs. For RM1 through RM4, maintenance costs are calculated based on the estimated number of annual failures (and necessary repairs) for each device. The emphasis of this report is on understanding how the available marine resource and key technology drivers affect LCOE. To better isolate technology and resource specific cost drivers, we applied the same set of assumptions about operations costs to all four reference models, including the cost of shore-side labor and the cost of insurance. We assumed that insurance costs, detailed in Section 2.3.3.4, are driven primarily by the perceived risk of a particular technology or array. As described in that section, we assume insurance rates drop to 1% for 50 units and 0.5% for 100 units.

Within the equation for LCOE (Eq. 2-1), a fixed charge rate (FCR) is used to represent the total cost of financing. It is the annual amount per dollar of initial capital cost required to cover the capital cost, a return on debt and equity, and various other fixed charges; the FCR calculation is based on the discount rate, the present value of depreciation, and the effective tax rate. We do not provide a methodology for selecting the parameters used to calculate FCR. To better isolate technology- and resource-specific cost drivers, we calculated LCOE using a consistent set of parameters across all RMs. The default values shown in Table 2-6 are presented in DOE's "Standardized Cost and Performance Reporting for Marine and Hydrokinetic Technologies" (LaBonte et al. 2013). As discussed above, we completed our analyses for RM1 through RM4 prior to the issuance of the new DOE costing guidance developed by LaBonte et al. (2013). The key financial parameters used to calculate the FCR (11.3%) used for our LCOE estimates for RM1 through RM4 are listed in Table 2-7.

Table 2-6. Standardized financial variables.

Symbol	Variable	Standard Value
r	Real discount rate (i.e. real WACC[14])	.07
i	Inflation rate	.025
τ	Composite federal-state tax rate	.396
D	Present value of depreciation tax shield	.309
N	Project economic life	20 Years
FCR	Fixed charge rate	10.8%[15]

[14] Weighted Average Cost of Capital

[15] The approach to calculating FCR used for Reference Models 1 through 4 (Re Vision 2011) was slightly different than that presented in (Eq. 2-3), so even though the values of several parameters are the same (e.g., project life and federal tax rate), several parameters differed from those presented in Table 2-6 and the FCR used for Reference Models 1 through 4 was slightly different: 11.3%. While the FCR value will affect the final estimate of LCOE, resulting differences in LCOE estimates are due only to differences in financial assumptions, not the technology itself or the marine resource.

Table 2-7. Financial parameter assumptions used in RM1 through RM4 analyses.

Project Economic Life (years)	20
Federal Tax Rate	40%
State Tax Rate	0%
Effective Tax Rate	40%
Construction Finance Rate	8%
Construction Time	2.0 years
Equity	50.0%
Return on Equity / Internal Rate of Return (IRR)	10.0%
Debt	50.0%
Return on Debt	8.0%
After Tax Weighted Average Cost of Capital (WACC)	7.25%
Fixed Charge Rate (FCR)	11.3%
Tax Assumptions: 1. No Investment Tax Credit (ITC) or Production Tax Credit (PTC) 2. 5 year MACRS	

Present value of depreciation, *D*, is calculated as:

$$D = \tau \times \sum_{t=1}^{t=6} \frac{MACRS_t}{(1+r)^t * (1+i)^t} \qquad (2\text{-}2)$$

and fixed charge rate is calculated as:

$$FCR = \frac{r}{1-\frac{1}{(1+r)^N}} \times \frac{1-D}{1-\tau}. \qquad (2\text{-}3)$$

$MACRS_t$ (Modified Accelerated Cost Recovery System) in Equation (2-2) represents the particular value for depreciation in year *t* according to the $MACRS_t$ table published by the Internal Revenue Service (IRS). We opted to use these default values because, as previously mentioned, the emphasis of this report is on modeling and understanding how key technology and resource drivers affect LCOE. A simple sensitivity analysis around the financial assumptions would illustrate the impact of these assumptions on LCOE. One approach would be to adjust the FCR directly (for example, changing FCR from 10.8% to 10.3% or 11.3%); another would be to modify assumptions about specific parameters such as the discount rate or inflation rate. We did not perform this type of sensitivity analysis for this RMP study.

2.5 Uncertainty

We used the uncertainty matrix shown in Table 2-8 to qualitatively evaluate the accuracy analyzing the device performance, structural design, PCC design, site resource (physical and environmental), and economics. Categorical levels of uncertainty (low, medium, high, or very high) were assigned for each of these analyses.

- **Low uncertainty** was assigned to the analyses if: 1) the numerical models for hydrodynamic and structural design and analysis were validated; 2) models for the PCC design were validated, or 3) costs of original equipment manufacturer (OEM) parts were validated, or actual data was available for resource assessment and costs.
- **Medium uncertainty** was assigned if the numerical models for hydrodynamic and structural design and analysis were not validated and if the PCC design was not validated—in other words, validated numerical models (not actual data) were used for resource assessment or costs were based on model simulations.
- **High uncertainty** was assigned when engineering judgment was used for device performance and for the structural and PCC design, as well as for resource assessment. The uncertainty of cost estimates is also high if they are based on renewable energy analogues.
- **Very high uncertainty** was assigned if no analysis was performed for design, resource assessment, or cost estimation.

In addition to evaluating the uncertainty for the analyses undertaken for RM design, analysis, and economics, a more detailed assessment of cost uncertainty was performed for CBS categories in CapEx and OpEx. As described under 2.4.2, for CapEx, these categories include costs for development, infrastructure, foundation/mooring, device structural components, PCC fabrication, installation, subsystem integration and profit margin, contingency, decommissioning, and pre-installation environmental studies. For OpEx these costs include marine operations, shoreside operations, replacement parts, consumables, insurance, and post-installation environmental monitoring. Similar to the uncertainty matrix in Table 2-8, categories are assigned uncertainty levels of low, medium, high, or very high based on the amount of actual analysis or data available. Results of this uncertainty analysis are discussed in Chapter 7

Table 2-8. Uncertainty matrix for RM design, analysis and LCOE estimation.

Uncertainty	Device Performance	Structural Design	PCC Design	Hydrokinetic Resource	Environmental Compliance	Economic*
Low	Validated model	Validated model	Validated model or OEM parts	Actual data	Actual data	Actual data
Medium	Model simulation, no scaled test or field data	Model simulation, no scaled test or field data	Model simulation, no test data	Validated model	Validated model	Model simulation, no supporting data
High	Engineering judgment	Engineering judgment	Engineering judgment	Engineering judgment	Engineering judgment	Economic assumption based on similar renewable resource
Very High	Issue not addressed	Issue not addressed	Issue not addressed	Issue not addressed	Issue not addressed	Issue not addressed

*NOTE: Includes infrastructure, installation and operation and maintenance costs.

3 Reference Model 1 (RM1): Tidal Current Turbine

3.1 RM1 Description

The RM1 device is a dual variable-speed variable-pitch (VSVP) axial-flow tidal turbine device, designed for the Tacoma Narrows tidal current energy resource site in Puget Sound, Washington. The concept design for the RM1 device, illustrated in Figure 3-1, was inspired by the SeaGen system (http://www.seageneration.co.uk/). RM1 comprises a monopile foundation and a cross-arm assembly to mount the two rotors. The cross-arm assembly is nearly neutrally buoyant so the attached rotors can be recovered and redeployed with a minimal amount of lifting crane capacity; therefore, the design minimizes the handling requirements during deployment and recovery, which reduces overall cost in all O&M activities including access to the power conversion chain (PCC).

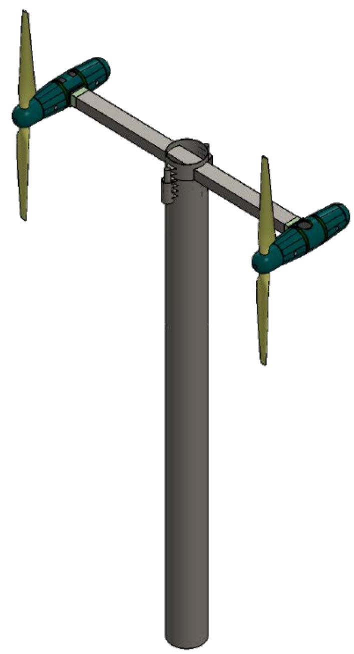

Figure 3-1. RM1 device design.

The dimensions of the RM1 device are illustrated in Figure 3-2. The site deployment depth (assumed to be uniformly 50 m deep for modeling purposes) permitted a rotor diameter of 20 m. The dual rotors on each unit are offset by 28 m from each rotor centerline. The total width of the device from blade tip to tip is therefore 48 m. The rotor centerlines are submerged 20 m (one rotor diameter) below the free surface to reduce cavitation potential and are positioned one and a half diameters (30 m) above the seabed to reduce boundary layer effects that can cause velocity, turbulent shear, and loading asymmetries across the rotor. The tower height is 45 m, with an embedment depth of 15 m.

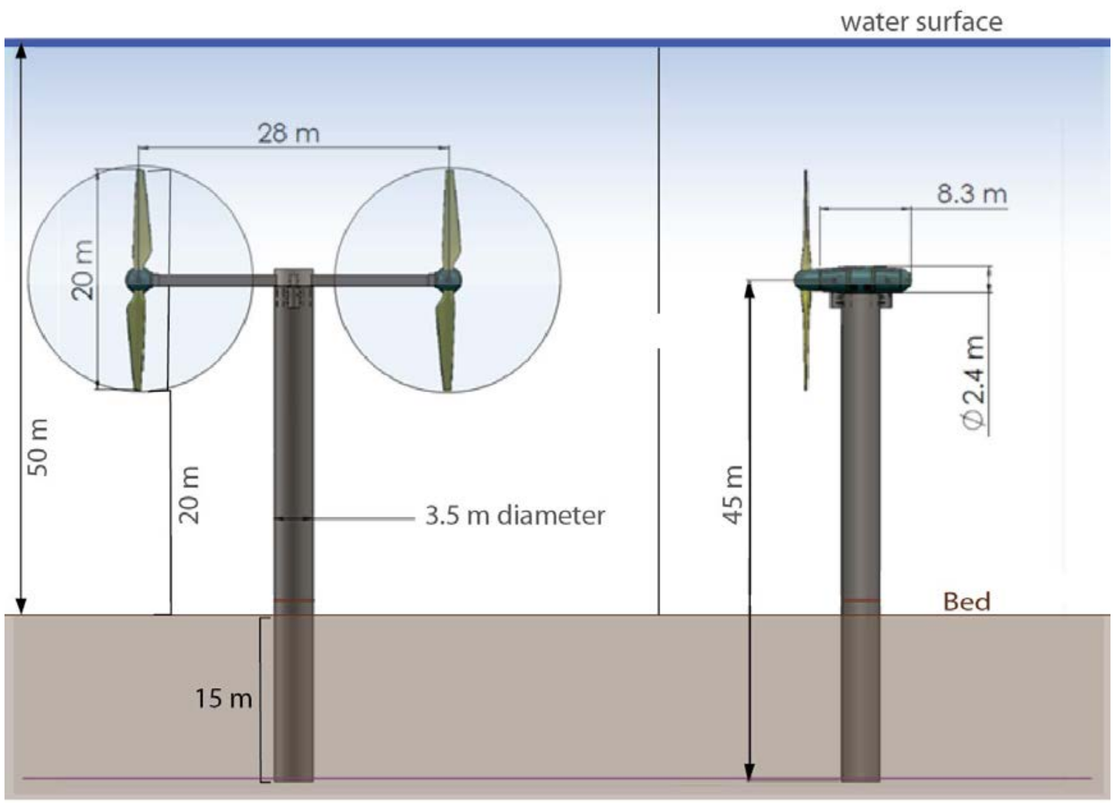

Figure 3-2. RM1 device profile and plan views dimensions.

3.1.1 Device Design and Analysis

As noted in Design Methodology for a Single Device, Section 2.1.1, the first step in the device design process was to develop a conceptual design appropriate for the modeled reference resource site. Once the conceptual design was completed, we refined designs using simulation tools originally developed for design and analysis of wind turbines. For the RM1 design and analysis, we leveraged methods and tools developed for designing and analyzing horizontal axis wind turbines (HAWT). The rotor for the concept device was designed and optimized using HARP-Opt (http://wind.nrel.gov/designcodes/simulators/HARP_Opt/) and WT-Perf (http://wind.nrel.gov/designcodes/simulators/wtperf/). Lawson et al. (2013, in preparation) provides more details on this modeling. The WT_Perf model, which was validated with measurements from scaled testing of a single rotor at the U.S. Naval Academy (Luznik et al. 2012), was used to simulate power performance characteristics for the turbine. These results were integrated with the reference resource site's current frequency histogram to estimate the annual energy production (AEP). Additional model validation data will be collected during scaled testing of the complete dual-rotor turbine in early 2014 at St. Anthony Falls Laboratory (SAFL) using their open-channel flume as described in Neary et al. (2012b). We estimated extreme hydrodynamic loads to evaluate the structural and PCC designs using Blade Element Momentum Theory (BEMT) code calculations and computational fluid dynamics (CFD) simulations.

3.1.2 Arrays: Design and Analysis

As noted in Section 2.1.1, due to the lack of developed array optimization models, we did not perform the detailed array design and analysis described in the general methodology. This adds to the uncertainty in the AEP estimate for arrays. However, we do lay out a hypothetical array for the reference site. The configuration for the RM1 array is depicted in Figure 3-3. Devices were separated in the longitudinal direction by 400 m (20 rotor diameters). With 20 rows, the longitudinal dimension of the array footprint for the 100-unit array is approximately 7600 m, which is the length of the trunk cable. The number of units in a row and their lateral spacing was dictated by the width of each unit (48 m) and the flat bottom width of the tideway (700 m). With five units in each row, the lateral spacing between units is 115 m, which is almost 2.5 times the width of each dual-rotor unit.

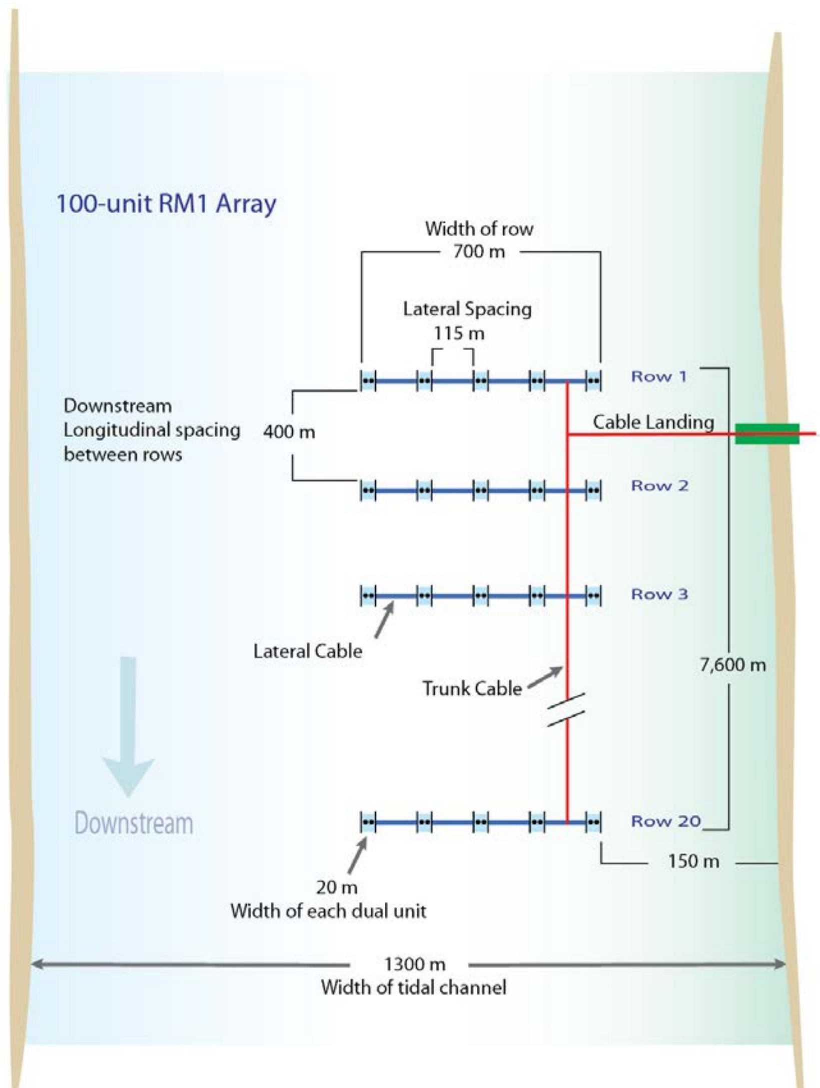

Figure 3-3. Array layout and subsea cabling (plan).

.

The total array capacity at 100 units is approximately 110 MW. We selected a 3-phase AC transmission cable with a voltage level of 30 kilovolts (kV). All transmission cables included fiber optic lines to allow communication from each device to shore. Cable landing is accomplished by directionally drilling a conduit that connects the cable out to the first row of devices. This approach minimizes installation and maintenance costs.

3.2 Module Inputs

3.2.1 Site Information

The reference tidal current energy resource for RM1 was developed from site information on the Tacoma Narrows tidal site in Puget Sound, Washington as summarized by Polagye (2011b). Figure 3-4 shows the water depth profile for the Tacoma Narrows site.

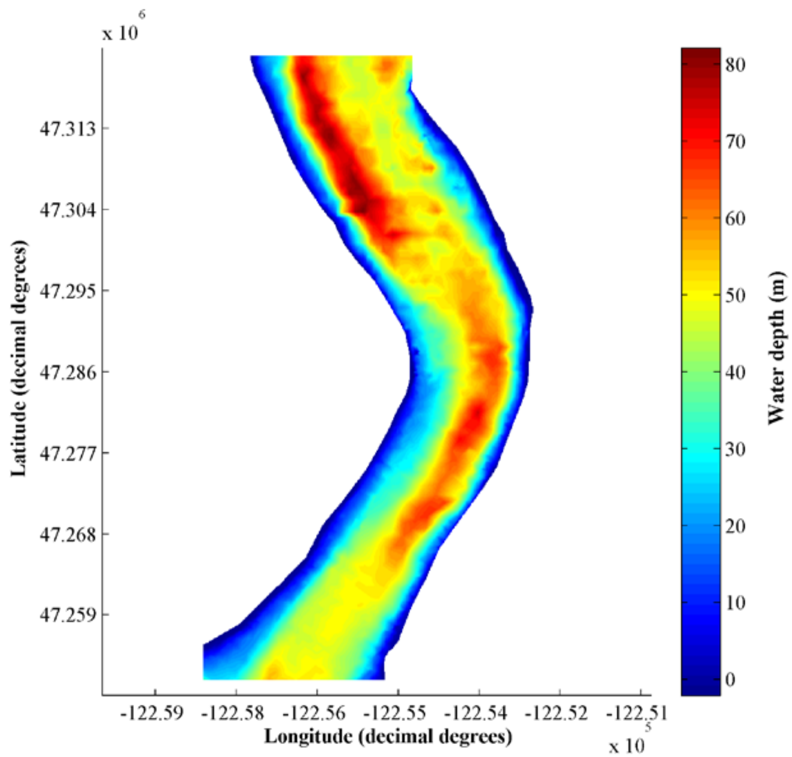

Figure 3-4. Water depth in Tacoma Narrows.

3.2.1.1 Bathymetry and Bed Sediments

As described in Section 2.2.1, the reference site's sea bed morphology and sediment regime are important features that influence the selection and design of: 1) foundations and moorings used for technology deployment, 2) electric cables used for interconnection between devices and electricity transfer to shore, and 3) potential environmental impacts to the sediment regime, bed morphology, and benthic organisms. Bathymetry and bed sediments were not assessed for the RM1 reference resource site.

3.2.1.2 Current Speed Frequency Histogram

Normalized mid-depth velocity frequency histograms and vertical current speed profiles derived from data collected at the Tacoma Narrows site were used to refine the design for individual RM1 units in the array as described by Polagye (2011b). The vertical current speed profile at each site was measured over a period between one to three months. The frequency histogram of the mid-depth (z/D=0.5) normalized current speeds in Puget Sound are shown in Figure 3-5. A value of 3 m/s was judged to be appropriate for U_{max} based on extensive velocity measurements at the site (Polagye and Thomson 2013). A 1/7th power law was applied to extrapolate the current speed frequency histogram measured at mid-depth (Table 3-1) to the rotor centerline (z/D=3/5). The 1/7th power law profile was used in prior studies and was applied to describe the variation of current speed with depth for our model of the reference site (e.g., EPRI feasibility assessments).

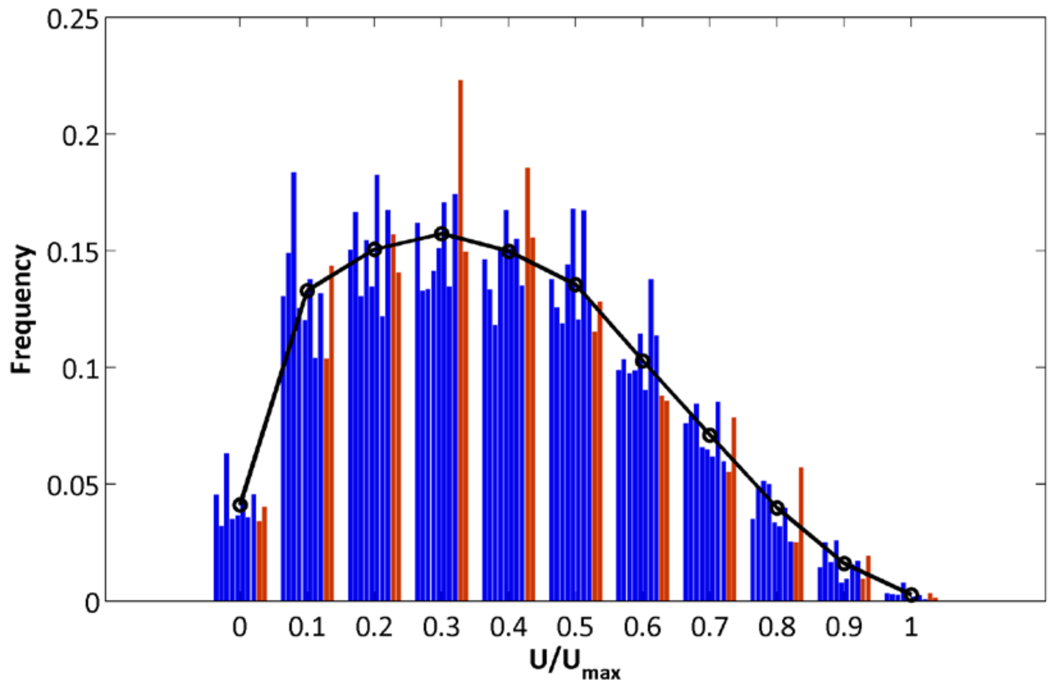

Figure 3-5. Non-dimensional mid-depth current speed frequency histograms, Puget Sound.

NOTE: Blue bars denote sites in northern Admiralty Inlet. Red bars denote sites in Tacoma Narrows. The black line denotes the reference current speed frequency histogram selected for the reference model (mean of all sites) with U_{max}=3 m/s.

Table 3-1. Reference resource mid-depth (z/D=0.5) current speed histogram for a mixed, mainly semidiurnal tidal regime.

U/U_{max}	0	0.1	0.2	0.3	0.4	0.5	0.6	0.7	0.8	0.9	1
Frequency	0.041	0.133	0.151	0.157	0.150	0.136	0.103	0.071	0.040	0.016	0.003

NOTE: U = current speed. U_{max} = maximum current speed. Normalized current speed = U/U_{max}

In our analysis, we assumed a straight tidal channel with no environmental constraints that would limit the array footprint. The site bathymetry was modeled as a trapezoidal cross-section with dimensions approximating those of the Tacoma Narrows (Figure 3-6). The channel is 1.3 km wide and has a flat central section that is 50 m deep and 700 m wide.

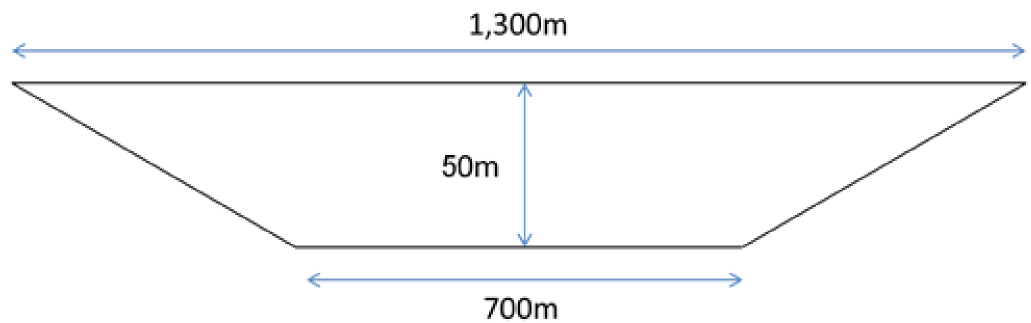

Figure 3-6. RM1 reference tidal current energy site, idealized cross-section.

3.2.1.3 Extreme Hydrodyamic Loads

Two extreme hydrodynamic load conditions derived from the tidal site current speed measurements were considered as described by Bir et al. (2011): 1) a load caused by a current speed twice the cut-out speed (6.0 m/s) that acts on a stalled turbine with feathered blades; and 2) a load caused by an instantaneous tidal current gust that is 1.5 times the near-rated current speed (1.5 x 1.9 m/s = 2.85 m/s) acting during normal operation with blades pitched at zero degrees.

3.2.1.4 Adjacent Port Facilities and Grid Options

Seattle was selected as the port facility from which service operations could be based. All LCOE calculations only considered power delivered to shore. Costs for overland transmission and grid connection to sub-stations were excluded.

3.2.2 Device/Array Information

In the conceptual design, we determined design specifications based on site resource characteristics borrowed from successful commercial technologies, and by applying engineering judgment, economic considerations, and simple hand calculations. The SeaGen turbine design specifications were directly adopted for the RM1 device and include a 20 m diameter rotor with an installed power capacity of 550 kW at a rated current speed of 2.0 m/s. A summary of the design specifications is given in Table 3-2.

Table 3-2. RM1 design specifications.

Description	Specification	Justification	Details
Deployment depth	50-60 m	Resource location	Sufficient depth for large rotor diameter.
Operational depth (hub centerline)	20 m (1 diameter)	Site resource characteristics	Surviving rough seas due to hurricanes is possible if the device is sufficiently below the free surface. The 20 m depth provides sufficient clearance for most ocean-going ships to safely pass over the device. High hydrokinetic power density.
Number of rotors per device	2	Economics	A multi-rotor device will have a lower LCOE.
Power per rotor	0.5 MW	Same as SeaGen	
Rated power	1 MW	Hand calculation	Two times installed capacity of each rotor.
Rotor diameter	20 m	Hand calculation	A 20 m rotor provides 0.5 MW at the most frequently occurring current speed.
Rated current speed	2.0 m/s	Engineering judgment	Wind turbines typically have their rated current speed 1.3–1.5 times the most frequently occurring current speed, depending on the current frequency histogram. We selected a lower rated current speed to increase the capacity factor, enabling an array of RM1 devices to provide a reliable base load to the grid.
Operational current speeds	0.5 – 3.0 m/s	Site resource characteristics	The reference resource site has a measured current speed between 0 and 3.0 m/s at hub height.
Array configuration	Linear with 20 rotor diameter longitudinal separation	Engineering judgment	A simple array configuration was selected because array modeling tools are not yet sufficiently developed to enable detailed array analysis. Longitudinal separation is sufficient to preserve inflow conditions for downstream devices based on observations from wake flow recovery experiments with scaled model hydrokinetic turbines (Neary et al. 2013b).

We selected a NACA 63_1-424 airfoil shape for the blades because of its relatively large minimum pressure coefficient, which makes this airfoil resistant to cavitation. The NACA 63-series airfoils are also known to delay stall and are less sensitive to leading edge roughness than the NACA 4- and 5-series airfoils (Lawson et al. 2013, in preparation). Given that the blade design was intended for a VSVP turbine, we assumed a circular cross-section at the blade root (to allow for a blade-pitching mechanism) that transitioned to the NACA 63_1-424 airfoil shape at 20% of the blade span. Future efforts could improve the performance of the blade by using several different airfoil shapes for the blade geometry.

3.3 Design, Analysis, and Cost Modules

3.3.1 Design & Analysis (D&A) Module

3.3.1.1 Performance Analysis and AEP Estimation

As described in Performance Analysis and AEP Estimation, Section 2.3.1.1, the potential and AEP are calculated from the power performance curve and the current frequency histogram. We used HARP-Opt, a combination of a Blade Element Momentum Theory (BEMT) code, WT-Perf, and an optimization algorithm, to optimize the blade shape and performance characteristics of the rotor (see Lawson et al. 2013 for details). The predicted single rotor operating characteristics are shown in Figure 3-7. The installed capacity for each rotor occurs at 2 m/s and is 550 kW; therefore, the rated power for the dual rotor unit is 1.1 MW (see figure note). As is typical of a VSVP turbine, the rotor operates with a zero degree (0°) pitch angle at the maximum tip-speed-ratio (TSR) from the cut-in speed until the turbine reaches rated power and its maximum rotor rotation rate at a current speed of 1.9 m/s. As the current speed increases past 1.9 m/s, the rotation rate remains constant, TSR decreases, and the blades are pitched towards the feathered position to decrease the rotor torque. As described in Section 2.3.1.1, the power curve and the current frequency distribution (adjusted to the current speed at hub height with the $1/7^{th}$ power law velocity profile) were combined to estimate an AEP of 2727 MWh for the dual-rotor system, which gives a capacity factor of 0.3. The rated power and annual output per device, dual-rotor, are given in Table 3-3. For arrays, the total AEP is determined by multiplying this estimated AEP per unit by the number of devices in the array. As stated earlier in Chapter 2, this assumes inflow conditions do not vary spatially and are not affected by turbulent wakes from upstream devices.

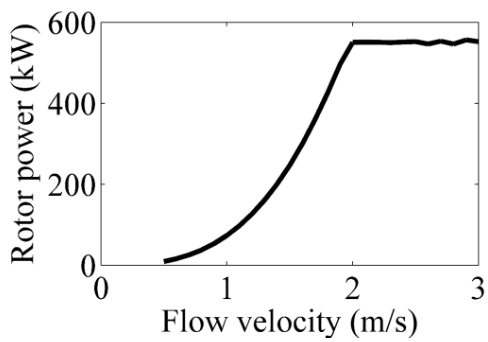

Figure 3-7. Rotor power vs. flow velocity (current speed).

NOTE: The rated power for each rotor occurs at 2 m/s and is 550 kW; therefore, the rated power is 1.1 MW.

Table 3-3. RM1 rated power and AEP output for single device.

Performance Variable	Per Unit
Rated Power	**1.1 MW**
Annual Energy Production	**3 GWh**

3.3.1.2 Materials Specifications and Structural Analysis

As described in Section 2.3.1.2, structural analysis of the main components of the RM device was performed to determine material specifications from which certain component costs can be estimated. This section provides details on this analysis for the RM1 device.

3.3.1.2.1 Estimation of Maximum Loads that Drive Structural Designs

As described in Extreme Hydrodynamic Loads, Section 3.2.1.3, the structural design and materials specifications for all RM1 device components considered the maximum of two extreme load conditions along the horizontal direction, as described earlier and detailed in Bir et al. (2011). Vertical loads on the rotors and cross arm (drag and submerged weight) during retrieval were also considered. Design factors were implemented to account for uncertainties in structural loads, environmental loads, and material properties.

Table 3-4 presents the component weight breakdown for the RM1 device. A design factor of 1.5 (1.3 load factor and 1.15 material factor) was selected. Maximum allowable deflection of the tower and cross-arm was 0.25 m.

Table 3-4. Tidal turbine component weight breakdown.

	Qty	Weight per Unit (Mg)	Total Weight (Mg)	in %
Tower	1	146.2	146.2	55
Cross-arm	1	37.2	37.2	14
Nacelle	2	40.1	80.2	30
Rotor	2	1.2	2.4	1
Total			**265.9**	

NOTE: 1 Megagram (Mg) = 1 metric ton

1 metric tonne = 1.1023 short tons; 1 short ton = 2,000 lb = 0.907185 metric tonnes

3.3.1.2.2 Cross-arm Design

The cross-arm was designed to create a neutrally buoyant structure with sufficient strength to withstand thrust loads from the rotors, drag loads on the structure, and the nacelle (turbine housing) weight. The cross-arm made with a rectangular box beam, as shown in Figure 3-8, accommodates the major static and dynamic loads.

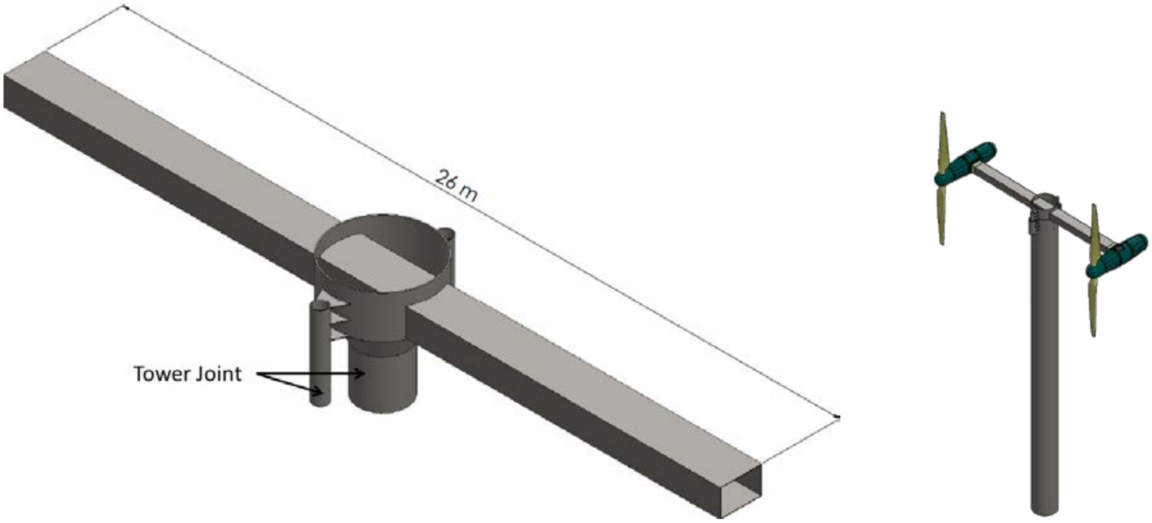

Figure 3-8. Tidal turbine cross-arm.

The flow disturbances of upstream towers can have major effects on the dynamic load characteristics of an operational rotor (Lawson et al. 2013, in preparation). Figure 3-8 does not show the fairings, which will streamline the flow around the cross-arm and reduce the wake disturbance onto the rotors of downstream devices. Table 3-5 lists the turbine cross arm specifications. The tower joint cross-arm connection uses a 1.5 m diameter central cylinder and two smaller cylinders as guides in the stream-wise direction. These guides help to align the cross-arm as it is lowered back onto the tower and secures the cross-arm into place.

Table 3-5. Tidal turbine cross-arm material specifications.

Material	A36 Steel
Yield Strength	248 MPa (36 ksi)
Length	26.0 m
Crossbeam	1.5 m x 1.0 m
Crossbeam Thickness	30.0 millimeters (mm)

Quasi-static analysis of the cross-arm loading resulted in a factor of safety of 1.53 and a deflection of 0.07 m in the stream-wise direction because of rotor thrust.

3.3.1.2.3 Tower Design

The tidal turbine tower, depicted in Figure 3-9, was designed as an un-tapered (i.e., same diameter from top to bottom) steel pile with a three-guide cross-arm connection joint at the top. Table 3-6 lists the tower material specifications. When installed, the tower joint on the cross-arm engages the three tower guides to provide a solid structural connection.

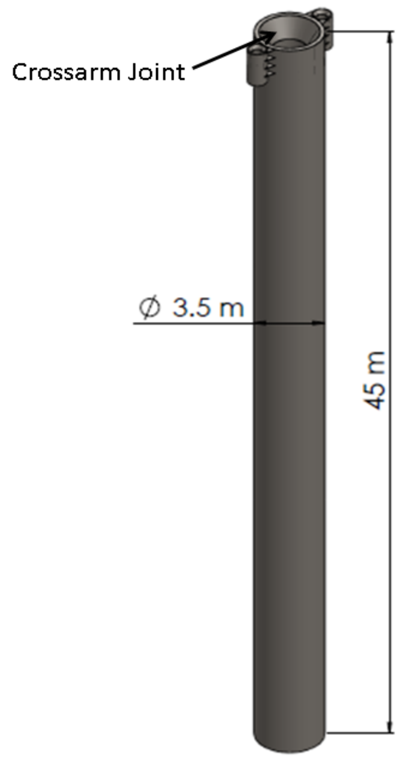

Figure 3-9. Tidal turbine tower.

Table 3-6. Tidal turbine tower material specifications.

Material	A36 Steel
Yield Strength	248 Mpa (36 ksi)
Length	45.0 m
Diameter	3.5 m
Thickness	39.0 mm
Tower Embedment Depth	15.0 m

Structural analysis of the loading on the tower produced a factor of safety of 1.65 and a maximum deflection of 0.20 m in the stream-wise direction.

3.3.1.2.4 Nacelle Design

The two nacelles, located at each end of the cross-arm, contain the complete rotor/drivetrain assembly (Figure 3-10).

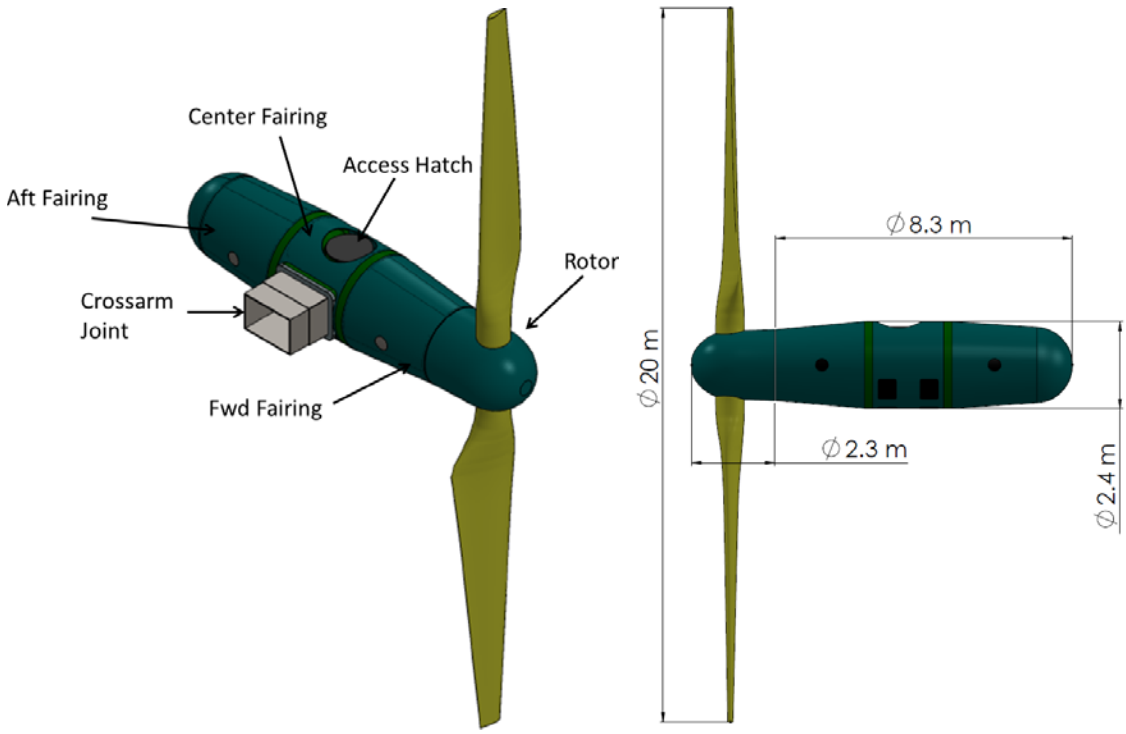

Figure 3-10. Tidal turbine nacelle.

The nacelle housing, which was designed as a pressure vessel, has three major fairing sections—forward, central, and aft. Table 3-7 lists the nacelle specification. The center fairing surrounds a center structure that connects the nacelle to the cross-arm. The center structure contains one access hatch topside and four smaller maintenance hatches on the underside. Forward and aft fairings are stiffened in the longitudinal direction to increase the strength of the pressure vessel.

Table 3-7. Nacelle structure material specifications.

Material	A36 Steel
Yield Strength	248 MPa (36 ksi)
Length	8.26 m
Diameter	2.44 m
Wall Thickness	10.0 mm

3.3.1.3 Power Conversion Chain (PCC) Design

The PCC was designed by Applied Research Laboratory at Pennsylvania State (ARL) (Beam et al. 2011a, Beam et al. 2012) and is the same as a PCC for a wind turbine with additional seal elements to allow for underwater operation. Figure 3-11 shows an exploded view of the nacelle with all fairings removed to better show the internal structure of the powertrain. The powertrain consists of the following key components:

- **Seal and bearing assembly –** keeps the enclosure water-sealed and transfers the loads from the rotor-shaft to the nacelle.
- **Rotor support structure –** transfers loads from the rotor to the center structure and cross-arm. The steel rotor support consists of six rectangular tubes connecting the two large annular flanges.
- **Seal and bearing flange**
- **Center structure –** connects the nacelle to the cross-arm and supports all of the nacelle's weight.
- **Drivetrain assembly –** Refer to details in Figure 3-13.

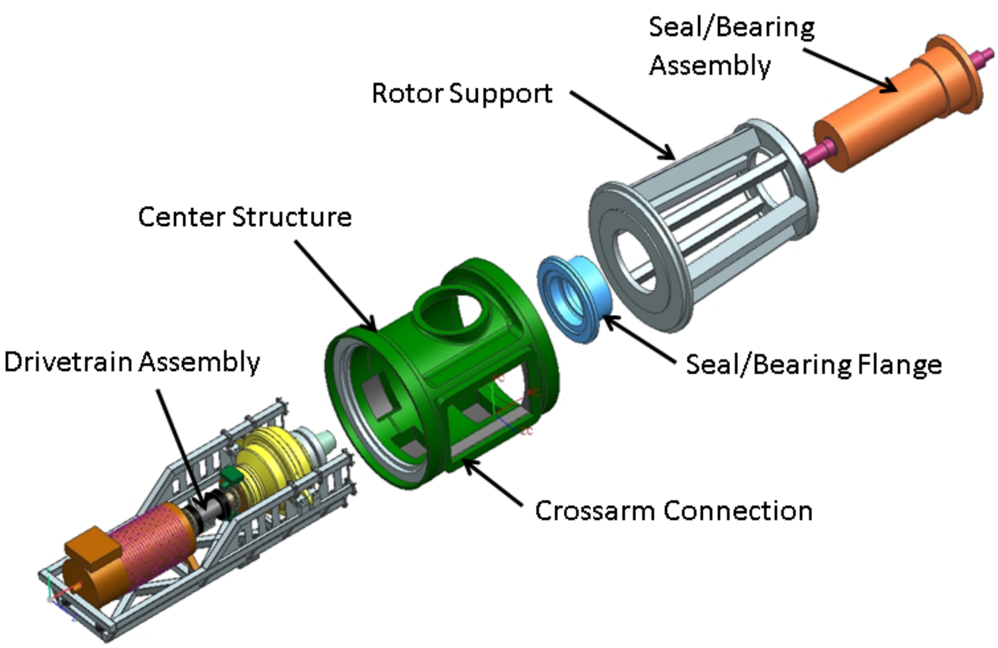

Figure 3-11. Nacelle internal components.

The seal/bearing assembly houses the rotor driveshaft, bearings, and seal components (Figure 3-12). This assembly consists of the following components:

- **Seal gland –** for the rotor shaft end.
- **Rotor shaft –** contains both bearings and end seals on the rotor shaft.
- **Bearing package canister –** centers and mounts the rotor shaft to the rotor support structure.

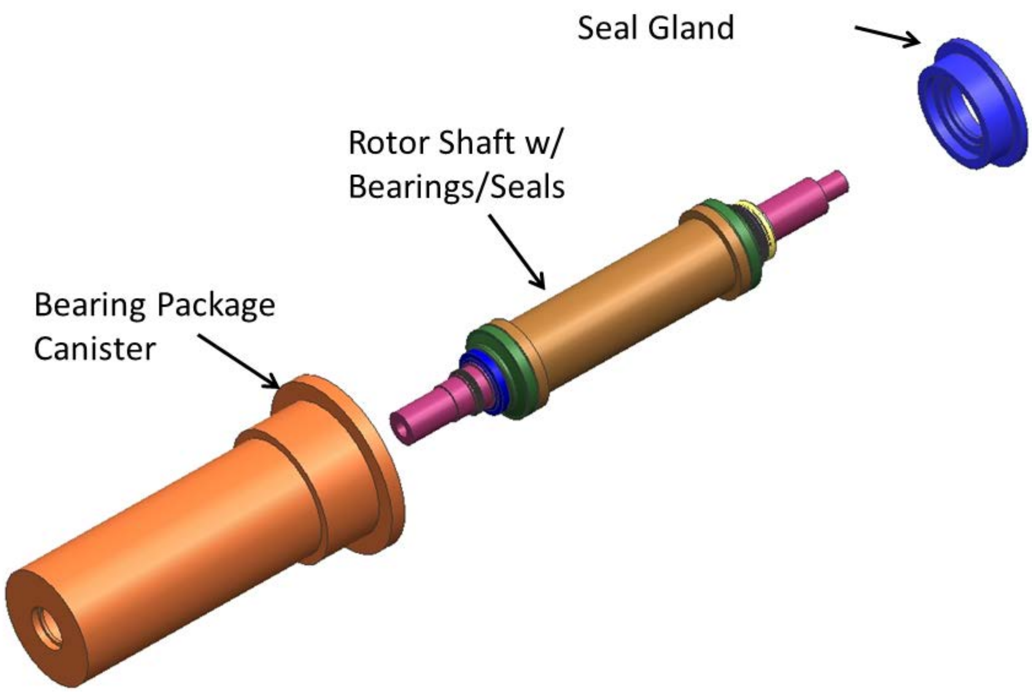

Figure 3-12. Rotor shaft seal and bearing assembly.

The gearbox and generator are mounted within the drivetrain sled, shown in Figure 3-13. The sled, which is fabricated from welded square steel tubing, was designed as a unit that can be installed through the aft end of the nacelle.

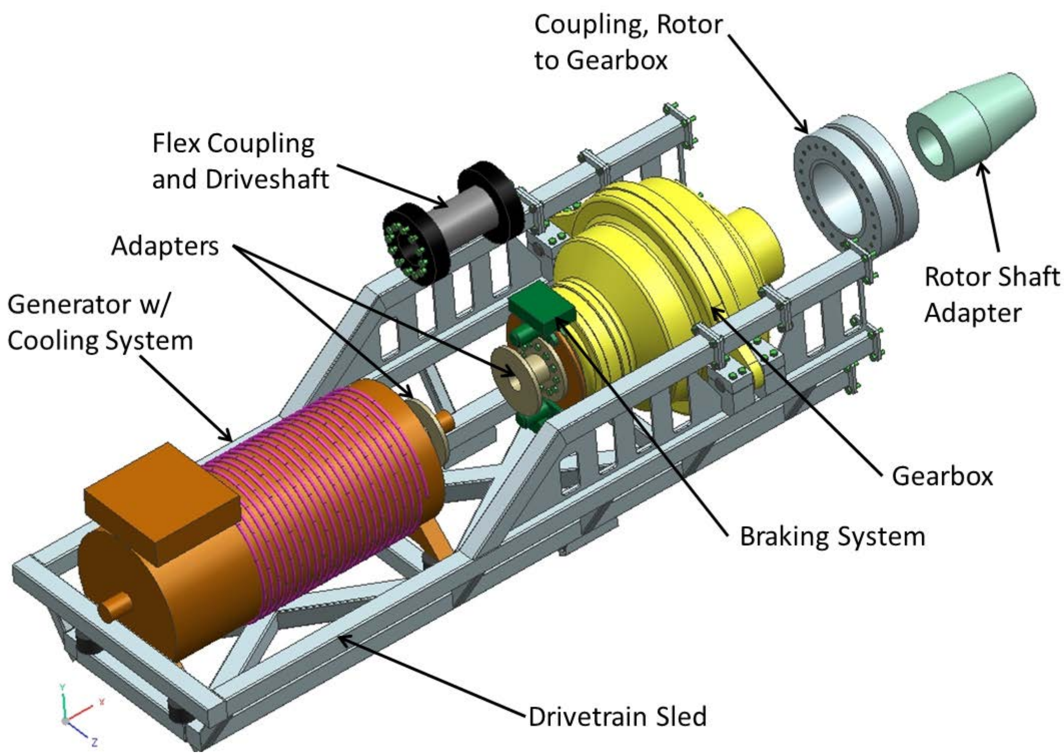

Figure 3-13. Drivetrain assembly mounted in drivetrain sled.

The drive train includes a stainless steel (17-4PhSS H900) drive shaft with a nominal bearing bore of 31.75 cm (12.5 inches) designed with a safety factor of 11 under normal loading, and 2.5 under extreme gusts. The shaft rotates within Timken tapered roller bearings with a design life of approximately 4.6 years. The design specifies:

- a Rexroth 53:1 ratio gearbox with an efficiency of 92%;
- an input rotational speed of 11.5 rpm (4.1×10^6 torque); and
- an output rotational speed of 600 rpm (7.9×10^6 torque).

The ABB 60 Hz permanent magnetic generator has a 97% efficiency and generates 690 V producing 500 kW of power at 600 rpm.

A weight breakdown of the nacelle's internal components is listed in Table 3-8. Note that nearly 50% of the total internal weight comes from the gearbox and the generator.

Table 3-8. Nacelle internal component weight breakdown.

Component	Weight Mg)	%
Rotor Shaft with all Bearings & Seals	2.4	12.9
Bearing Package Canister	1.6	8.5
Rotor Shaft Adapter	0.7	3.8
Coupling, Rotor to Gearbox	2.1	11.2
Gearbox, Orbital 2	5.4	29.5
Flex Coupling and Driveshaft	0.036	0.2
Generator with Cooling System	3.1	16.9
Drivetrain Sled	1.59	8.6
Cables & Connectors	1.56	8.5
Total	18.4	100

NOTE: Megagram (Mg) = 1 metric ton

As currently designed the assembly and housing for the PCC is a good conceptual design—but only for single-unit production. While most of the mountings can be built using welded structural steel, some of the parts, such as the center structure, will require some machining. Optimizing the nacelle for assembly line production will require substituting the machined and welded elements with mostly cast elements and simplifying the pressure vessel design. However, the cost uncertainty for the turbine PCC design and its components was generally low due to the detailed design and commercial off-the-shelf (COTS) hardware specified for the system.

3.3.2 Manufacturing & Deployment (M&D) Strategy Module

3.3.2.1 Manufacturing Strategy and Costs

As described in Manufacturing Strategy and System Component Costs, Section 2.3.2.1, this module assumes the use, where possible, of both commercially available components (e.g., generators and anchors) and conventional materials (e.g., A36 steel, standard fasteners, mooring cables). Manufacturing costs of system components for RM1 at different array scales (1, 10, 50 and 100 units) are summarized in Figure 3-14 and Figure 3-15. Figure 3-14 shows the cost breakdown for the nacelle and the structural support components. The monopile is the largest contributor to the costs followed by the nacelles. Figure 3-15 shows the cost breakdown for the energy capture and PCC components.

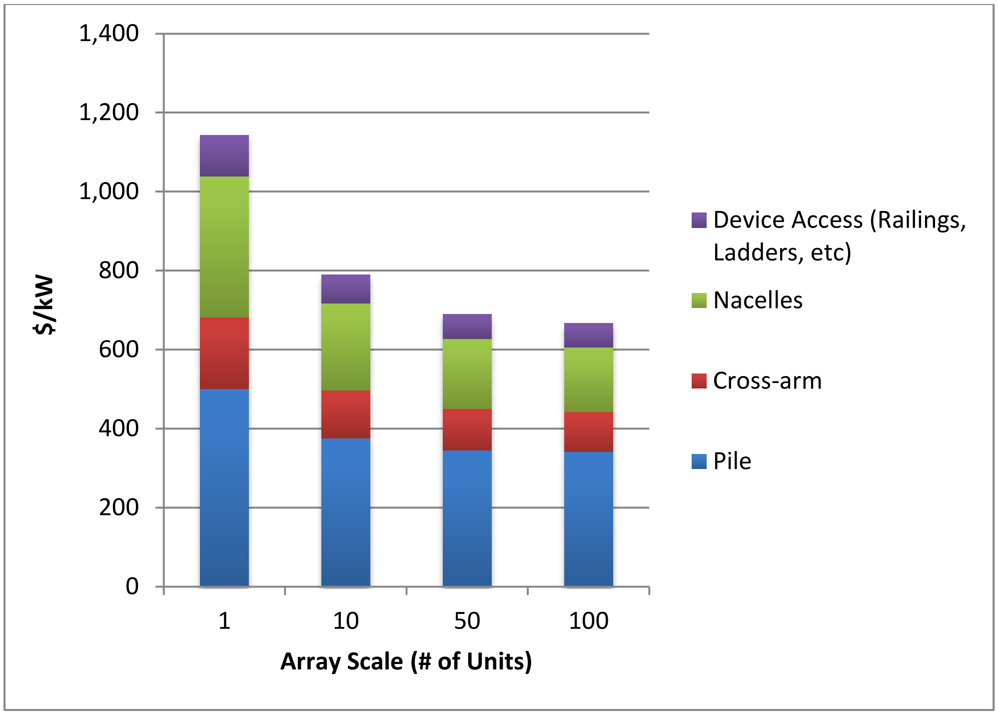

Figure 3-14. Structural cost breakdown ($/kW) per deployment scale.

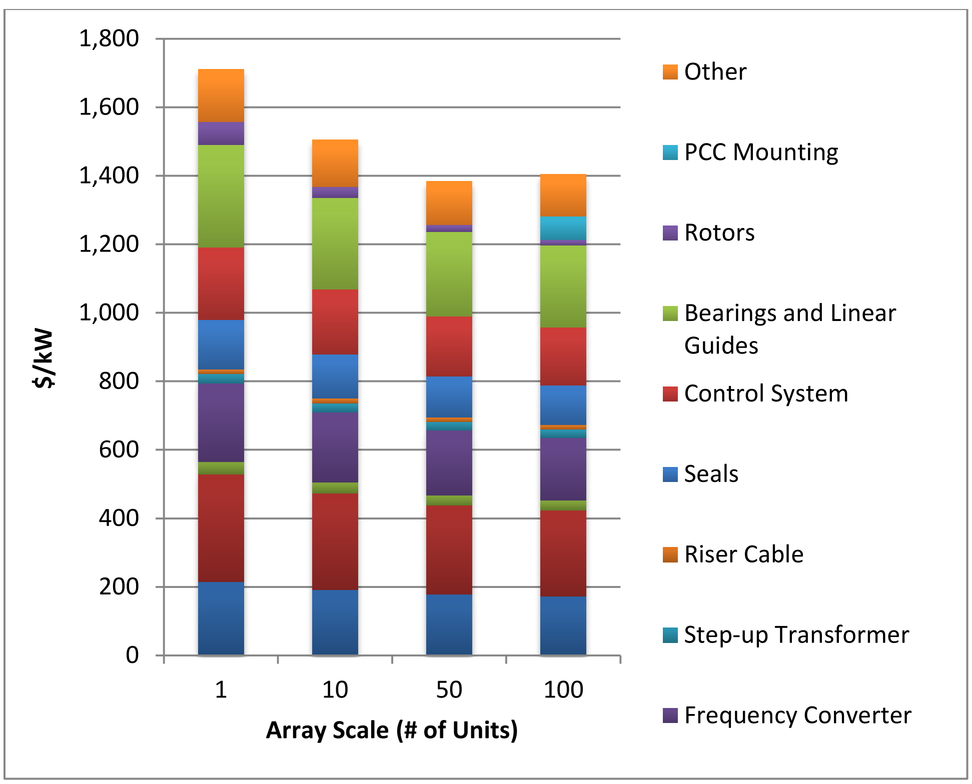

Figure 3-15. Cost breakdown ($/kW) for the energy capture and PCC components per deployment scale.

Using a series of estimates and vendor quotes, ARL developed a cost estimate for the production of a single PCC—approximately $1,710/kW. The cost estimate for production at a larger scale (e.g., 100 units) is approximately $1,400/kW[16]. At mature production levels, the cost of the PCC is likely to be similar to the cost of a wind-turbine PCC.

To estimate the cost at commercially mature production levels, results from the NREL Wind Partnerships for Advanced Component Technology (WindPACT) study (Poore and Lettenmaier, 2003) were adapted to account for:

- Lower revolutions per minute (rpm) of the rotor for equivalent power rating resulting in an increase in gearbox cost;
- Difference in rotor blade design;
- Redundancy measures required to reduce intervention cycles; and
- Sealing requirements.

The pressure vessel design and cost are discussed in the structural section. Blade cost was estimated from the NREL rotor design study that showed a structural weight of 614 kg per blade.

Table 3-9 compares the cost ($/kW) for a wind-turbine PCC, a tidal turbine PCC, and a hardened tidal turbine PCC. Figure 3-16 illustrates the relative cost differences. However, because the hardened version adds redundant measures, the operational costs over its design life will be significantly less because the hardened PCC will require less frequent service interventions. For this reason, we selected a hardened PCC for the RM1 design.

[16] A detailed cost breakdown of the PCC (also referred to as the power take-off) is included in the spreadsheet developed by ReVision, entitled "Reference Model 1 CBS.xlsx" (October 26, 2012).

Table 3-9. 500 kW powertrain cost comparison.

Component	Wind ($/kW)	Tidal ($/kW)	Redundant Tidal ($/kW)
Control, Safety System, and Condition Monitoring	69	69	138
Gearbox	52	136	136
Variable speed electronics	51	51	51
Generator	42	42	42
Main frame	38	38	38
Electrical connections	34	51	51
Hub	34	34	34
Blades	14	14	14
Hydraulic, Cooling system	8	8	16
Pitch mechanism & bearings	6	6	12
Low speed shaft	3	3	3
Yaw drive & bearing	2	0	0
Mechanic brake, HS coupling, etc.	1	1	2
Bearings	1	1	1
Spinner, Nose Cone	0	0	0
Main shaft seal	0	27	27
Total	**355**	**481**	**565**

NOTE: Comparison from WindPACT Scaling Study.

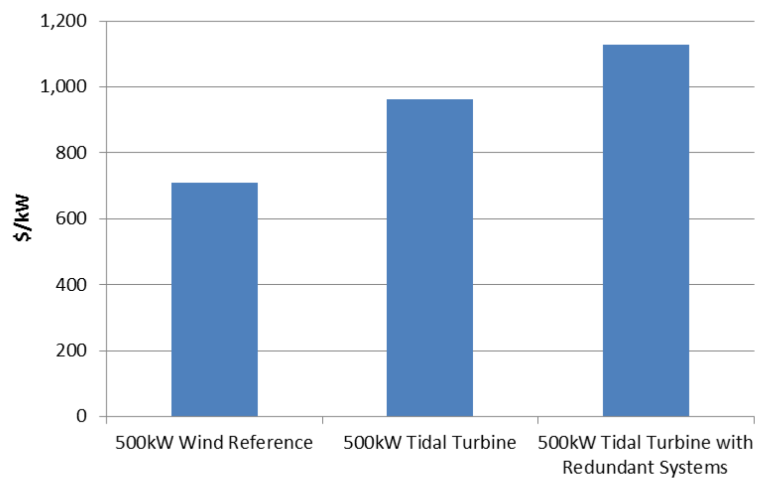

Figure 3-16. PCC cost comparison.

NOTE: Comparison is at commercial manufacturing scale.

3.3.2.2 Deployment Strategy and Costs

The deployment strategy accounts for the installation of the RM1 turbine monopile, the subsea cable infrastructure, and the device structure itself. Three types of vessels would be required:

- **Pile Installation Crane Barge –** A crane barge will be used to lift and handle the equipment and components used in the pile-driving operations. We assumed this project will require a crane barge with a lift capacity of more than 454 Mg (454 metric tonnes or 500 short tons). An example barge is shown in Figure 3-17. This barge will also require a six-point mooring system capable of holding station.
- **Cable Installation Vessel –** For installing the subsea buried cable, a separate cable installation vessel will be required.
- **DP-2 Vessel with moonpool –** Finally, for installing the devices, a DP-2 vessel with a moonpool will be used. This custom vessel would also serve as the project's dedicated service vessel.

Total installation costs were developed using the assumed day rates for these vessels and assumed installation durations presented in Table 3-10.

Figure 3-17. Example of a 500-tonne capacity crane barge.

NOTE: This crane barge was built by Mason Construction.
www.mansonconstruction.com/derrick-barges-clamshell-dredges

Table 3-10. RM1 M&D Strategy Module cost assumptions.

		1 Unit			100 Units		
Operational Detail	**Vessel Status**	**No. Days**	**Vessel Day Rate**	**Cost**	**No. Days**	**Vessel Day Rate**	**Cost**
Pile Installation Vessel							
Mobilize Vessel in West Coast Home Port	At Dock (Mob/Demob)	4.0	$110,725	$442,900	4.0	$110,725	$442,900
Transit from home port to Tacoma Narrows & set mooring	Transit/ Anchoring	2.0	$166,600	$333,200	2.0	$166,600	$333,200
Drive Piles at 3 per day	Pile Installation	0.3	$164,200	$54,733	33.3	$164,200	$5,473,333
Recover anchors & transit back to Home port	Transit/ Anchoring	2.0	$166,600	$333,200	2.0	$166,600	$333,200
Operational Contingency (weather included) at 25% of time to drive piles	Standby	0.1	$149,850	$12,488	8.3	$149,850	$1,248,750
Demobilize at West Coast Home Port	At Dock (Mob/Demob)	3.0	$110,725	$332,175	3.0	$110,725	$332,175
	Subtotal for Ops only	11.4		$1,508,696	52.7		$8,163,558
Gunderboom Sound Barrier				$4,500,000			$4,500,000
Frame to transport barrier system				$50,000			$50,000
Mob/Demob of Sound Barrier System				$70,000			$70,000
	Total			**$6,128,696**			**$12,783,558**

Continues

Cable Installation using Cable Install Vessel									
Transit to site	At Dock (Mob/Demob)			1.0	$45,432	$45,432	1	$45,432	$45,432
Install Cables to device	Installation Ops	2	per day	0.5	$74,784	$37,392	50	$74,784	$3,739,200
Secure/Unsecure cable segment to pile	Installation Ops	2	per day	0.5	$74,784	$37,392	50	$74,784	$3,739,200
Splice interconnect cables between each J-Box	Installation Ops	2	per day	0.5	$74,784	$37,392	10	$74,784	$747,840
Fairleading cables in the field	Installation Ops			5.0	$74,784	$373,920	5	$74,784	$373,920
Shore End cable through HDD	Installation Ops			2.0	$74,784	$149,568	2	$74,784	$149,568
Lay/Burial of Trunk Cable	Installation Ops			4.0	$74,784	$299,136	4	$74,784	$299,136
Standby for testing and commissioning	Standby			4.0	$62,924	$251,696	4	$62,924	$251,696
Transit back to Home port	Transit			1.0	$45,432	$45,432	1	$45,432	$45,432
Operational Contingency (weather included) at	Standby	25%		4.125	$62,924	$259,562	31.25	$62,924	$1,966,375
Demobilization at Home Port	At Dock (Mob/Demob)			2.0	$45,876	$91,752	2	$45,876	$91,752
			Total	**24.625**		**$1,628,674**			**$11,449,551**
Device Installation Using DP-2 Vessel									
Mobilize Vessel - usually in state of readiness	At Dock			4	$74,026	$296,104	4	$74,026	$296,104
Transit to site	Transit			1	$78,682	$78,682	1	$78,682	$78,682
Install Devices, 2 per day	Installation Ops			0.5	$106,014	$53,007	50	$106,014	$5,300,700
Secure cable segment to pile, 2 per day	Installation Ops			0.5	$106,014	$53,007	50	$106,014	$5,300,700
Fairleading of cables in field	Installation Ops			2	$106,014	$212,028	2	$106,014	$212,028
Transit back to Home port	Transit			1	$86,854	$86,854	1	$78,682	$78,682
Operational Contingency (weather included) at	Standby	25%		1.3	$74,026	$92,533	25.5	$86,854	$2,214,777
Demobilize at Home Port							2	$74,026	$148,052
			Total	**9.0**		**$872,215**	**133.5**		**$13,629,725**

For the M&D and O&M Strategy Modules, we assumed a custom service vessel (described in Section 3.3.3.1) for O&M servicing would also be used both to deploy the RM1 turbine cross-arm and to service the device (or array). We assumed this dual role would reduce the total installation cost because the same permanent crew and vessel are used.

Large diameter pile installation requires large pile-driving equipment and it may also require a sound attenuation system (SAS) to protect marine life. However, it is not yet clear if such a sound barrier system will be required by regulators for the pile-installation activities at the reference site. Generally, noise attenuation is necessary for large pile driving projects since the sound can harm or kill fish, marine mammals, and other marine life (Knik Arm Bridge and Toll Authority 2005). Because traditional sound barriers such as bubble curtains are ineffective in strong (tidal) currents, we designed a custom pile-driving device with the help of Gunderboom, a company that has developed a sound barrier system that encapsulates pockets of air in a large curtain that is placed around the pile and pile-driving equipment. Figure 3-18 illustrates the system. The system cost, approximately $4.5 M, is included in the deployment CapEx of the array.

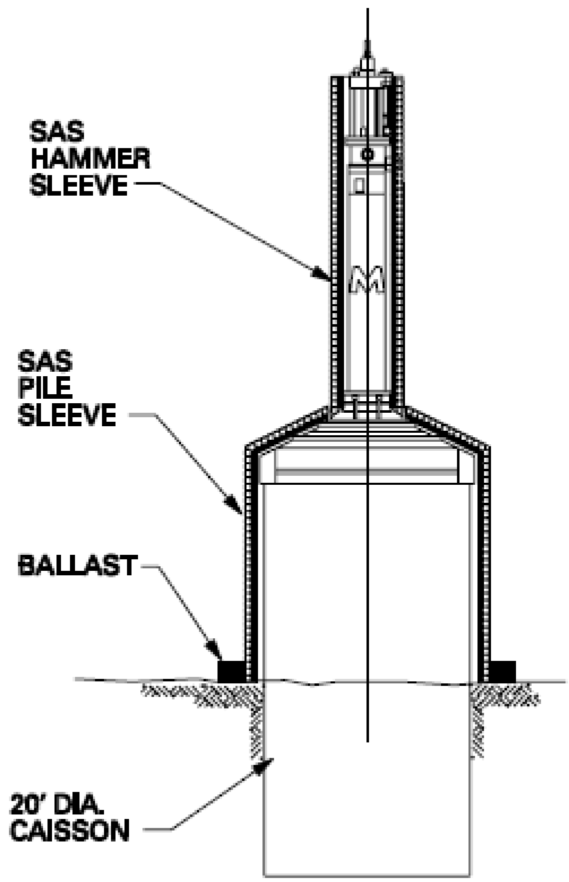

Figure 3-18. Sound barrier system for high-current environments.

NOTE: This design was conceived through collaboration with Gunderboom. www.gunderboom.com

To drive the 3-meter diameter pile, a 454 Mg (500.45 short tons) pile-driving hammer is required. Additional equipment required on board the crane barge includes:

- Burial tool
- Small crane
- Cable tower and spread
- Stern chute
- Rigging van and tools
- Generators

For installation using the crane barge, we estimated that a total crew of 26 personnel is needed, including dive support. The primary installation vessel would be supported by two tugs, a transport barge, and a supply boat. The cable landing would be installed using directional drilling from shore.

Depending on array size, one to four directionally drilled conduits with an inner diameter of 0.2 to 0.3 m (8 to 12 inches) would be placed to accommodate the subsea cables. Installation trade-offs were studied through discussions with offshore operators and specialty offshore equipment suppliers to determine cost levels.

Figure 3-19 shows the total installation cost as a function of deployment scale (1, 10, 50 and 100 units). Installation cost of a single device is driven primarily by the cost to install the mooring system, whereas installation costs of a 100-unit array are more evenly distributed between devices, cables, and mooring systems. Note that costs for transport to the staging site are not included because the Puget Sound area has a good industrial base and it is assumed that construction is mostly done locally. In addition, it was very difficult to estimate device commissioning for RM1. Because it is not a cost driver, especially for larger deployment scales, we left this out of the installation costs.

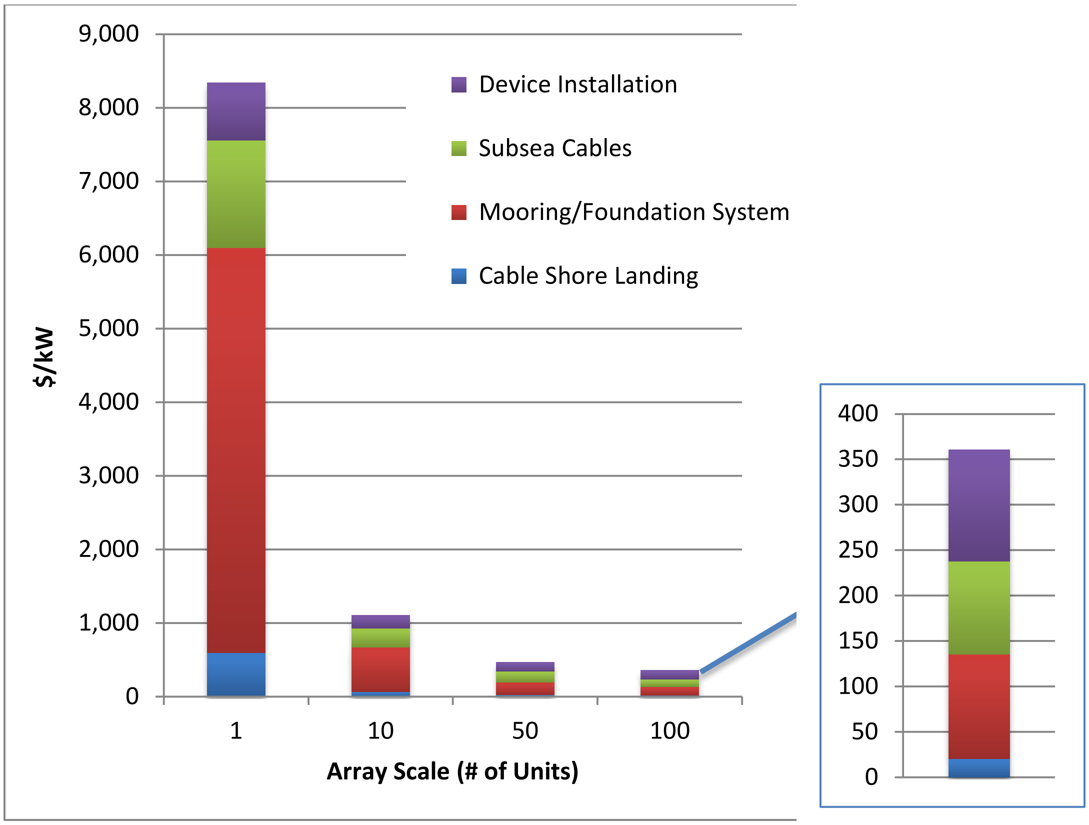

Figure 3-19. Installation cost breakdown ($/kW) per deployment scale.

3.3.3 Operations & Maintenance (O&M) Strategy Module

The O&M Strategy Module for RM1 was developed for a concept design that reduces O&M costs, specifically shore-side PCC maintenance and repairs, by adopting a dual-rotor design, mounted on a retrievable cross-arm assembly from a single monopile foundation. As noted earlier, the cross-arm assembly is close to neutrally buoyant to further reduce recovery and redeployment costs by reducing the lifting crane capacity. The PCC design was also hardened with redundant subsystems to reduce the frequency of shore-side repairs.

For full recovery of both rotors to allow shore-side repairs, a stab-pipe would connect the dynamically positioned vessel on the surface to the pile on the seabed and use an integrated lift-mechanism to move the cross-arm assembly up and down the pipe as illustrated in Figure 3-20. Active dynamic positioning of the stab-pipe allows the tip of the pipe to be accurately inserted into the top of the bottom-mounted pile and compensates for small vessel movements on the surface that may be induced by turbulent flows.

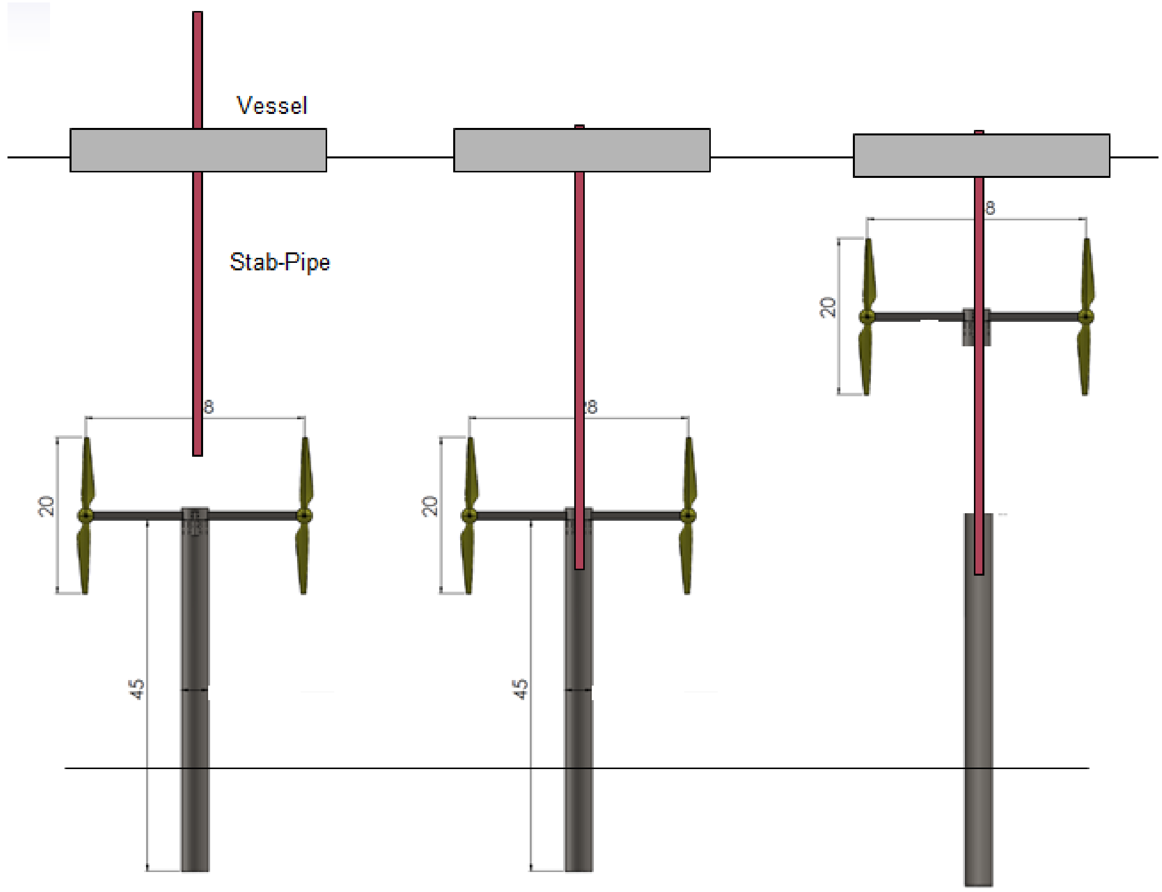

Figure 3-20. Conceptual cross-arm deployment/ recovery.

3.3.3.1 Service Vessel Specifications

After reviewing handling requirements and the potential of meeting owners/captains with 'Vessels of Opportunity,' it was determined that the most cost-effective approach to O&M would be to secure a custom-designed vessel that would be an integral part of the MEC array and to staff it with a permanent crew. This is similar to the approach taken by many leading tidal device manufacturers who are realizing that a specialty vessel equipped to meet the requirements of the task is the best way to address the challenges of vessel operations.

The custom-designed vessel conceptualized for RM1 was a dynamic positioning (DP)-2 vessel with a large moonpool that could transport the cross-arm assembly to shore while it was completely immersed. Using dynamic positioning instead of a mooring system provides significant operational efficiencies and makes the deployment and recovery procedures possible during relatively short-period slack water windows.

The moonpool vessel, illustrated in Figure 3-21, eliminates the need to lift the very heavy cross-arm assembly out of the water. An artificial bow, forming a protected moonpool, shields the immersed turbine assembly from floating debris during transit. It also reduces the handling requirements on the winch system and the buoyancy and stability requirements of the overall vessel. The moonpool is large enough for an entire cross-arm and rotor assembly to be transported fully shielded. General dimensions of the vessel in feet are shown in Figure 3-22.

A 20-person crew was considered adequate to carry out operational activities safely. Initial cost estimates for such a vessel vary from $13M to $16M. Section 2.3.3 details requirements and costs for the shore-side crew of technicians and administrative personnel needed for carrying out repairs and maintenance activities. Although the dedicated vessel will be used for O&M, the cost to acquire such a vessel is considered a capital expense, and was included in the CapEx portion of the Cost Breakdown Structure (CBS); the vessel purchase is not an OpEx cost.

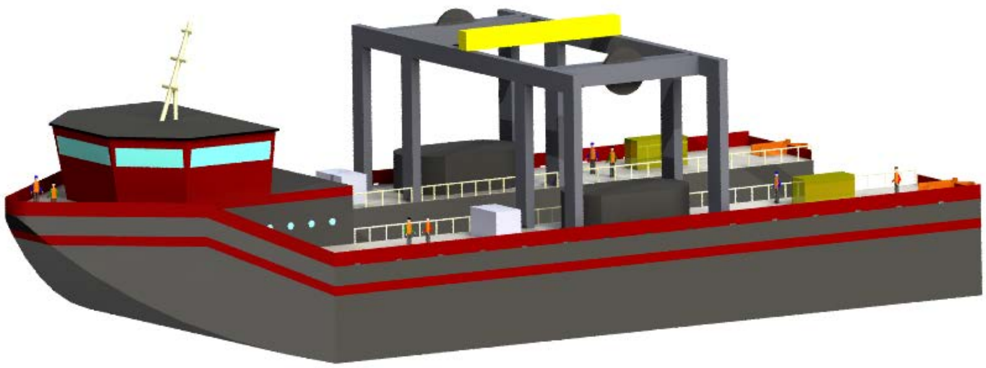

Figure 3-21. Custom DP-2 vessel with moonpool.

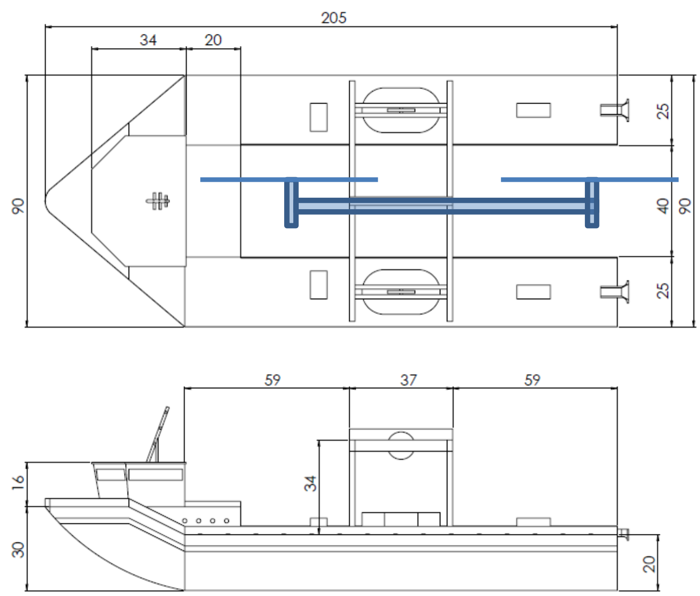

Figure 3-22. Custom DP-2 moonpool vessel.

NOTE: Dimensions in feet.

3.3.3.2 Failure Rates

Failure Rates, Section 2.3.3.2, details the failure (reliability) matrix adopted for device and infrastructure (BOS) components, which accounts for the likelihood of failure of each component along with the requirements for the repair, and the number and unit cost of service trips. Based on reported failure rates for wind turbine technologies (Poore and Lettenmaier 2003), we assumed an average of 3.9 repairs each year. Table 3-11 shows the typical number of failure events for a 100-unit wind turbine farm (1MW rated capacity) adapted to a 100-unit project with the two-bladed rotor used in the tidal turbine case.

To reduce the number of expected interventions for RM1, it was assumed that the PCC could be hardened by introducing redundancy in the systems highlighted in light blue in Table 3-11. The introduction of such redundant systems was assumed to decrease the number of failures (and required repairs) to one per rotor per year, or two per year for a dual-rotor machine, such as the RM1 tidal turbine. We assumed scheduled maintenance tasks such as removing biofouling and replacing gearbox oil and filter elements would be carried out once a year. At that point, non-critical repairs/maintenance would also be conducted.

Table 3-11. Failure rate summary of typical wind turbine powertrain.

System	Component	Parts in Project	Total Failures over 20 yrs / initial qty parts in fleet (%)	# Failures 100 Units
Rotor	Blade--struct. repair	200	5%	10
	Blade--nonstruct. repair	200	100%	200
	Pitch bearing	200	0%	0
	Pitch motor	200	123%	246
	Pitch gear	200	143%	286
	Pitch drive	200	117%	234
Drivetrain	Main bearing	100	5%	5
	High-speed coupling	100	39%	39
Gearbox and Lube	Gearbox--gear & brgs	100	5%	5
	Gearbox--brgs, all	100	67%	67
	Gearbox--high speed only	100	67%	67
	Lube pumps	300	147%	441
	Cooling Fan, Gearbox Cooling	200	97%	194
Generator and Cooling	Generator--rot. & brgs	100	5%	5
	Generator--brgs only	200	92%	184
	Motor, generator coolant fan	200	97%	194
	Contactor, generator	300	78%	234
Brakes & Hydraulics	Brake caliper	300	194%	581
	Brake Pads	200	10%	20
	Accumulator	100	340%	340
	Hydraulic pump	100	146%	146
	Hydraulic valve	400	148%	590
Control System	Control board, Top	100	117%	117
	Control board, Main	100	117%	117
	Control Module	200	117%	234
	Sensor, static	1700	128%	2183
	Sensor, dynamic	200	156%	312
Electrical and Grid	Main Contactor	100	77%	77
	Main Circuit Breaker	100	37%	37
	Frequency Converter	100	160%	160
Misc. (All others)	Miscellaneous Parts	100	5%	5

NOTE: The table shows values for a 100-unit project using dual-rotors for each unit. The blue shading indicates redundant systems.

3.3.3.3 Annual O&M Costs

Based on the above number of interventions and replacement part values, the annual O&M cost was estimated for the different scales of deployment (Figure 3-23) in terms of $/kW. Figure 3-23 shows the breakdown of the likely annual OpEx cost ($/kWh) as a function of the number of units in an array. See Section 2.3.3.4 for details on how insurance costs were estimated. Note that the post-installation monitoring is a part of environmental monitoring and regulatory compliance costed under the Environmental Compliance (EC) Module (see Section 3.3.4) and is included in the total OpEx costs shown in Figure 3-23. Initial environmental compliance and monitoring activities prior to start up would fall under CapEx as explained in the following section.

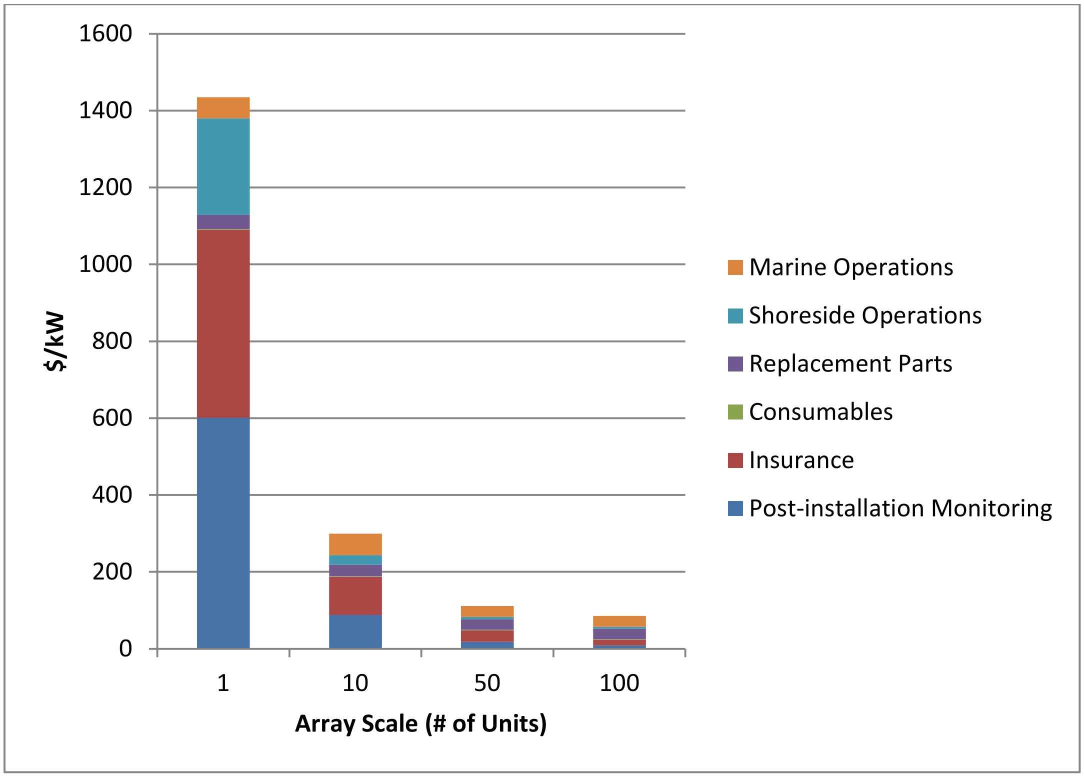

Figure 3-23. Annual OpEx cost ($/kW) per array size.

3.3.4 Environmental Compliance (EC) Module

The methods developed by Copping and Geerlofs (2011) were applied for the RM1 turbine and reference resource site based on the Tacoma Narrows tidal energy site to estimate environmental CapEx and OpEx for pilot (1 unit), small commercial (10 units), and large commercial (> 50 units) scale deployments. As described in Section 2.3.4, CapEx and OpEx under the EC Module includes costs broken out as follows:

- **CapEx Cost:** NEPA project phases, siting and scoping, pre-installation (including recreational impact study costs), and upfront (first-year) costs for post-installation contribute to the CapEx of the project.
- **OpEx Cost:** Post-installation monitoring continues for the duration of the life of the project and contributes to the annual OpEx.

Tidal sites are generally small in geographic size, requiring limited seabed surveys. However, these sites tend to be located at water-body constrictions, often encompassing the major ingress and egress pathways for marine life to pass from one estuarine basin to another. This heightened sensitivity to interaction with marine mammals, fish, and other highly valued organisms may drive up pre-installation studies and post-installation monitoring costs. Spinning tidal turbine blades and acoustic noise from rotors may pose risk to marine animals from strike and acoustic masking, and may require extensive post-installation monitoring to verify and inform risk assumptions. Since the tip of the turbine blades are submerged 10 m below the free surface and many diving sea birds dive within this depth range, seabird surveys will be needed to characterize the species present and their feeding habitat at the reference site location. Tidal sites generally are within fairly well studied bodies of water, so that some environmental data may be available for scoping and pre-installation assessment.

Until environmental effects of tidal energy development are better understood, we assume the first two years of post-installation will require an extensive set of studies, followed by a reduced level of near-field monitoring for any animals determined to be at risk, and periodic special studies including those to evaluate far-field effects. No regulatory timeframe has been established to date for intensive post-installation studies; the two-year timeframe cited here has been extrapolated from requirements made on U.S. projects under development; this timeframe could be lengthened or shortened, based on future regulatory requirements. Together these studies can be used to estimate ecosystem risk. Using the cost ranges developed to estimate the capital costs of monitoring equipment, as well as the costs of carrying out specific studies, sample analysis, and analysis and interpretation of the data, estimates for total CapEx normalized by installed power for the NEPA process, siting and scoping, pre-installation studies, and first-year post-installation studies as a function of array scale are summarized in Figure 3-24. Detailed breakdown of the costs and assumptions made is shown in Copping and Geerlofs (2011).

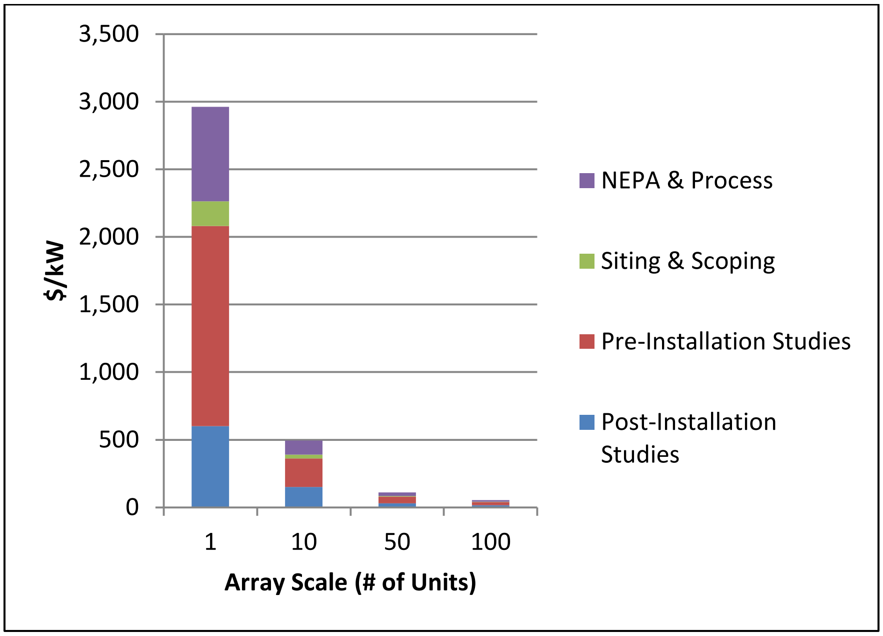

Figure 3-24. Total environmental CapEx estimate per deployment scale (1, 10, 50 or 100 units).

High and low bounds for the environmental compliance cost estimate were approximately +/-30% relative to the mean value shown in Figure 3-24 and were derived from regional and site-specific differences in the sensitivity of animal populations and habitats that might be expected. This is carried forward into the analysis of the array cost and economic assessments. It is clear that with increasing numbers of devices, the cost per installed power decreases significantly.

Post-installation environmental monitoring continues for the duration of the project and contributes to the annual costs (OpEx). Similar to the Environmental CapEx, the costs for OpEx, shown in Figure 3-25, also decreases with larger arrays.

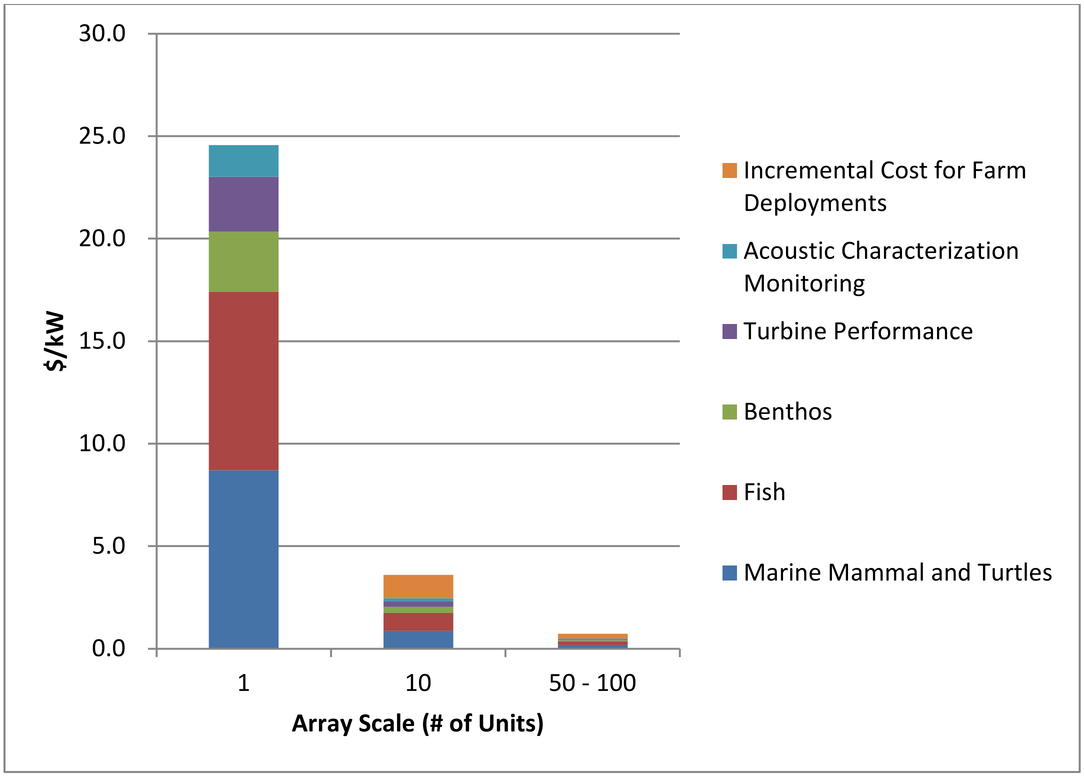

Figure 3-25. Annual cost of post-installation monitoring per deployment scale.

NOTE: Because post-installation monitoring is highly uncertain, commercial scales of 50 and 100 units are grouped together and assumed to be the same cost.

3.4 LCOE Calculation

The levelized cost of energy (LCOE) estimate for a 10-unit RM1 array is 41 cents/kWh based on the FCR, AEP, CapEx, and OpEx estimates described below. The estimated AEP for this array is 27,272 MWh per year. Table 3-12 gives a detailed breakdown of the LCOE estimate. The cost of M&D is the greatest LCOE driver for RM1, contributing 53% of the total LCOE. The next largest driver is O&M which contributes nearly 30% of the total LCOE. These findings indicate that the most critical area for targeting potential cost savings is M&D.

Table 3-12. RM1 LCOE breakdown by cost category (10-unit array).

	cents/kWh	% of total LCOE
Development	3.1	7.7%
M&D	21.7	53.3%
Subsystem Integration & Profit Margin	1.1	2.6%
Contingency	2.6	6.4%
O&M	12.2	30.0%
Total	40.7	100.0%

Figure 3-26 illustrates the total LCOE for RM1, and shows how the cost of energy decreases as a function of installed capacity.

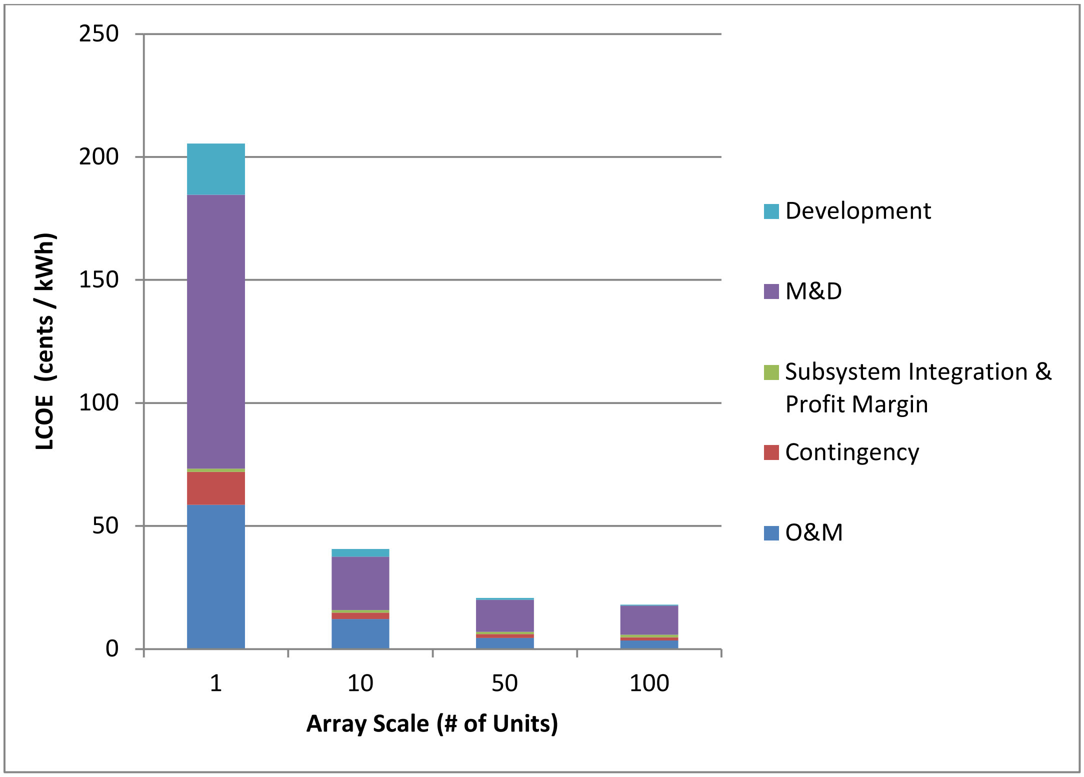

Figure 3-26. High-level LCOE (cents/kWh) breakdown per deployment scale for RM1.

The total CapEx for a single unit deployment was estimated to be approximately $31,900/kW, whereas the total CapEx per unit for a 100-unit array was estimated to be $3,170/kW. While there are some cost savings to be expected simply by increasing the manufacturing and fabrication volume from one to 100, major per-unit cost savings are expected to be realized within the installation cost category and the infrastructure cost category.

Figure 3-27 shows the contribution of capital costs to the RM1 LCOE. Note that Mooring/Foundation is not applicable for RM1 (foundation/pile is covered in the device structural component costs).

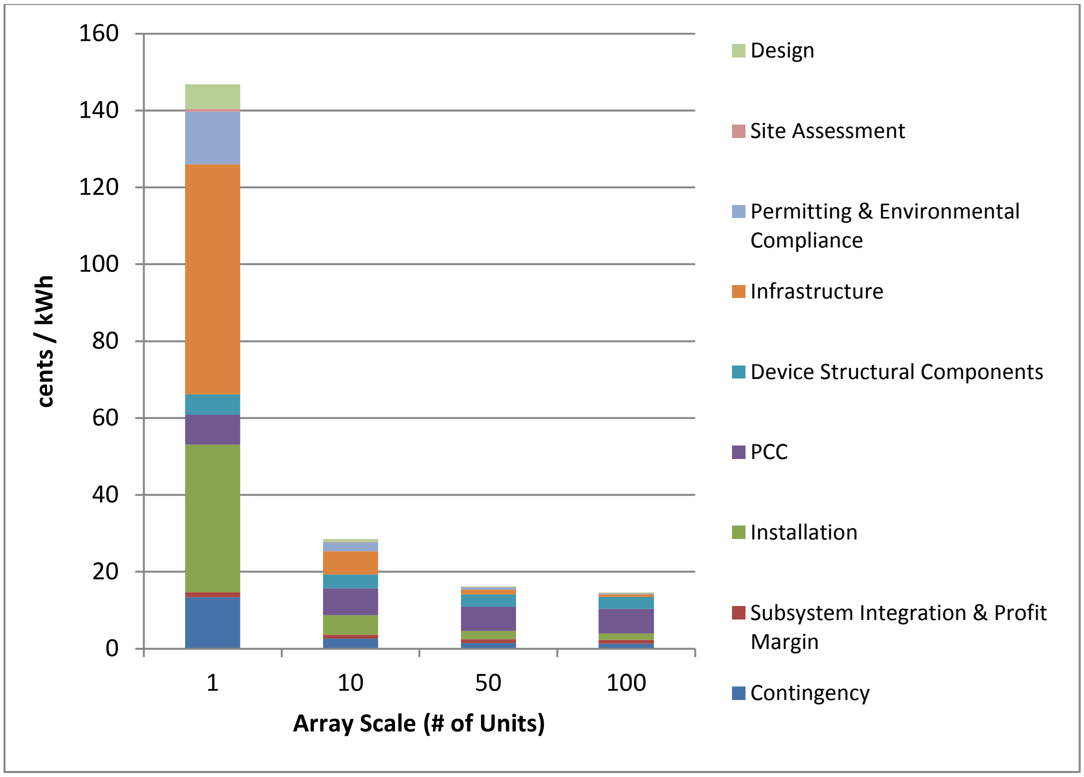

Figure 3-27. RM1 CapEx contributions to LCOE (cents/kWh) per deployment scale.

A detailed breakdown of major CapEx cost categories, in terms of LCOE, is provided in Table 3-13 for a commercial array.

Table 3-13. Breakdown of RM1 CapEx contributions to LCOE (10-unit array).

	cents/kWh	% of total CapEx
Design	0.8	2.6%
Site Assessment	0.12	0.4%
Permitting & Environmental Compliance	2.3	8.0%
Infrastructure	6.0	21.2%
Mooring/Foundation	0.0	0.0%
Device Structural Components	3.6	12.8%
PCC	6.9	24.3%
Installation	5.1	17.9%
Subsystem Integration & Profit Margin	1.1	3.7%
Contingency	2.6	9.1%
Total	28.5	100.0%

Annual OpEx for a single unit deployment was estimated to be approximately $1,435/kW, whereas the annualized OpEx per unit for a 100-unit array was estimated to be $85/kW. Similarly to the capital cost contributions to LCOE, the operational cost contributions to the RM1 LCOE are shown in Figure 3-28.

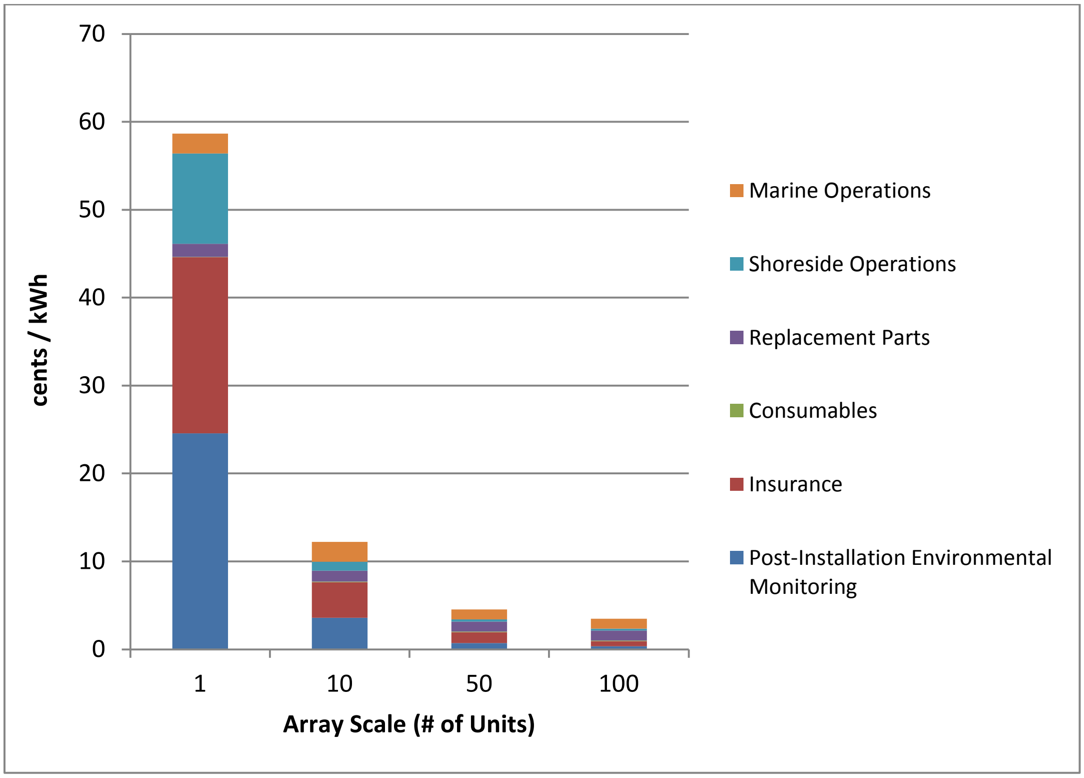

Figure 3-28. RM1 OpEx contributions to LCOE (cents/kWh) per deployment scale.

A detailed breakdown of major OpEx cost categories in terms of LCOE is provided in Table 3-14.

Table 3-14. Breakdown of RM1 OpEx contributions to LCOE (10-unit array).

	cents/kWh	% of total OpEx
Marine Operations	2.3	18.4%
Shoreside Operations	1.0	8.4%
Replacement Parts	1.2	10.1%
Consumables	0.1	0.6%
Insurance	4.0	33.1%
Post-Installation Environmental Monitoring	3.6	29.5%
Total	12.2	100.0%

4 Reference Model 2 (RM2): River Current Turbine

4.1 RM2 Description

The RM2 is a variable speed dual-rotor cross-flow river turbine that is deployed at the water's surface. It was designed for deployment at a reference site modeled after a reach in the Mississippi River near Baton Rouge, Louisiana. As shown in

Figure 4-1, the rotors are anchored to a two-pontoon vessel platform. The concept design for this device was inspired by the EnCurrent Power Generation (EPG) system developed by New Energy Corporation (n.d.) (http://www.newenergycorp.ca/). The EPG system has undergone extensive testing and is at a high Technology Readiness Level (TRL) of approximately 7-8 (refer to introduction in Chapter 2). The EPG system only deploys a single rotor, while the RM2 device deploys two counter-rotating rotors on a shared pontoon platform to further reduce manufacturing and deployment (M&D), operations and maintenance (O&M), and environmental costs. Surface deployment of the turbine also minimizes the handling requirements during deployment and recovery and reduces overall costs for all O&M activities, including allowing for easy access to the power conversion chain (PCC). The design (two rotors per platform) also reduces the environmental footprint and associated environmental compliance costs. Details of the RM2 design are provided in Barone et al. (2011).

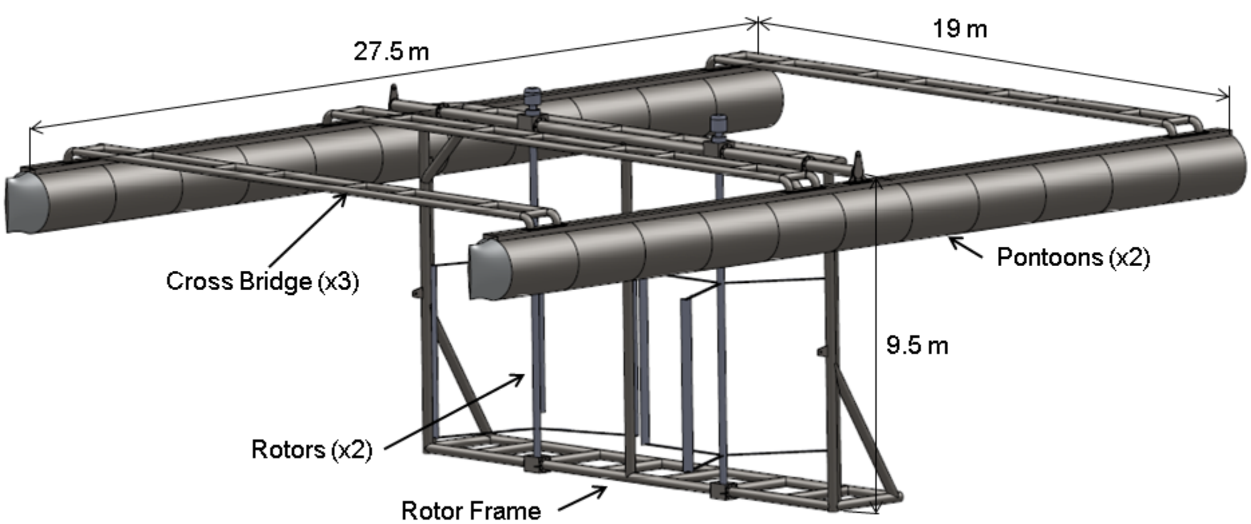

Figure 4-1. RM2 device design.

The dimensions of the RM2 device are illustrated in Figure 4-2. Plan dimensions of the pontoon are 28 m by 20 m. The diameter of each rotor is 6.45 m. The dual-rotors on each unit are offset by one and a half diameters (9.675 m) from each rotor centerline. The rotor centerlines are submerged one blade length (4.84 m) below the free surface to guard against cavitation. As compared to the RM1 tideway resource site, the water depth at the RM2 river resource site can vary greatly; this fact restricts the height of each rotor to 4.8 m. Even at shallow depths, which occur with reduced discharges, the rotors remain well above the riverbed (at least 5 m of clearance above the bottom). This reduces potential boundary layer effects that can cause velocity, turbulent shear, and loading asymmetries across the rotor.

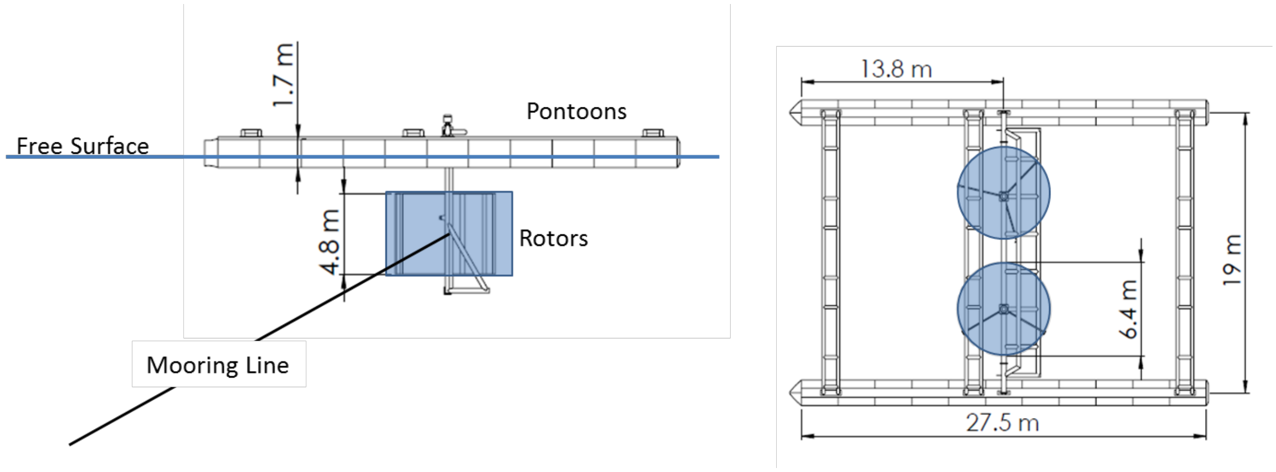

Figure 4-2. RM2 profile and plan views with dimensions.

4.1.1 Device Design and Analysis

As noted in Design Methodology for a Single Device, Section 2.1.1, the first step in the device design process was to develop a conceptual design appropriate for the modeled reference resource site. Once the concept design was completed, detailed device design was developed using simulation tools originally developed for design and analysis of wind turbines. For the RM2 design and analysis, we leveraged methods and tools developed for designing and analyzing vertical-axis wind turbines (VAWT). The rotor for the concept device was designed and optimized using Sandia's wind turbine design code, CACTUS (Code for Axial and Cross-flow Turbine Simulation), which employs a free wake vortex method (Murray and Barone 2011). CACTUS simulations provided the performance characteristics of the RM2 device to derive an estimate of the annual energy production (AEP) at the reference resource site. CACTUS was also used to estimate extreme structural loads on the rotor components. Measurements from physical scaled model experiments at the University of Minnesota, St. Anthony Falls Laboratory (SAFL), as described by Neary et al. (2012b), will be available in 2014 to validate the CACTUS model.

4.1.2 Array (Farm) Design and Analysis

As noted in Section 2.1.1, due to the lack of developed array optimization models, we did not conduct detailed array design and analysis as described in the general methodology, which adds to the uncertainty in the AEP estimate for arrays. Our proposed configuration for the RM2 array is depicted in Figure 4-3. The spacing between rows, in the longitudinal downstream direction, is 400 m (63 rotor diameters). With 20 rows, the longitudinal dimension of the array footprint for the 100-unit array is approximately 8000 m, which is the length of the trunk cable. The width of each dual-rotor unit (20 m) and the surface width of the river (800 m) constrain both the number of units that can be placed in a row and the lateral spacing between the devices. We selected an array with five units in each row allowing for a 50 m lateral spacing between the units, which is 2.5 times the width of each dual-rotor unit.

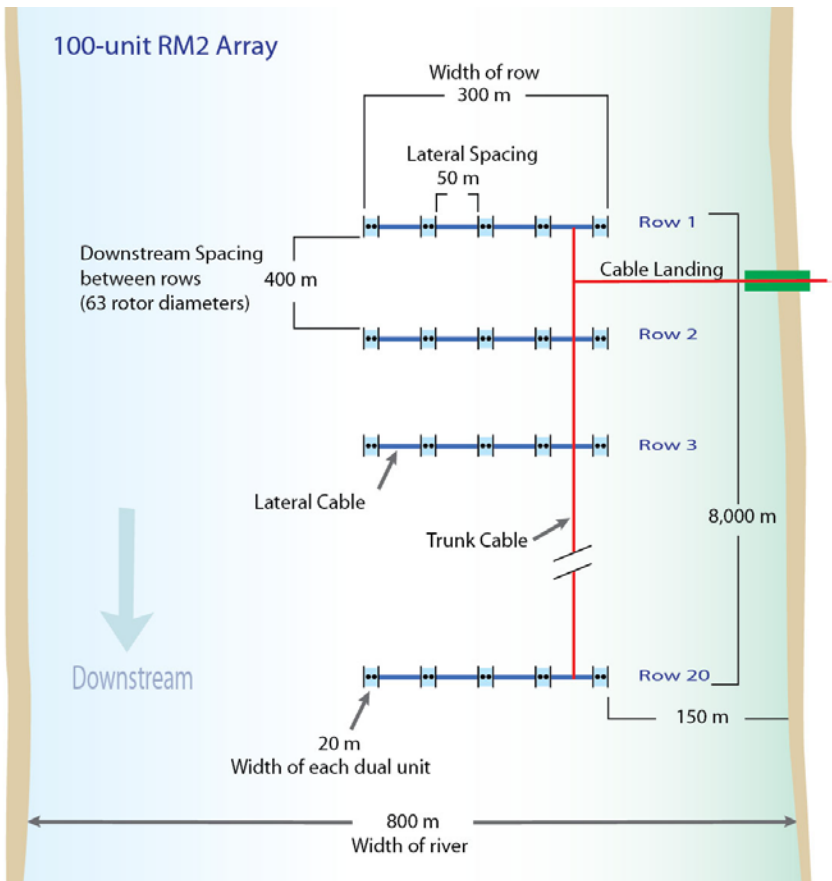

Figure 4-3. Array layout and subsea cabling (plan).

NOTE: The 100-unit array footprint is approximately 8,000 m x 300 m.

The total array capacity at 100 units is approximately 10 MW. We selected a 3-phase AC transmission cable with a voltage level of 11 kilovolts (kV). All transmission cables included fiber optic lines to allow communication from each device to shore. The cable landing is accomplished by directionally drilling a conduit that connects the cable out to the first row of devices. This approach minimizes installation and maintenance costs.

4.2 Module Inputs

4.2.1 Site Information

The reference river current energy resource for RM2 was developed from site information on the Mississippi River reach at Baton Rouge, Louisiana as summarized by Neary (2011). Figure 4-4 shows three typical cross-sectional profiles, which can be approximated as trapezoidal sections with top widths of 800 m and bottom widths of 500 m. For the purpose of this site design, it was assumed that only half of the river width can be occupied by the array footprint and that the first 150 m from shore is not included to allow device placement in the highest flow-velocity region of the river. This leaves an area of approximately 300 m width for device deployment.

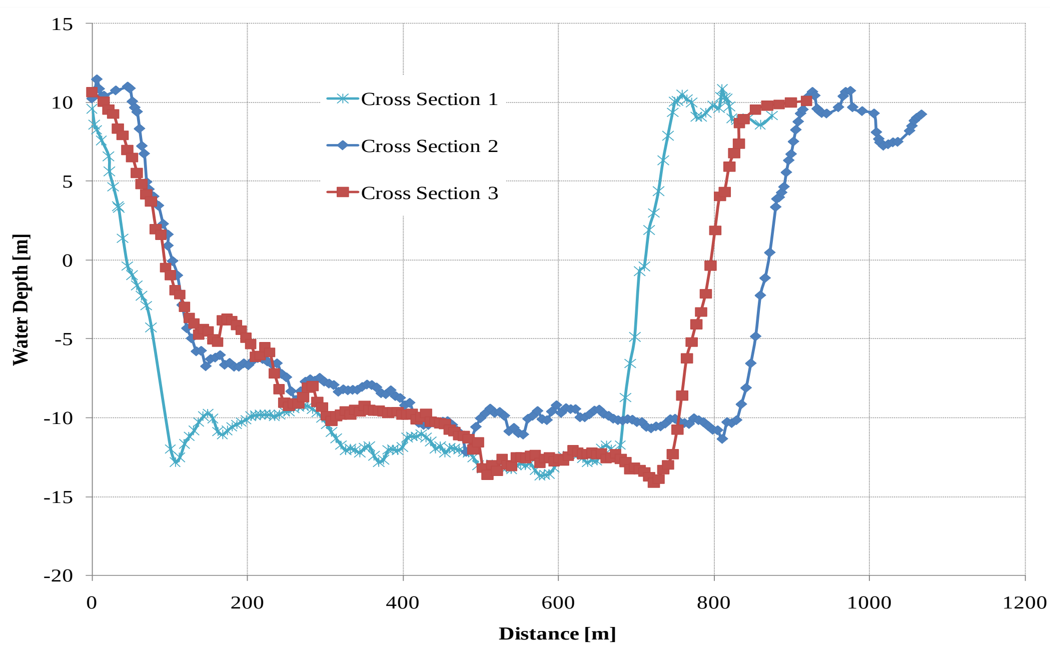

Figure 4-4. Typical river cross-sections near Baton Rouge, LA.

4.2.1.1 Bathymetry and Bed Sediments

As described in Section 2.2.1, the reference site's river bed morphology and sediment regime are important features that influence the selection and design of: 1) foundations and moorings used for technology deployment; 2) electric cables used for interconnection between devices and electricity transfer to shore; and 3) potential environmental impacts to the sediment regime, bed morphology, and benthic organisms. We did not assess the bathymetry and bed sediments for the RM2 reference resource site.

4.2.1.2 Current Speed Frequency Histogram

The surface current speed histogram for the site, in bins of 0.1 m/s, is shown in Figure 4-5. The variation of the river water depth with the river current speed is shown in Figure 4-6 (a). As demonstrated by Neary et al. (2013 a), the velocity profile in a river can be reasonably modeled using a 1/6th power law, where the elevation above the bed (z) is non-dimensionalized by the water depth and the velocity is non-dimensionalized by the surface current, as shown in Figure 4-6 (b).

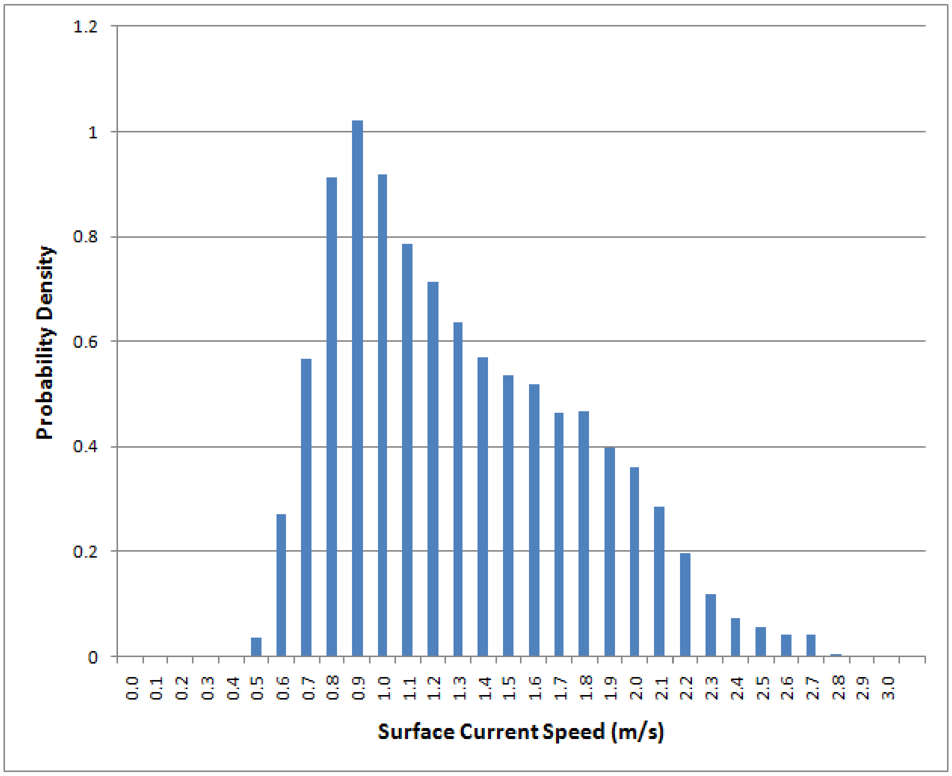

Figure 4-5. Surface current speed frequency histogram, daily averages in 0.1 m/s bins.

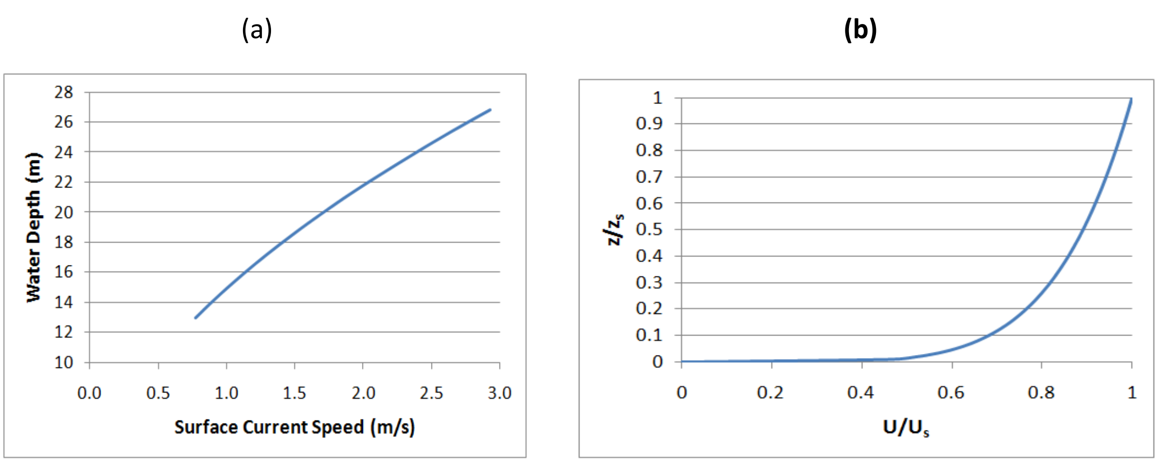

Figure 4-6. (a) Water depth vs. surface current speed; (b) 1/6th power law velocity profile.

4.2.1.3 Extreme Hydrodyamic Loads

An extreme hydrodynamic load condition based on a 3.25 m/s current speed was used to generate the design hydrodynamic flap-wise loads for the blade structure. The extreme hydrodynamic load condition for the struts was assumed to derive from a uniform gust with vertical velocity equal to 25% of the current speed during a parked condition with a surface current speed of 3.5 m/s. Both extreme hydrodynamic load condition current speeds were higher than the 50-year return period surface current speed of 2.81 m/s, and the 100-year return period current speed of 2.92 m/s.

4.2.1.4 Adjacent Port Facilities and Grid Options

Baton Rouge was selected as the port facility from which service operations could be based. All LCOE calculations only considered power delivered to shore. Costs for overland transmission and grid connection to sub-stations were excluded.

4.2.2 Device/Array Information

In the conceptual design, we determined design specifications based on site resource characteristics borrowed from successful commercial technologies and by applying engineering judgment, economic considerations, and simple hand calculations. The EnCurrent turbine design specifications influenced those for the RM2 device, which has an installed power capacity of approximately 100 kW at a rated current speed of 2.3 m/s. A summary of the design specifications is given in Table 4-1.

Table 4-1. RM2 design specifications.

Description	Specification	Justification	Details
Deployment at free surface	Flow depth 13-27 m	Site resource characteristics	Sufficient depth for 50 kW cross-flow turbine.
Operational depth (rotor centerline)	3 m (1 rotor height)	Engineering judgment	Device surface deployed from floating pontoon at free surface. High hydrokinetic power density near free surface.
Number of rotors per device	2	Economics	A multi-rotor device will have a lower LCOE.
Power per rotor	50 kW	Same as EnCurrent	
Rated power	100 kW	Hand calculation	Two times installed capacity of each rotor.
Rotor diameter	6.5 m	Hand calculation	A 6.5 m rotor provides 50 kW at the most frequently occurring current speed.
Rated current speed	2.3 m/s	Engineering judgment	Wind turbines typically have their rated current speed 1.3–1.5 times the most frequently occurring current speed, depending on the current frequency histogram. We selected a lower rated current speed to increase the capacity factor, enabling an array of RM2 devices to provide a reliable base load to the grid.
Operational current speeds	0.7 – 2.6 m/s	Site resource characteristics	The reference resource site has a measured current speed between 0 and 2.7 m/s at hub height.
Array configuration	Linear with 64 rotor diameter longitudinal separation	Engineering judgment	A simple array configuration was selected because array modeling tools are not yet sufficiently developed to enable detailed array analysis. Longitudinal separation sufficient to preserve inflow conditions for downstream devices.

4.3 Design, Analysis, and Cost Modules

4.3.1 Design & Analysis (D&A) Module

4.3.1.1 Performance Analysis and AEP Estimation

As described in Performance Analysis and AEP Estimation, Section 2.3.1.1, the potential and AEP were calculated from the power performance curve and the current frequency histogram. We used CACTUS to simulate the power performance curve for the RM2 device. The predicted single rotor power curve is shown in Figure 4-7. A maximum power rating of 51 kW occurs at just over 2 m/s. A CACTUS simulation of tandem counter-rotating rotors showed only a minor decrease in predicted rotor performance with a separation distance (blade-to-blade) of one radius. As described in Section 2.3.1.1, the power curve and the given current frequency distribution were combined to estimate an AEP of 274.2 MWh for the dual-rotor system, which gives a capacity factor of 0.3 (30%). The rated power and annual output per device, dual-rotor, are given in Table 4-2. For arrays, the total AEP is determined by multiplying this estimated AEP per unit by the number of devices in the array.

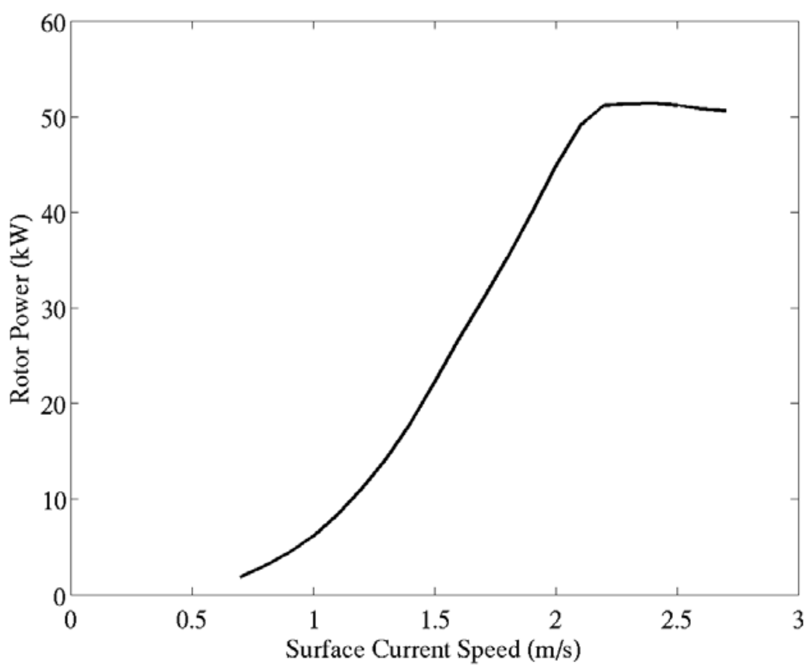

Figure 4-7. Rotor power vs. current speed.

Table 4-2. RM2 rated power and AEP output for single device.

Performance Variable	Per Unit
Rated Power	**100 kW**
Annual Energy Production (AEP)	**204 MWh**

4.3.1.2 Materials Specifications and Structural Analysis

As described in Material Specifications and Structural Analysis, Section 2.3.1.2, we performed structural analysis for the main components of the RM device to determine material specifications from which certain component costs can be estimated. This section provides details on this analysis for the RM2 device. ASTM A36 carbon steel was chosen as the material for the major components of the pontoon-float structure. Although we initially selected aluminum for the design of the pontoons due to its higher corrosion resistance and strength-to-weight ratio; however, the reduced strength of welded aluminum and higher cost made the design unfeasible.

4.3.1.2.1 Estimation of Maximum Loads that Drive Structural Designs

Similar to the RM1 device, the structural design and materials specifications for all RM2 device components considered the maximum of two extreme load conditions along the horizontal direction, as described for extreme hydrodynamic loading in Section 4.2.1.3.

4.3.1.2.2 Pontoon and Frame

The rotor frame was designed with a pivot joint at the pontoon connection with a 90 degree stop to allow for the rotor frame to be lifted to the surface for maintenance and transportation. Details of the structural design of the pontoon and frame are provided in Re Vision Consulting, LLC (2011b). Figure 4-8 shows the dimensions of a single RM2 pontoon. We used standard design factors to account for structural loads, environmental loads, and material properties. A design factor of 1.5 (1.3 load factor and 1.15 material factor [Det Norske Veritas, 2011]) was selected. Table 4-3 shows the device weight breakdown.

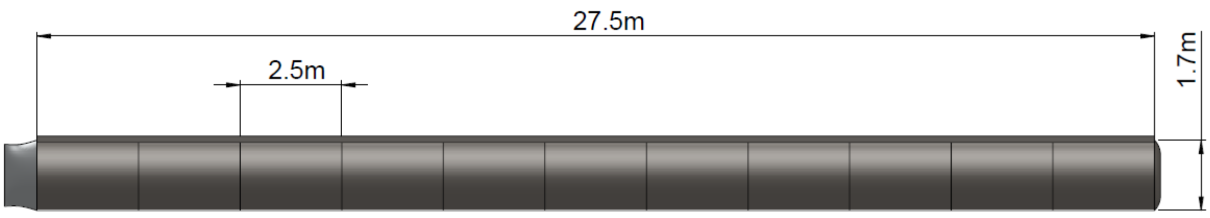

Figure 4-8. Device pontoon.

Table 4-3. RM2 device weight breakdown.

	Qty	Weight per Unit (Mg)	Total Weight (Mg)	Weight %
1.73m (68-in) diameter pontoons	2	11.4	22.6	57.6
Cross-bridge	3	2	5.9	14.8
Rotor frame	1	11	11	27.6
Device Total			39.8	

A wide channel is welded to the top of each pontoon to connect with the three cross-bridges. Each cross-bridge (Figure 4-9), which has eight cross-members, connects the two pontoons together and provides lateral rigidity to the platform. The mid cross-bridge will serve the additional purpose of providing an access walkway to the PCC units for service.

The pontoons were sized to allow for approximately 50% submersion during operation. The pontoon is fabricated as rolled and welded cylinder sections. Its material properties are listed in Table 4-4.

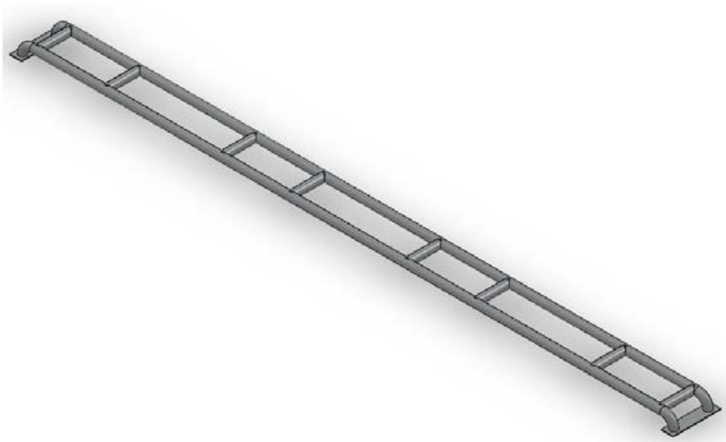

Figure 4-9. Cross bridge.

Table 4-4. Pontoon material specifications.

Material	A36 Steel
Yield Strength	248 MPa (36 ksi)
Length	27.5 m
Diameter	1.7 m
Wall Thickness	6.35 mm

Each cross-bridge component under direct loading in the structure is fabricated using full penetration welding to ensure maximum weld strength. Material specifications for the cross-bridge are given in Table 4-5.

Table 4-5. Cross-bridge material specifications.

Material	Steel (A36, A500) 0.2 m (8-in.) Schedule 40 Pipe
Yield Strength	248 Mpa (36 ksi)
Length	19 m

The rotor frame structure, shown in Figure 4-10, supports the rotors and the entire PCC. Like the cross-bridge, the rotor frame design uses steel because of the high loads transferred throughout the frame due to the rotor drag, generator and drivetrain weight, and structural weight. Maximum rotor drag loads during operation are 68 kilonewtons (kN) per rotor. Only quasi-static loads were considered for the design.

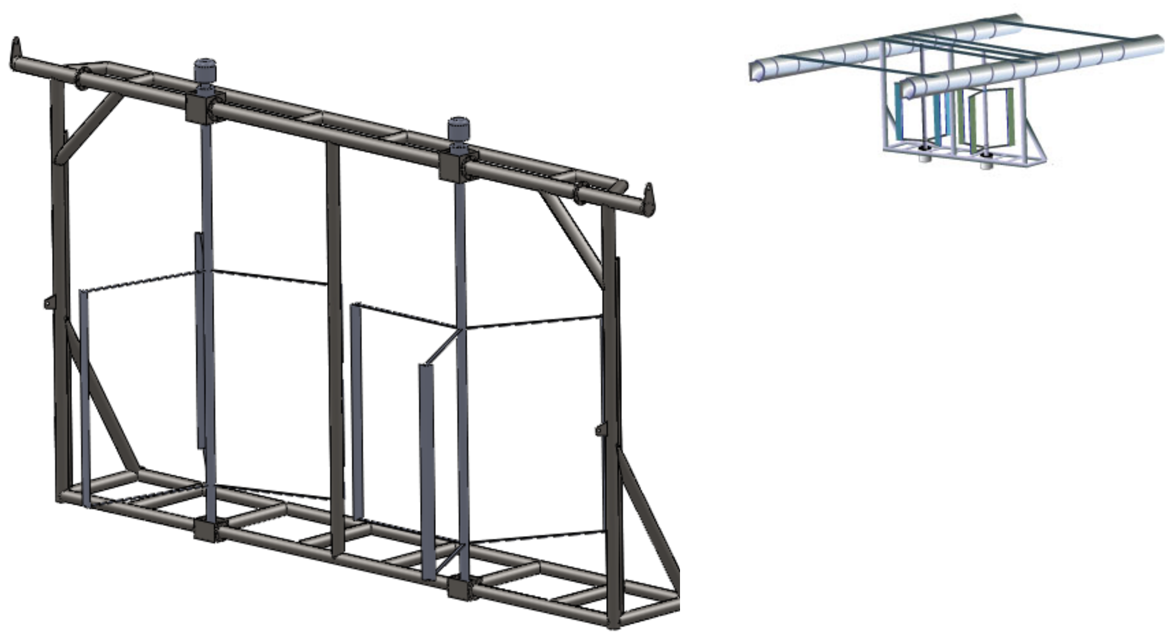

Figure 4-10. Rotor frame with rotors.

The central vertical support as well as the downstream lateral bracing is designed to reduce both vertical and downstream deflection of the frame due to loading. Thin sheet metal fairings are used on the main vertical members to reduce the drag on the rotor frame. Mooring attachment points for the device are located on the rotor frame at the vertical centerline of the rotor drag.

Material specifications for the rotor frame are listed in Table 4-6.

Table 4-6. Rotor frame material specifications.

Material	Steel (A36, A500) 0.2 m (8-in.) Schedule 40 Pipe
Yield Strength	248 MPa (36 ksi)
Width	19 m
Height	9.5 m

As described in Manufacturing Strategy and System Component Costs, Section 2.3.2.1, the device structural cost data for different unit scales was estimated by using a steel manufacturing cost model previously developed by Re Vision Consulting (Previsic et al. 2004). This model provided insight into the manufacturing cost drivers.

4.3.1.2.3 Blades and Struts

For blades and struts, glass-only materials were utilized to reduce material cost. A high fraction of unidirectional materials were needed along with thick laminates to resist the loads. Table 4-7 lists the material properties for the unidirectional and double-bias materials. Elastic properties and ultimate stress for the blade/strut laminates were determined by *rule of mixtures* (Alger 1997) with a 90% unidirectional and a 10% double-bias. The rule of mixtures provides a good approximation of single cycle (ultimate) failure stresses and was also used to determine ultimate tensile and compressive stresses.

Table 4-7. Material property data selected from SNL/MSU database.

Laminate Definition			Longitudinal Direction								Shear
			Elastic Constants				Tension		Compression		
VARTM Fabric/resin	lay-up	V_F %	E_L GPa	E_T GPa	υ_{LT}	G_{LT} GPa	UTS_L MPa	ε_{max} %	UCS_L MPa	ε_{min} %	τ_{TU} MPa
E-LT-5500/EP-3 (“uni”)	$[0]_2$	54	41.8	14.0	0.28	2.63	1151	2.97	-740	-1.79	30
Saertex/EP-3 (“double bias”)	$[\pm 45]_4$	44	13.6	13.3	0.51	11.8	144	2.16	-213	-1.80	----
Blade and strut laminate	90% uni, 10% double bias		39.0	13.9	0.3	3.55	1051	n/a	-687	n/a	n/a

E_L – Longitudinal modulus, υ_{LT} – Poisson’s ratio, G_{LT} and τ_{TU} – Shear modulus and ultimate shear stress, UTS_L – Ultimate longitudinal tensile strength, ε_{MAX} – Ultimate tensile strain, UCS_L – Ultimate longitudinal compressive strength, ε_{MIN} – Ultimate compressive strain.

Wind turbine design standards were used to determine a combined safety factor. A factor for loads of 1.1 was used for the extreme load condition selected for these analyses, which is considered an abnormal condition. A factor for materials of 2.205 was used, which assumed state-of-the-art manufacturing and includes aging and temperature effects. Therefore, the combined safety factor for materials and loads is 2.43.

For the 90/10 laminate, the allowable stresses were: 432 MPa for the allowable tension, and -282 MPa for the allowable compression. These were determined using the combined safety factor of 2.43. Compressive stress was the design driver.

Flap-wise loads for the rotor azimuth position with the largest loading (54-degree location) were selected for the blade design. We did not consider edge-wise and torsional loads in this design iteration because the flap-wise loads were considerably larger. Inertial loads were also not included as they were estimated to be small compared to the hydrodynamic loads.

For the strut design, we considered two load scenarios: 1) Land-based fabrication—the dry weight of blades and struts during fabrication, and 2) operations—the "wet" weight of blades and struts plus the hydrodynamic flap-wise loads during operation. The "wet" weight is determined as the dry weight of the blade/strut minus the weight of water displaced by the blade/strut. Hydrodynamic loads were determined using the CACTUS code (see Section 4.3.1.1).

To account for the blade/strut attachment joint, we assumed the blades were solid in cross section from the blade strut attachment point to 0.807 m along the span. To reduce the blade's weight, we designed a shell laminate from the 0.807-m span to the blade tip (2.42 m). No shear webs were included in this design. We designed the shell thicknesses along the span conservatively (with respect to local span-wise bending stress) to account for the potential need of additional weight of shear webs that may be needed to prevent shell buckling. Therefore, the shell thickness was determined according to the loads. The PreComp code (Bir 2007) was used to determine the blade cross-sectional properties for the outboard sections. The resulting tapered half-blade mass was 45.2 kg. For comparison, a solid, tapered half-blade (2.42 m in length) with 0.4-m root chord and 0.24-m tip chord has mass of 63.2 kg. The design root bending moment, corresponding to the maximum load during the extreme operational condition, for the half-blade was 34,437 N-m. The resulting root bending stress was 169 MPa, which is significantly less than the allowable of 282 MPa.

Figure 4-11 shows a plot of the blade stress distribution along the half-blade span. The blue curve represents the designed blade with a mass of 45.2 kg, while the red curve represents a solid blade with 63.2-kg mass. The plot demonstrates that a sizeable stress margin exists with respect to the allowable stress. Alternatively, this margin may allow for deployment in more energetic sites than the current reference site.

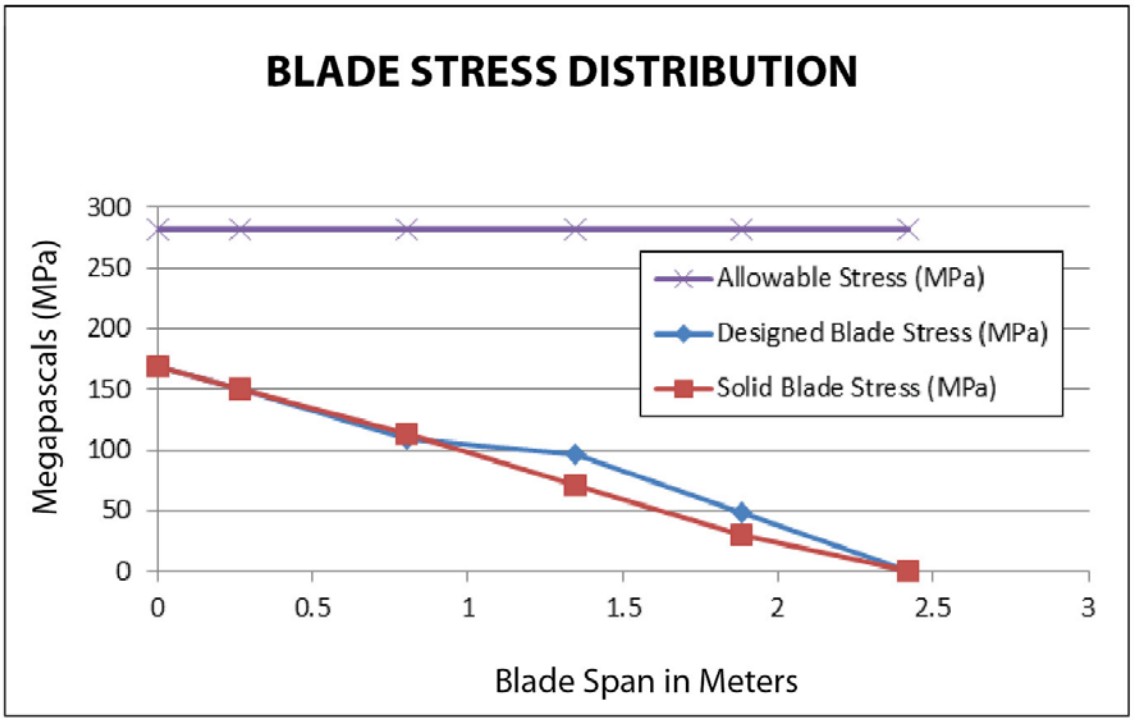

Figure 4-11. Blade stress distribution.

The half-blade shell thickness is tabulated in Table 4-8. Span is defined from the root of the half-blade to the tip. Each half-blade is identical above and below the blade/strut attachment location. From 0 to 0.807 m, the blade is of solid cross section. At 0.807 m, the shell is 0.018-m thick. From 0.807 m to 1.344 m, the thickness linearly varies from 0.018 m to 0.012 m. Likewise, from 1.334 m to 1.882 m, the thickness linearly varies from 0.012 m to 0.010 m. From 1.882 m to 2.42 m, the thickness is a constant 0.010 meters.

Table 4-8. Blade thickness distribution (root = 0 m and tip = 2.42 m).

Span (m)	Chord (m)	Shell thickness (m)
0	0.4	Solid
0.269	0.382	Solid
0.807	0.346	0.018
1.344	0.311	0.012
1.882	0.275	0.010
2.42	0.24	0.010

To account for the blade-strut attachment joint (see Figure 4-12) as well as the strut/tower attachment joint, the initial 0.25 m at each end of the strut was designed to be of solid cross section. A constant strut chord of 0.36 m was analyzed, which is in line with the current blade/strut attachment joint design (see the next section). The loads that were considered for the strut analysis include a uniform distributed 3-kN/m hydrodynamic load, the weight of the blades at the tip of the strut, and the distributed strut weight. The blade and strut weights were considered for both the dry and wet cases. We determined that the root bending moment for the dry case (land-based fabrication) was 4,454 N-m and for the wet case (during operation) 17,166 N-m. Therefore, the wet case was chosen for analysis. The interior shell, between the solid end sections of 0.25-m length, was designed such that the entire load (17,166 N-m) could be carried at any point along the span (to be conservative). The maximum stress in the shell section was determined to be 149 MPa, which is significantly less than the 282 MPa allowed. The design mass of the strut was 58.8 kg. For comparison, a solid strut would have mass of 100.6 kg.

The strut shell thickness is tabulated in Table 4-9. Span is defined from the root of the strut (at the strut/tower connection) to the blade/strut attachment. From 0 to 0.25 m, the strut is of solid cross section. At 0.25 m, a shell of 0.010-m thickness begins. From 0.25 m to 2.73 m, the thickness is constant 0.010 m. From 2.73 to 3.23 m, the strut is of solid cross section.

Table 4-9. Strut thickness distribution.

Span (m)	Chord (m)	Shell thickness (m)
0	0.36	Solid
0.25	0.36	0.010
2.73	0.36	0.010
3.23	0.36	Solid

NOTE: Root = 0 m and blade attachment point = 3.23 m.

The blade-strut attachment design assumes the strut and two semi-blades will be permanently bonded together with a “tee” joint with mortise-and-tenon connections, as shown in Figure 4-12. The length of each tenon is about 150 mm and the interface between parts is about 100 mm from the center of the tee joint.

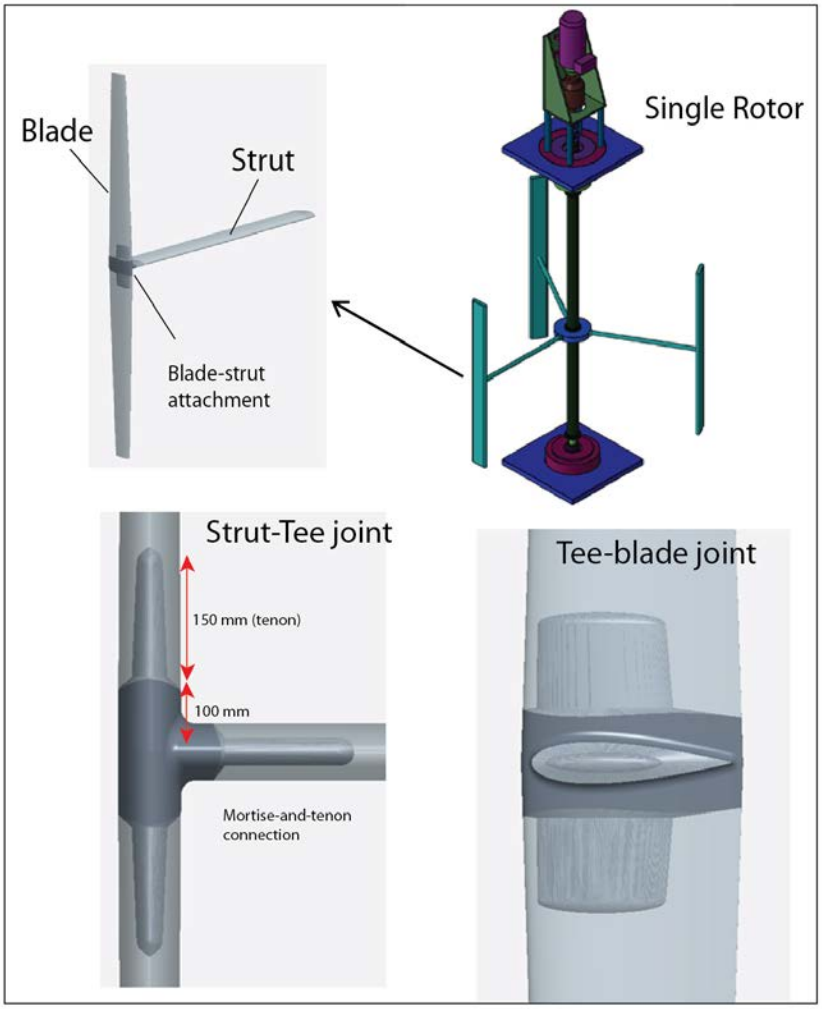

Figure 4-12. Blade-strut attachment design.

There are two attachments to be analyzed: 1) the strut-tee attachment and 2) the tee-semi-blade attachment.

The solid model of one semi-blade was imported into ANSYS BladeModeler software for a static analysis. The goal of this analysis was to find the shear stress at the joint surfaces.

The semi-blade was loaded with the maximum hydrodynamic forces of 9 kN in the tangential direction toward leading edge and 29 kN toward the center of rotation. These forces were applied at the approximate load center of 1.72 m from the semi-blade root.

After a *brief* consideration of available adhesives, Plexus MA550 was selected for the first design cycle because this product is classified as a marine adhesive and Plexus adhesives are commonly used to build wind blades. Plexus MA550 has a lap shear strength of 8.9 to 12.4 MPa.

Figure 4-13 shows the shear stress results. For most of joint interface, the shear stress is around 1.1 MPa; however, there are stress concentrations that bring the maximum stress up to 17 MPa. This initial analysis indicates that an all-adhesive joint is feasible, but additional attention is required to stress concentrations in the detailed design.

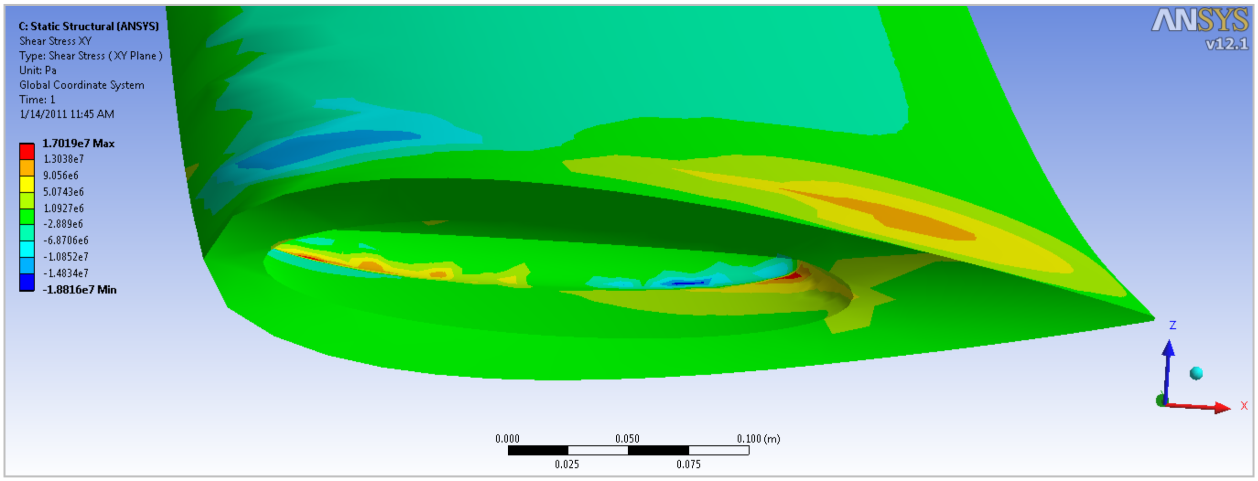

Figure 4-13. Shear stress at the tee/blade joint.

NOTE: This figure was created using ANSYS BladeModeler software. Information available at: www.ansys.com/Products/Simulation+Technology/Fluid+Dynamics/Turbomachinery+Products/ANSYS+BladeModeler.

The strut/tee joint design was analyzed with some basic hand calculations. The highest axial force directed outward is -35.92 kN and occurs at 324 degrees rotor azimuth. The highest axial force directed inward is 57.6 kN and occurs at 54 degrees rotor azimuth.

Centrifugal force assuming a full-blade weight of 2x (45.2 kg) = 90.4 kg and rotor speed of 14 RPM (1.466 rad/s) is

$$F = -mr\Omega^2 = -(90.4)(3.225)(1.466)^2 = -0.63 \text{ kN}$$

When the axial force on the strut is directed inward, the load is offset by the centrifugal force of the blade weight. When the axial force on the strut is directed outwardly (negative), the axial force and centrifugal force combine to give a greater load. Given the small magnitude of the centrifugal force, we use the 57.6-kN inward axial force as the design driver and consider the centrifugal force to be negligible.

The required surface area of the bonded joint can be calculated given the design load and allowable shear stress of the adhesive. We use the same combined safety factor of 2.43 that was used previously.

$$A = SF \times \frac{F_{axial}}{\tau_{allow}} = 2.43 \times \frac{57.6\text{kN}}{8.9\text{ Mpa}} = 0.0157\text{ m}^2 = 15700\text{ mm}^2$$

The bond surface area per longitudinal distance along the strut was calculated for two design cases. It was assumed that the wall thickness for a "mortise-and-tenon" style joint would be between 10 and 20 mm. The surface area per joint length for the two cases is approximately 640 mm^2/mm and 500 mm^2/mm, respectively. Assuming the wall thickness will be closer to 20 mm, the required bond length to withstand the axial load is 15700 mm^2/500 mm^2 per mm = 32 mm.

Bending loads at the strut to full-blade joint have not been considered in the current analysis. In addition, allowance must be made for defects introduced during assembly. For these reasons, the bond length in the current design has been increased to 150 mm.

The "tee" component (see Figure 4-12) has a volume of 0.009 m^3. Assuming fiberglass construction with the 90/10 material specified previously, the mass is 17.2 kg.

Table 4-10 lists the inputs of material weights for the rotor cost model. The estimated rotor production cost was $13.38/kg.

Table 4-10. Rotor cost model inputs.

Parameter	Value
Single Blade Mass	90.4 kg
Single Strut Mass	58.8 kg
Total Single Rotor Mass (3 Blades + 3 Struts)	447.6 kg

4.3.1.3 Power Conversion Chain (PCC) Design

The PCC was designed by Applied Research Laboratory (ARL) at Pennsylvania State (Beam et al. 2011b). Figure 4-14 shows an exploded view of the PCC from the driveshaft to the generator. The overall arrangement, shown in Figure 4-15, consists of the following key components:

- Generator and gearbox in shovel mount (illustrated in Figure 4-15)
- Shafts and bearings
- Power conditioning electronics on platform (not shown)
- Drivetrain assembly, including rotor driveshaft, bearings and U-joint

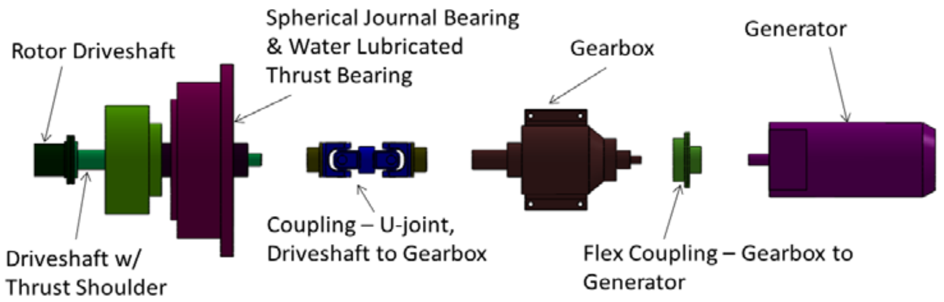

Figure 4-14. Coupling of rotating components.

As illustrated in Figure 4-15, the PCC is oriented vertically. The entire assembly is located above the water surface on the pontoon platform and, therefore, does not require additional water sealing, unlike the RM1 PCC, which is completely submerged.

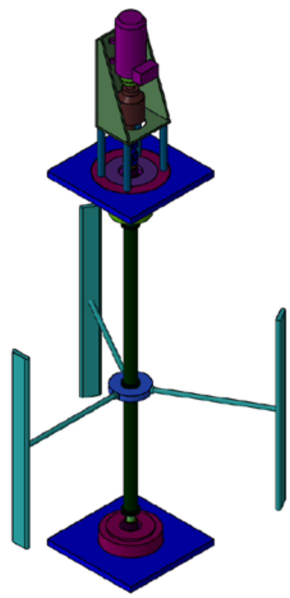

Figure 4-15. Overall component configuration.

Referring to Figure 4-14, the drive train includes a 254 mm diameter modular drive shaft fabricated from a Schedule 80 stainless steel pipe. The mounting shaft bearings within spherical seats can operate in excess of 12 000 rpm. Journal bearings allow the shaft to float axially. The design specifies a Rexnord 13.8:1 ratio gearbox with an advertised efficiency of 97% (94% overall). An ABB 60 Hz generator with a 90% efficiency generates a voltage of 460 V and 53 kW of power at 146 rpm. Details of the drive train design are given in Beam et al. 2011b.

Table 4-11 lists a weight breakdown of the PCC components. Note that nearly 70% of the total internal weight comes from the gearbox and the motor.

Table 4-11. PCC component weight breakdown.

Component	Weight (Mg)	%
Motor	1.59	42.7
Gearbox	0.91	24.4
Generator	0.50	13.4
Couplings	0.11	3.0
Drive System	0.01	0.3
Control System	0.01	0.2
Flow Sensors	0.18	4.9
Transformer	0.09	2.4
Cooling System	0.16	4.3
Switch Gear	0.05	1.2
Cables & Connectors	0.005	0.1
Monitoring Sensors	0.005	0.1
System Enclosure	0.08	2.2
Total	3.7	100

Uncertainty for the turbine PCC design and component costs was generally low due to the detailed design and commercial off-the-shelf (COTS) hardware specified for the system.

4.3.1.4 Mooring Design

The RM2 turbine pontoon is moored to the riverbed by attaching a mooring leg to each side of the turbine frame as shown on Figure 4-16. Using two anchor legs ensures that the unit can maintain station if one leg fails.

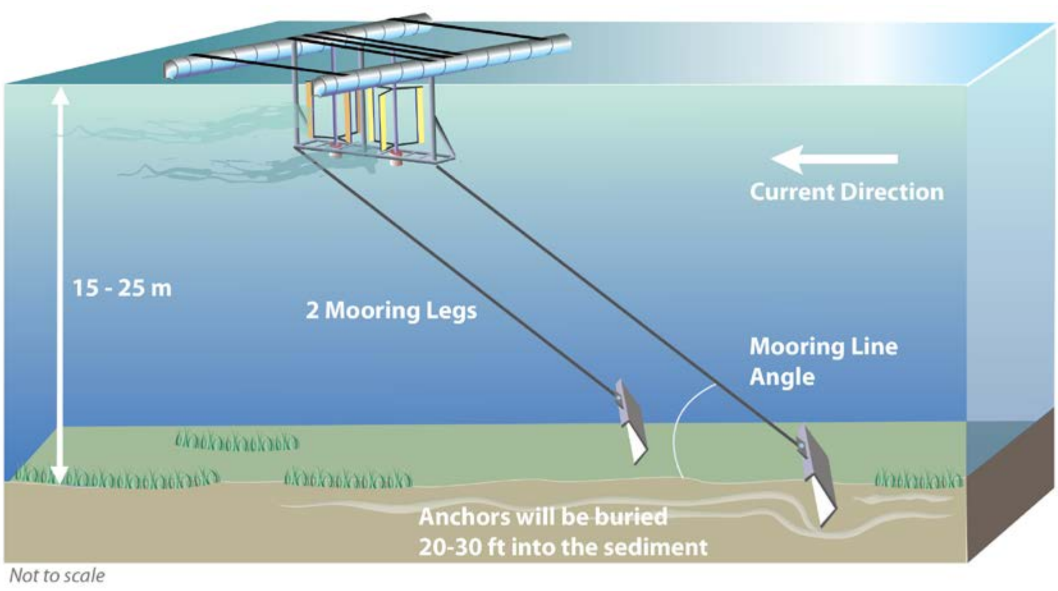

Figure 4-16. Mooring configuration.

Mooring design details are given in Re Vision (2011b). Mooring legs are stainless steel chains and are connected to a plate anchor at the riverbed. Chain, rather than wire or synthetic cables, was selected to withstand higher loads caused by debris impacts and fouling. Mooring components and their weights are summarized in Table 4-12.

Table 4-12. Mooring components and weights.

Component	Size	Unit Weight	QTY
Anchor Joining Link	25 mm	6.5 kg	4
Chain	25 mm	14.2 kg/m	110 m
Chain Joining Link	25 mm	2.3 kg	2

A 75-meter long mooring line was considered adequate to maintain a 20 degree angle from the seabed to the device and allow for sufficient anchor embedment depth. To determine the adequate size for both the chain anchor legs and the plate anchors, both rotor drag and pontoon drag were taken into account in our analysis. We calculated the static current load on the pontoons would be 0.4 kN, much less than the rotor drag load of 68 kN per rotor (DoD 2005). At a mooring line angle of 20 degrees, the vertical force on the moorings is about 47 kN. The total tension on the chain is 72 kN per rotor, and for this analysis, we assumed each chain will hold half of the load. We applied a minimum factor-of-safety (FOS) for the break strength of 4.0. With a 72 kN load per rotor and a 4.0 minimum FOS, we used a design load of 288 kN. To provide an adequate design factor, we selected a 25 mm grade two stud-link chain with a breaking strength of 372 kN, resulting in a FOS of 5.1. We selected this chain size because it is commonly stocked by marine suppliers (Anchor Marine and Industrial Supply 2011).

For anchoring, we selected a 0.9 m by 1.2 m plate anchor similar to the one shown in Figure 4-17 to provide an adequate design factor and provide a reasonable cost estimate. This embedment plate anchor is driven about 6.1 to 9.1 m (20 to 30 ft) into the riverbed soil to provide adequate holding strength. Plate embedment anchors should have a minimum FOS of 3.0 (DoD 2005). Using the rotor drag loads, the total vertical load is near 100 kN, and the anchor is more than adequate. Although a smaller plate anchor could be used, the cost of the larger anchor system and its installation is not significantly higher. A detailed mooring design would depend on the river bed substrate characteristics and would need to be proof-load tested prior to operation to verify its strength.

Figure 4-17. Plate anchor with pad eye.

4.3.2 Manufacturing and Deployment (M&D) Strategy Module

4.3.2.1 Manufacturing Strategy and Costs

As described in Manufacturing Strategy and System Component Costs, Section 2.3.2.1, the M&D Strategy Module assumes the use of COTS components (e.g., generators and anchors) and conventional materials (e.g., A36 steel, standard fasteners, mooring cables, etc.) where possible. Manufacturing costs of system components for RM2 at different array scales (1, 10, 50 and 100 units) are summarized in Figure 4-18, Figure 4-19, and Table 4-13. Figure 4-18 shows the structural cost breakdown and Figure 4-19 shows the cost breakdown for the Energy Capture and PCC components by array scale.

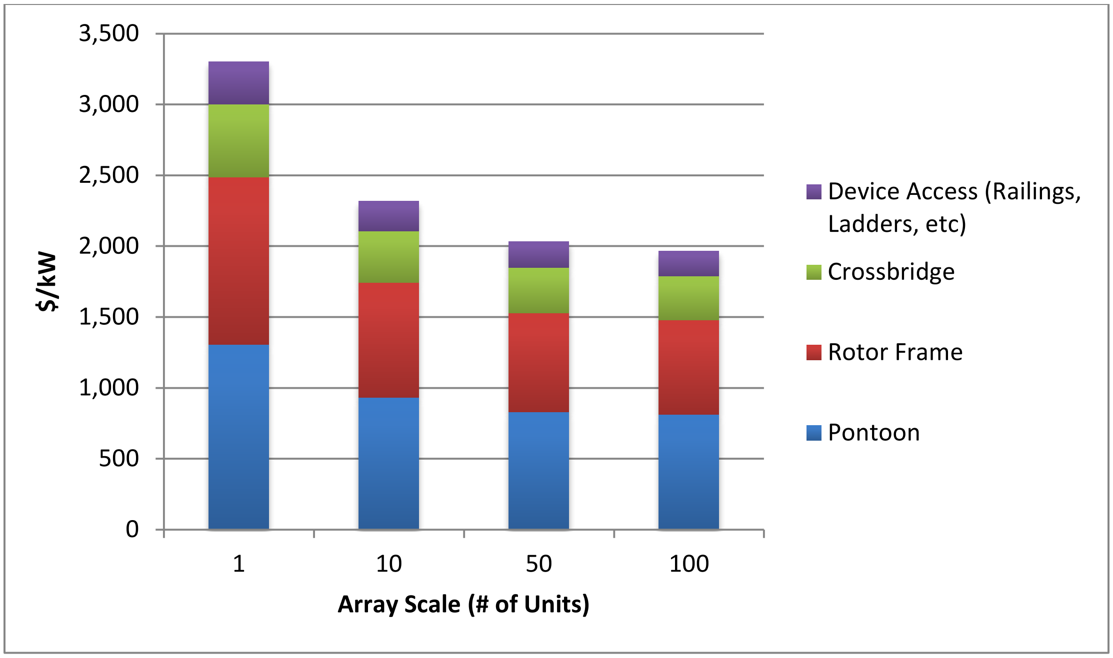

Figure 4-18. Structural cost breakdown ($/kW) per deployment scale.

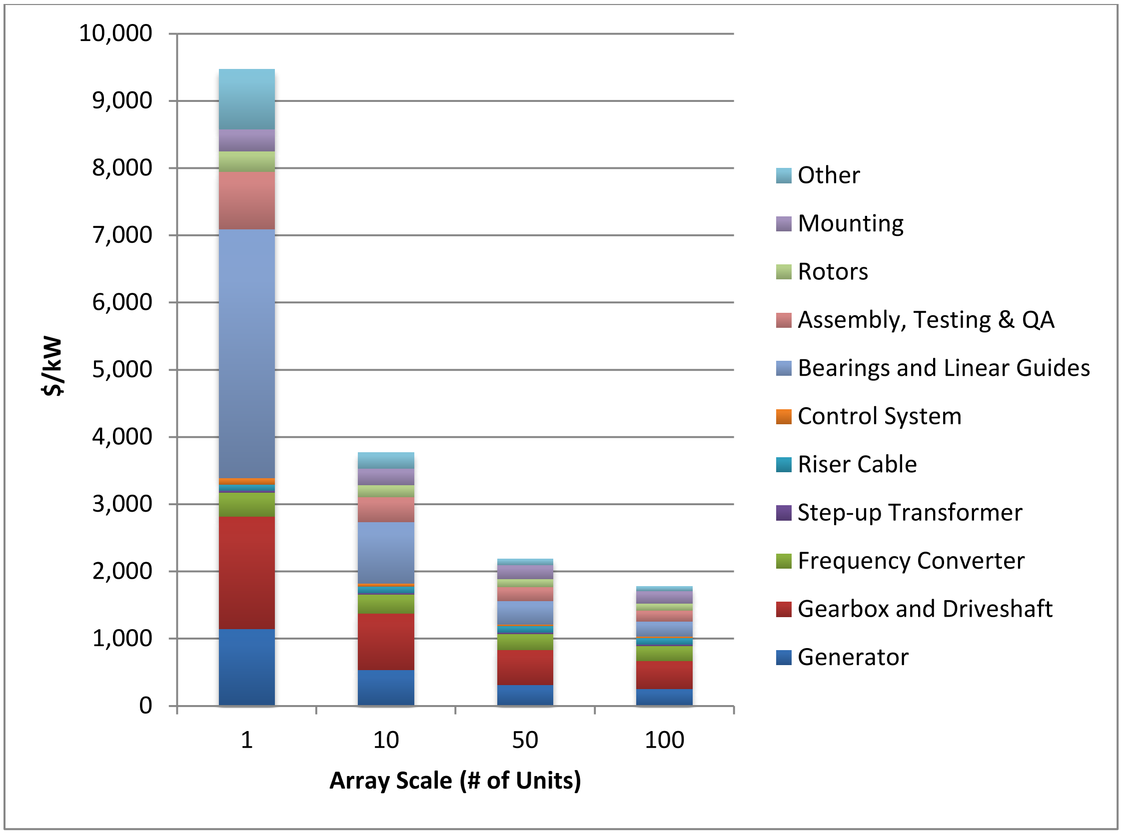

Figure 4-19. Cost breakdown ($/kW) for the energy capture and PCC components per deployment scale.

The cost breakdown of the mooring components is shown in Table 4-13. The components consist of two plate anchors, 120 m of 38-mm chain mooring, and shackles and other mooring hardware.

Table 4-13. Mooring component cost breakdown ($/kW) per unit.

	Cost ($/kW)
Mooring lines/chain	134
Anchors	89
Connecting Hardware (shackles etc.)	19
Total	242

NOTE: This table assumes that the mooring component costs remain consistent regardless of number of units deployed.

4.3.2.2 Deployment Strategy and Costs

The deployment strategy accounts for the installation of the RM2: 1) mooring system, 2) subsea cable infrastructure, and 3) the devices themselves (including commissioning). We assumed a DP-2 class vessel (described in Section 3.3.2.2) would be mobilized from the Gulf of Mexico region and used for the mooring installation. A separate Cable Installation Vessel would be used for cable installation, and the device would be connected to the mooring system and commissioned using the same vessel that will be used for O&M. Total installation costs were developed using the assumed day rates for these vessels and assumed installation durations presented in Table 4-14. Although costs were determined for 1, 10, 50, and 100 units, the table only compares results for 1 and 100 units.

Table 4-14. RM2 M&D Strategy Module cost assumptions.

	1 Unit			100 Units		
Operational Detail	**No. Days**	**Vessel Day Rate**	**Cost**	**No. Days**	**Vessel Day Rate**	**Cost**
Mooring Installation						
Mobilize Installation barge	7	$11,875	$83,125	7	$11,875	$83,125
Set and Move Installation Barge Anchors	2	$30,275	$60,550	12	$30,275	$363,300
Installation Activities	1	$21,100	$21,100	50	$21,100	$1,055,000
Demobilization	4	$11,875	$47,500	4	$11,875	$47,500
Operational Contingency	0.3	$8,800	$2,640	6.2	$8,800	$54,560
Total	**14**		**$214,915**			**$1,603,485**
Cable Shore Landing						
Horizontal Directional Drilling (distance is 500 m)			$170,000			$170,000
Cable Installation						
Shore End of Trunk Cable (assumes one)	2	$21,100	$42,200	2	$21,100	$42,200
Lay cable between junction boxes	0	$21,100	$0	9	$21,100	$189,900
Operational Contingency	0.2	$8,800	$1,760	1.1	$8,800	$9,680
Dive Support and Shore-Side Ops			$65,000			$65,000
Total			**$108,960**			**$306,780**
Device Installation						
Device Assembly (Shoreside)			$33,260			$181,750
Device Installation (River-Side)	`		$1,280			$0
Total			**$34,540**			**$181,750**

NOTE: Ops Day-rate for 3-person device installation crew:
$1,080 + $200 for fuel and consumables => $1,280.

Cable costs were generated through vendor estimates for unit deployments of 1, 10, 50, and 100 units. At scales of 1 and 10 units, only one subsea cable was assumed to be needed, but for the larger arrays of 50 and 100 units, two cables were assumed. The cost for the cable system was $0.17, $0.32, $3.12, and $7.87M for 1, 10, 50, and 100 units, respectively.

Figure 4-20 shows the total installation cost per RM2 device at different deployment scales. Single unit deployment cost is dominated by the cost to install the mooring system and the cable shore landing. The installation cost, in terms of $/kW, is significantly higher for the deployment of a single unit than an array (even arrays of only 10 units). The per-kW cost of installation is estimated to fall from more than $5,900/kW for a single unit deployment, to approximately $800/kW for a 10-unit deployment, and just over $300/kW for a 100-unit deployment. An increase in device capacity/unit would reduce that cost.

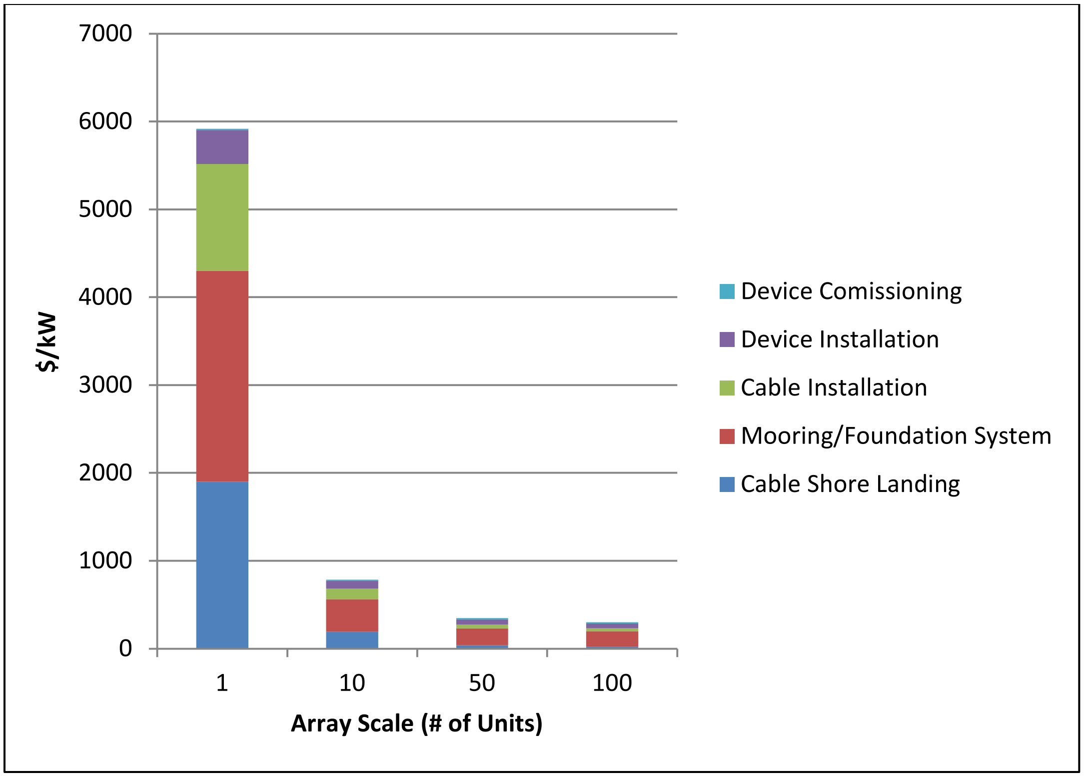

Figure 4-20. Installation cost breakdown ($/kW) per deployment scale.

4.3.3 Operations and Maintenance (O&M) Strategy Module

The O&M Strategy Module for RM2 was developed based on the RM1 strategy. Similar to the RM1 concept design, the RM2 concept design was developed to reduce O&M costs by: 1) deploying a dual-rotor system from a single platform; 2) mounting the units on a floating platform (which allows retrieval for shore-side PCC maintenance and repairs); and 3) placing the generators above water. We did not, however, include the cost of mooring line repairs for RM2 because repairs are likely to be infrequent over the life of the project.

4.3.3.1 Service Vessel Specifications

Both shore-side facilities and an adequate vessel were specified to carry out O&M activities. The service vessel requirements include: 1) a 3,000-pound crane to handle mooring lines, and 2) sufficient deck space to accommodate moorings and provide a sufficient working area, good maneuverability, and a redundant power system.

Based on discussions with a number of operators, an aluminum vessel with dimensions of 3.7 m x 11.6 m (12 ft x 38 ft) was considered to be adequate. Figure 4-21 shows an example of the type and size vessel envisioned. It would be outfitted with appropriate handling capabilities.

Figure 4-21. O&M workboat type.

NOTE: Type of workboat required as part of the operational assets.

Crew size for the vessel will likely be between three and six personnel to effectively carry out different types of operational activities. Onshore facilities require dock-space or a ramp that can be used for device haul-out and a covered warehouse equipped with appropriate cranes to perform repairs on the device components. The general discussion for the O&M Strategy Module, Section 2.3.3, details requirements and costs for the shore-side crew of technicians and administrative personnel needed for carrying out repairs and maintenance activities.

4.3.3.2 Failure Rates

Section 2.3.3.2 details the failure (reliability) matrix adopted for device and infrastructure (i.e., BOS) components, which accounts for the likelihood of failure of each component along with the requirements for the repair, and the number and unit cost of service trips. Because the power train of the RM2 turbine is similar to a wind-turbine, we used failure rates from a wind-turbine powertrain as an analogue (Poore and Lettenmaier, 2003). While this data is somewhat outdated, it provides likely failure rate distributions for the components of a typical wind-power drive-train and is in the public domain. Given that the major components are very similar in this application, we re-used the same data. To simplify the analysis, we simply averaged the number of failures instead of following the more typical Weibull failure-rate distribution of many of the subsystems and components. This approach was deemed appropriate, given the uncertainties in estimating failure rates for technologies with no operational experience.

From a cost assessment perspective, there are two important factors that will drive O&M schedule and cost—replacement part cost and the number and type of operational interventions. To compute replacement part cost, we assumed that failures were evenly distributed over the 20-year project life and replacement part cost was equal to the value of the part/subsystem in the original device. We then computed the number and type of interventions expected in the economic life of the project; failures were divided into two groups: repair activities that could be carried out onboard the device and activities that would require recovery to land. The high-level failure data in Table 4-15 was derived from this analysis.

Table 4-15. Failure event frequency and single unit cost.

		Total Events	Replacement Events	Part Cost ($/kW)	# Parts	# Interventions (per device-year)	$/kW-Year
Powertrain							
	Generator	272%	97%	$671	2	0.27	$33
	Gearbox	139%	139%	$509	2	0.14	$35
	Frequency Converter	160%	160%	$203	1	0.08	$16
	Step-up Transformer	10%	10%	$30	1	0.01	$0
	Switchgear	37%	37%	$37	1	0.02	$1
	Cooling System	244%	244%	$12	2	0.24	$1
	Control System	117%	59%	$49	1	0.06	$1
Rotor							
	Blades (2 rotors)	105%	53%	$166	2	0.11	$4
	Shaft (Stainless)	5%	5%	$196	2	0.01	$0
	Bearings/Couplings	44%	44%	$281	4	0.09	$6
Total				$2,155	18	1.02	$99

NOTE: Values listed are for a 100-unit project with dual-rotors for each unit. The 'Total Events' column calculates the total number of expected failures over the 20-year design life divided by the initial number of parts in the fleet and multiplies the result by 100.

Each failure event requires the recovery of the device to shore for repair. The total events column represents all failure events, even minor ones such as the repair of the generator cooling fan. The replacement events frequency is used to estimate replacement part cost and is just capturing the major failure events.

4.3.3.3 Annual O&M Costs

Based on the above number of interventions and replacement part values, the annual O&M cost was computed at different scales of deployment (Figure 4-22). Figure 4-22 shows the breakdown of the likely annual OpEx cost ($/kWh) as a function of the number of units in an array. See Section 2.3.3.4 for details on how insurance costs were estimated. Note that the post-installation monitoring is a part of environmental monitoring and regulatory compliance costed under the Environmental Compliance (EC) Module (see Section 4.3.4) and is included in the total OpEx costs shown in Figure 4-22. Initial environmental compliance and monitoring activities prior to start up would fall under CapEx as explained in the following section.

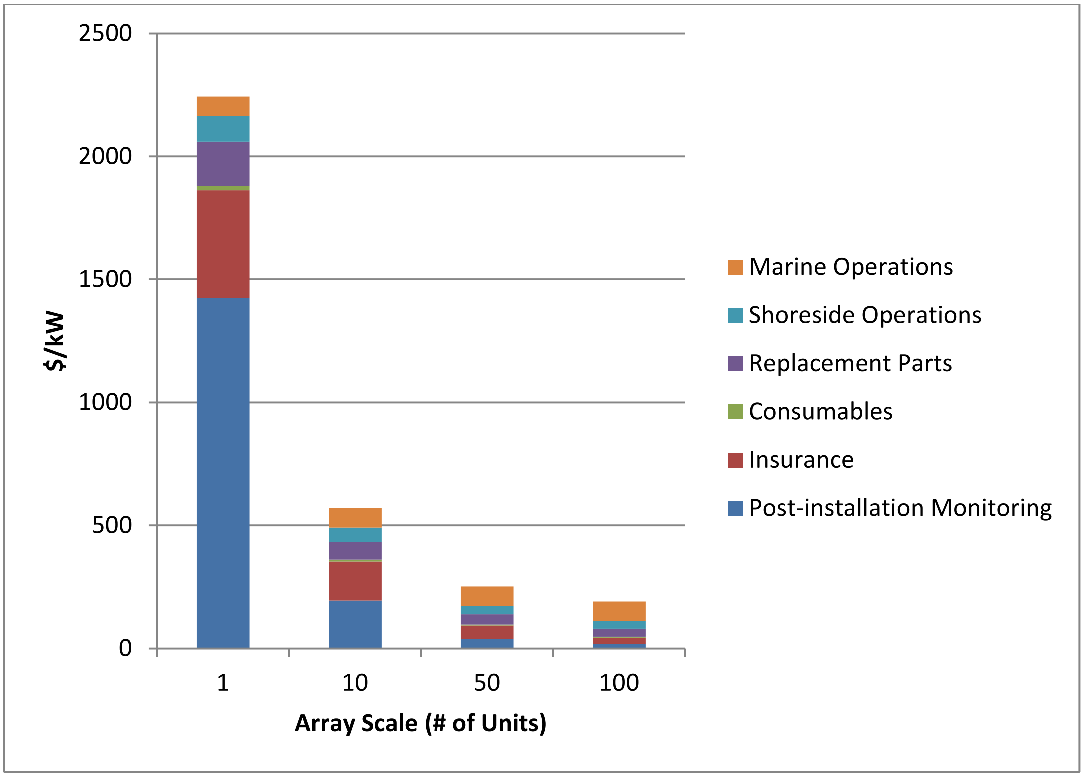

Figure 4-22. Annual OpEx cost ($/kW) per array size.

4.3.4 Environmental Compliance (EC) Module

The EC Module for RM2 is based, in part, on previous studies conducted at the RM2 reference site. Deployment of a river stream turbine requires extensive siting and permitting studies to ensure the responsible development of river stream hydrokinetic technology. The siting and permitting analysis for RM2 has been completed for the Baton Rouge reference site (USGS 07374000), a developed river with freshwater animals and habitat. This study has established cost estimates for pilot (1 unit), small commercial (10 units), and large commercial (>50 units) scale deployments. This work was completed by Copping and Geerlofs (2011) from Pacific Northwest National Laboratory (PNNL) as described in Section 2.3.4.

Rivers that are suitable for MHK energy development are often large industrialized stretches that are impacted by other anthropogenic activities. Animals and plants living in these areas may be considered to be less sensitive than those in marine waters, with the exception of animals that are under special protection (such as listed on the U.S. Endangered Species Act). Working in rivers is easier and less costly than working in marine waters; as a result, survey and study costs can be expected to be lower. In addition, environmental sensitivities may be lower in Louisiana (generic location for the river reference model) than in Washington State (tidal reference model, RM1) and California (wave reference model, RM3), resulting in lower costs for engaging in the public process and conducting many permitting activities.

Each phase requires individual environmental studies, based on regulatory requirements, and the specific animals, habitats, and ecosystem processes found in the proposed location. A cost range has been developed to estimate the capital costs of monitoring equipment, as well as the costs of carrying out specific studies, sample analysis, and the analysis and interpretation of the data. There is considerable uncertainty associated with each cost estimate, with the greatest uncertainties for post-installation monitoring. No costs have been assigned for long-term mitigation activities that will be required for environmental risks. The total estimate of environmental CapEx normalized by installed power is summarized on Figure 4-23. for pilot and commercial scales.

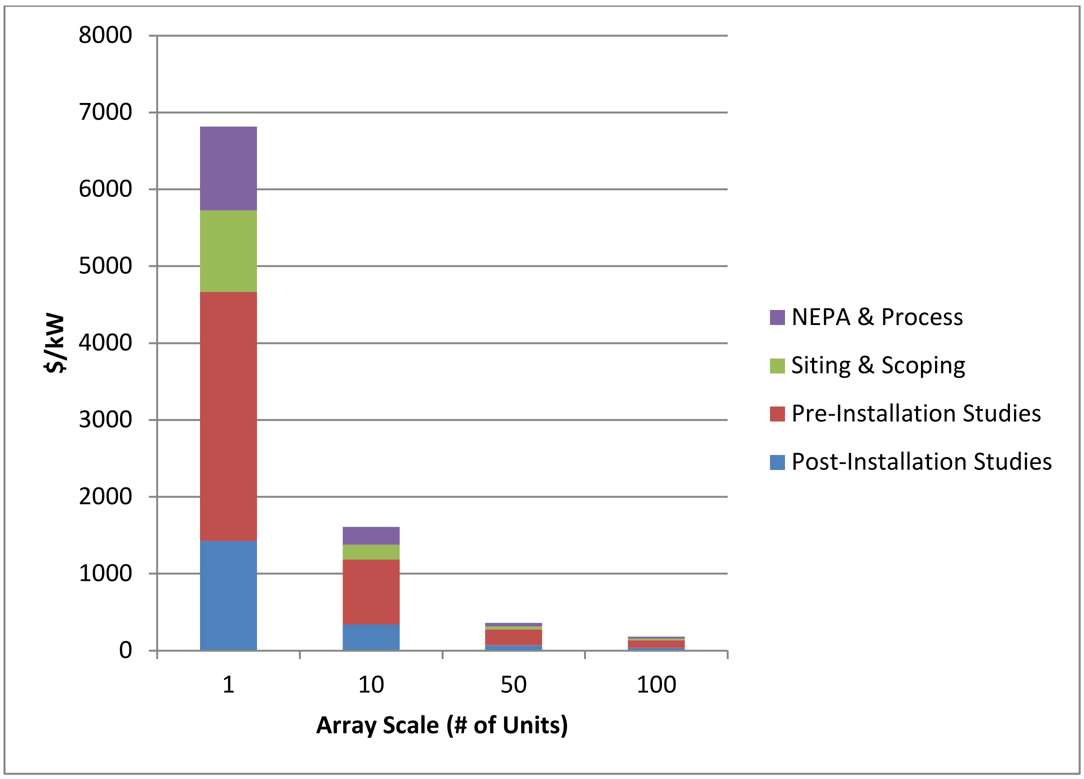

Figure 4-23. Total environmental CapEx estimate per deployment scale (1, 10, 50 or 100 units).

High and low bounds for the environmental compliance cost estimate were approximately +/- 20% relative to the mean value shown in Figure 4-23. This is carried forward into the analysis of the array cost and economic assessments. Annually recurring costs for post-installation monitoring over the life of the project are shown in Figure 4-24. As with RM1, all costs normalized by installed power decrease significantly for larger arrays.

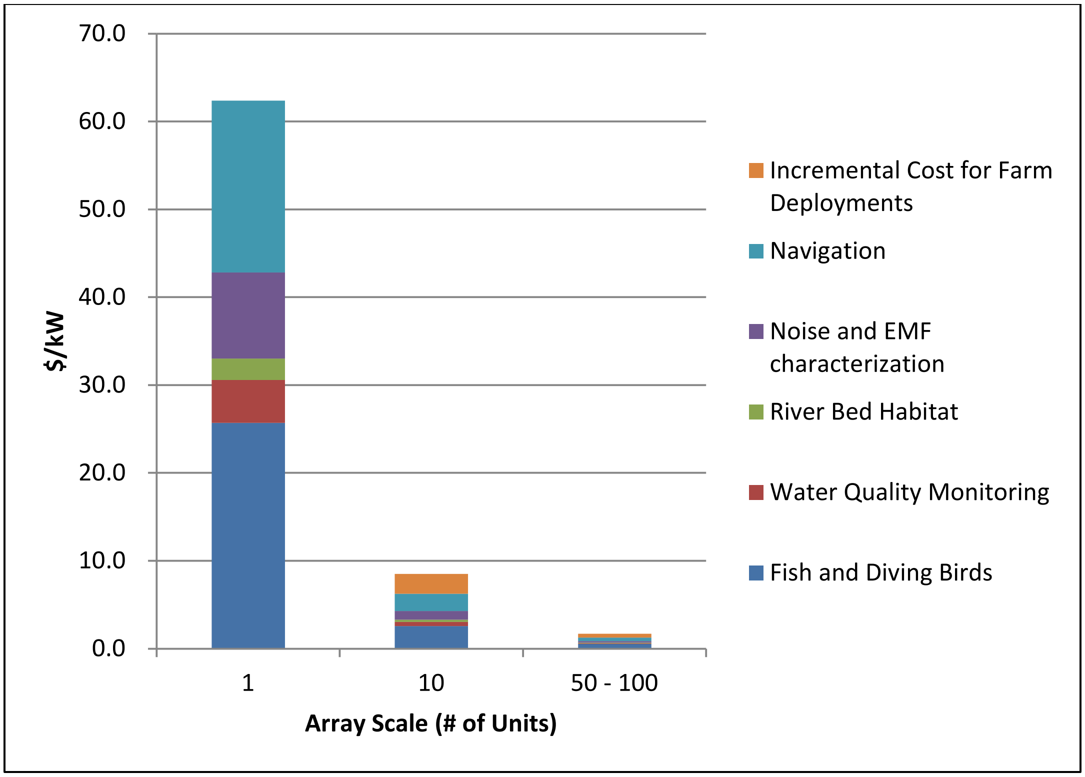

Figure 4-24. Annual cost of post-installation monitoring per deployment scale.

4.4 LCOE Calculation

The LCOE estimate for a 10-unit RM2 array is 80 cents/kWh based on the FCR, AEP, CapEx and OpEx estimates described below. The estimated AEP for this array is 2,044 MWh per year. Table 4-16 gives a detailed breakdown of the LCOE estimate. The largest cost contributors to the LCOE is M&D, which accounts for approximately 45% of the LOCE, followed by O&M costs, which account for approximately 31% of the LCOE. These findings indicate that the most critical area for targeting potential cost savings is M&D.

Table 4-16. RM2 LCOE breakdown by cost category (10-unit array).

	cents/kWh	% of total LCOE
Development	11.0	13.7%
M&D	36.3	45.2%
Subsystem Integration & Profit Margin	3.0	3.7%
Contingency	5.0	6.3%
O&M	25.0	31.1%
Total	80.3	100.0%

Figure 4-25 shows the total LCOE for RM2 and shows how the cost of energy decreases as a function of installed capacity.

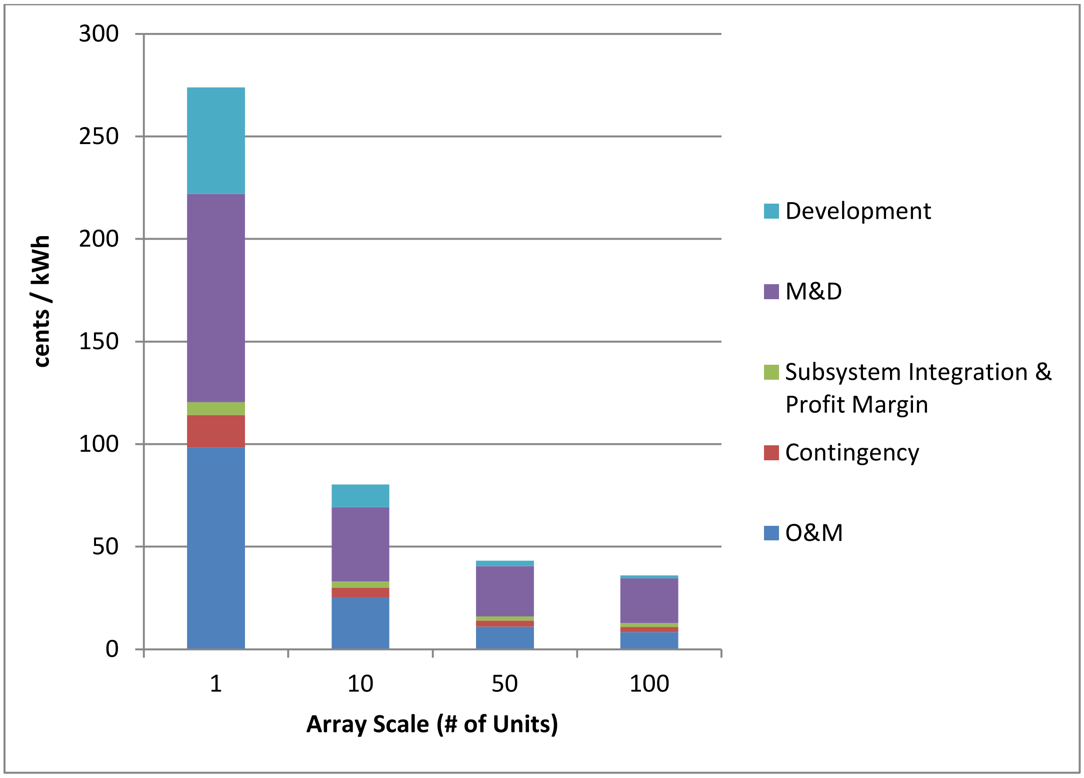

Figure 4-25. High-level LCOE (cents/kWh) breakdown per deployment scale for RM2.

The total CapEx for a single unit deployment was estimated to be approximately $35,600/kW, whereas the total CapEx per unit for a 100-unit array was estimated to be $5,600/kW. While there are some cost savings to be expected simply by increasing the manufacturing and fabrication volume from 1 to 100, major per-unit cost savings are also expected to be realized within the installation cost category. Figure 4-26 shows the contribution of capital cost (CapEx) to the LCOE.

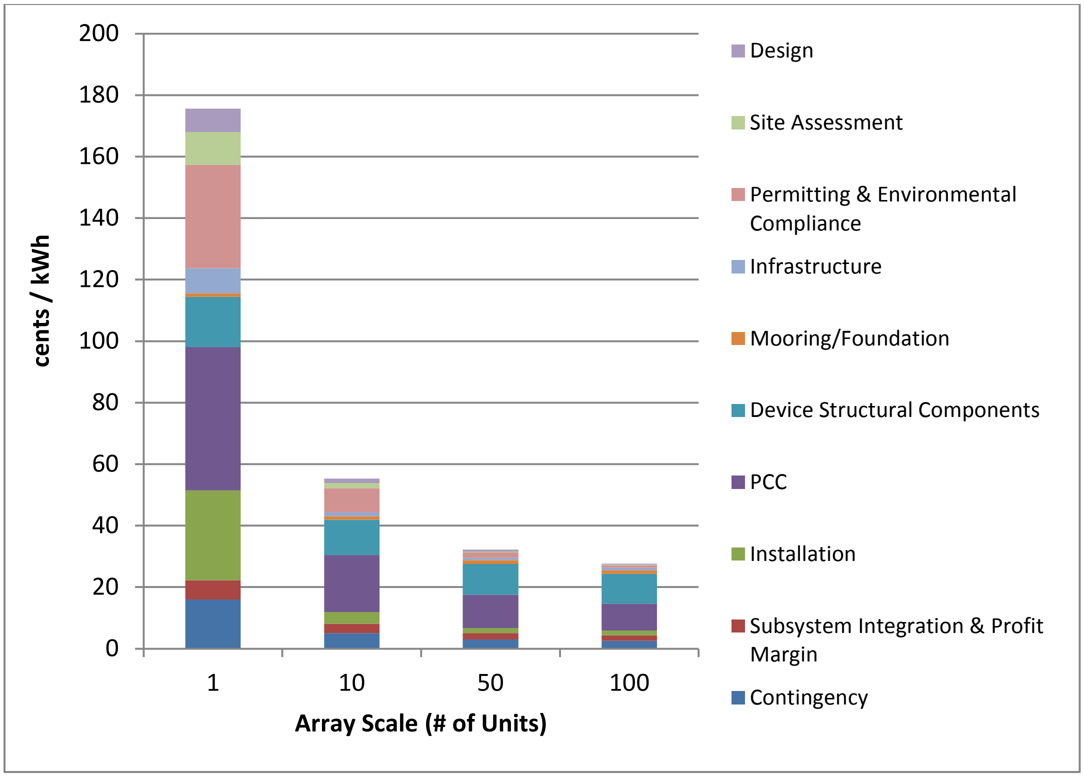

Figure 4-26. RM2 CapEx contributions to LCOE (cents/kWh) per deployment scale.

A detailed breakdown of major CapEx cost categories, in terms of LCOE is provided in Table 4-17.

Table 4-17. Breakdown of RM2 CapEx contributions to LCOE (10-unit array).

	cents/kWh	% of total CapEx
Design	1.5	2.6%
Site Assessment	1.6	2.9%
Permitting & Environmental Compliance	7.9	14.3%
Infrastructure	1.2	2.2%
Mooring/Foundation	1.2	2.2%
Device Structural Components	11.4	20.7%
PCC	18.6	33.6%
Installation	3.9	7.0%
Subsystem Integration & Profit Margin	3.0	5.4%
Contingency	5.0	9.1%
Total	55.3	100.0%

Annual OpEx for a single unit deployment was estimated to be approximately $2,240/kW, whereas the annualized OpEx per unit for a 100-unit array was estimated to be $190/kW. Similarly to the capital cost contributions to LCOE, the operational cost contributions to LCOE are shown in Figure 4-27.

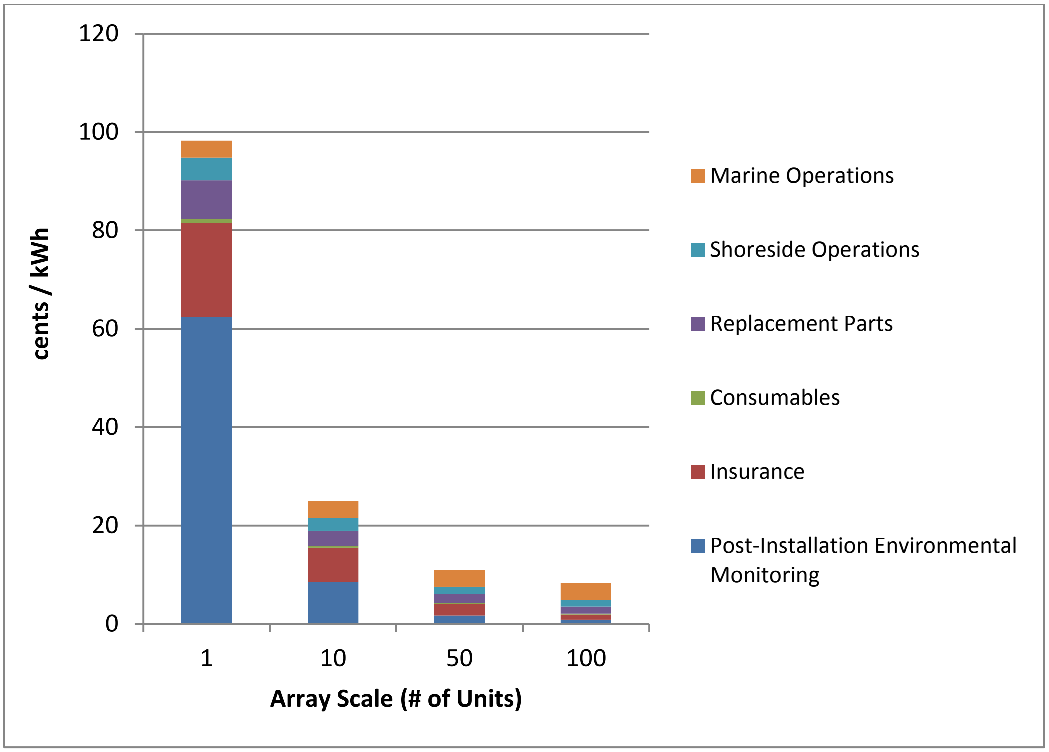

Figure 4-27. RM2 OpEx contributions to LCOE (cents/kWh) per deployment scale.

A detailed breakdown of major OpEx cost categories, in terms of levelized cost of energy, is listed in Table 4-18.

Table 4-18. Breakdown of RM2 OpEx contributions to LCOE (10-unit array).

	cents/kWh	% of total OpEx
Marine Operations	3.5	13.9%
Shoreside Operations	2.6	10.3%
Replacement Parts	3.1	12.5%
Consumables	0.3	1.3%
Insurance	7.0	27.9%
Post-Installation Environmental Monitoring	8.5	34.1%
Total	25.0	100.0%

5 Reference Model 3 (RM3): Wave Point Absorber

5.1 RM3 Description

The RM3 wave point absorber, also referred to as a wave power buoy, was designed for a reference site located off the shore of Eureka in Humboldt County, California. The concept design for this device was inspired by the Ocean Power Technology's PowerBuoy (http://www.oceanpowertechnologies.com), which is a two-body floating point absorber (FPA) designed to convert ocean wave energy into electrical power. The design of the device consists of a surface float that translates (oscillates) with wave motion relative to a vertical column spar buoy, which connects to a subsurface reaction plate (Figure 5-1 and Figure 5-2). This two-body point absorber converts wave energy into electrical power predominately from the device's heave oscillation induced by incident waves; the float is designed to oscillate up and down the vertical shaft up to 4 m. The bottom of the reaction plate is about 35 m below the water surface. The device is targeted for deployment in water depths of 40 m to 100 m. The point absorber is also connected to a mooring system to keep the floating device in position. Our RM3 design assumed a hydraulic PCC system, which is placed inside the vertical column. The optimum energy capture of a wave point absorber occurs when the system is at resonance, in other words, when the oscillating body velocity is in-phase with the hydrodynamic wave excitation force.

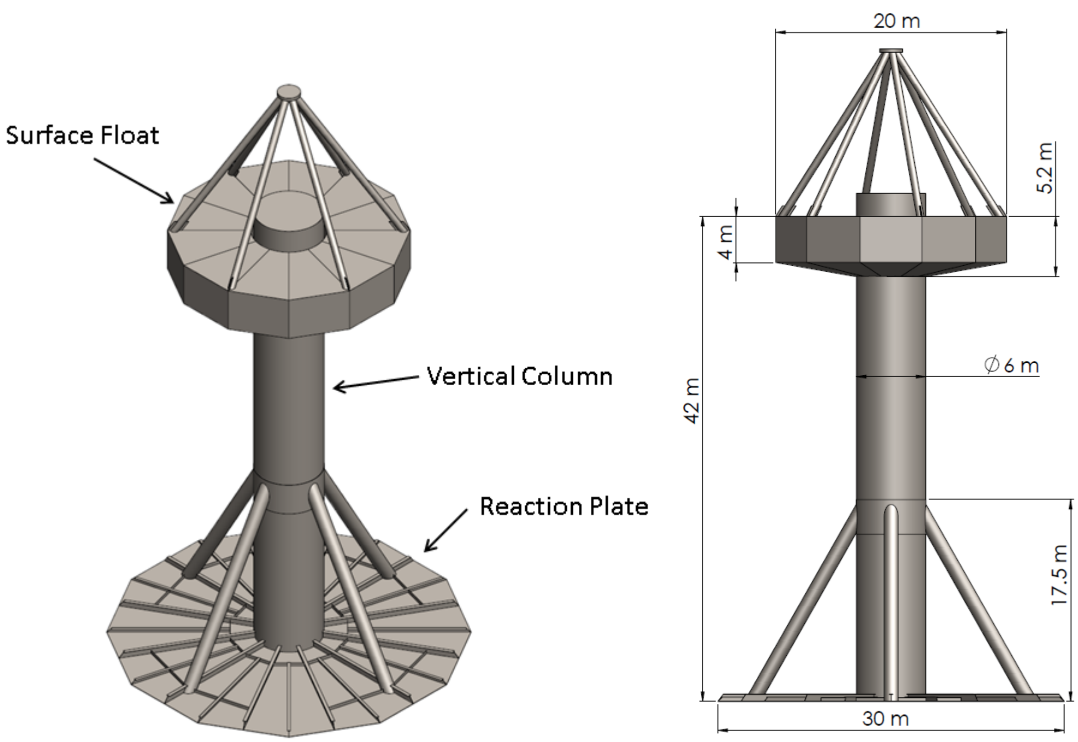

Figure 5-1. RM3 device design and dimensions.

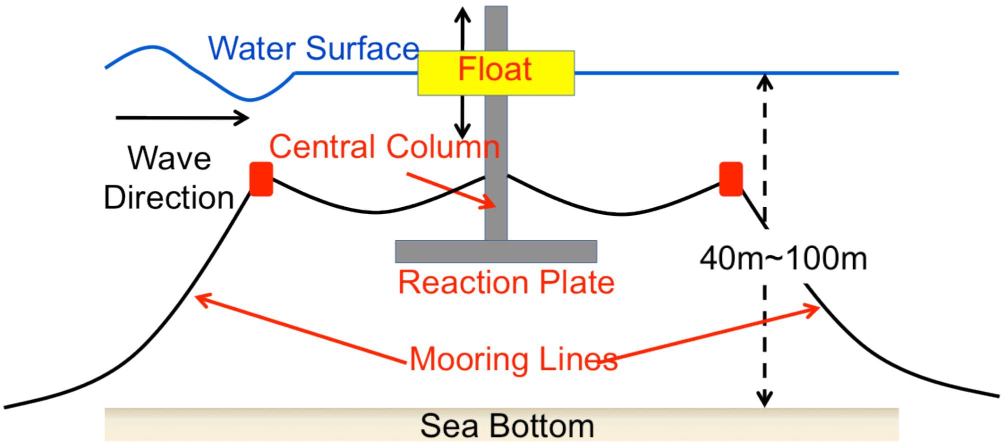

Figure 5-2. The schematic (side view) of the FPA concept design.

NOTE: The float moves up and down on the central column in relation to the reaction plate.

5.1.1 Device Design and Analysis

As noted in Design Methodology for a Single Device, Section 2.1.1, the first step in the device design process was to develop a conceptual design for a Wave Energy Converter (WEC) device appropriate for the modeled reference resource site. Once the concept design was completed, a detailed device design was developed using a combination of numerical modeling tools and testing scaled physical models. For the RM3 design and analysis, we conducted a series of experimental tanks tests and numerical analyses, including the use of reduced order radiation and diffraction numerical methods and computational fluid dynamics (CFD) simulations to determine the RM3 device's geometry and to estimate the power generation performance of the device at a potential deployment site. The annual energy capture of the RM3 design was determined based on the wave characteristics of the wave resource from the Northern California Coastal region and the power matrix of the device that gave the estimated power prediction of the device for a range of sea states. Extreme loads were determined using wave tank testing at 1:100 scale. Based on those extreme loads, we established the final structural design.

5.1.2 Arrays (Farm) Design and Analysis

As noted in Section 2.1.1, due to the sparsity of developed array optimization models, we did not perform detailed array design and analysis as described in the general methodology, and this adds to the uncertainty in the AEP estimate for arrays. In the RM3 wave point absorber analysis, we assumed a maximum of 100 units could be deployed at the reference site in order to take advantage of reduced costs through economies of scale, thus lowering the LCOE estimates. The array layout (number of units and spacing) was determined based on the bathymetry and the potential installation space available at the deployment site. The required spacing between the devices to accommodate moorings and avoid river traffic collisions was 600 m (Figure 5-3). This spacing also minimizes the fluid dynamic interaction between devices to ensure that the loss of energy in the array is negligible (Babarit 2012).

The total array capacity at 100 units is approximately 30 MW. For the main cable (cable to shore), we selected a 3-phase AC transmission cable with a voltage level of 30 kilovolts (kV). All transmission cables included fiber optic lines to allow communication from each device to shore. For the RM3 array, groups of 10 devices (only nine are shown in Figure 5-3) are connected with interconnect cables that run between individual units (Figure 5-4). Riser cables transmit electricity via a riser cable to a junction box and a trunk cable connects each junction box. Cable landing is accomplished by directionally drilling a conduit that connects the cable out to the first row of devices. This approach minimizes installation and maintenance costs.

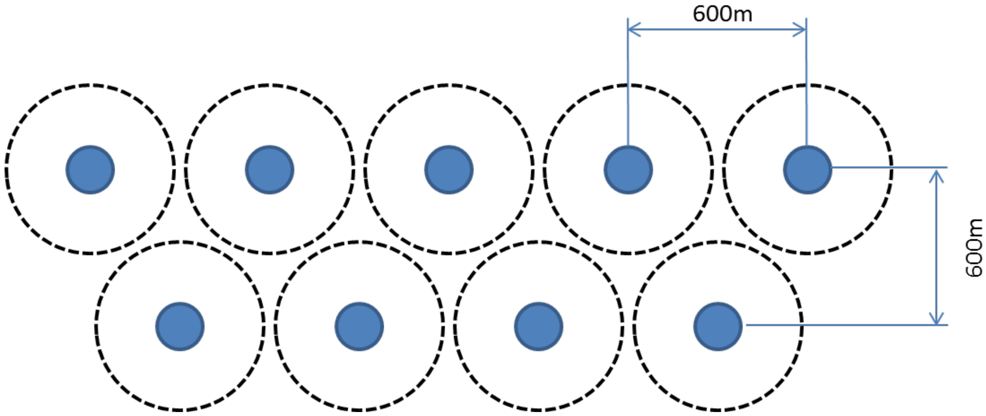

Figure 5-3. Array layout (plan).

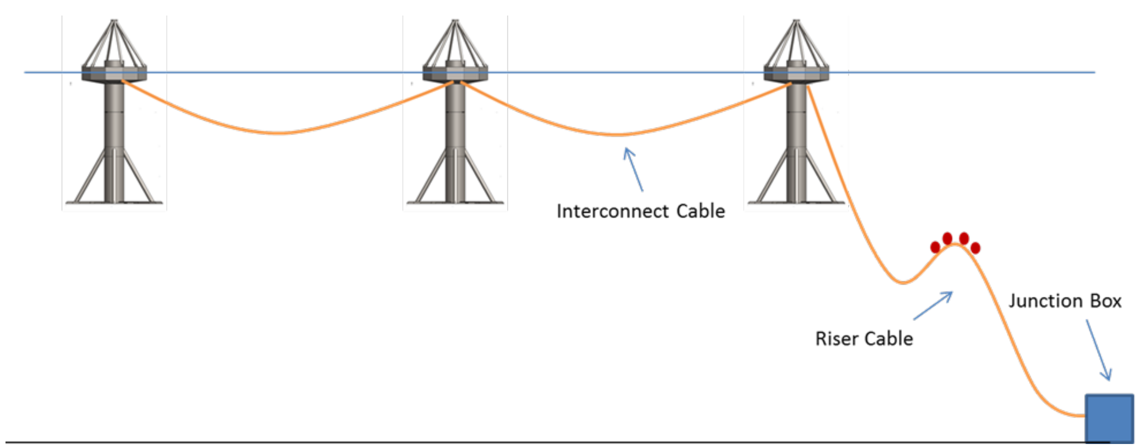

Figure 5-4. Device interconnection cable, riser cable, and junction box (profile).

5.2 Module Inputs

5.2.1 Site Information

The reference wave energy resource for RM3 was developed from site information collected near Eureka, in Humboldt County, California. This wave energy site was identified as a promising future deployment site and has a wave climate representative of the West Coast of the U.S. There is also a wide range of high-fidelity oceanographic data sets available from this area. The Eureka coast reference site was also the proposed site for Pacific Gas & Electric's WaveConnect™ pilot project test bed. The methodology used in this study could be expanded to include potential deployment sites in other parts of the U.S. and the world.

5.2.1.1 Bathymetry and Bed Sediments

As shown in Figure 5-5, the deployment site features a gently sloping seabed without many irregularities (such as canyons, located farther to south) that could disturb the local wave field. It is therefore likely that the wave-field is homogeneous over the deployment area of interest. The RM3 wave point absorber was designed for deep-water deployment, where the water depth is in the range between 40 m and 100 m.

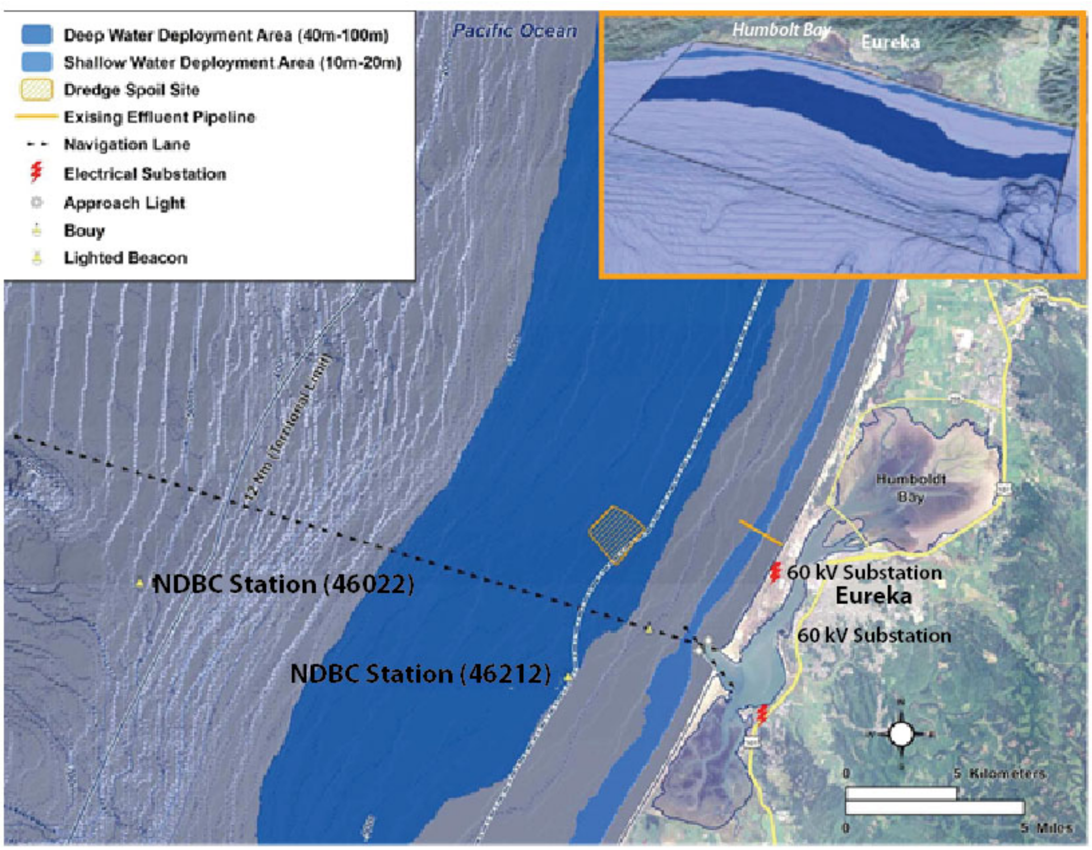

Figure 5-5. Local site bathymetry plan and reference site grid interconnection options.

Sediment classification enabled a detailed seabed characterization at the reference site, which is a sedimentary shelf throughout the deep-water deployment zone. This information is also very important to assess the impacts that the RM3 device and array will have on the marine environment and ecosystem. Most of the seabed in the near shore region of the Humboldt site consists of soft sediments (sand and clay). There are rocky areas near Trinidad Head to the north, but these areas can be avoided. Sediments within the proposed cable route and deployment area are well suited for subsea cable burial and anchoring.

5.2.1.2 Operational Wave Characteristics

According to linear wave theory, the wave energy flux for irregular waves in deep water is

$$J_s = \frac{\rho g^2}{64\pi} H_s^2 T_e$$

where J_s is the wave energy flux per unit of wave-crest length for irregular waves, H_s is the significant wave height, T_e is the wave energy period, ρ is the water density, and g is the acceleration of gravity. Based on this equation, more wave power is available when the wave height is larger and the wave period is longer. But a point absorber extracts maximum energy when the system is at resonance. It is therefore important to design the wave point absorber with a natural frequency that closely matches the dominant wave frequencies at the deployment site.

The wave statistics data[17] are often presented in terms of their joint probability distribution (JPD), which indicates the probability of a significant wave height and wave energy period pair that occurs during a year for the reference resource. The JPD at the reference site, shown in Table 5-1 was obtained from a WAVEWATCH III[18] simulation, and the details of the development of the wave spectra for the reference resource were described in the report by Re Vision Consulting (Previsic 2011a).

[17] Wave statistics data is often referred to as wave spectrum plot and wave scatter diagram.
[18] WAVEWATCH III is a numerical model developed by National Oceanic and Atmospheric Administration and National Centers for Environmental Prediction for predicting the sea states.

Table 5-1. Wave statistics data for reference resource.

Joint Probability Plot (%)																
	Te															
Hs	4.5	5.5	6.5	7.5	8.5	9.5	10.5	11.5	12.5	13.5	14.5	15.5	16.5	17.5	18.5	19.5
0.25	0.0%	0.0%	0.0%	0.0%	0.0%	0.0%	0.0%	0.0%	0.0%	0.0%	0.0%	0.0%	0.0%	0.0%	0.0%	0.0%
0.75	0.0%	0.0%	0.6%	0.8%	0.5%	0.5%	0.2%	0.0%	0.0%	0.0%	0.0%	0.0%	0.0%	0.0%	0.0%	0.0%
1.25	0.0%	1.0%	2.7%	3.7%	4.1%	2.9%	1.5%	0.4%	0.1%	0.0%	0.0%	0.0%	0.0%	0.0%	0.0%	0.0%
1.75	0.0%	1.0%	4.4%	4.3%	4.1%	3.4%	2.0%	1.1%	0.6%	0.1%	0.0%	0.0%	0.0%	0.0%	0.0%	0.0%
2.25	0.0%	0.2%	3.5%	4.2%	3.6%	4.1%	3.1%	1.5%	1.2%	0.3%	0.0%	0.0%	0.0%	0.0%	0.0%	0.0%
2.75	0.0%	0.0%	1.5%	2.5%	1.9%	3.2%	3.3%	1.8%	1.1%	0.4%	0.1%	0.1%	0.0%	0.0%	0.0%	0.0%
3.25	0.0%	0.0%	0.1%	0.9%	0.9%	2.0%	2.4%	1.4%	0.8%	0.4%	0.1%	0.0%	0.0%	0.0%	0.0%	0.0%
3.75	0.0%	0.0%	0.0%	0.1%	0.2%	1.0%	1.9%	1.5%	0.5%	0.3%	0.2%	0.1%	0.0%	0.0%	0.0%	0.0%
4.25	0.0%	0.0%	0.0%	0.0%	0.0%	0.2%	1.0%	1.3%	0.5%	0.3%	0.2%	0.1%	0.0%	0.0%	0.0%	0.0%
4.75	0.0%	0.0%	0.0%	0.0%	0.0%	0.0%	0.3%	0.4%	0.4%	0.2%	0.1%	0.1%	0.0%	0.0%	0.0%	0.0%
5.25	0.0%	0.0%	0.0%	0.0%	0.0%	0.0%	0.1%	0.2%	0.3%	0.2%	0.1%	0.0%	0.0%	0.0%	0.0%	0.0%
5.75	0.0%	0.0%	0.0%	0.0%	0.0%	0.0%	0.0%	0.2%	0.1%	0.1%	0.1%	0.0%	0.0%	0.0%	0.0%	0.0%
6.25	0.0%	0.0%	0.0%	0.0%	0.0%	0.0%	0.0%	0.1%	0.1%	0.1%	0.0%	0.0%	0.0%	0.0%	0.0%	0.0%
6.75	0.0%	0.0%	0.0%	0.0%	0.0%	0.0%	0.0%	0.0%	0.0%	0.0%	0.0%	0.0%	0.0%	0.0%	0.0%	0.0%
7.25	0.0%	0.0%	0.0%	0.0%	0.0%	0.0%	0.0%	0.0%	0.0%	0.0%	0.0%	0.0%	0.0%	0.0%	0.0%	0.0%
7.75	0.0%	0.0%	0.0%	0.0%	0.0%	0.0%	0.0%	0.0%	0.0%	0.0%	0.0%	0.0%	0.0%	0.0%	0.0%	0.0%
8.25	0.0%	0.0%	0.0%	0.0%	0.0%	0.0%	0.0%	0.0%	0.0%	0.0%	0.0%	0.0%	0.0%	0.0%	0.0%	0.0%
8.75	0.0%	0.0%	0.0%	0.0%	0.0%	0.0%	0.0%	0.0%	0.0%	0.0%	0.0%	0.0%	0.0%	0.0%	0.0%	0.0%
9.25	0.0%	0.0%	0.0%	0.0%	0.0%	0.0%	0.0%	0.0%	0.0%	0.0%	0.0%	0.0%	0.0%	0.0%	0.0%	0.0%
9.75	0.0%	0.0%	0.0%	0.0%	0.0%	0.0%	0.0%	0.0%	0.0%	0.0%	0.0%	0.0%	0.0%	0.0%	0.0%	0.0%

NOTE: H_S = significant wave height; T_e = wave energy period.

5.2.1.3 Extreme Sea States

A WEC system must be designed to survive extreme wave conditions at the deployment site. Data for extreme sea states during storms was evaluated using 10 National Data Buoy Center (NDBC) buoys located off the west coast of the U.S. (red labels in Figure 5-6). For each buoy, Table 5-2 shows the 50-year return period significant wave height, $H_{s,50}$, and the 100-year return period significant wave height, $H_{s,100}$. Both the maximum measured height (MMH) of waves and the 95% confidence interval (CI) for each buoy are also listed in the table. The data was measured by these buoys over a period of approximately 20 years. At these measurement locations, a typical 100-year significant wave height during storms is generally in the range between 8 m and 13 m. Specific extreme wave conditions during storms near Humboldt site (station 46022) were described by Berg (2011), where the 100-year return period significant wave height was estimated to be between 11 m and 12 m, and the peak wave period was estimated at 17 sec. The values were then used as a guide to design the survivability wave tank test in our study for determining the extreme wave load. Note that, although the largest wave heights can be found at 17-second periods, this is not usually the design-load case. Berg (2011) investigated the design loads as a function of wave period of the extreme wave. The results from his study (Figure 5-7) and the experimental wave tank test measurement were then used to determine the design load.

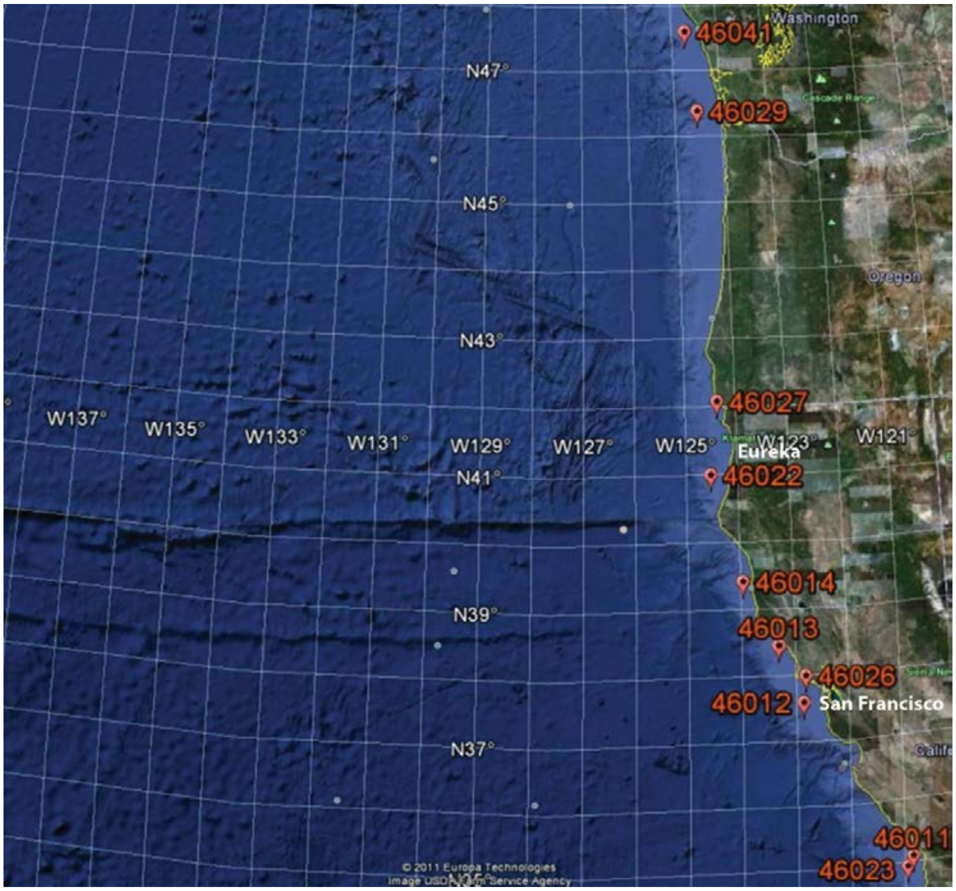

Figure 5-6. NDBC buoy locations for extreme wave measurements.

Table 5-2. Extreme wave measurements at NDBC stations.

Buoy number	Data period	MMH (m)	50 years (m)		100 years (m)	
			$H_{s,50}$	95% CI	$H_{s,100}$	95% CI
46011	1980-2008	9.1	8.8	7.9, 9.5	9.1	8.0, 10.0
46012	1980-2008	8.7	8.9	8.2, 9.6	9.2	8.3, 10.1
46013	1981-2008	9.6	9.4	8.5, 10.2	9.7	8.7, 10.8
46014	1981-2008	9.8	10.2	9.4, 11.0	10.6	9.7, 11.5
46022	1982-2008	11.5	11.2	10.0, 12.3	11.6	10.2, 13.0
46023	1982-2008	8.0	8.1	7.7, 8.5	8.2	7.7, 8.7
46026	1982-2008	8.0	8.1	7.4, 8.7	8.3	7.5, 9.1
46027	1983-2008	9.6	10.3	9.4, 11.3	10.7	9.7, 11.9
46029	1984-2008	12.8	12.5	10.9, 14.0	13.0	11.1, 14.8
46041	1987-2008	11.4	11.2	9.8, 12.5	11.6	10.0, 13.3

NOTE: Table adapted from Mackay et al., 2010.
MMH = maximum measured height of wave

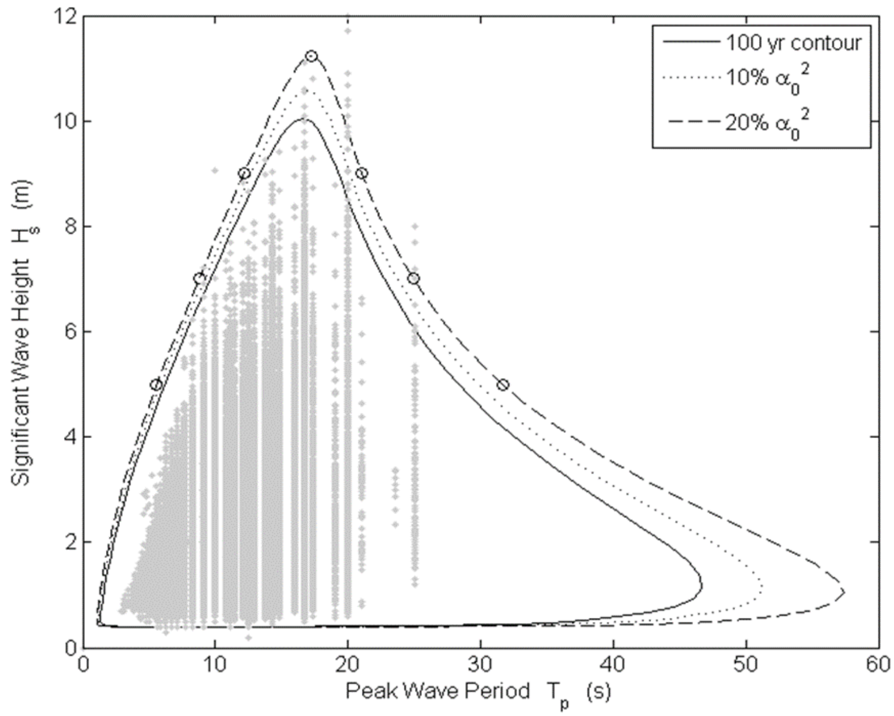

Figure 5-7. 100-year contour for NDBC buoy 46022 (Berg 2011).

5.2.1.4 Adjacent Port Facilities and Grid Options

The port nearest to the area is located within Humboldt Bay and serves as the only deep-water port on California's North Coast. Figure 5-8 shows a nautical chart of the Humboldt Bay area of interest. The facilities are well suited for installation and operational activities that would be required by nearby wave farms. Multiple piers within the bay would also greatly facilitate the launching of any WEC installation project and provide some of the necessary infrastructure for operational activities.

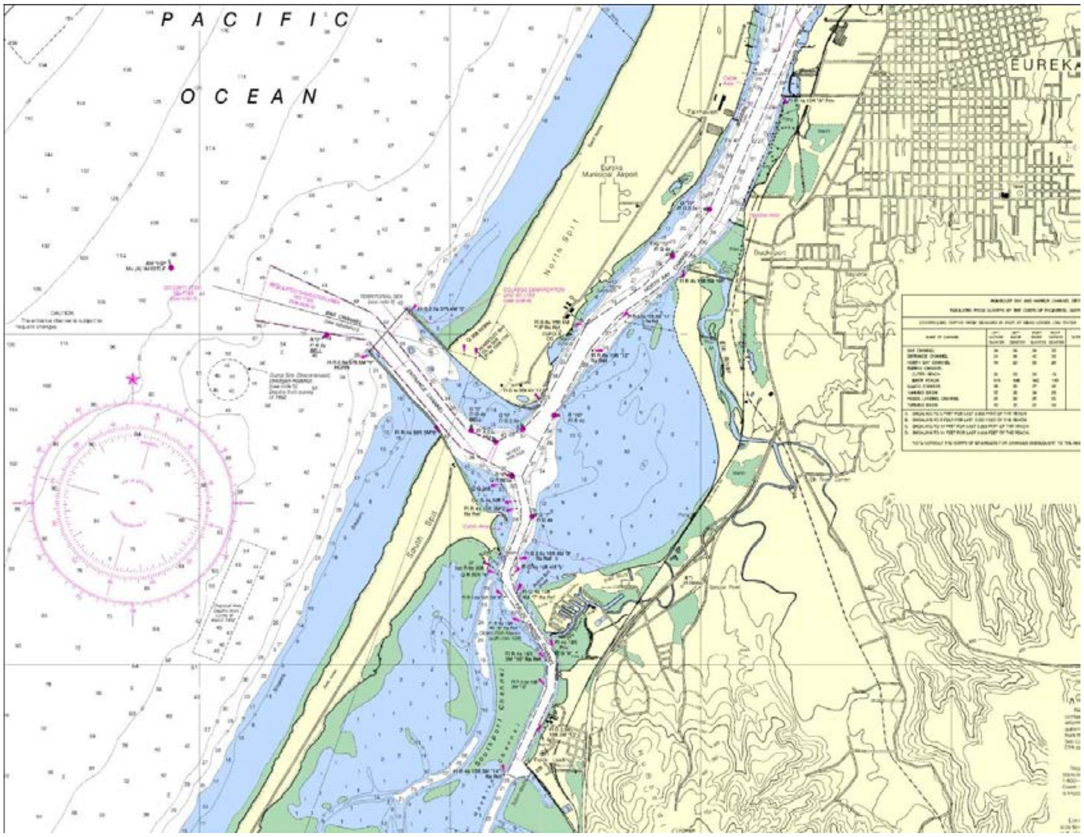

Figure 5-8. NOAA nautical chart (Humboldt Bay).

Approximately 5 miles north of the Humboldt Bay inlet, there is a 60 kV substation in very close proximity to the coastline. This station would serve as the interconnection point to the local electrical grid. An existing outfall location (orange line shown in Figure 5-5) could be used to accommodate the proposed electrical subsea cable and eliminate the need to directionally drill to shore to accommodate the power cable landing. However, this option was not considered for estimating installation costs in this study.

5.2.2 Device/Array Information

In the conceptual design, we determined design specifications based on site resource characteristics borrowed from successful commercial technologies and by applying engineering judgment, economic considerations, and simple hand calculations. A summary of the design specifications is given in Table 5-3.

Table 5-3. RM3 design specifications.

Description	Specification	Justification	Details
Deployment at free surface	Water depth 40 - 100 m	Site resource characteristics	Sufficient depth for deep-water WEC design.
Operational depth	Free surface	WEC architecture	Point absorber.
Mooring system	3-mooring line design	Standard design for buoys	Designed for mooring loads under extreme 100-year return period sea state.
Rated power	300 kW	Numerical simulation with a capacity factor of 30%	Assumed a capacity factor of 30% based on literature (Carbon Trust 2006; Department of Trade and Industry 2007; RenewableUK 2010; and Previsic et al. 2012).
Float diameter	20 m	Economies of Scale	A 20 m float (based on the results from operational sea state wave tank test).
Operational sea states	T_e=5sec~18sec; H_s=0.75m~6m	Site resource characteristics	Based on the wave statistic data (i.e., JPD) at the reference site estimated from the WAVEWATCH III model.
Array configuration	Staggered with 30 float diameter separation	Literature. Engineering judgment	Avoid device interaction according to Babarit (2012). Sufficient space to accommodate mooring connections and accommodate device watch circle.

5.3 Design, Analysis, and Cost Modules

5.3.1 Design & Analysis (D&A) Module

5.3.1.1 Performance Analysis and AEP Estimation

As described in Performance Analysis and AEP Estimation, Section 2.3.1.1, the AEP for a WEC is calculated by multiplying the predicted mechanical power matrix for the device $P_m\left(H_{s_i}, T_{e_i}\right)$ with the joint probability distribution (JPD) that describes the reference resource site's sea state. The mean reference site wave energy density (33.5 kW/m) was obtained based on the JPD at the reference resource site (Table 5-1) assuming linear wave theory. The irregular sea states were characterized by significant wave height H_s and peak wave period T_p (or energy period T_e) and were represented numerically in the time-domain by the superposition of many monochromatic waves using a Brechtschneider spectrum. The RM3 mechanical power matrix (Table 5-4) was calculated by ReVision Consulting using a time-domain radiation and diffraction method. An optimal velocity-dependent damping term was determined using an iterative approach for each sea-state. The power performance results were validated by NREL using a similar approach and CFD. More details on the NREL power performance calculation were described in Yu et al. (2013, in preparation). In addition, a series of wave tank tests for analyzing the operational wave condition RM 3 design power performance were carried out at Scripps in San Diego by Re Vision Consulting and NREL to further validate the models.

Table 5-4. Mechanical power matrix for the TRL 4 RM3 design

Mechanical Power Matrix																	
		Te															
		4.5	5.5	6.5	7.5	8.5	9.5	10.5	11.5	12.5	13.5	14.5	15.5	16.5	17.5	18.5	19.5
Hs	0.25	0	1	1	1	1	1	1	1	1	1	1	0	0	0	0	0
	0.75	4	7	9	11	12	12	11	9	8	6	5	4	3	3	2	2
	1.25	11	18	26	31	34	32	29	25	21	17	14	12	9	8	6	5
	1.75	22	36	50	60	64	62	56	48	40	33	27	22	18	15	13	10
	2.25	36	59	82	99	105	101	90	78	65	54	44	36	30	25	20	17
	2.75	54	88	121	145	154	148	133	114	96	79	65	53	44	36	30	25
	3.25	75	123	168	201	212	203	182	157	131	109	89	73	60	50	42	35
	3.75	100	163	222	264	277	265	238	205	172	142	117	96	79	66	55	46
	4.25	128	208	283	335	351	335	301	259	218	180	148	122	100	83	69	58
	4.75	159	259	352	414	433	413	370	319	268	222	183	150	124	103	86	72
	5.25	194	315	426	501	522	497	445	384	323	268	220	181	150	124	104	87
	5.75	232	377	508	595	618	588	526	454	382	317	261	215	178	148	123	104
	6.25	274	443	596	696	722	685	614	529	446	370	305	252	208	173	144	121
	6.75	319	515	691	804	832	789	706	610	514	427	352	291	240	200	167	140
	7.25	367	592	792	919	949	899	805	695	586	487	402	332	275	228	191	161
	7.75	418	674	899	1040	1072	1015	909	785	662	551	455	376	311	259	217	182
	8.25	473	760	1013	1169	1202	1137	1018	880	743	618	511	422	350	291	244	205
	8.75	530	852	1132	1303	1339	1265	1132	979	827	689	570	471	391	325	273	230
	9.25	591	949	1257	1444	1481	1399	1252	1083	915	763	632	523	433	361	303	255
	9.75	655	1050	1388	1591	1630	1538	1377	1191	1008	841	696	576	478	399	334	282

By multiplying the mechanical power matrix with a PCC conversion efficiency, we obtained the electrical power matrix, which was capped at the rated power (also referred to as capacity) to reduce the size of generator and cost. The relationship for estimating the electrical power is

$$P_e = P_m \times \eta_1$$

where P_e is the estimated electrical power that can be generated by the RM3 design under each given sea state, P_m is the mechanical power, and η_1 is the PCC efficiency that accounts for the losses between the generated mechanical power and the electrical power output. We assumed a hydraulic PCC is used in the RM3 design and assumed a PCC conversion efficiency of 80% (Cargo et al. 2011) for estimating P_e.

The annual averaged electrical power P_{ae} was then obtained by summing the product of the electrical power matrix and the joint power distribution (JPD) for the reference site.

Note that the annual averaged electrical power, P_{ae}, was first calculated using an initially assumed device-rated power. The rated power depends on the capacity factor (C_f) and P_{ae}, which is defined as

$$P_{rated} = \frac{P_{ae}}{C_f}$$

Therefore, the next step in the process was to iteratively change the machine-rated power until the assumed capacity factor equaled 30%, which was selected for the RM3 design as listed in the design specifications (Table 5-3). The resulting electrical power matrix for the RM3 device is shown in Table 5-5.

Table 5-5. Electrical power matrix for the RM3 device (rated power with a capacity factor of 30%).

Electrical Power Matrix																	
		Te															
		4.5	5.5	6.5	7.5	8.5	9.5	10.5	11.5	12.5	13.5	14.5	15.5	16.5	17.5	18.5	19.5
Hs	0.25	0	1	1	1	1	1	1	1	1	1	0	0	0	0	0	0
	0.75	3	5	7	9	10	10	9	7	6	5	4	3	3	2	2	2
	1.25	9	15	20	25	27	26	23	20	17	14	11	9	8	6	5	4
	1.75	18	29	40	48	52	50	45	38	32	27	22	18	15	12	10	8
	2.25	29	48	65	79	84	81	72	62	52	43	35	29	24	20	16	14
	2.75	43	71	97	116	123	118	106	91	77	63	52	43	35	29	24	20
	3.25	60	98	134	161	169	162	145	125	105	87	71	59	48	40	33	28
	3.75	80	130	178	211	222	212	190	164	138	114	94	77	63	52	44	37
	4.25	102	167	227	268	281	268	241	207	174	144	119	97	80	67	55	47
	4.75	128	207	281	286	286	286	286	255	214	178	146	120	99	82	69	58
	5.25	155	252	286	286	286	286	286	286	258	214	176	145	120	99	83	70
	5.75	186	286	286	286	286	286	286	286	286	254	209	172	142	118	99	83
	6.25	219	286	286	286	286	286	286	286	286	286	244	201	166	138	115	97
	6.75	255	286	286	286	286	286	286	286	286	286	282	232	192	160	134	112
	7.25	286	286	286	286	286	286	286	286	286	286	286	266	220	183	153	129
	7.75	286	286	286	286	286	286	286	286	286	286	286	286	249	207	173	146
	8.25	286	286	286	286	286	286	286	286	286	286	286	286	280	233	195	164
	8.75	286	286	286	286	286	286	286	286	286	286	286	286	286	260	218	184
	9.25	286	286	286	286	286	286	286	286	286	286	286	286	286	286	242	204
	9.75	286	286	286	286	286	286	286	286	286	286	286	286	286	286	267	226

Finally, the practical AEP (in the unit of MWh) was calculated

$$AEP = P_e \times 8766 \times \beta$$

where $\beta = \eta_2 \eta_3$ is the parameter, accounting for the losses due to device availability $\eta_2 = 0.95$ (95%) and transmission efficiency $\eta_3 = 0.98$ (98%).

A summary of the power performance for the RM3 design wave point absorber at the reference site is listed in Table 5-6.

Table 5-6. RM3 rated power and AEP output for single device.

Performance Variable	Per Unit
Rated Power	**286 kW**
Annual Energy Production (AEP)	**700 MWh**

5.3.1.1.1 Device Dimension and Geometry Design

As noted earlier, the power generation performance of a wave point absorber highly depends on the dominant sea states at the deployment sites and the resonant frequency of the system, which is influenced by the dimension and geometry of the device. We conducted iterative experimental wave tank tests and used numerical analyses to determine the final dimensions and geometry for the RM3 device. Three sets of experimental wave tank tests were performed between August and November of 2011 at Scripps Institution of Oceanography located at the University of California San Diego (UCSD) to validate the computational models. The RM3 design was then refined to improve the power generation performance during the design and analysis process.

Two floating-point absorber designs were considered in the study. The dimensions and the properties of the two tested subscale models are shown in Figure 5-9. The Model 2 design was refined in an effort to increase energy capture after completing the first series of tests in Scripp's wave tank. The diameter of the float, the vertical column and the reaction plate were all increased in the Model 2 design. The float diameter was increased to improve power output, and the vertical column diameter was increased to improve upright stability and simplify the mooring design. These all contributed to a lower LCOE.

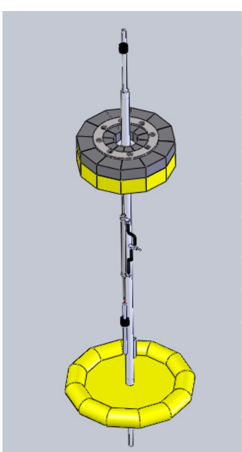

Figure 5-9. RM3 design models (1/33 scale) used for wave tank tests conducted at Scripps, UCSD.

NOTE: The full-scale dimensions for Models 1 and 2 are listed at the top of the figure. The properties of the test model (1/33 scale) are listed in the shaded boxes.

Figure 5-10 shows the experimental setup for the Scripp's wave tank tests. In the first set of tests, a carriage-connected heave guide was used, so that the WEC model (Model 1) was only allowed to move freely in heave. In the second and third test sets with Model 2, the WEC was connected to a set of four mooring lines, allowing for a fully coupled full 6-DoF motion of the device. To attach the mooring lines, four metal piles were installed on the tank's sidewalls (two piles on each side). Each mooring line was then connected to the metal pile on the sidewall. Wave periods between 5 and 20 sec (full scale) were selected to test the response of the model to sinusoidal waves. This corresponds roughly to the range of wave periods encountered at most deployment sites of interest, globally.

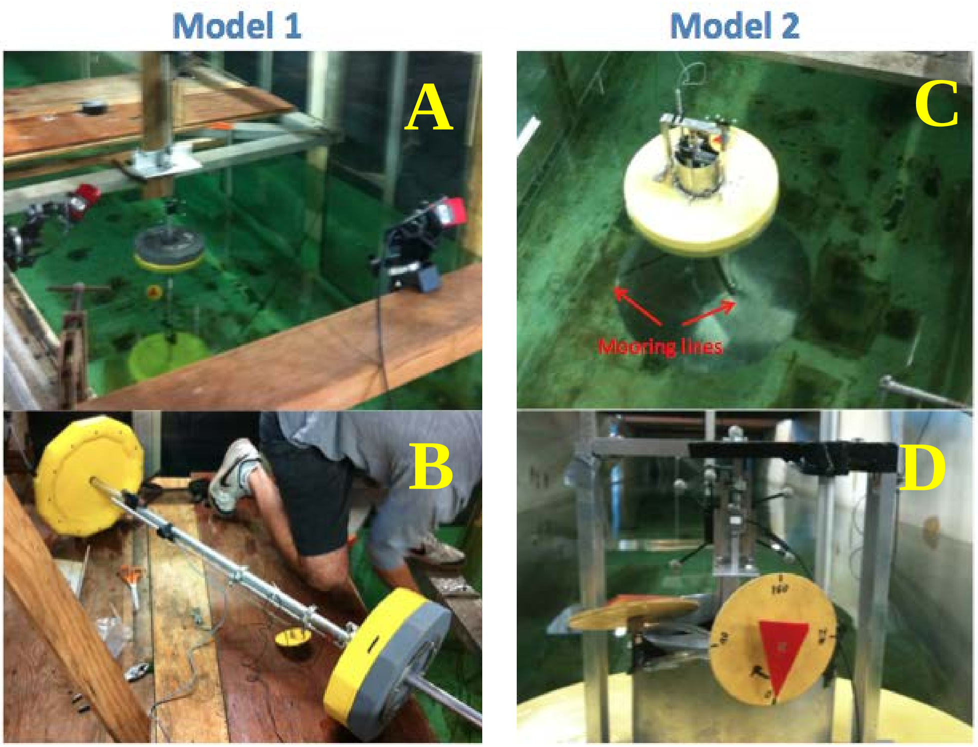

Figure 5-10. UCSD experimental wave tank test settings (A–D described below).

NOTE: (A) Device and heaving guide setup for Model 1

(B) PCC damping system tank test design for Model 1

(C) Device and mooring setup for Model 2

(D) PCC damping system tank test design for Model 2

Figure 5-11 compares the power output from the two RM3 subscale models. The larger float on the Model 2 design increases the amount of power that can be converted from ocean waves, and its maximum power output is much closer to the theoretical power output. An increase in the mass moments of inertia of the Model 2 design reduced its resonant frequency closer to the dominate wave frequencies at the reference resource site. The Model 2 design was therefore selected as the final Technology Readiness Level 4 (TRL 4) RM3 design.

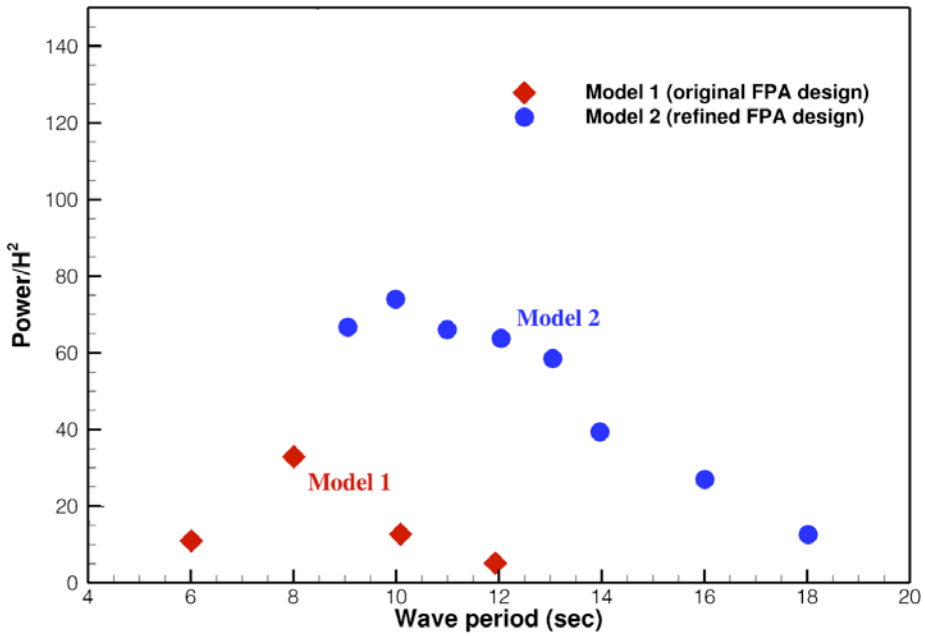

Figure 5-11. Comparison of power performance (in full scale) of FPA models from the experimental tank test under operational condition.

NOTE: C_{PCS} for FPA Model 1 is around 1500 kNs/m and C_{PCS} for FPA Model 2 is around 7000 kNs/m.

5.3.1.1.2 Radiation and Diffraction Numerical Model

We used reduced order radiation and diffraction numerical methods to estimate the RM3 device's power performance. The method first simulated the device hydrodynamics using a boundary element method (BEM) in the frequency-domain. We then solved the system dynamic equations of the RM3 device based on the forces obtained from the hydrodynamic simulations. This method is frequently used for predicting the power performance of wave energy converters (Li and Yu 2012; Previsic et al., 2012), particularly during early stage design and optimization. The hydrodynamic added-mass and radiation hydrodynamic coefficients and wave diffraction and excitation forces were calculated numerically using a frequency-domain boundary element method (WAMIT[19]). The viscous damping coefficients were selected based on the prescribed oscillation CFD simulation by Nelessen (2012) and introduced in the time-domain model. The total loads on the device were then used to calculate the dynamic response of the RM3 device and to estimate its power performance in different sea-states. An iterative approach was used to find an optimal linear damping term for each sea-state. Performance estimates presented here therefore, only used slow-tuning and not advanced control strategies, which have the potential to substantially improve the device's performance.

[19] WAMIT is a boundary element method-based code developed by WAMIT Inc. It solves the radiation and diffraction problem and is developed for modeling the linear hydrodynamic interaction between waves and various types of floating and submerged bodies.

To validate the radiation and diffraction numerical simulations, we simulated the power performance of the Model 1 and Model 2 designs and compared the simulation results to those obtained from experimental wave tank tests and CFD simulations (Yu and Li 2013). Figure 5-12 shows a plot of the estimated mechanical power against the incident wave period for the Model 1 device. The theoretical limit and the (in viscid) potential flow solution are also presented in the figure for reference.

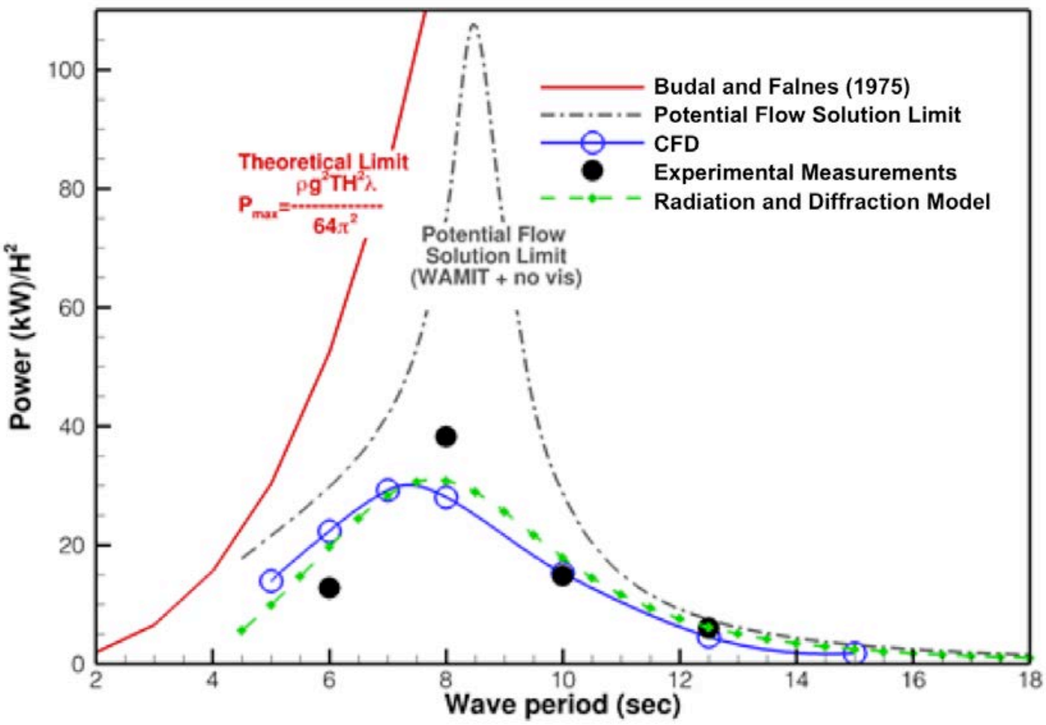

Figure 5-12. Mechanical power performance (scaled by the wave height) for the Model 1 wave point absorber design.

NOTE: (1) An incoming wave height of 2.5 m and a PCC damping of 1200 kNs/m were used.
(2) The potential flow solution limit was calculated using the radiation and diffraction method without specifying any drag coefficient for the device.

Figure 5-13 shows the Model 2 design power performance, where the radiation and diffraction simulation results were compared to those observed in the experiment for different PCC damping values. The study showed that the radiation and diffraction numerical simulation results agreed well with the CFD solutions and the experimental data. The slight differences could be attributed to the difference in the model geometries, the selection of the viscous damping coefficients at a particular wave frequency, the nonlinear characteristics in the PCC, and small the variability in the wavemaker.

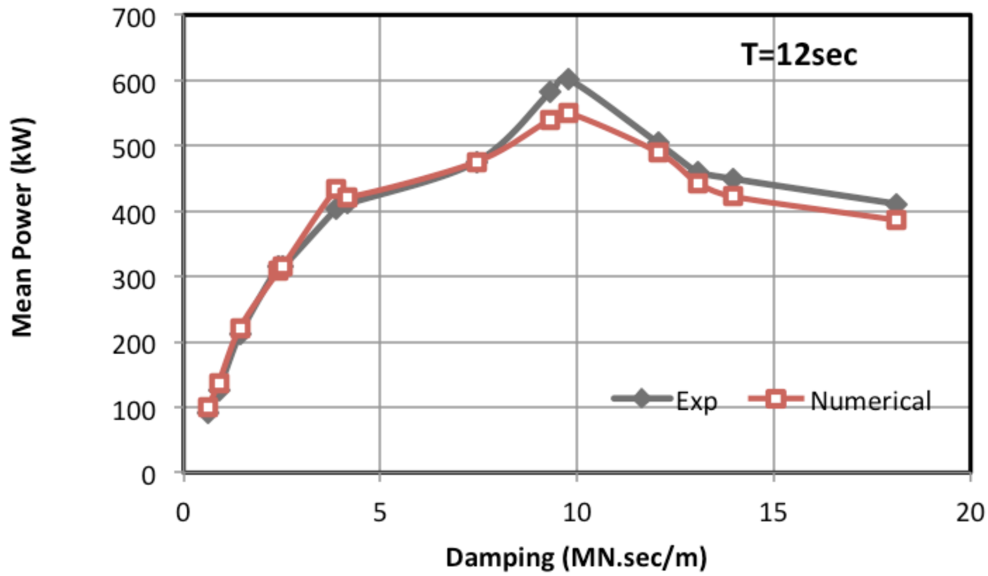

Figure 5-13. Comparison of mechanical power performance for the Model 2 wave point absorber design with different PCC damping values at T = 12 sec.

5.3.1.2 Materials Specifications and Structural Analysis

WEC devices must be designed to sustain the extreme sea states during severe storms. This section discusses the structural design and stress analysis of the RM 3 wave point absorber. In contrast to the current energy converter (CEC) RM designs, the extreme wave loads for the RM3 WEC design were obtained from scaled model wave tank test measurements. These loads were scaled up and input into subsequent finite element analysis (FEA) models for determining the structural design of the RM3 device. We did not consider fatigue loads at this preliminary state in the design process.

5.3.1.2.1 Extreme wave load estimation

An experimental test set was performed at the UC Berkeley wave tank to measure the wave load and analyze the structural performance of the RM3 device under an extreme event. Berkeley's wave tank is 68 m long and 2.4 m wide. The water depth was set at 1.5 m. The dimension of the wave tank and the experimental settings are shown in Figure 5-14 and Figure 5-15.

The WEC device was connected to eight mooring lines and each mooring line was connected to the metal pile on the sidewall. To measure the wave-induced loads on the device, the load cell was positioned between the float and the damping plate. A two-dimensional (2D) motion-tracking system was used to capture the surge, heave, and pitch motions of the device. A target plate, attached to the buoy with passive markers, served as targets for the motion tracking system.

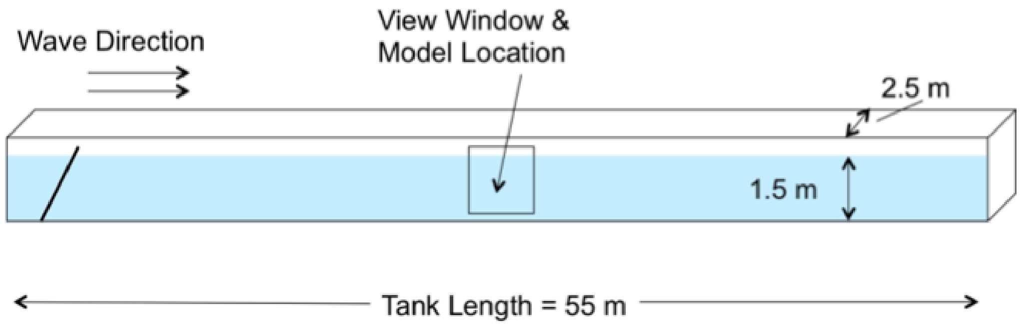

Figure 5-14. Wave tank dimensions for extreme wave load estimation.

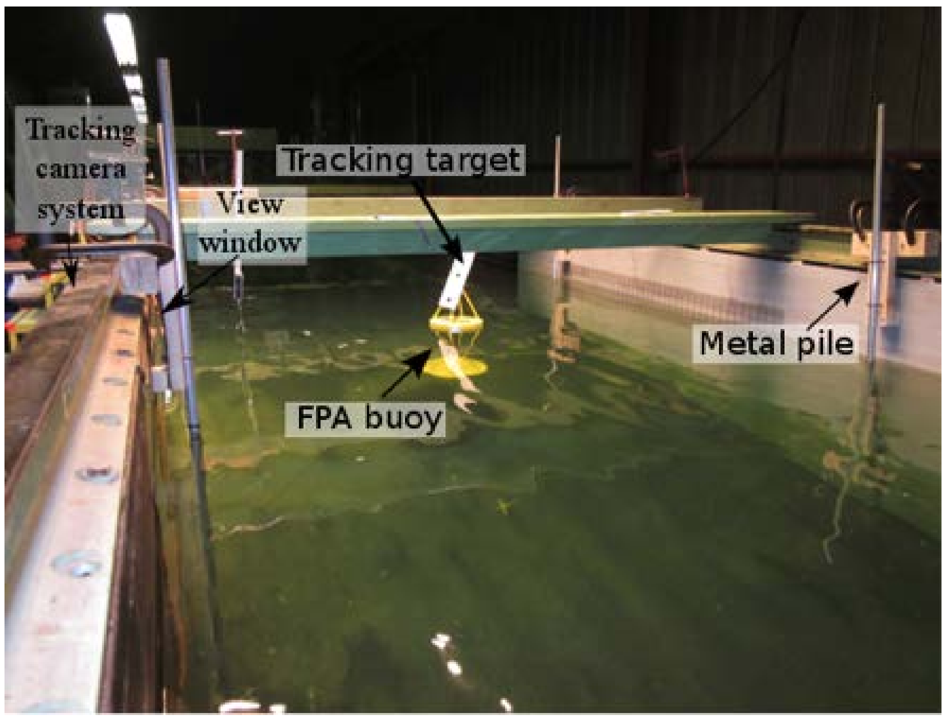

Figure 5-15. Wave tank setup for survivability analysis.

Based on the 100-year return sea states estimated from the NDBC buoy near Humboldt Bay, the experimental extreme wave test was performed with a range of large wave heights between 8 m and 15 m and the wave period between 6 sec and 20 sec (full scale). Only regular wave tests were performed due to limitations of the wavemaker using a 1/100 scale device model. The model's geometry and its dimensions are shown in Figure 5-16. More details on the extreme wave tank test setting and the model dimensions and weight are described in Yu et al. (2013, in preparation).

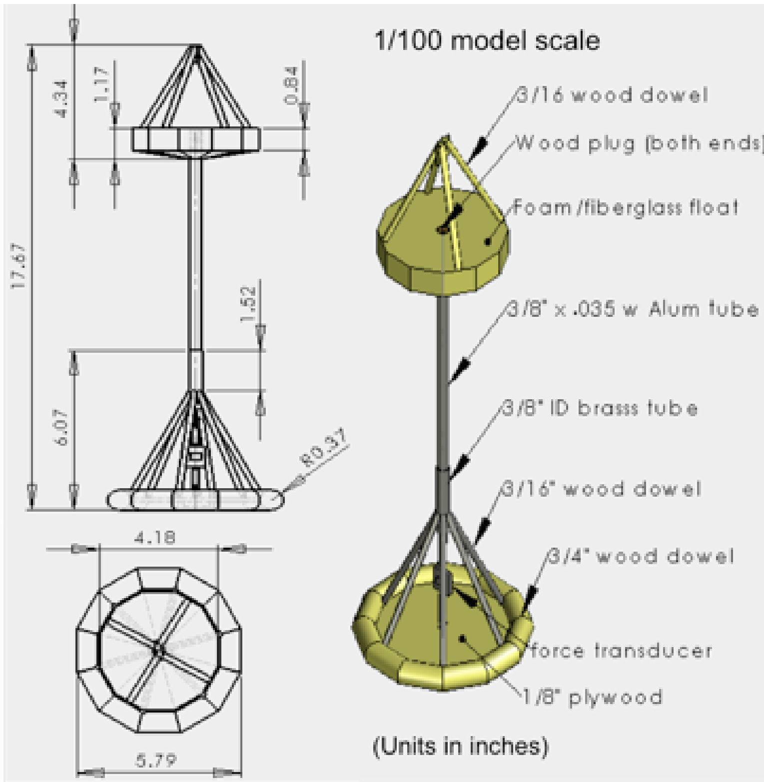

Figure 5-16. The dimensions and the geometry of the 1/100 scale model.

From the experimental wave tank test measurements, the peak tensile load was between 2500 kN and 2700 kN (H≈15m; in full scale), and the maximum compressive load was around 1400 kN. We used the measured extreme wave load for the structural design, and used Froude number scaling to scale the measured forces to the full-scale RM3 device.

Because of the limitations of the wave tank's capabilities and the scale of the model, it is difficult to accurately model the complex fluid structure interactions and predict the load that a full-scale WEC device would encounter during storm conditions. Therefore, some uncertainty remains in these load predictions that could be addressed through testing larger scale models and conducting CFD modeling.

5.3.1.2.2 Structural Analysis

We used the FEA method to perform the stress analysis. The results for the float are shown in Figure 5-17. As shown in the figure, the surface float was compartmentalized into 12 watertight sections that join together to form the float diameter. All major load bearing joints were continuously welded using full penetration welding to maximize the joint strength.

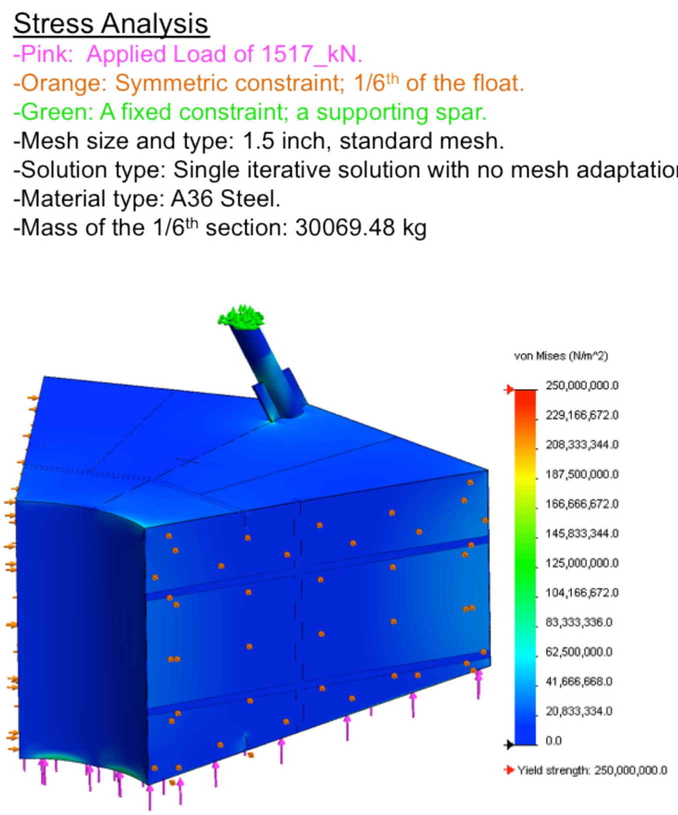

Figure 5-17. Finite Element Analysis model used to test stress in the RM3 design float.

Inside each float section are both horizontal and vertical stiffeners, which strengthen and limit deflection of the float body during operation. The peak tensile load of 8500 kN was selected for both tensile and compressive load analysis for our RM 3 device. The material specifications for the float are listed in Table 5-7.

Table 5-7. Float material specifications.

Material	A36 Steel
Yield Strength	36 ksi (36 000 psi)
Float Diameter	20.0 m
Float Height	5.2 m
Plate Thickness	0.44 in → 0.56 in
Tubular Structure	24 in OD Pipe x 0.5 in thick

The internal float layout (Figure 5-18) shows the stiffener design. Bottom-side float plates required thicker steel due to operational loading (pressure forces on the underside of the float) while the top and side plates have reduced thickness to minimize the total design weight.

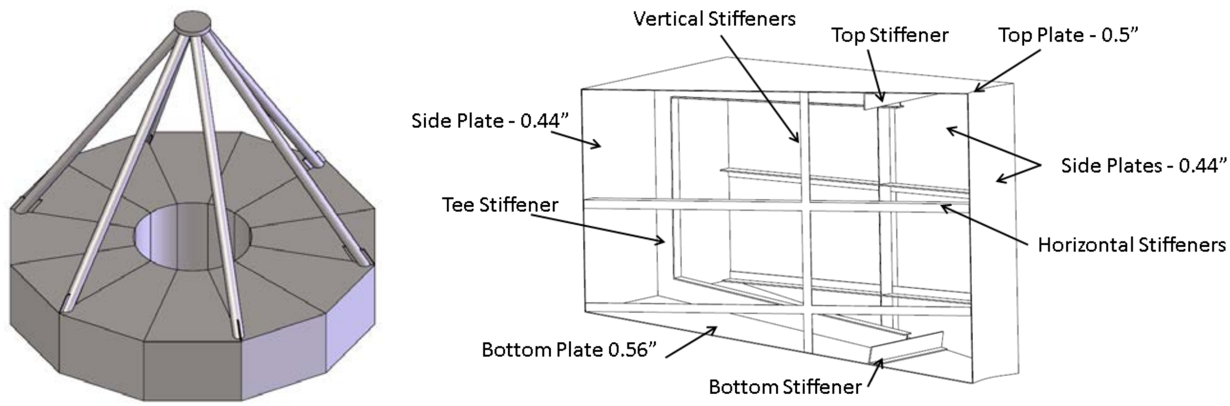

Figure 5-18. External and internal views of RM3 device float.

The vertical column (stiffener) was designed as a single rolled and welded pipe (Figure 5-19). An internal diaphragm plate separates the ballasting tank on the bottom of the column from rest of the column. Internal plate stiffeners support the diaphragm plate as well as the upper and bottom of the column.

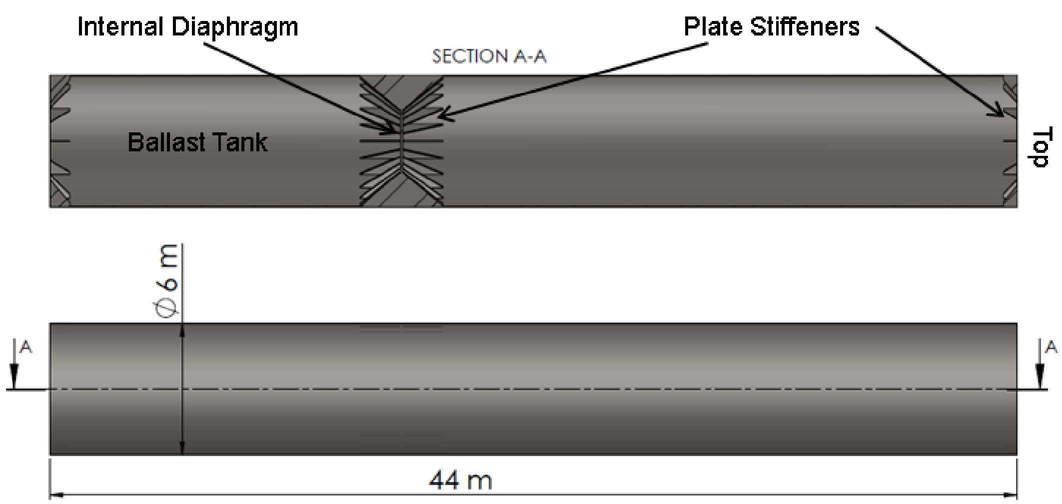

Figure 5-19. Vertical column.

Material specifications for the vertical column are listed in Table 5-8. Each component under direct loading in the structure is fabricated using full penetration welding to ensure maximum weld strength.

Table 5-8. Vertical column material specifications.

Material	Steel A36
Yield Strength	36 ksi
Length	44.0 m
Outer Pipe Diameter & Thickness	236.2 in x 1.0 inch thick

Because of the vertical column length, buckling of the component was evaluated since failure due to buckling can occur significantly below the steel yield stress. Buckling depends not on material strength, but on the materials modulus of elasticity and the slenderness ratio, a ratio which depends on the length and profile of the column. Longer members undergo increased lateral deflection leading to failure if forces exceed the critical load for that member. Our analysis found that column buckling had a factor of safety above 3 due to the large cross-sectional profile.

Figure 5-20 shows the stress analysis results for the reaction plate and Figure 5-21 shows the design of the reaction plate. The plate has 24 radial T-stiffeners to limit the deflection of the 1 inch plate during operation. The material specifications for the reaction plate materials are listed in Table 5-9. Because of the increased diameter, the buoyancy tanks were replaced by the ballasting tank in the vertical column, which raises the structure into a horizontal position at the water surface. A tubular structure joins to the vertical column to transfer loads between the heaving surface float and the reaction plate.

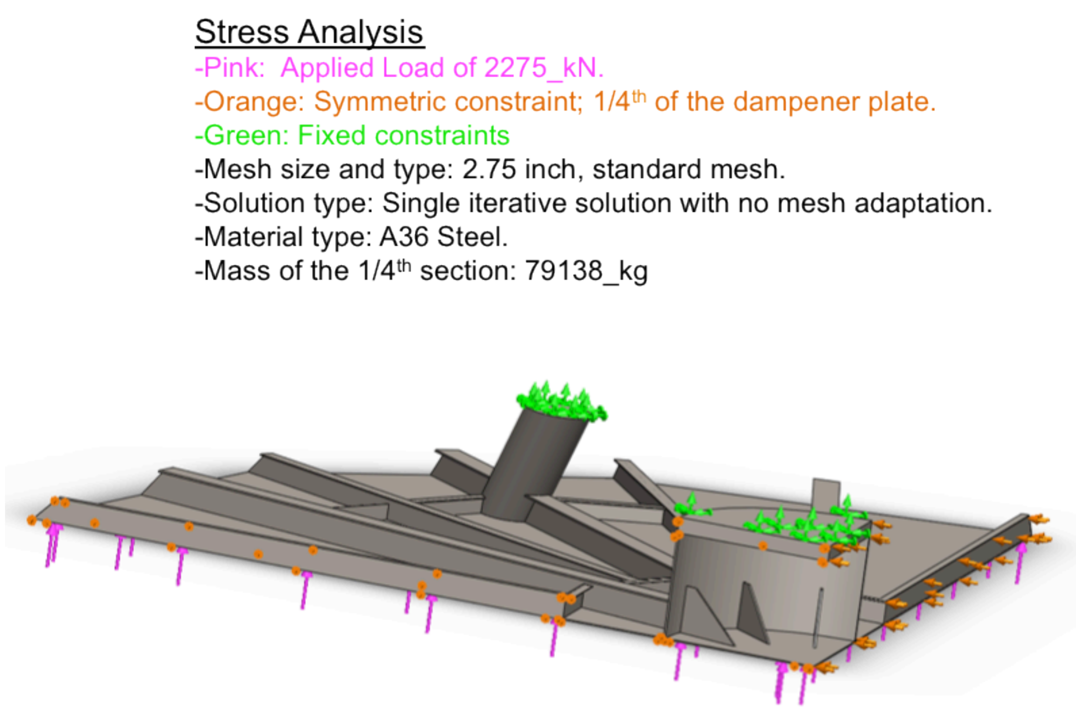

Figure 5-20. Stress analysis for the design plate.

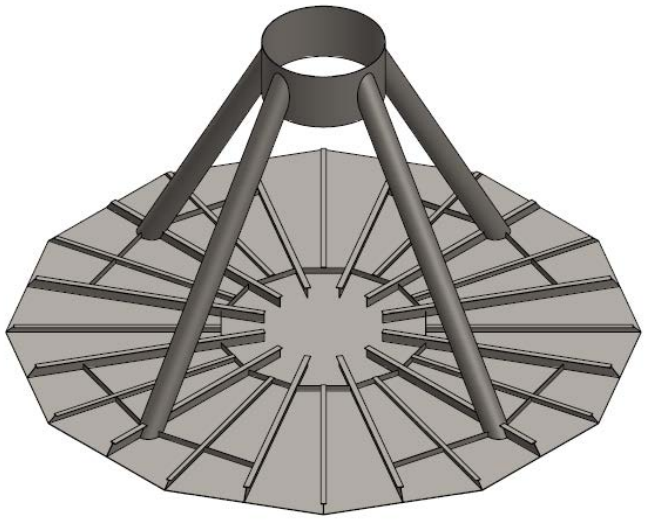

Figure 5-21. Reaction plate.

Table 5-9. Reaction plate material specifications.

Material	Steel A36
Yield Strength	36 ksi
Diameter	30.0 m
Plate Thickness	1.0 in
Tubular Structure	48-inch OD Pipe x 1.0 in thick

The reaction plate and the vertical column are ballasted to remain neutrally buoyant during operation, so that during still water conditions there is no net force between the reaction plate assembly and the absorber buoy. The vertical column is ballasted during operation to achieve neutral buoyancy for the column and the reaction plate. Ballast is added to the surface float as well to submerge the float topside with about 2 m above the waterline. A design factor of 1.5 (1.3 load factor and 1.15 material factor [Det Norske Veritas 2011]) was selected during the structure design analysis. Table 5-10 shows the weight breakdown of the device.

Table 5-10. Device weight breakdown.

	Weight (Mg)	Weight %
Surface Float	207.6	30.5%
Vertical Column	223.6	32.9%
Reaction Plate	244.7	36.0%
Enclosure for PCC	4.1	0.6%
Total	680.0	

5.3.1.3 Power Conversion Chain (PCC) Design

In order to characterize the likely impacts of the hydraulic power conversion system on cost, performance and maintenance, a simple conceptual hydraulic PCC design was established in the early phases of this effort by a joint effort between Re Vision Consulting and Oregon State University. More detail on the PCC can be found in the Re Vision report (Previsic 2011 a).

Figure 5-22 shows a schematic of the hydraulic circuit. The hydraulic circuit consists of a primary hydraulic ram that converts the relative movement between the wave energy absorber device and the central column to hydraulic pressure. The hydraulic pressure is then converted into mechanical rotation using a fixed displacement motor/pump. The motor/pump in turn drives the generator. A frequency converter, step-up transformer, and associated switch-gear are then used to convert the electricity produced by the generator into an output that can be fed into the electric grid.

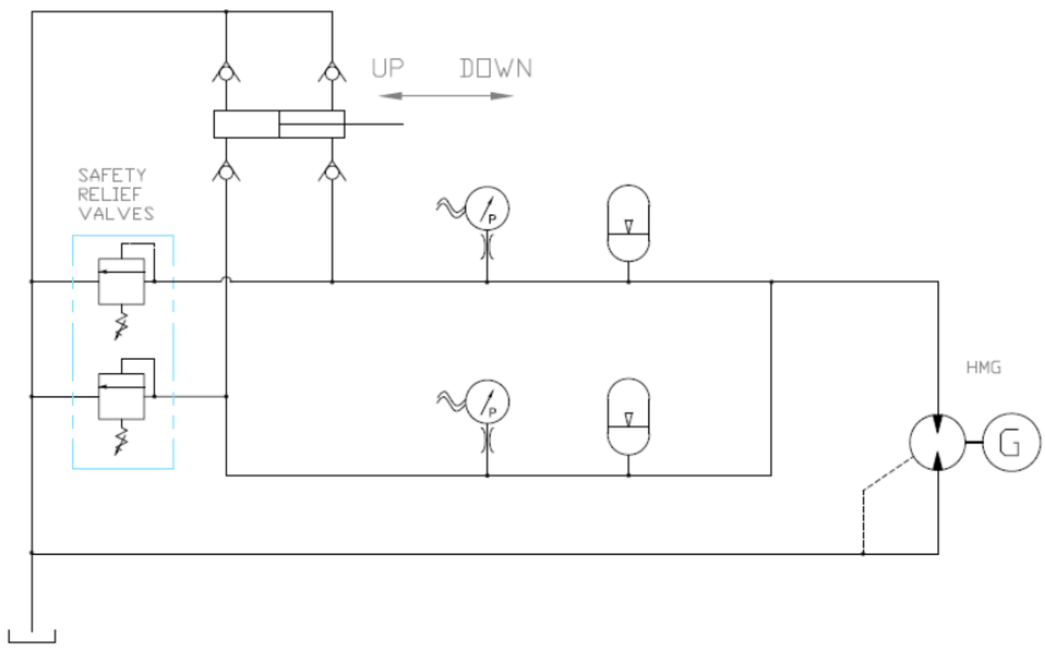

Figure 5-22. Hydraulic circuit.

The internal components of the power conversion system located inside the vertical column are shown in Figure 5-23. The rated capacity of this unit is 286 kW with conversion efficiency of 80% from mechanical to electrical energy. Also shown in the assembly is a set of pressure accumulators, which can be used to smooth the cyclical power output coming from the cylinder.

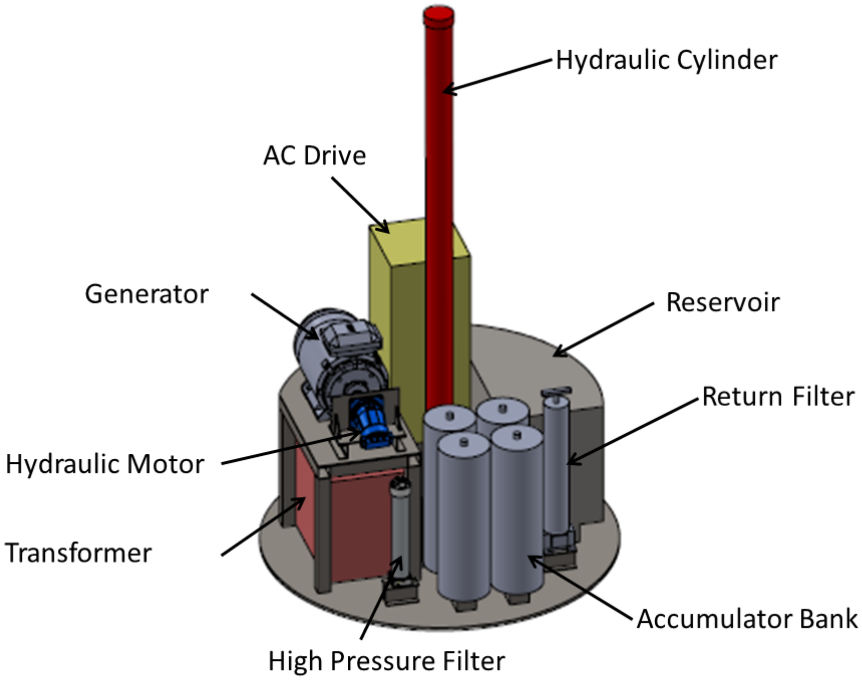

Figure 5-23. PCC internal assembly.

Table 5-11 provides a weight breakdown of the power conversion system. The power conversion system requires about 300 gallons of hydraulic fluid (not listed in the weight break down table). We selected an environmentally benign fluid to reduce environmental risks. The PCC assembly was designed so that it can be removed as an integrated unit from the RM3 device and replaced with a new one. The original PCC unit can then be transported in its entirety back to shore for maintenance and refurbishment.

Table 5-11. Power conversion system weight breakdown.

Component	Weight (total, kgs)	Weight %
Power Converstion System		
Hydraulic Cylinder	907	7.9%
AC Drive	399	3.5%
Generator	725	6.3%
Hydraulic Motor	73	0.6%
Transformer	760	6.6%
High Pressure Filter	50	0.4%
Return Filter	90	0.8%
Accumulator Bank (x4)	452	3.9%
Reservoir	454	3.9%
Structural		
Enclosure/Mounts	7584	66.0%
total	11494	

NOTE: Data from RM3 CBS Excel Spreadsheet. Sandia National Laboratories Energy, Climate, and Infrastructure Security website: http://energy.sandia.gov/rmp

5.3.1.4 Foundation and Mooring Design

The mooring system also needs to withstand extreme events, allowing the device to ride-out extreme waves without unnecessarily constraining its motion and thereby increasing the mooring loads, while still providing adequate spring-stiffness to keep the device on station. Using nylon, instead of more traditional wire-rope, allowed increased compliance (stretching), while reducing overall loads. Basic design requirements for the mooring are shown in Table 5-12.

Table 5-12. Mooring design requirements.

Water Depth	70 m
100-year Significant Wave Height (Hs)	11.9 m
100-year Significant Wave Period (Tp)	17.1 s
100-year current speed	0.59 m/s
Seafloor composition	Sand/Clay
Mooring legs	Nylon & Chain
Anchors	Drag Embedment

Figure 5-24 shows the major design elements of the mooring system. We used ANSYS-AQWA to model the mooring-line and system dynamics and to establish a suitable mooring design. Subsea buoys with a net uplift capacity of 55 kN were used near the surface to reduce vertical force components of the mooring legs and keep the mooring attachments on the surface if the WEC device is removed from its moorings.

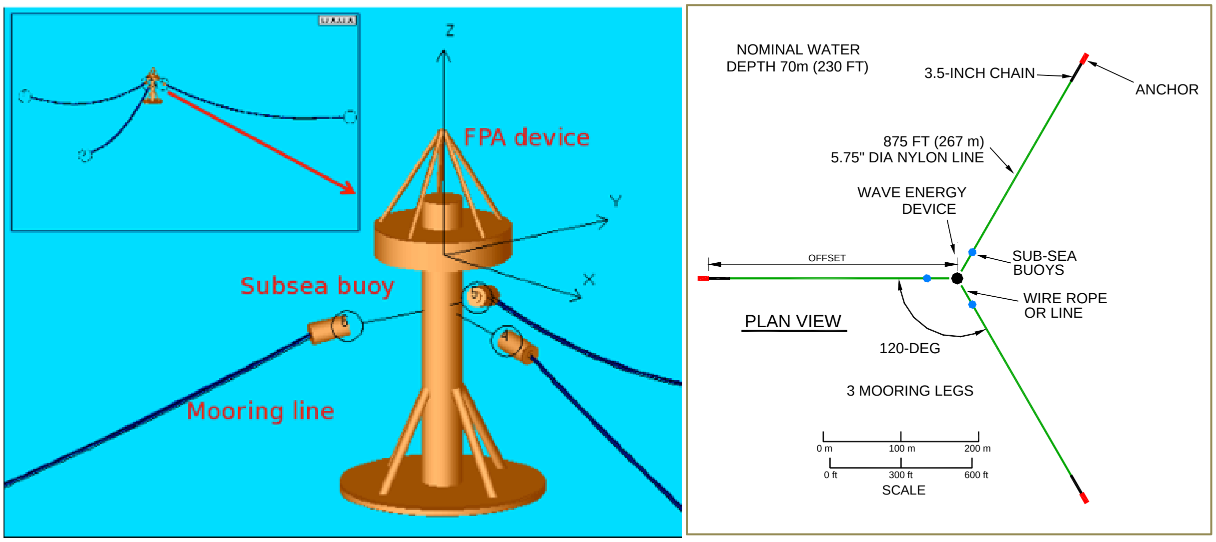

Figure 5-24. Mooring arrangement and dimensions.

The extreme mooring load under a 100-year return event was estimated at 1886 kN, which with a 1.95 safety factor gives the required break strength of 3680 kN. A 146-mm (5.75-in) diameter nylon line provides sufficient break strength and was, therefore, selected as the main mooring line for the RM3 design. The main mooring line was also connected to an 89-mm (3.5-in) chain at the bottom. A 10-ton clump weight is attached to the chain portion of the mooring leg (not shown in the figure above) to reduce the angle of the mooring-line to the anchor. We selected a 9-ton Bruce anchor (Figure 5-25) to attach the mooring line to the sea bed and accommodate the required ultimate loading capacity to maintain the WEC's position.

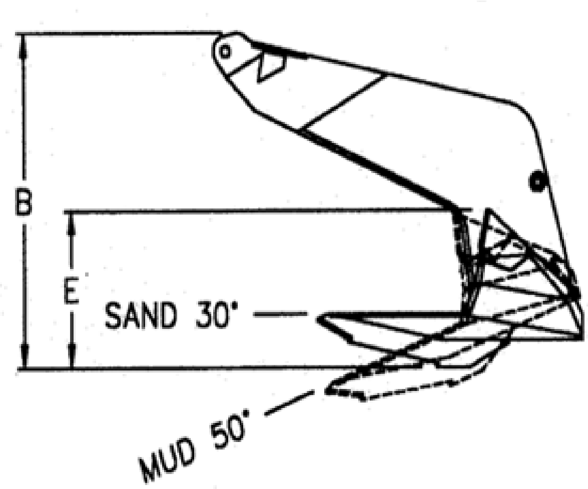

Figure 5-25. Anchor: 9-tonne Bruce® FFTS MK 4 anchor.

NOTE: The FFTS Mark 4 anchor (patented) shown above is from the Bruce® Anchor Group equipment data sheet. Website: www.bruceanchor.co.uk

5.3.2 Manufacturing & Deployment (M&D) Strategy Module

5.3.2.1 Manufacturing Strategy and Costs

Manufacturing costs of system components for RM3 at different array scales (1, 10, 50, and 100 units) are summarized in the figures and tables below. Figure 5-26 shows the cost breakdown of the device structure subcomponents, including the surface float, vertical column, and reaction plate. Each subcomponent contributes approximately one-third of the total structural cost of these; the reaction plate contributes the most because it is the heaviest component.

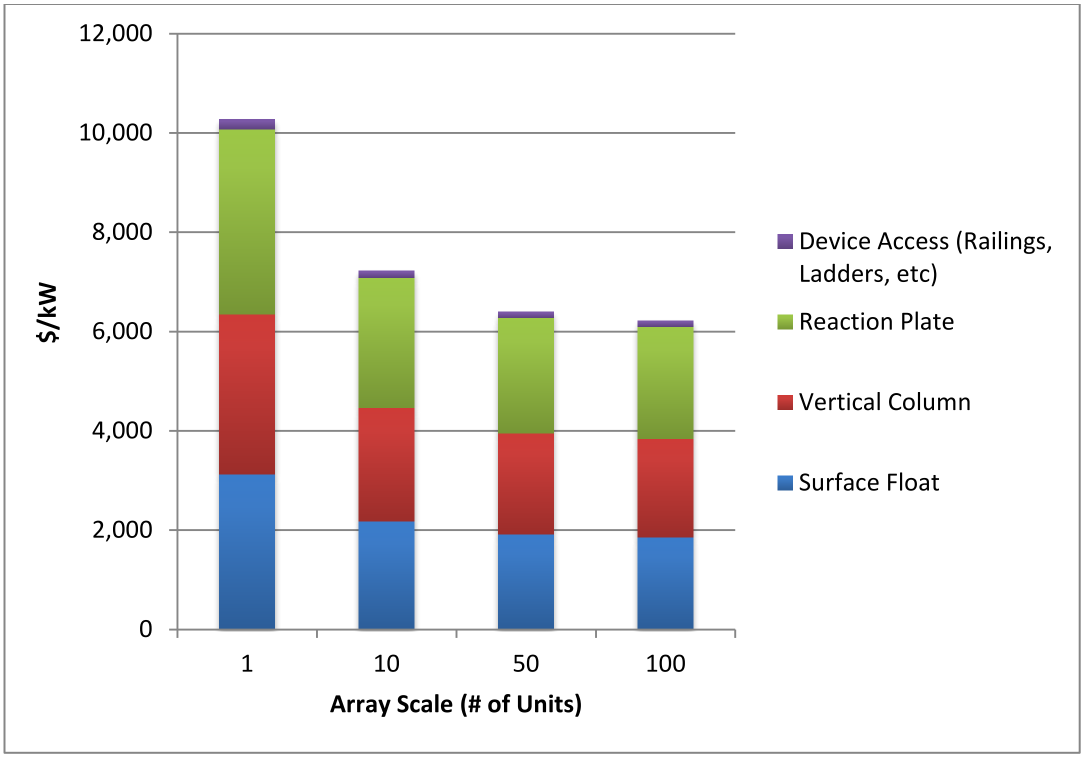

Figure 5-26. RM3 structural cost breakdown ($/kW) per deployment scale.

Figure 5-27 shows cost breakdown for the energy capture and PCC components of the RM3. The greatest contributors to the cost for this PCC system are the hydraulic components and the bearings and linear guides.[20]

[20] No design was available for the linear guides, so the cost was estimated at 20% of the total PCC cost.

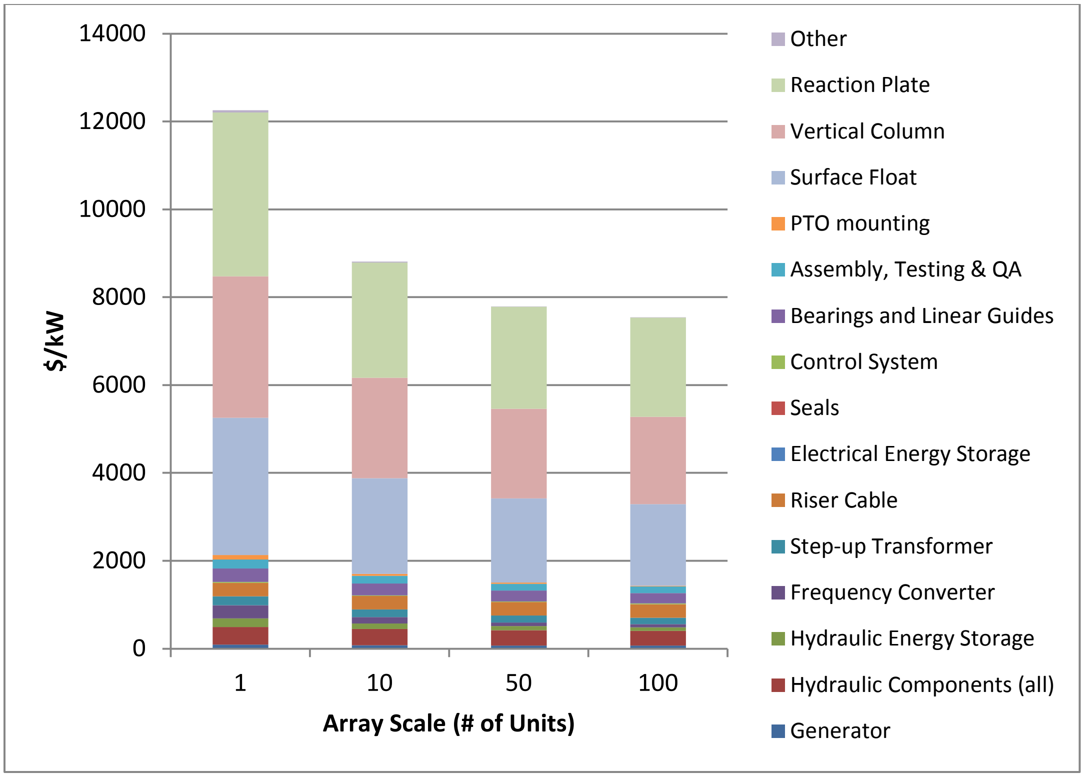

Figure 5-27. Cost breakdown ($/kW) for the PCC components per deployment scale.

NOTE: The riser cable was incorrectly included in the PCC cost breakdown used in this study, but it is not a subcomponent of the PCC based on the definition provided in the footnote 5 in Section 2.1.1. The riser cable should be included as part of the installation cost.

Mooring component costs, including: 1) mooring lines and chains, 2) anchors, 3) subsurface buoys, and 4) connecting hardware ready for installation were estimated at nearly $525,000 for a single device deployed as a single unit, or nearly $475,000 per device at larger deployment scales (10, 50, or 100 units). Table 5-13 shows the estimated cost of the components of the mooring system at different deployment scales.

Table 5-13. Mooring system component cost breakdown.

	Cost ($/kW) (1 unit deployment)	Cost ($/kW) (10-, 50-, or 100- unit deployments)
Mooring lines/chain	638	574
Anchors	629	566
Buoyancy	210	189
Connecting Hardware (Shackles etc.)	358	322
Total	**1,835**	**1,651**

5.3.2.2 Deployment Strategy and Costs

The deployment strategy accounts for the installation of the: 1) mooring system, 2) subsea cable infrastructure, and 3) the devices themselves (including commissioning). Our analysis assumed a DP-2 class vessel would be mobilized from the Gulf of Mexico region and used for the mooring installation. A separate Cable Installation Vessel would be used for installing the cable. The device[21] would be connected to its mooring system and commissioned using the same workboat/custom service vessel that will be used for O&M activities.

Table 5-14 lists the total installation costs using the assumed day rates for these three types of vessels and the assumed installation durations for the key steps in the installation process.

[21] This analysis assumed devices could be assembled in a suitable fabrication facility in Oregon and barged down to the installation site about 300 miles south.

Table 5-14. RM3 M&D Strategy Module cost assumptions.

Operational Detail	1 Unit			100 Units		
	No. Days	Vessel Day Rate	Cost	No. Days	Vessel Day Rate	Cost
Mooring Installation (DP-2 Vessel)						
Transit (5,000 miles)	46	$58,754	$2,690,933	46	$58,754	$2,690,933
Mob/Demob of Vessel	4		$422,000	4		$422,000
Dockside Support			$7,350			$735,000
At Dock Loading	0.4	$70,485	$26,079	37	$70,485	$2,586,800
Transit to Site and back	0.2	$76,610	$18,386	24	$76,610	$1,869,284
On-site working	0.4	$73,810	$27,310	37	$73,810	$2,708,827
Total	**51**		**$3,192,059**			**$11,012,844**
Cable Shore Landing						
Horizontal Directional Drilling (distance is 500 m)			$667,000			$1,534,000
Cable Installation (using Cable Install Vessel)						
Mob/Demob CIV	11	$66,350	$729,850	11	$66,350	$729,850
Load Cable	1	$75,625	$53,694	3	$75,625	$257,125
Transit to Site	2	$101,275	$202,550	2	$101,275	$202,550
Install Cable & Surface Lay	1	$101,075	$55,591	55	$101,075	$5,559,125
Cable Burial and S/E	3	$101,075	$313,333	3	$101,075	$313,333
Contingency	2	$87,855	$152,868	3	$87,855	$221,395
Total	**19**		**$1,507,885**			**$7,283,377**
Device Installation (same workboat as for O&M)						
Mob/Demob			$181,750			$181,750
Installation	1	$66,775	$66,775	100	$66,775	$6,677,500
Contingency	0.1	$66,775	$6,678	0	$66,775	$0
Total	**9.0**		**$255,203**	**100**		**$6,859,250**

Figure 5-28 shows the total installation cost normalized by installed power at different deployment scales. Single unit deployment cost is dominated by the cost to install the mooring system and the cable shore landing. The installation cost, in terms of $/kW, is significantly higher for the deployment of a single unit as compared to an array (even arrays with only 10 units). The dollars per-kW cost of installation is estimated to fall from more than $20,000/kW for a single unit deployment, to approximately $3,000/kW for a 10-unit deployment, and just over $1,000/kW for a 100-unit deployment. An increase in device capacity/unit would further reduce that cost.

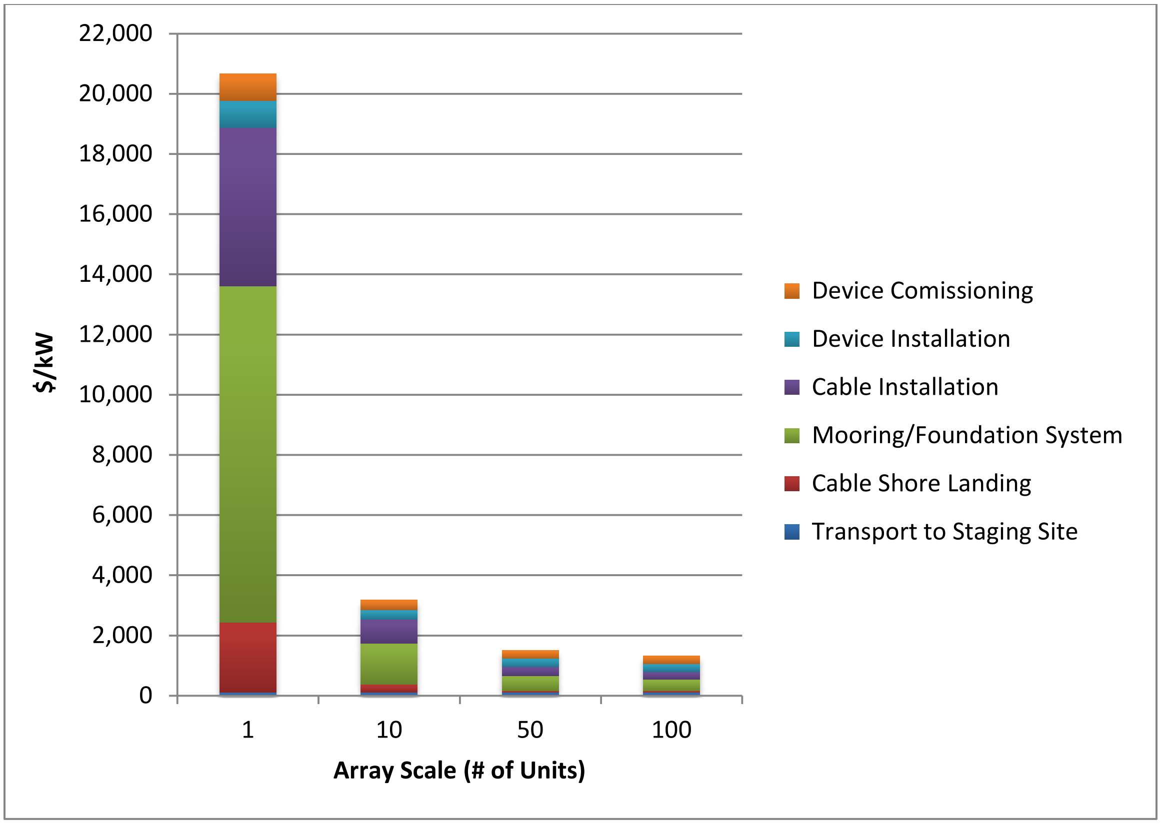

Figure 5-28. Installation cost breakdown ($/kW) per deployment scale.

5.3.3 Operations & Maintenance (O&M) Strategy Module

Similar to the other RMs, the RM3 concept design was developed to reduce O&M costs. As discussed earlier, cassette-type approach is envisioned for the PCC to allow the entire PCC unit to be easily lifted out of the main device structure and replaced with a new one. The original unit would then be brought back to shore for maintenance. Secondly, in the case of arrays (more than one device), all subsea cables are buried along the cable route, which minimizes installation and maintenance costs.

5.3.3.1 Service Vessel Specifications

To operate a WEC farm effectively, the purchase of a dedicated service vessel will likely become feasible at larger unit scales. We envision that a small offshore supply/workboat in the 85 ft to 125 ft range, as shown in Figure 5-29, would be suitable. The vessel requirements include: 1) sufficient deck-space to handle mooring lines and cable repair; 2) dynamic positioning (DP-1) to allow for more effective operation; and 3) crane lifting capacity of 5 Mg at 20-foot radius. Total cost estimates for the vessel are on the order of $4M to $5.5M assuming it was built new. A 10-person crew, approximately, would be required to operate the vessel and carry out repair and maintenance activities. Operations would take place only during daylight hours (12-hours per day) and the vessel would return to port at night.

Figure 5-29. General type of medium sized workboat.

NOTE: Refer to www.sunmachinery.com/workboats_for_sale.html for this and other workboat images.

The cost of marine operations is based on the number of interventions and the cost of the vessels used for operations.

Based on the failure rate assumptions (see next section) and operational frequency, it was found that the device would require a total of two interventions per year. There are two major types of interventions: those requiring device recovery and those requiring only PCC recovery. The vessel day rates are the same for both types of interventions with the exception of the cost of fuel and consumables; the rate is higher for device retrieval. The operational cost would be expected to drop if the WEC farm used a custom-built service vessel that is purchased as part of the project rather than employing a vessel of opportunity.

5.3.3.2 Failure Rates

Table 5-15 provides first order approximations by Previsic (2011a) of component costs and failure rates for the 286 kW WEC device. The L-50 life was assumed to be the mean-time of the subsystem requiring complete replacement. The cost of replacement parts was assumed to equal the value of the part/subsystem of the original device. Annual replacement part costs were calculated from the part cost and the estimated number of failures per year (Table 5-15).

Table 5-15. Cost and failure rate assumptions for WEC components (single unit cost).

Hydraulic System		$/Unit	# Units	L50	$/Year	# Failures/Year
	Hydraulic Cylinder	$26,741	1	8	$3,343	0.13
	Check Valves	$1,167	4	20	$233	0.05
	Relief Valve	$332	1	5	$66	0.20
	Pressure Sensor	$644	2	8	$161	0.13
	Valve Subplate	$2,008	2			
	Accumulator	$56,628	4			
	HP Filter	$2,568	1			
	Return Filter	$7,344	1			
	Fixed Displacement Motor	$23,626	1	5	$4,725	0.20
	Reservoir	$20,020	1			
Electrical Systems		$0				
	Generator	$20,037	1	10	$2,004	0.10
	Frequency Converter	$85,800	1	7.5	$11,440	0.13
	Step-up Transformer	$57,200	1	15	$3,813	0.07
External Systems						
	Riser Cable	$88,000	1	10	$8,800	0.10
	Moorings	$524,775	1	50	$10,496	0.02
	Linear Guides	$87,270	1	10	$8,727	0.10
Total					$53,808	1.22

NOTE: The values in the table are for a 100-unit project.

5.3.3.3 Annual O&M Costs

Based on the estimated number of interventions and replacement part values, the annual O&M cost was computed at different scales of deployment. Figure 5-30 shows the breakdown of the likely annual cost per WEC device. Increasing the unit scale of the farm would have a dramatic impact in reducing operational costs because the costs for the service vessel (and the number of the crew) will increase at a lower rate as the deployment scale goes up. See Insurance, Section 2.3.3.4, for details on how insurance costs were estimated. Note that the post-installation monitoring is a part of environmental monitoring and regulatory compliance costed under the Environmental Compliance (EC) Module (see Section 5.3.4) and is included in the total OpEx costs shown in Figure 5-30. Initial environmental compliance and monitoring activities prior to start up would fall under CapEx as explained in the following section.

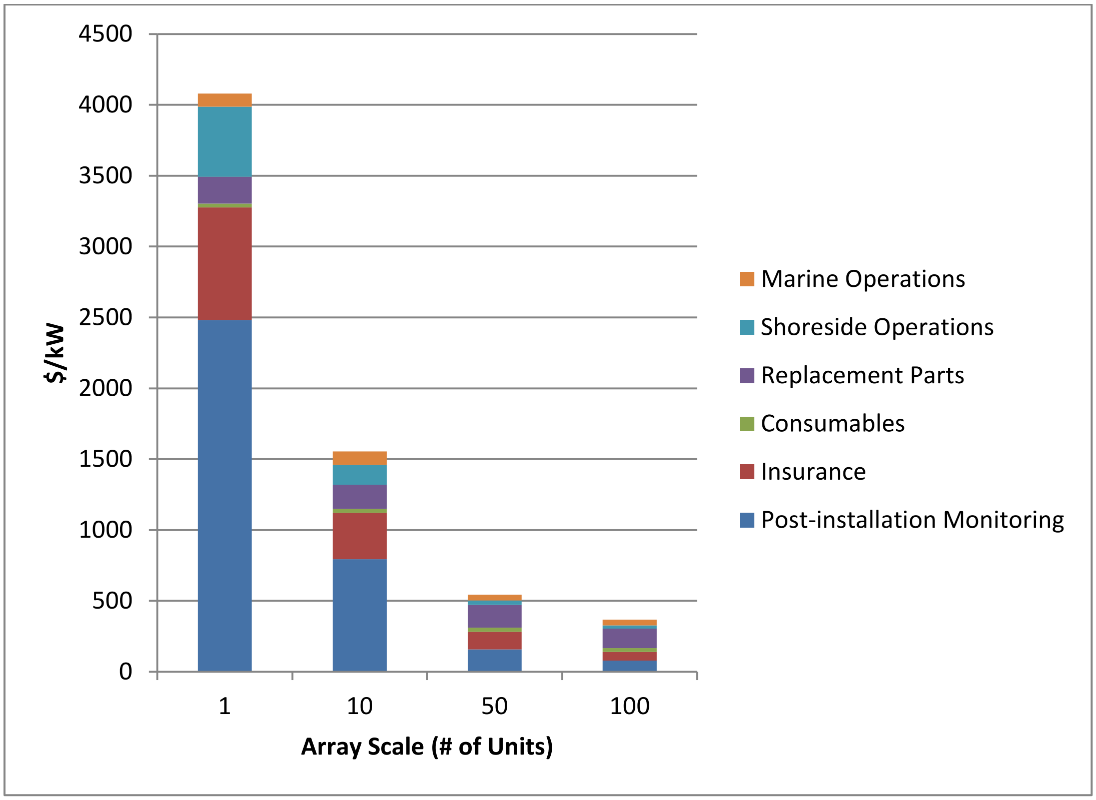

Figure 5-30. Annual OpEx cost ($/kW) per array size.

5.3.4 Environmental Compliance (EC) Module

Deployment of a wave power buoy requires extensive siting and permitting studies to ensure the responsible development of wave hydrokinetic technology. The siting and permitting analysis for RM3 has been completed for the Northern California reference site, a temperate open coastline with protected marine animals and habitat. This study has established cost estimates for pilot (1 unit), small commercial (10 units), and large commercial (> 50 units) scale deployments. This work was completed by Pacific Northwest National Laboratory (PNNL).

Wave sites appropriate for power generation are most commonly found in coastal areas, encompassing large expanses of ocean. Work in the open ocean is costly, and may require large areas to be surveyed for migratory species, habitat quality, and seabed variations. In addition, coastal sites are likely to support commercial and recreational fisheries and other ocean uses, requiring more extensive environmental scoping and outreach. Seabirds and sea turtles, as well as marine mammals and large fish, become important marine receptors of concern for pre-installation studies. However, most wave sites have sea room for passage of migratory animals, and may not require a high level of year-round monitoring of marine mammals, fish, and sea turtles. Open coastal areas are less likely to have extensive environmental data sets available, driving pre-installation survey costs higher.

As described in the general discussion of the EC Module, Section 2.3.4, the NEPA project phases, siting and scoping, pre-installation, and initial post-installation activities contribute to the capital costs (CapEx) of the project. Post-installation monitoring will continue for the duration of the project and this will contribute to the annual OpEx costs; the first few years of post-installation are assumed to require an extensive set of studies, followed by a reduced level of near-field monitoring for any animals determined at risk, and periodic special far-field studies to estimate ecosystem risk. Each phase may require individual environmental studies, based on regulatory requirements, and the specific marine animals, habitats, and ecosystem processes found in the location. The total estimate of environmental CapEx normalized by installed power is summarized in Figure 5-31.

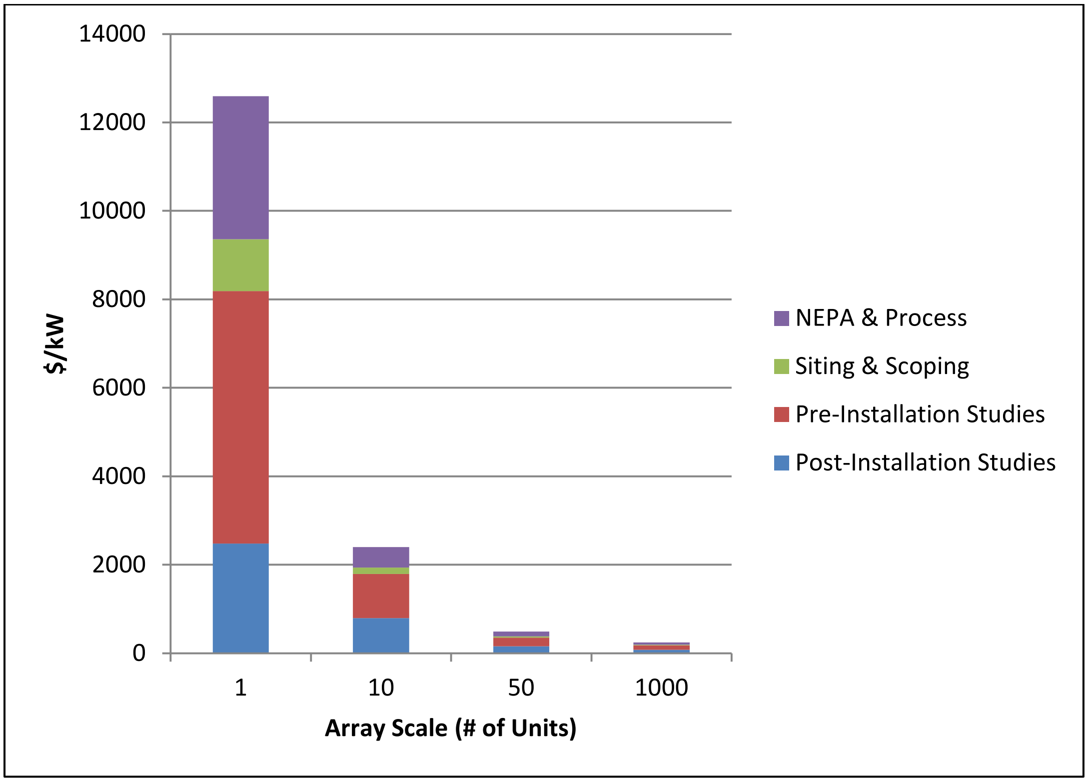

Figure 5-31. Total environmental CapEx estimate per deployment scale (1, 10, 50 or 100 units).

High and low bounds for the environmental compliance cost estimate were approximately +/-20% relative to the mean value shown in Figure 5-31. This is carried forward into the analysis of the array cost and economic assessments. Annually recurring costs for post-installation monitoring over the life of the project are shown in Figure 5-32. As with RM1-2, normalized costs decrease with larger arrays.

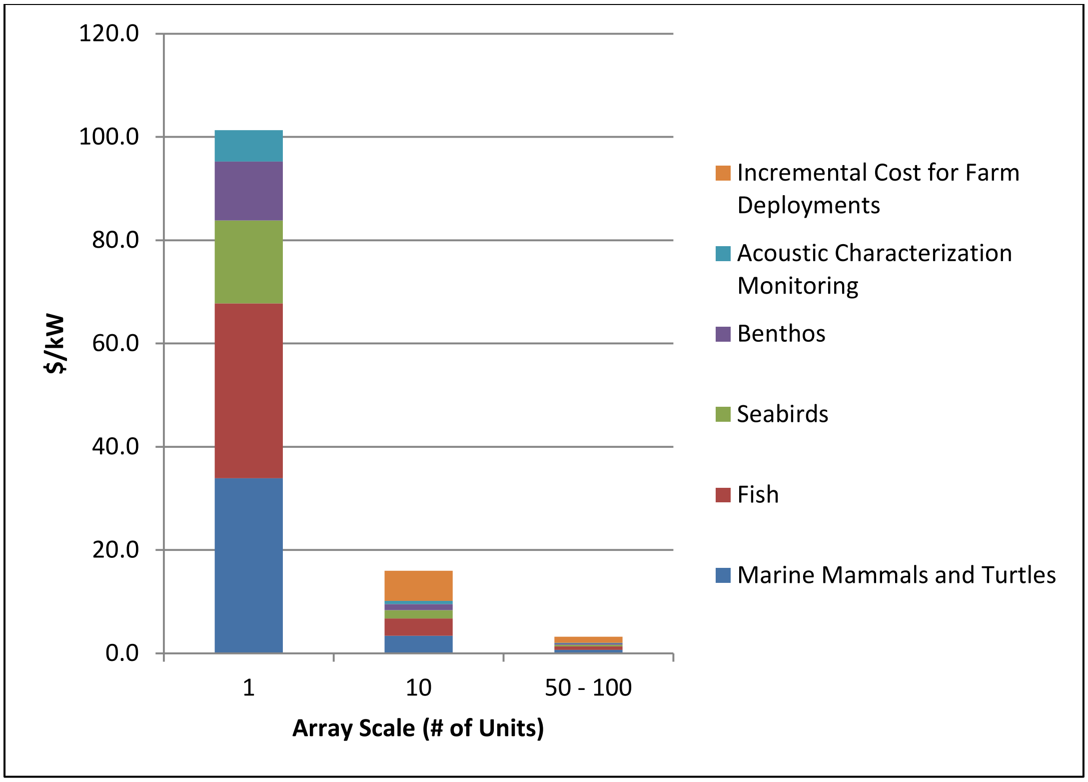

Figure 5-32. Annual cost of post-Installation monitoring per deployment scale.

5.4 LCOE Calculation

The LCOE estimate for a 10-unit RM3 array is 145 cents/kWh based on the FCR, AEP, CapEx, and OpEx estimates described below. The estimated AEP for this array is 7000 MWh per year. Table 5-16 gives a detailed breakdown of the LCOE estimate. The M&D cost contributes 49% of the total LCOE, followed by O&M costs, which account for approximately 32% of the LCOE. These findings indicate that the most critical area for targeting potential cost savings is M&D.

Table 5-16. RM3 LCOE breakdown by cost category (10-unit array).

	cents/kWh	% of total LCOE
Development	14.1	9.7%
M&D	71.1	49.0%
Subsystem Integration & Profit Margin	4.1	2.8%
Contingency	8.9	6.1%
O&M	47.0	32.4%
Total	145.3	100.0%

Figure 5-33 shows significant economies of scale at larger deployment scales.

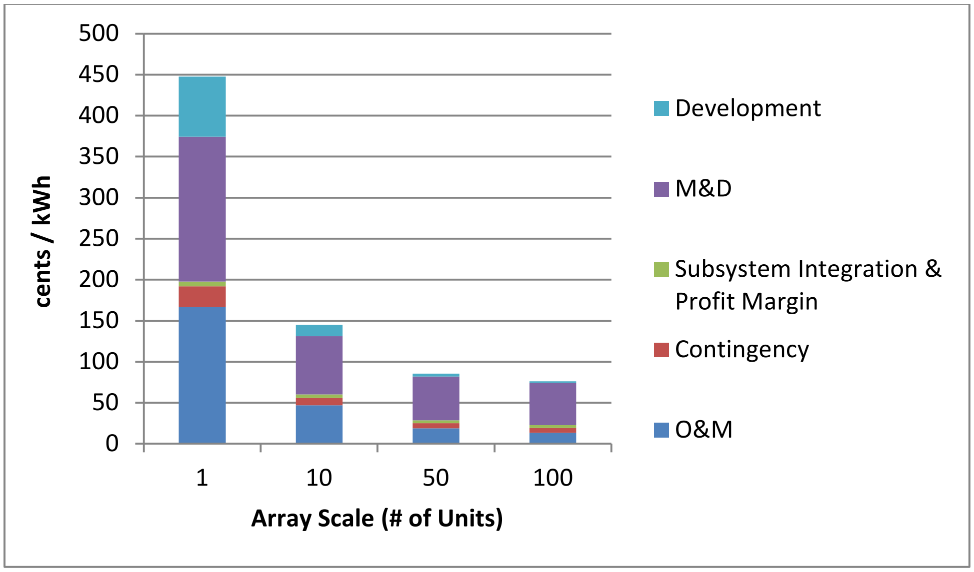

Figure 5-33. High-level LCOE (cents/kWh) breakdown per deployment scale for RM3.

The total CapEx for a single unit deployment was estimated to be approximately $61,100/kW, whereas the total CapEx per unit for a 100-unit array was estimated to be $13,600/kW. While there are some cost savings to be expected simply by increasing the manufacturing and fabrication volume from one to 100, major per-unit cost savings are expected to be realized within the installation cost category and the infrastructure cost category as well. Figure 5-34 shows the contribution of CapEx to the RM3 LCOE.

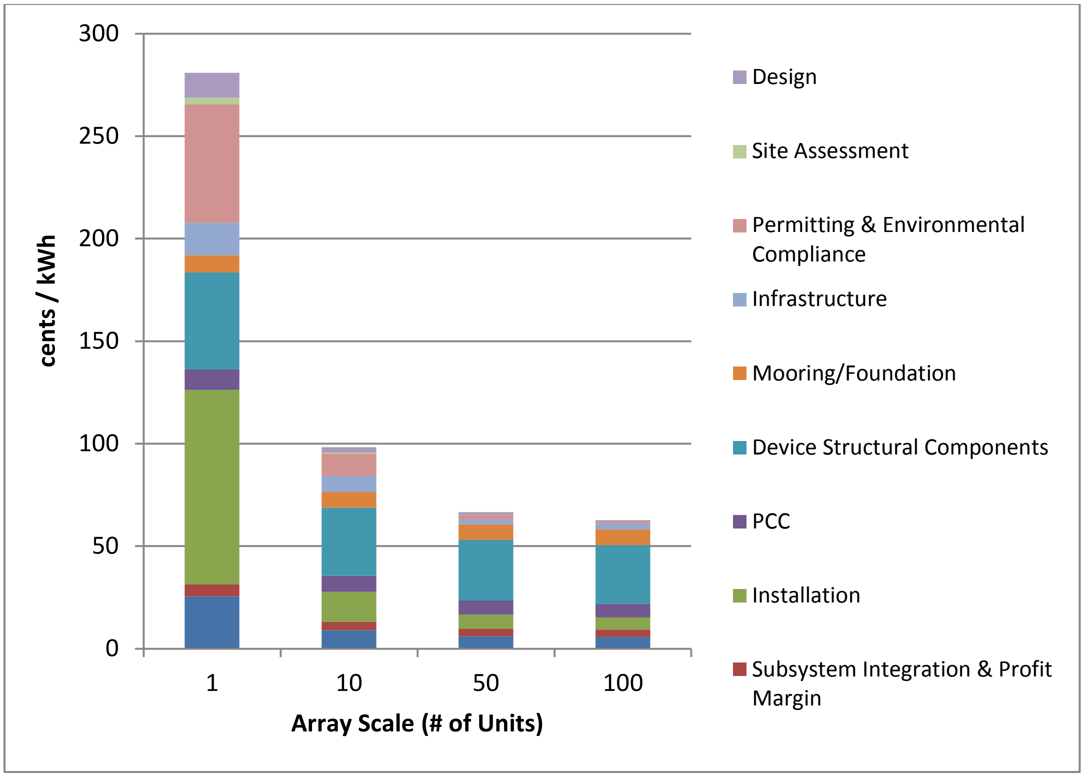

Figure 5-34. RM3 CapEx contributions to LCOE (cents/kWh) per deployment scale.

A detailed breakdown of major CapEx cost categories, in terms of levelized cost of energy, is provided in Table 5-17.

Table 5-17. Breakdown of RM3 CapEx contributions to LCOE (10-unit array).

	cents/kWh	% of total CapEx
Design	2.6	2.6%
Site Assessment	0.47	0.5%
Permitting & Environmental Compliance	11.0	11.2%
Infrastructure	7.8	7.9%
Mooring/Foundation	7.6	7.7%
Device Structural Components	33.2	33.8%
PCC	7.9	8.1%
Installation	14.6	14.8%
Subsystem Integration & Profit Margin	4.1	4.2%
Contingency	8.9	9.1%
Total	98.3	100.0%

Annual OpEx for a single unit deployment was estimated to be approximately $4,080/kW, whereas the annualized OpEx per unit for a 100-unit array was estimated to be $192/kW. Similarly to the capital cost contributions to LCOE, the operational cost contributions to LCOE are shown on Figure 5-35.

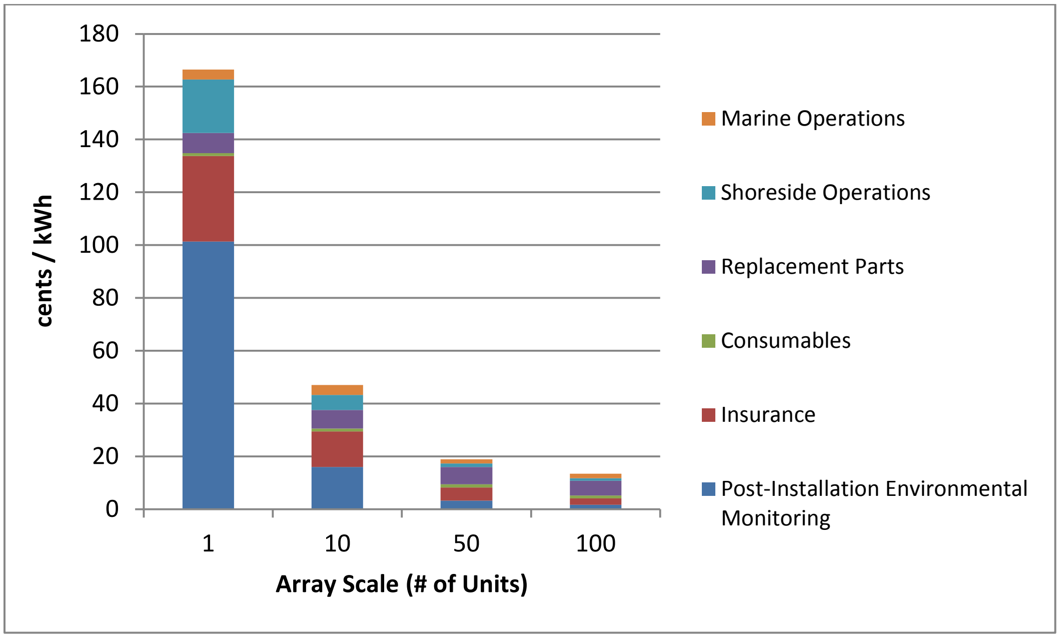

Figure 5-35. RM3 OpEx contributions to LCOE (cents/kWh) per deployment scale.

A detailed breakdown of major OpEx cost categories, in terms of LCOE, is provided in Table 5-18.

Table 5-18. Breakdown of RM3 OpEx contributions to LCOE (10-unit array).

	cents/kWh	**% of total OpEx**
Marine Operations	3.8	8.1%
Shoreside Operations	5.7	12.1%
Replacement Parts	7.0	14.9%
Consumables	1.1	2.4%
Insurance	13.4	28.4%
Post-Installation Environmental Monitoring	16.0	34.0%
Total	47.0	100.0%

6 Reference Model 4 (RM4): Ocean Current Turbine

6.1 RM4 Description

The RM4 ocean current turbine is a "flying-wing" concept intended for deployment in the Gulf Stream off the southeast coast of Florida. The concept design was inspired by the Aquantis C-Plane device, a marine current turbine with two rotors attached by angled wing spars to a center hub (http://ecomerittech.com). By contrast, the RM4 device has four rotors, with a rotorless center nacelle housing the power electronics, attached on a straight wing 120 m long (Figure 6-1). The device is designed to be submerged ~50 m below the surface and is moored to the seabed. The RM4 uses buoyancy within the wing and the five nacelles to maintain its position in the water column. Each rotor has a diameter of 33 m and has a 1-MW power rating, yielding a total device rated power of 4 MW. The rotors on the left and right side of the wing rotate in opposite directions in order to balance the torque applied to the device. The rotorless center nacelle housing the power electronics serves to condition the power generated by the rotors before it is delivered to the grid.

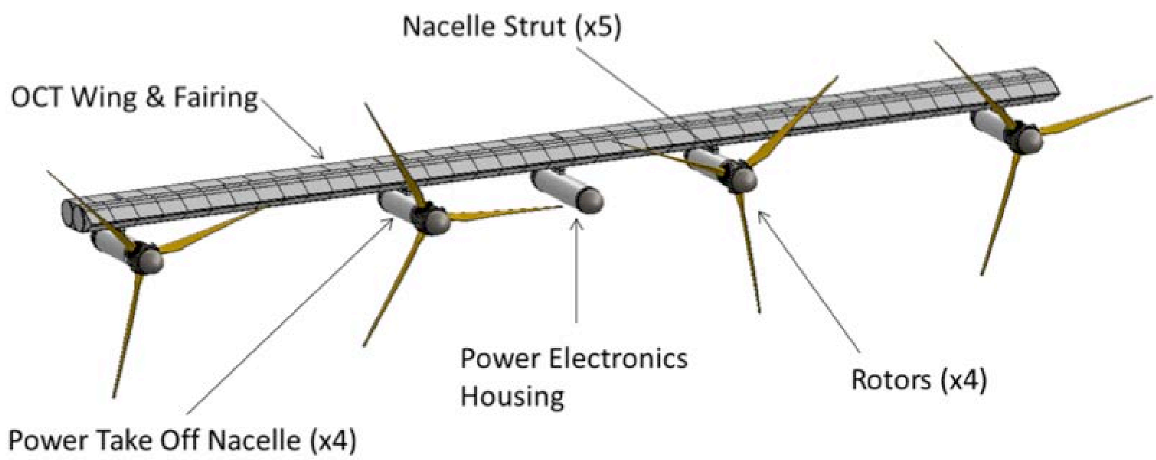

Figure 6-1. RM4 device design.

The two-point mooring system configuration and dimensions are shown in Figure 6-2. The system consists of a tension (or buoyancy) and thrust mooring lines that are secured to the seafloor using a suction pile and a drag embedment anchor (DEA), respectively. As the name indicates, the thrust mooring line supports the thrust loads produced by the turbine in operational conditions. The buoyancy tanks and tension mooring provide the necessary buoyancy to keep the device at an approximately stationary position in the water column, for the range of thrust values that the turbine will produce during operation.

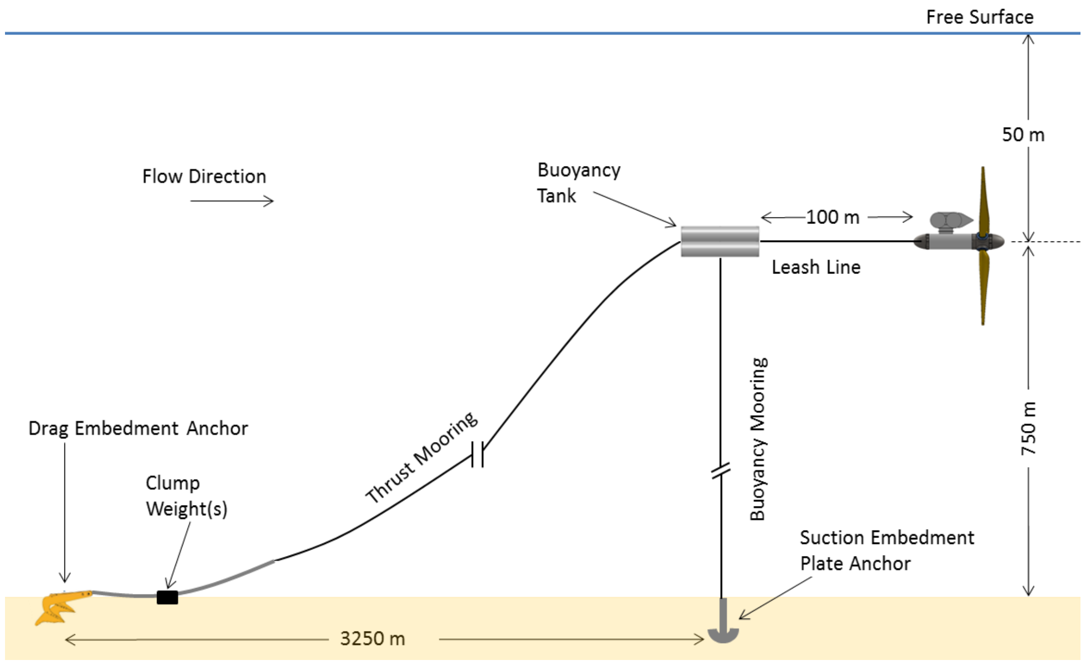

Figure 6-2. RM4 device dimensions.

6.1.1 Device Design and Analysis

As noted in Design Methodology for a Single Device, Section 2.1.1, the first step in the device design process was to develop a conceptual design appropriate for the modeled reference resource site. Once the concept design was completed, detailed device design was accomplished using simulation tools originally developed for use by the offshore and wind turbine industries. Specifically, the rotor design and optimization codes, HARP-Opt (http://wind.nrel.gov/designcodes/simulators/HARP_Opt/) and WT-Perf (http://wind.nrel.gov/designcodes/simulators/wtperf/), were used to design and analyze the performance of the rotor. WT_Perf simulations provided the performance characteristics of the RM4 device to derive an estimate of the annual energy production (AEP) at the reference resource site. The stability and dynamics of the wing and the mooring system's performance were modeled using the commercial software OrcaFlex. Detailed drive train and structural designs were then developed using commercial finite element analysis (FEA) tools (e.g., Solidworks), engineering judgment, analytical calculations, and design standards developed by the offshore oil and gas and shipping industries, as described in detail later in this chapter.

6.1.2 Arrays (Farm) Design and Analysis

As noted in Section 2.1.1, due to the lack of developed array optimization models, we did not perform detailed array design and analysis as described in the general methodology section. This adds to the uncertainty in the AEP estimate for arrays. It was assumed that a maximum of 100 units could be deployed at the reference site to reduce costs through economy of scale, which would lower the LCOE estimates. Figure 6-3 illustrates the array design for the RM4 device. Devices were spaced in a uniform grid with a 1 km separation between the devices in each row and a 1 km separation between the rows to ensure the mooring systems from the different devices do not interact. With this large device spacing, which is equivalent to approximately 30 rotor diameters, we assumed that wakes from upstream devices did not affect the performance of downstream devices.

The total array capacity at 100 units is approximately 400 MW. We selected a 3-phase AC transmission cable with a voltage level of 110 kilovolts (kV). All transmission cables included fiber optic lines to allow communication from each device to shore. Since wet mateable connections for this voltage do not exist in the commercial market, these connections would require custom design; therefore, there is great uncertainty estimating the cost of these components. Cable landing is accomplished by directionally drilling a conduit that connects the cable out to the first row of devices. This approach minimizes installation and maintenance costs.

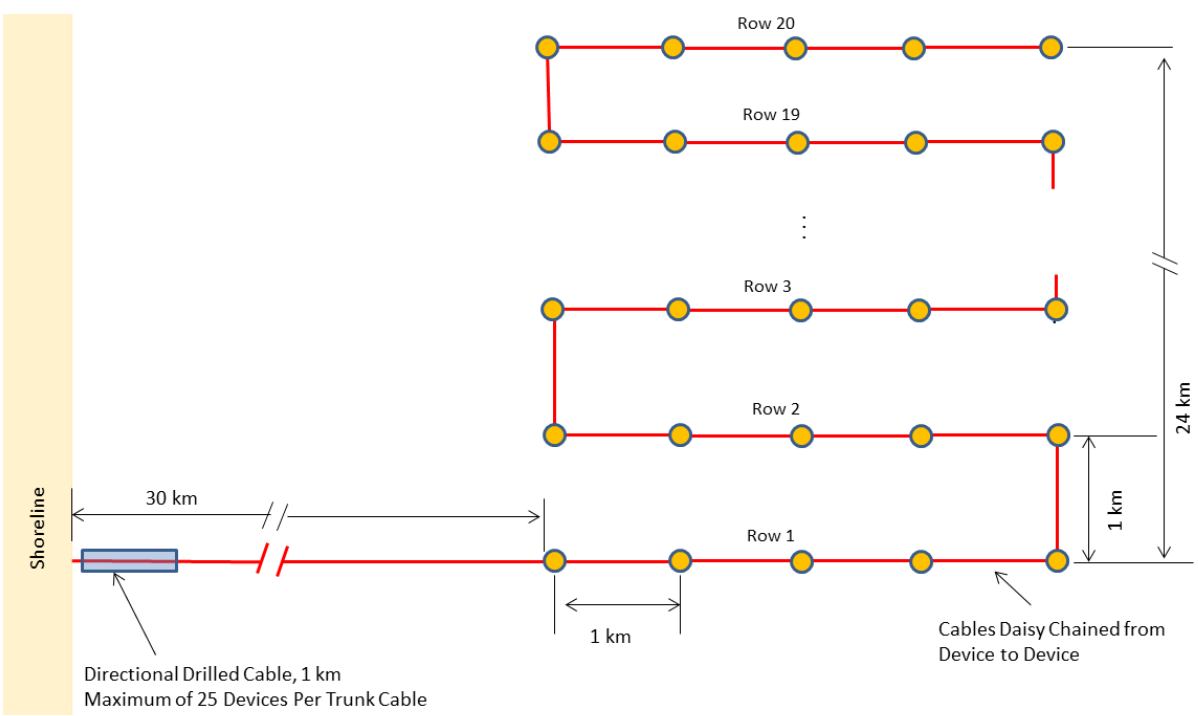

Figure 6-3. Array layout and subsea cabling (plan).

6.2 Module Inputs

6.2.1 Site Information

The reference wave energy resource for RM4 was developed from site information collected in the Florida Strait off the east coast of Florida. The Florida Current flows northward between the east coast of Florida and Grand Bahama Island. On average, the western edge of the Florida current is within 16 km of shore from Ft. Lauderdale and the high-velocity core of the current is about 20 km wide. The red arrows shown in Figure 6-4 illustrate the formation of the Gulf Stream off the southern coast of Florida.

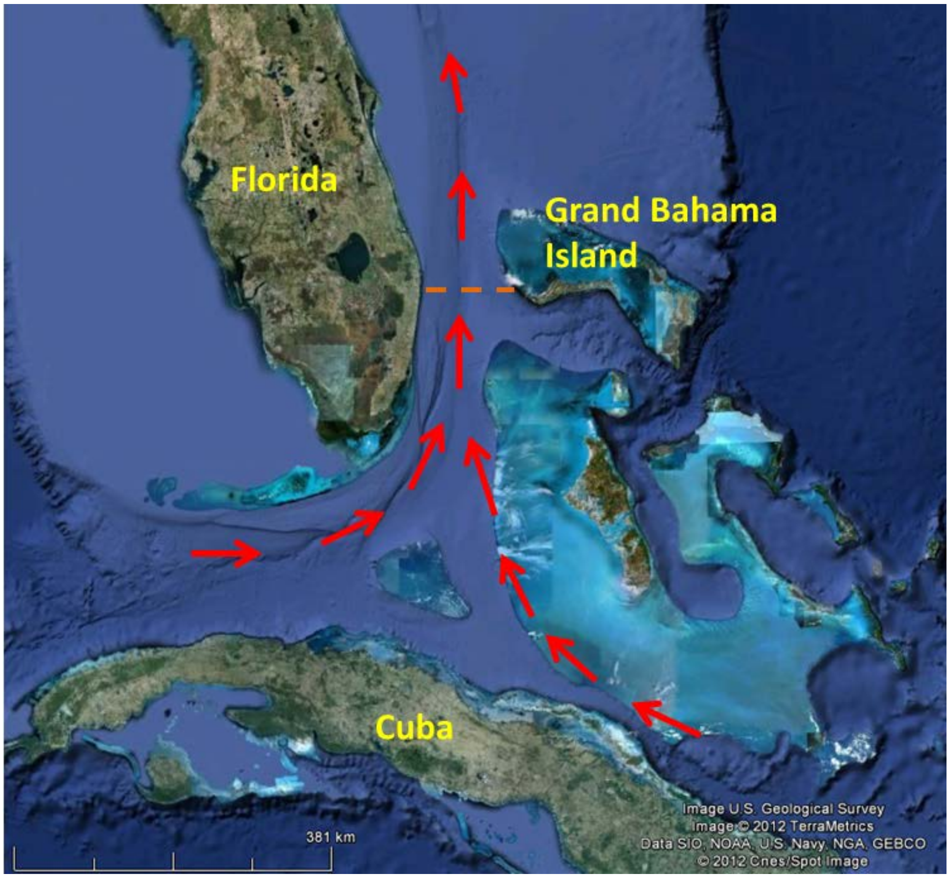

Figure 6-4. The Gulf Stream through the Florida Strait.

The deployment site selected for the RM4 project was located near 26.1 N, 79.8 W latitude and longitude. The site is about 30 km east of Fort Lauderdale and Port Everglades, which was selected as the staging and operational site. Because a large farm of devices cannot be deployed in a single location, a 5 km by 25 km region within the area of 26.1 N, 79.8 W, shown in Figure 6-5, was selected as the deployment region. This site lies within the high-current core of the Gulf Stream.

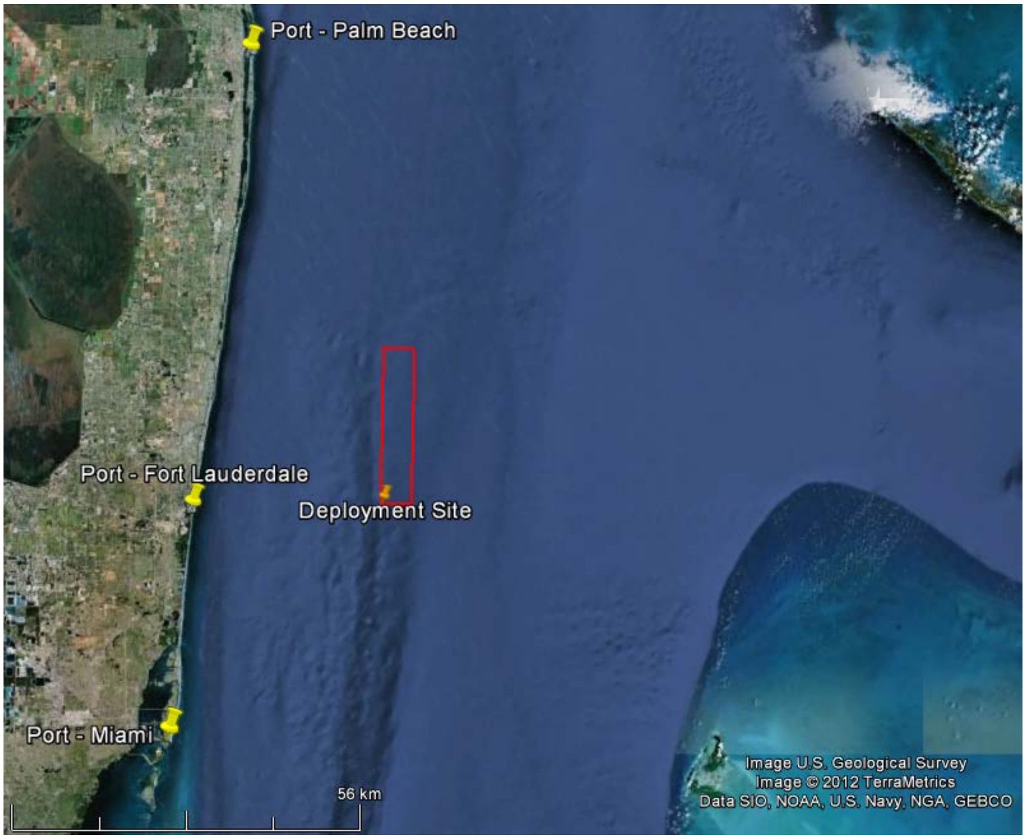

Figure 6-5. The location of the RM4 array deployment site (within the red rectangle).

6.2.1.1 Bathymetry and Bed Sediments

As described in Section 2.2.1, the reference site's sea bed morphology and sediment regime are important features that influence the selection and design of foundations, and moorings used for technology deployment, electric cables used for interconnection between devices and electricity transfer to shore, and potential environmental impacts to the sediment regime, bed morphology, and benthic organisms. We did not assess the bathymetry and bed sediments for the RM4 reference resource site; we assumed the bed sediments to be medium to coarse sands.

6.2.1.2 Current Speed Frequency Histogram

The only detailed data available to derive a current speed frequency histogram at the time of our study were Acoustic Doppler Current Profiler (ADCP) measurements collected by Florida Atlantic University (FAU) (Raye 2002). However, no Acoustic Doppler Velocimetry (ADV) data was available to characterize the effects of turbulence on design performance for this reference model site. Other data, including validated Hybrid Coordinate Ocean Model (HYCOM) simulations of current speed profiles at the reference site have since been published (Neary et al. 2012a).

For 19 months during 2000 and 2001, FAU deployed an ADCP in 330 m of water along the edge of the Miami Terrace at 26.18 N, 79.83 W. A current speed frequency histogram (Figure 6-6) was developed from the FAU data near the deployment location at the 50-meter depth where the

RM4 device would be deployed. Figure 6-7 presents the minimum, average, and maximum current speed observed during the 19 month FAU study (Raye 2002). In the absence of other data, we assumed the FAU ADCP measurements were representative of the ocean current hydrokinetic resource within the deployment region. Although this introduces some uncertainty into the estimate of the ocean current power in the deployment region, we assumed that any variation would be minimal because both the ADCP measurements and the deployment region are within the core of the Florida Current.

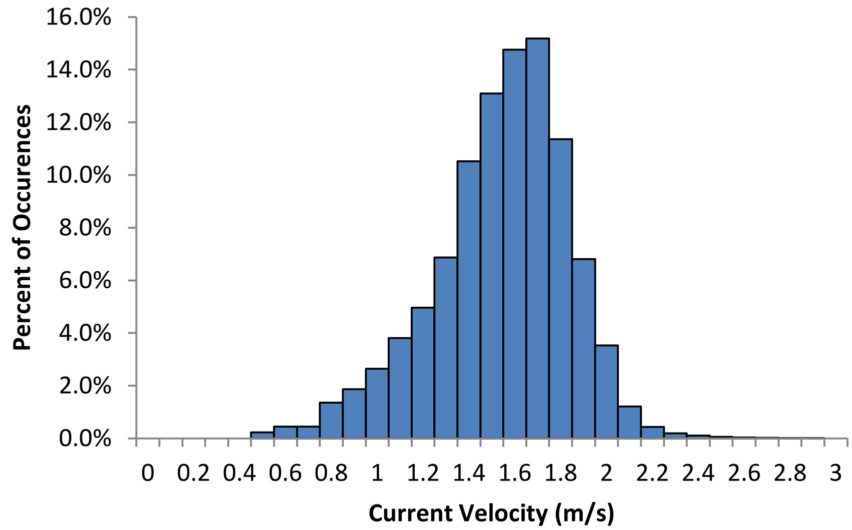

Figure 6-6. Frequency histogram of the current speed (horizontal velocity) at 50 m depth, measured using the FAU ADCP over a 19-month period (adapted from Raye 2002).

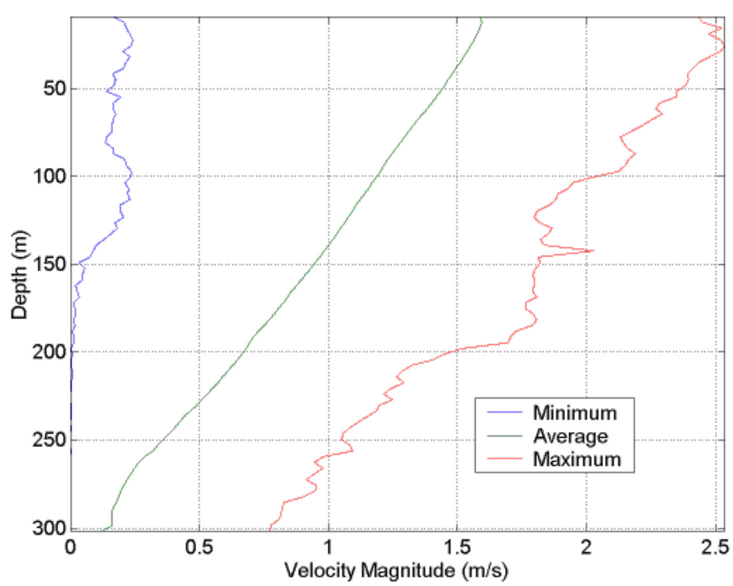

Figure 6-7. Minimum, average, and maximum current speed (horizontal velocity magnitude) profile at the device deployment site (adapted from Raye 2002).

6.2.1.3 Extreme Hydrodyamic Loads

In order to perform the wing and nacelle structural design, we considered one extreme hydrodynamic load condition based on a 2.4 m/s current speed that produces a 1400 kN thrust load on an operating turbine.

6.2.1.4 Adjacent Port Facilities and Grid Options

Ft. Lauderdale was selected as the port facility from which service operations could be based. All LCOE calculations only considered power delivered to shore. Costs for overland transmission and grid connection to sub-stations were excluded.

6.2.2 Device/Array Information

In the conceptual design, we determined design specifications based on site resource characteristics borrowed from successful commercial technologies, and by applying engineering judgment, economic considerations, and simple hand calculations. A summary of the design specifications for RM4 is given in Table 6-1.

Due to the consistent and predictable nature of the Gulf Stream Current, there was an opportunity to develop turbines with very high capacity factors (50% to 75%). To achieve high capacity factors, the turbine rotor was designed to achieve rated power at the most frequently occurring current speed of approximately 1.7 m/s.

The power rating for each rotor was selected to meet torque constraints of commercial off-the-shelf (COTS) drivetrain components.

A rotor diameter of 33 m was designed using the HARP-Opt turbine design code (NREL website reference) so the turbine achieved rated power at 1.7 m/s.

The blades designed for the RM4 device leveraged the blade design developed for the RM1 device. Specifically, the same NACA 63_1-424 airfoil was used as the primary airfoil shape because of its relatively large minimum pressure coefficient, which makes this airfoil resistant to cavitation. The NACA 63-series airfoils are also known to delay stall and are less sensitive to leading edge roughness than the NACA 4-and 5-series airfoils (Lawson et al. 2013, in preparation). In addition, as with the RM1 blade design, the rotor was designed as a VSVP device; therefore, we assumed a circular cross-section at the blade root (to allow for a blade-pitching mechanism) that transitioned to the NACA 63_1-424 airfoil shape at 20% of the blade span.

Table 6-1. RM4 design specifications.

Description	Specification	Justification	Details
Deployment depth	800 m	Resource location	The core of the gulf stream is located at an 800 m depth in the selected deployment region.
Operational depth (hub centerline)	50-60 m	Site resource assessment	Surviving harsh seas due to hurricanes is possible if the device is sufficiently below the free surface. The 50–60 m depth provides sufficient clearance for ocean-going ships to safely pass over the device.
Survival depth	200 m	Engineering judgment	All device components must be designed to withstand pressures at a 200 m depth, which could occur with buoyancy system failures.
Mooring line scope	4:1	Engineering judgment	A 4:1 mooring scope allows the mooring system to hold the necessary thrust load from the device without requiring large amounts of buoyancy.
Number of rotors per device	4	Economics	A multi-rotor device will have a lower LCOE.
Power per rotor	1 MW	Gearbox availability	OEM gearboxes were limited to 1 MW based on the torque requirements for turbines.
Rated power	4 MW	Hand calculation	Four times installed capacity of each rotor.
Rotor diameter	33 m	Hand calculation	A 33 m rotor provides 1 MW at the most frequently occurring current speed.
Rated current speed	1.7 m/s	Engineering judgment	Wind turbines typically have their rated current speed 1.3–1.5 times the most frequently occurring current speed, depending on the current frequency histogram. We selected a lower rated current speed to increase the capacity factor, enabling an array of RM4 devices to provide a reliable base load to the grid.
Operational current speeds	0.5 – 2.4 m/s	Resource based	The reference resource site has a measured current speed between 0 and 2.5 m/s at hub height.
Thrust mooring line anchor type	Drag embedment	Engineering judgment	This is the best option for the sandy bottom locations.
Buoyancy mooring line type	Suction embedment plate anchor	Engineering judgment	This is the best option for withstanding the vertical load the tension mooring must hold.
Array configuration	Linear with 1 km separation	Engineering judgment	A simple array configuration was selected because array modeling tools are not yet sufficiently developed to enable detailed array analysis.

6.3 Design, Analysis, and Cost Modules

6.3.1 Design & Analysis (D&A) Module

6.3.1.1 Performance analysis and AEP estimation

As described in Section 2.3.1.1, the potential and AEP were calculated from the power performance curve and the current frequency histogram. We used HARP-Opt, a combination of a Blade Element Momentum Theory (BEMT) code, WT-Perf, and an optimization algorithm, to optimize the blade shape and performance characteristics of the rotor. See Lawson et al. 2013 (in preparation) for details. The predicted single rotor operating characteristics are shown in Figure 6-8. The installed capacity for each rotor occurs at 1.7 m/s and is 1.1 MW; therefore, the rated power for the RM4 device is approximately 4 MW. As described in Section 2.3.1.1, the power curve and the given current frequency distribution were combined an AEP of 23 GWh for the dual-rotor system, which gives a capacity factor of 0.7. The rated power and annual output per device, dual-rotor, are given in Table 6-2. For arrays, the total AEP is determined by multiplying this estimated AEP per unit by the number of devices in the array.

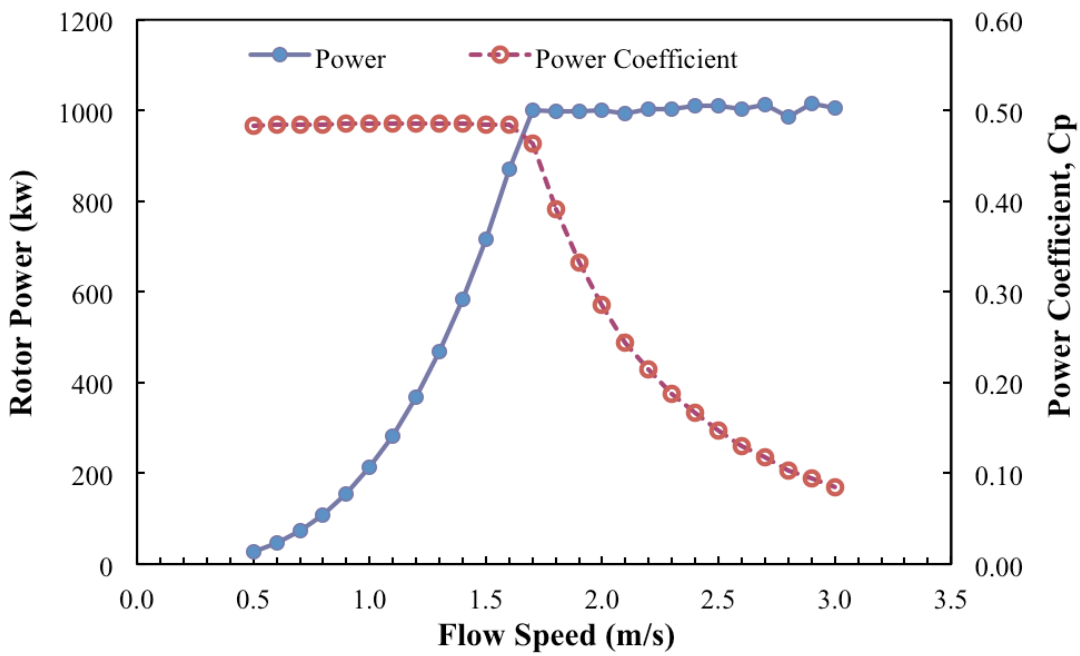

Figure 6-8. Rotor power (and power coefficient) vs. flow speed (current speed).

Table 6-2. RM4 rated power and AEP output for single device.

Performance Variable	Per Unit
Rated Power	4 MW
Annual Energy Production	23 GWh

6.3.1.2 Materials Specifications and Structural Analysis

As described in Section 2.3.1.2, structural analysis of the main components of the RM device was performed to determine material specifications from which certain component costs can be estimated. This section provides details on this analysis for the RM4 device. Note that since the blade structural design was scaled up from the RM1 blade design, no detailed blade structural design is presented in this chapter.

6.3.1.2.1 Estimation of Maximum Loads that Drive Structural Designs

In order to perform the wing and nacelle structural design, two extreme events that were determined most likely to cause extreme loading were identified. At this preliminary state in the design process, fatigue loads were not considered. The two extreme load cases are as follows:

> **Load Case 1:** The wing is submerged below the normal operational depth of 50 m—at a depth of 100 m—due to a depth-control system failure and for some reason the rotors continue to operate. At this depth, the device encounters a gust of 2.4 m/s causing a rotor thrust of 1400 kN (rounded up from 1381 kN). Table 6-3 summarizes the structural load assumptions (also see Lawson et al. 2011 and Bir 2011).
>
> **Load Case 2:** Due to a depth-control system failure the wing sinks to 200 m and the rotors have fully stopped. The wing structure experiences extreme hydrodynamic pressures and must maintain integrity and buoyancy at this depth. At this depth, the wing design is dominated by hydrostatic pressure loads, which would require additional internal stiffening of the pipe-sections.

The wing and nacelle structural components were then designed to withstand the loads during these two load case scenarios. In addition, handling loads due to lifting of the device during construction and instillation, as well as loads experienced during towing the device to the installation site were estimated using simple engineering calculations. High-fidelity simulations using finite element analysis and computational fluid dynamics simulations were not performed to estimate these loads.

Table 6-3. Load case 1 details.

Load	Value
Rotor Thrust (red)	1400 kN
Rotor Shear (green)	280 kN
Wing Drag (blue)	5.3 kN/m
Mooring Line R1 (black)	2800 kN
Mooring Line R2 (black)	2800 kN
Maximum Moment	27.5 MN-m
Maximum Compressive Force	3360 kN
Hydrostatic Pressure	10 bar

6.3.1.2.2 Wing Design

The 120-meter length of the wing, shown in Figure 6-9, allows for a 2.5 m tip-to-tip clearance between the rotors. Recent NREL research, based on results from a Large-Eddy Simulation (LES) model, shows that this tip clearance will not adversely affect rotor performance or power output (Churchfield et al. 2013). Figure 6-10 shows the wing cross-section and nacelle outer dimensions.

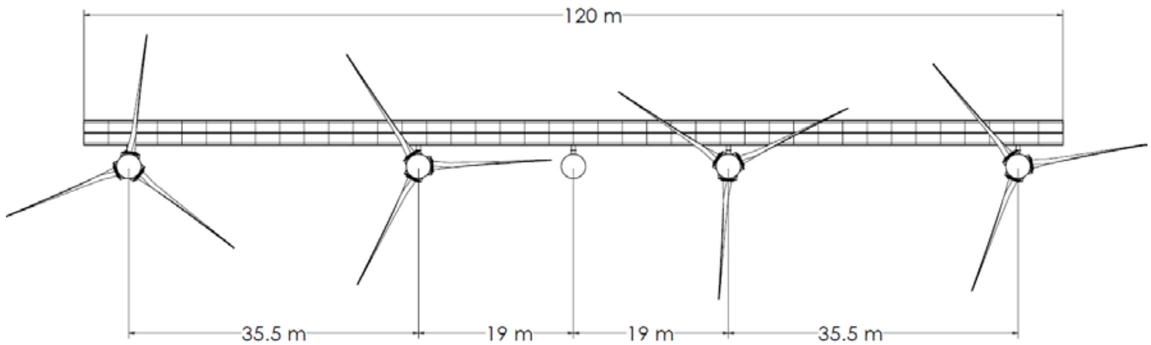

Figure 6-9. Front view of the RM4 device.

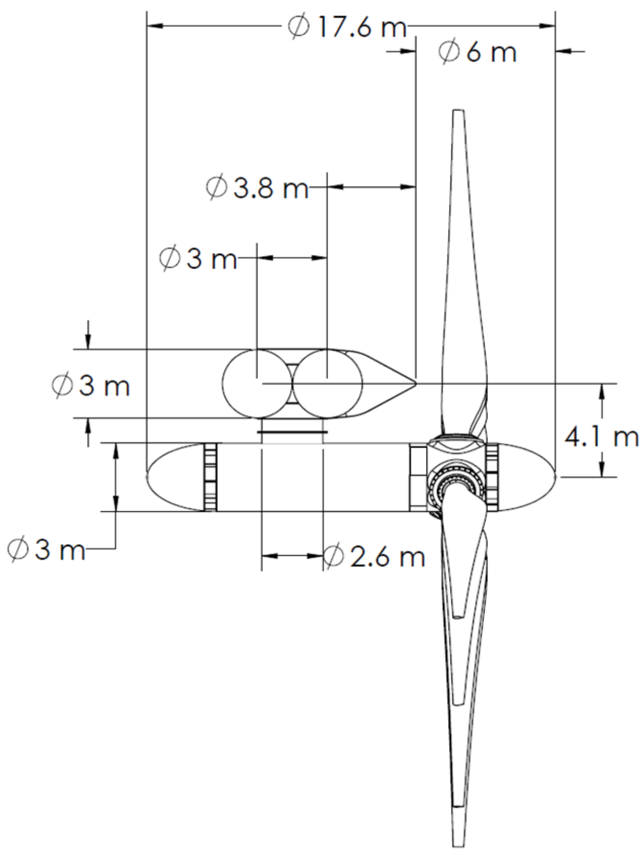

Figure 6-10. Side view of the RM4 device.

The wing design uses two side-by-side circular pipes that span the length of the wing. These members act as the primary load-carrying member of the wing. Both pipes are connected together along the wing with diagonal pipe trusses and perpendicular plate stiffeners (Figure 6-11) so that they form a rigid structure. The structural design of the wing is based on the American Petroleum Institute (API) recommended practice for planning, designing, and constructing fixed offshore platforms—the Working Stress Design standard, API RP-2A WSD, which was used for all circular sections of the design. Any noncircular sections (such as the perpendicular stiffeners) were designed using the API referred American Institute of Steel Construction (AISC) allowable stress specification for the design, fabrication, and erection of structural steel for buildings.

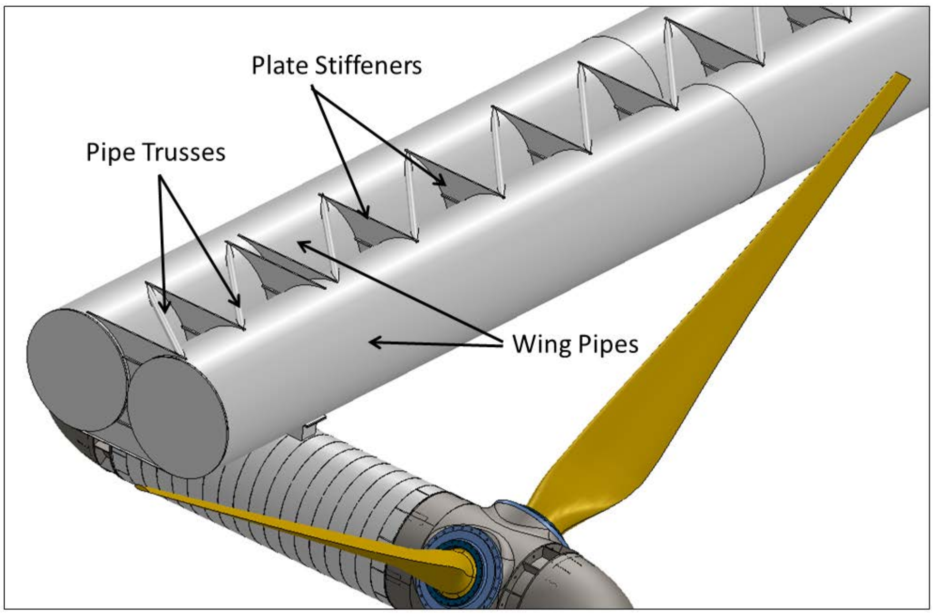

Figure 6-11. Designed wing members.

To design the wing structure, each wing pipe was assumed to support 50% of the structural loads. Therefore, each pipe acts independently and was designed with enough strength to transfer half of the rotor thrust, rotor shear, and wing drag loads from the device to the mooring system. Our assumption that the wing pipes act independently is conservative and eliminates the need to design the interconnecting braces. Interconnecting braces, however, are still required to insure that the two-pipes act as a single load-carrying structure. The size of the connecting braces is determined assuming the wing structure performs similar to a truss structure.

As described in Section 2.3.1.2, we did not consider dynamic loads to assess fatigue. The structural analysis and design procedure was based on conservative static load case assumptions described in Section 6.3.1.2.1.

Figure 6-12, Figure 6-13, and Figure 6-14 show the detailed structural design of the wing components. Table 6-4 presents material specifications of the pipe and plate materials used for the wing design. Inside the wing pipes, ring stiffeners were used to reinforce the section as required from Load Case 2. Additionally, five diaphragm plates are used to compartmentalize the wing into watertight sections. In the event that two compartments flood, the wing can still maintain positive buoyancy.

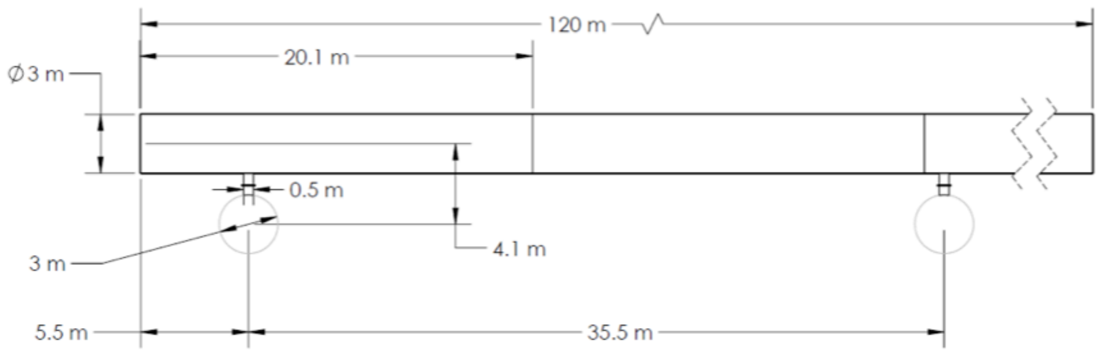

Figure 6-12. RM4 device wing front view.

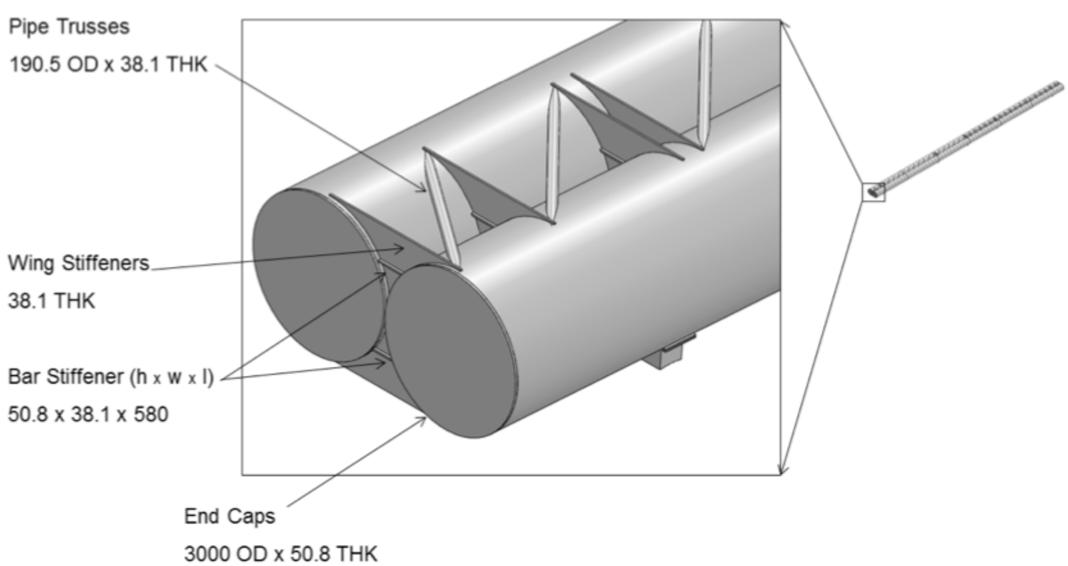

Figure 6-13. RM4 device wing outer stiffener detail (units in mm).

NOTE: The figure shows the end caps on one end of the double pipe structure.

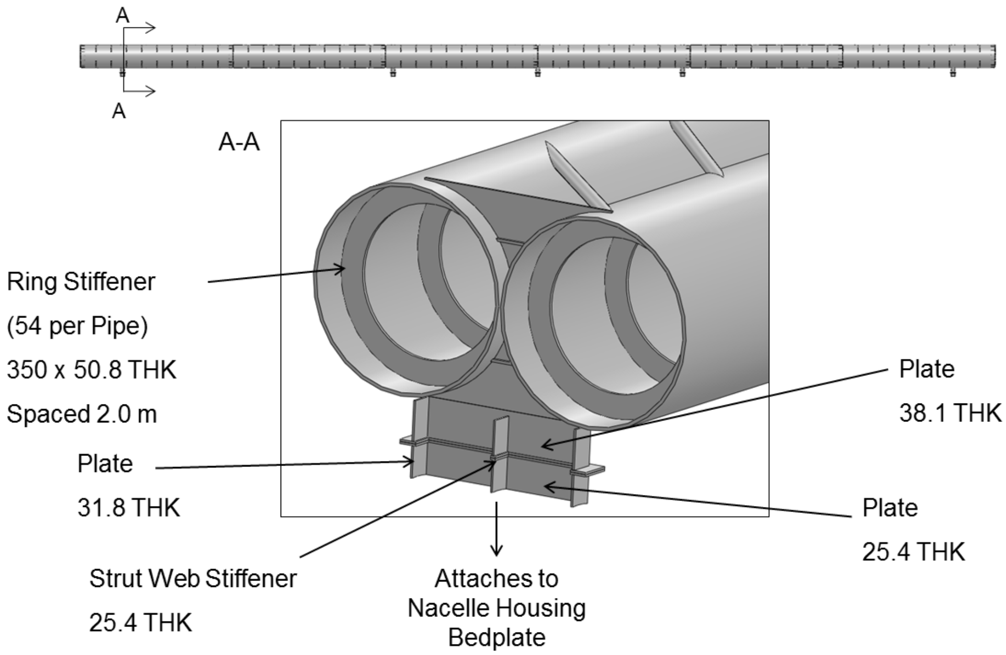

Figure 6-14. RM4 device wing inner stiffener detail (units in mm).

NOTE: Section view A-A shows interior pipe and nacelle strut detail.

Table 6-4. Wing material specifications.

Property	Value
Total Wing Mass	1170 Mg
Pipe Material	API 5L Grade X52
Plate Material	API 2H Grade 50
Pipe Yield Strength	359 MPa (52 ksi)
Plate Yield Strength	345 MPa (50 ksi)
Wing Length	120 m
Wing Pipe Diameter	3.0 m (2 Pipes)
Pipe Thickness	50.8 mm (2 in)

6.3.1.2.3 Nacelle Design

The PCC nacelle housing was designed by Penn State's Applied Research Laboratory (ARL) and modified by ReVision to reduce structural complexities and associated production costs. Modifications were minor so that strength and dimensions would be relatively unchanged. The external dimensions of the housing are shown below in Figure 6-15.

The support structure for the turbine was designed to house the drive components and to act as the means of connection to the wing spar. The center support housing of each nacelle provides the main support structure with attachment to the wing spar. It is also designed to provide access to the gearbox shown in Figure 6-15. The center support housing was designed with cylindrical end flanges to mate with the forward and aft nacelles. Figure 6-16 shows the nacelle components. The center housing could be made from cast steel or fabricated from steel as a weldment. The outer contour of the center support housing was made from thin rolled steel plate and could be attached to the center housing in split sections. Bulkheads were designed to be located at the forward and aft ends to mount the gearbox and to provide support for the drive components. Figure 6-17 lists the nacelle specifications and shows the results of preliminary finite element analysis (FEA) for nose and shell buckling.

The rotor hub was not included in the structural cost of the housing; rather it was included in the powertrain and rotor cost breakdown in the following section. A summary of the material specification and mechanical properties is listed in Table 6-5.

The nacelle was designed for easy system assembly and access for maintenance. The generator and gearbox assembly is mounted to a sliding rail system permitting easy access to these components through removal of the forward conical section.

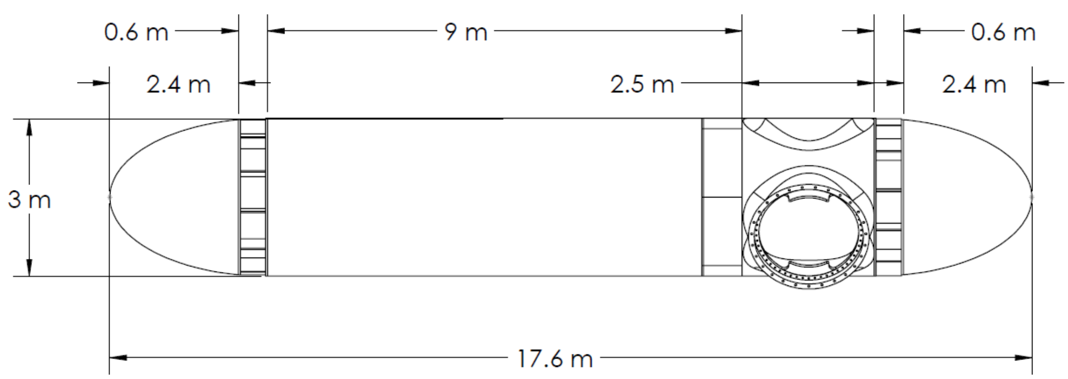

Figure 6-15. PCC nacelle housing major dimensions.

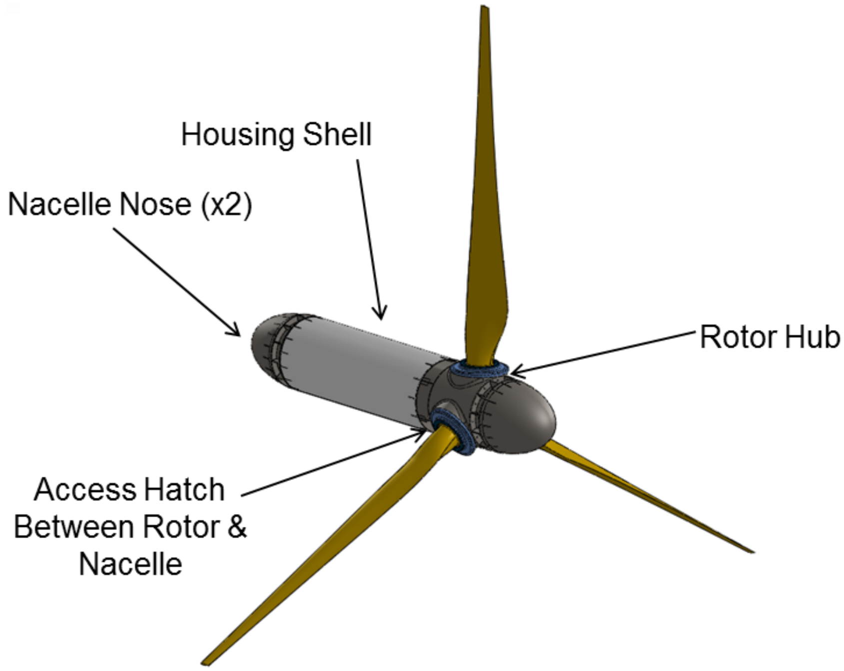

Figure 6-16. RM4 device nacelle components.

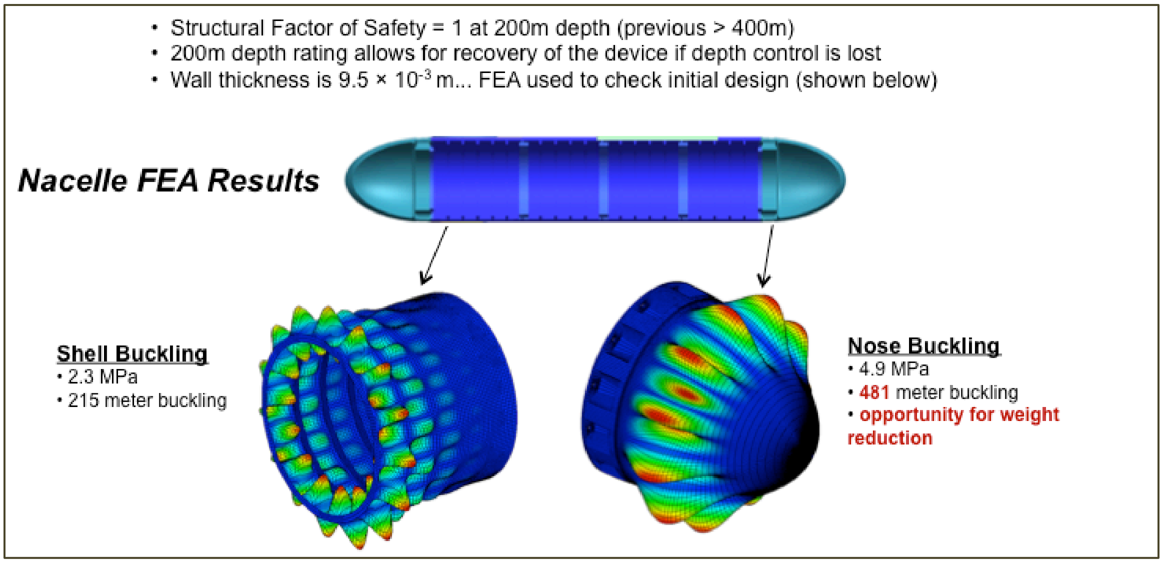

Figure 6-17. Nacelle specifications and structural analysis results.

Table 6-5. RM4 device PCC and power material specifications.

Property	Value
PCC Nacelle Housing Mass	23.5 Mg
Shell & Plate Material	API 2H Grade 50
Yield Strength	345 MPa (50 ksi)
Length	17.6 m
Diameter	3.0 m
Shell Thickness	9.5 mm

6.3.1.2.4 Nacelle Strut Design

During extreme rotor thrust events, the strut that connects the nacelle to the wing must withstand large loads. SolidWorks FEA simulations were used to check if the strut was sufficiently designed to withstand loads during Load Case 1, which will produce the largest strut loads. For the simulations, the rotor thrust and shear from Load Case 1 were applied at the rotor location. To assess the results, a load factor and a material factor were used to account for deviations from the loading condition and material strength. Load factors of 1.3 for both permanent and variable functional loads and a factor for steel of 1.15 were used, as recommended by DNV standards. The resulting combined safety factor is 1.5. The FEA analysis illustrated in Figure 6-18 showed that the effective factor of safety for the strut is 1.58, which satisfies the target design factor.

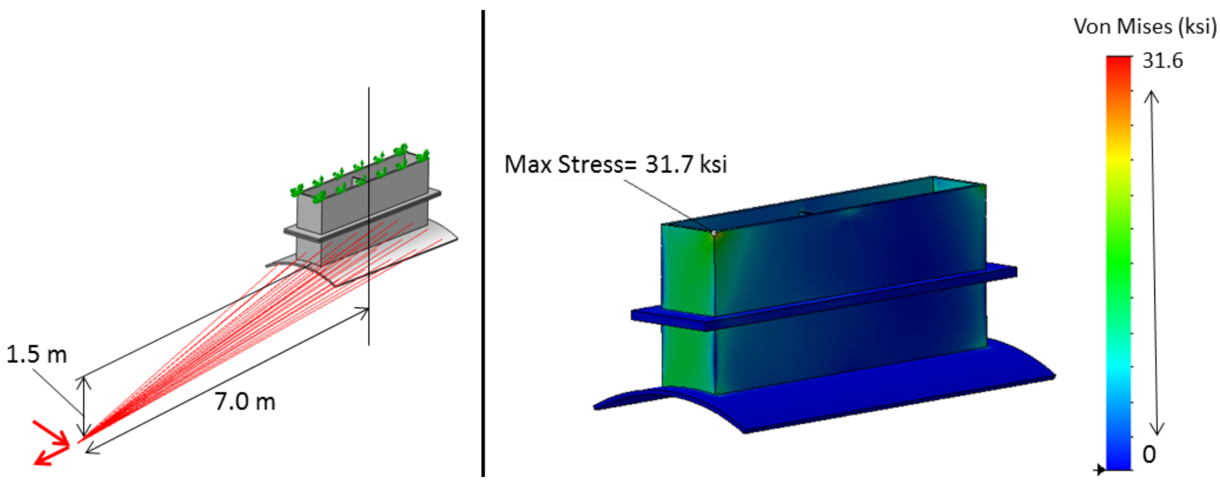

Figure 6-18. Nacelle strut thrust and shear loads.

NOTE: Forces in red are shown on the left. Von Mises Stress Distribution is shown on the right.

6.3.1.2.5 Wing Fairing Design

A fairing design was completed for the wing to reduce the wing wake. Reducing the wake decreases the unsteady loads the blades are exposed to as they sweep by the wing. The fairing design was conceptualized to develop a complete understanding of the cost profile, but was not optimized. Figure 6-19 and Figure 6-20 show the cross-section of the fairing. Table 6-6 presents a summary of the fairing design characteristics.

The structure of the fairing was determined by estimating the loads on the fairing and then designing a structure to withstand the loads. Pressure loads due to water flowing over the fairing dominate the fairing loads and XFOIL, an airfoil analysis code developed by the Massachusetts Institute of Technology (MIT), was used to estimate the pressure distribution. Based on preliminary assessments, the major dimensions of the fairing are representative of the structural complexity required for this type of design. However, additional studies of the fairing's ability to minimize flow-separation should be carried out to study the potential effect on the down-stream rotors.

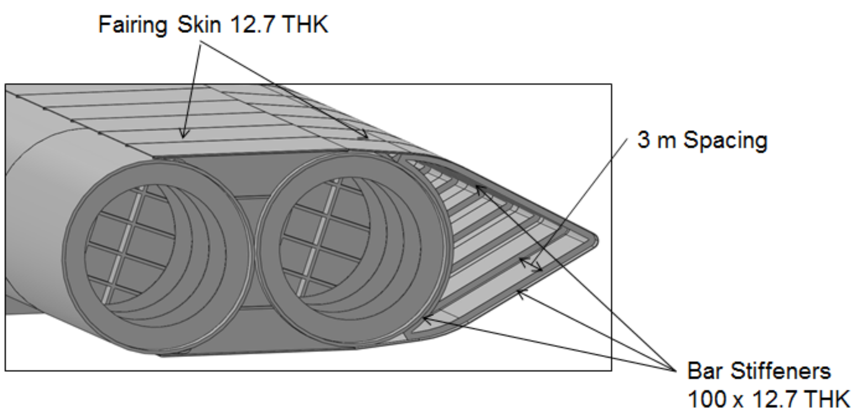

Figure 6-19. RM4 device fairing detail.

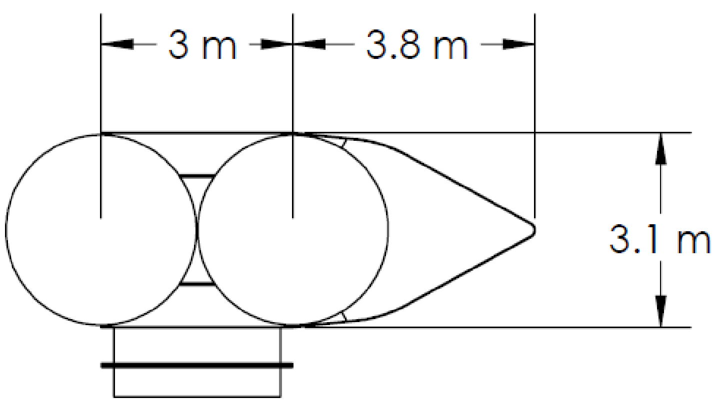

Figure 6-20. Fairing major dimensions.

Table 6-6. Summary of fairing properties.

Property	Value
Fairing Mass	177 Mg
Material	API 2H Grade 50
Yield Strength	345 MPa (50 ksi)
Fairing Thickness	12.7 mm

6.3.1.2.6 Buoyancy Tank Design

The buoyancy tank was designed to withstand the hydrostatic pressure at a water depth of 100 m. Figure 6-21 and Figure 6-22 show the structural design of this buoyancy tank and Table 6-7 lists the specifications. The four 16-meter length pipe sections provide 315.6 Mg (347.9 short tons) of net buoyancy. Due to the shallower design depth, ring stiffening is not required for the buoyancy tank according to API standards.

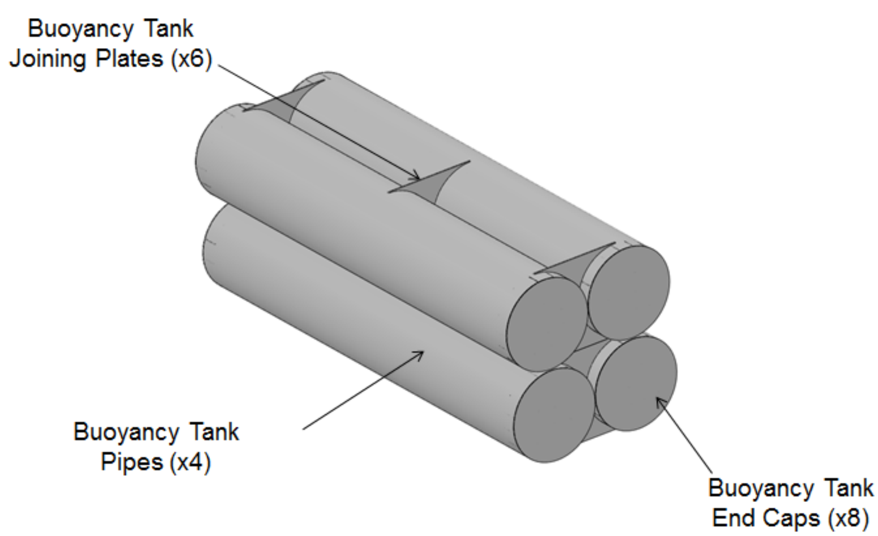

Figure 6-21. Bouyancy tank major components.

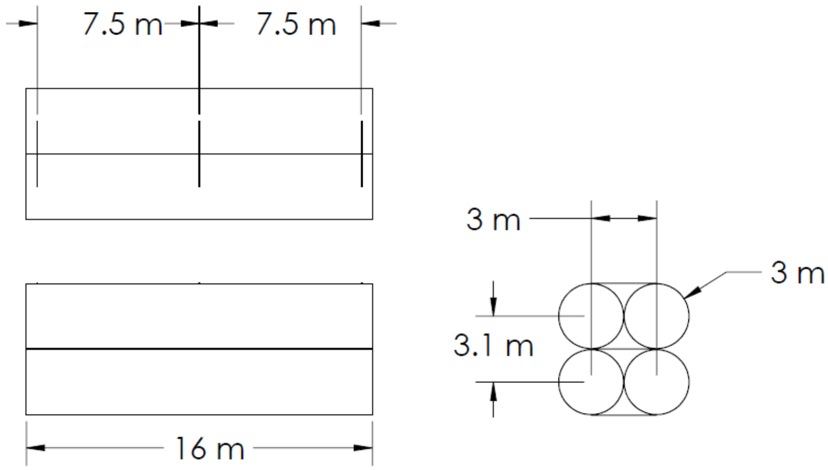

Figure 6-22. Buoyancy tank major dimensions.

Table 6-7. Buoyancy tank specifications.

Property	Value
Buoyancy Tank Mass	150 Mg
Pipe Material	API 5L Grade X52
Plate Material	API 2H Grade 50
Pipe Diameter	3.0 m
Pipe Thickness	25.4 mm

6.3.1.2.7 Total Mass and Buoyancy

The component masses listed in Table 6-8 include all subsystems contained within each component. For example, the PCC nacelle mass contains the mass of the housing, rotor, and powertrain components. The buoyancy breakdown of the device shows 295 Mg (325.2 short tons) of reserve buoyancy or about 14% of the total dry mass of the device.

Table 6-8. RM4 device component weight and buoyancy breakdown.

NOTE: The net submerged weight "+" is positively buoyant.

	Qty	Total Dry Weight (Mg)	% of Total Weight	Displacement (m^3)	Net Submerged Weight (Mg)
Wing	1	1,199	57	1,709	551
PCC Nacelle	4	677	32.2	499	-154
Power Nacelle	1	49	2.3	110	-166
Fairing	1	177	8.4	23	64
Device Total	**1**	**2,102**	**100**	**2,341**	**+295**
Buoyancy Tank	1	150	-	454	316

NOTE: 1 Megagram (Mg) = 1 metric tonne = 1.1 tons

6.3.1.3 Buoyancy Control

The main support of the wing base is a dual cylindrical spar system and an emergency recovery system was designed into the device in the case of loss of control or persistent descent. Salvage bags have been added to the wet spar in an activation system illustrated in Figure 6-23. A commercially available underwater lift bag system (Subsalve SP40000), capable of 40 000 lbs of buoyancy, per bag, is installed in the wet spar. The bag is activated by high pressure air stored in the dry spar—6000 psi tanks. Ultrahigh pressure (10 000 psi) tanks could be used for space and weight reduction. Valves would open to expel water from the wet spar as the bags inflate. While a reactive gas generation system could be used to reduce cost, weight and complexity, the compressed cylinder concept circumvents the need to pressure-rate the dry spar. The activation system needs to be determined based on depth sensing and device failure monitoring.

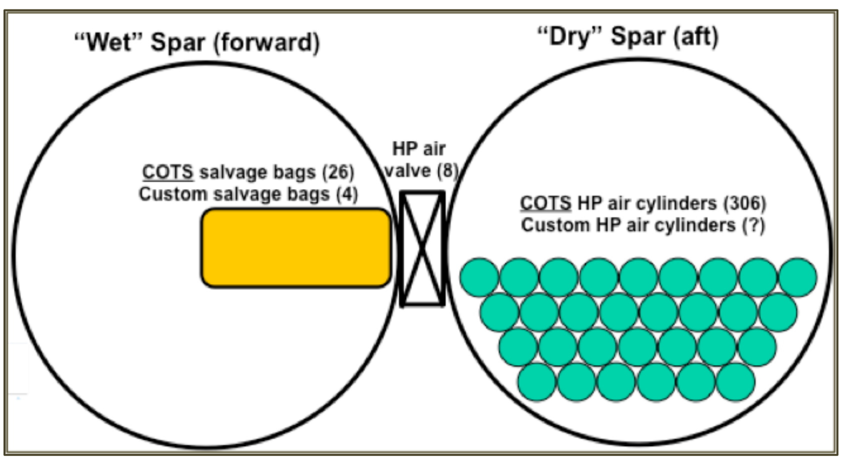

Figure 6-23. Emergency recovery system schematic.

The spars serve as: 1) a primary support structure for the nacelles and the wing fairings, 2) a space for dry storage (aft spar), and 3) a floodable forward spar for buoyancy control and recovery. The sealed aft spar will house power cables and transmission to the central power conditioning pod, and storage for the buoyancy control auxiliary equipment (logic controller and air supply). The buoyancy control is based on controlling the floodable volume in the forward spar. System components would include pumps and piping to expel water, valves to selectively flood or isolate the wet spar sections, distributed pressure sensors for depth sensing and a programmable logic control system. Power requirements for buoyancy control are estimated at less than 100 kW. Additionally, two small floodable segments were added to the dual-spar system later in the design, as shown in Figure 6-24, to reduce compressed air requirements and system complexity and provide for limited roll control.

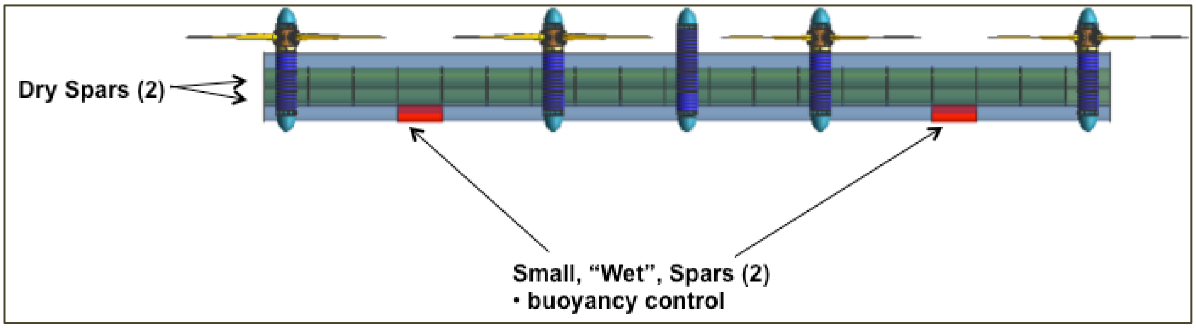

Figure 6-24. Alternate buoyancy control for roll control.

An emergency recovery system was designed into the device in the case of loss of control or persistent descent. Salvage bags have been added to the wet spar in an activation system illustrated in Figure 6-23**.**. A commercially available underwater lift bag system (Subsalve SP40000), capable of 40 000 lbs of buoyancy per bag is installed in the wet spar. The bag is activated by high pressure air stored in the dry spar—6000 psi tanks. Ultrahigh pressure (10 000 psi) tanks could be used for space and weight reduction. Valves would open to expel water from the wet spar as the bags inflate. While a reactive gas generation system could be used to reduce cost, weight and complexity, the compressed cylinder concept circumvents the need to pressure-rate the dry spar. The activation system needs to be determined based on depth sensing and device failure monitoring.

6.3.1.4 Power Conversion Chain (PCC) Design

The PCC design input parameters are provided in Table 6-9. All drive train components would be housed within a watertight nacelle to maintain overall system buoyancy and provide a closed seawater-tight system to permit use of standard industrial or wind turbine components. The watertight nacelle design eliminates the need to seal each component individually in a watertight, seaworthy environment.

Table 6-9. PCC design input parameters.

Physical Properties

- Four (4) turbines connected via a "support wing"
- Rotor diameter (single unit) = 33 m
- Three (3) turbine blades

Operation Parameters

- **Max Operating Depth= 200 m (656 ft) i.e. approx. 284 psi**
- Nominal Flow speed = 1.6 m/s
- Rotor speed = 7.67 rpm
- Shaft Torque = 1260 kN-m (929,200 ft-lbf)
- Thrust = 914 kN (205,475 lbf) & 1.5x @ Max Gust
- Potential Reverse Thrust = 457 kN (103,000 lbf.)
- Power = 1000 kW
- Rotor dry weight (hub & blades) = 58,535 kg (129,047 lb)
- **Gust Force = 1,371 kN (308,213 lbf)**
- **Gust induced moment = 2331 kNm (1,718,927 ft-lbf)**
- Hub O.D. 3 m (188.1 inches)

Figure 6-25 shows the proposed turbine PCC, nacelle, and wing spar. The RM4's PCC assembly consists of four major systems:

1) Bearing and seal assembly,

2) Gearbox and coupling section,

3) Generator section, and

4) Nacelle body.

For specific details relating to the drivetrain design, the interested reader should refer to (Beam et al. 2012).

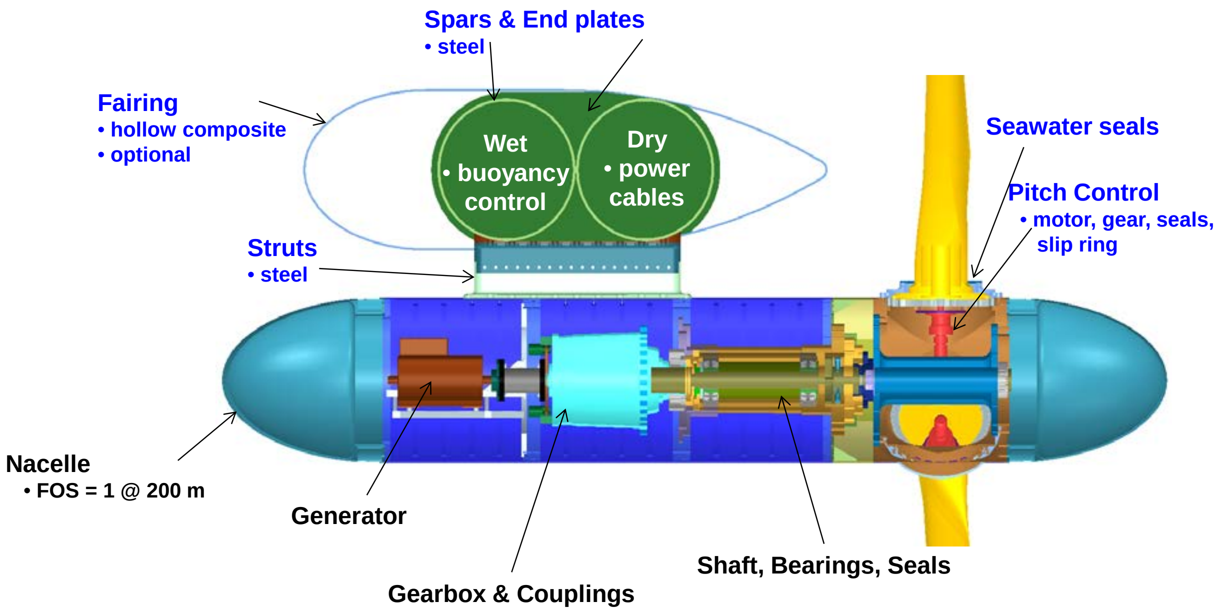

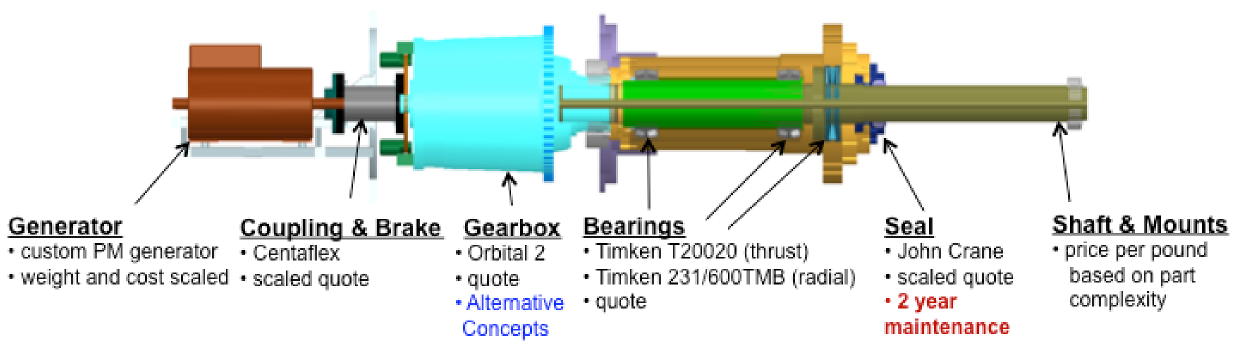

Figure 6-25. PCC schematic – nacelle housing components (top) and internal component detail (bottom).

6.3.1.4.1 Drive Train Design

The drive train design starts with the drive shaft specification. The drive train must withstand the operational loads described previously, and accommodate auxiliary equipment. Figure 6-26 illustrates the drive train assembly consisting of the drive shaft, bearings, and seals. The hollow drive shaft design allows for passage of power connectors for the blade pitch actuators. It is desirable to minimize drive shaft size while maintaining a performance specification with a factor of safety of at least 1.1 under maximum load to reduce weight, and improve selection of supporting components such as seals, bearings, and couplings.

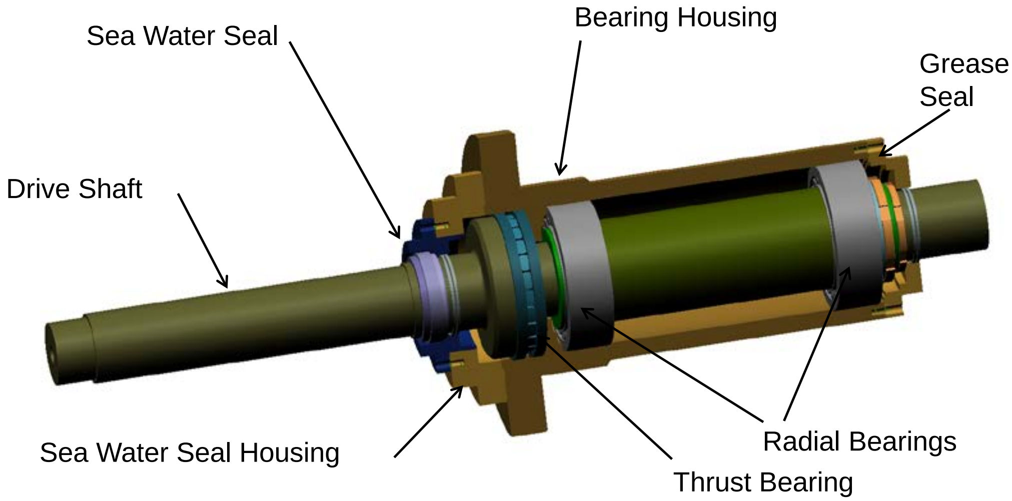

Assembled Weight= 32,057 kg (70,673 lbf)
Modular Design for Fast Change Out to Minimize Maintenance Turn Around

Figure 6-26. Bearing/seal package assembly.

6.3.1.4.2 Drive Shaft Design

Table 6-10 lists the drive shaft specifications for this design. All drive shaft specifications were focused on delivering an endurance limit—under normal operating conditions—of 50 million cycles, which corresponds to greater than 12 years of operation at the design shaft speed of 7.67 rpm. The endurance limit was selected to limit costly maintenance of the RM4 DEVICE, which requires bringing the device to the surface. The shaft size through the bearing bores was selected at 508 mm with a 117.5 mm bore through the center. The shaft material selected is 17-4 stainless steel. The material is specified to be at H1150 due to its greatly enhanced resistance to stress corrosion cracking when submersed in sea water. The table also lists the shaft design safety factors for normal operation and maximum loads. This design assumes that standard bearing locking nuts and hub attachment methods will be used. We did not consider these and their associated stress concentration effects in our calculations. We recommended that a rigorous stress and deflection analysis be performed prior to using our numbers for a final detailed design.

Table 6-10. Drive shaft specifications.

- Material: SS 17-4 Ph SS H1150
    - Recommended material for marine vessel shafting for cost and material performance.
    - Heat treat condition chosen for resistance to stress corrosion cracking in sea water.
- Size at Max. Diameter @ Thrust Shoulder = 940 mm (37 in)
- Size Through Rotor = 508 mm (20 in)
- Approximate Overall Length= 6.27 m (247 inches)
- Weight = 9115 kg (20 096 lbf)
- Bored Center Pass-Thru Diameter= 117.5 mm (4.625 in)
- Safety factor tensile yield (normal operation)= 5.4
- Safety factor shear yield (normal operation)= 2.4
- Safety factor tensile yield (worst case gust) = 2.6
- Safety factor shear yield (worst case gust) = 1.1

6.3.1.4.3 Bearing and Seal Design

The bearing and seal package was designed with the intent of protecting the balance of the drive train from sea water elements, supporting the turbine rotor and withstanding subsea gusting and unsteady loading, which can propagate into the drive train from the rotor plane. The design operational loads for the bearing and seal assembly are listed in Table 6-11. The drive train design needs to support the operational torque and thrust of the rotor and the system weight—the weight of the rotor and the connected couplings and components. The main rotor shaft is hollow to minimize weight and to provide a pass-through of electrical cables or hydraulic lines.

Table 6-11. The design operational loads for the bearing and seal assembly.

System	Sub-system	Maintenance Cycle / Life
Nacelle / Spar		--
Drive Shaft and Support	Shaft Bearings Seals	20 years 20 years 2 years
Gearbox and Brakes	Gearbox Wet Brake (Optional) Disc Brake and Coupling	-- -- --
Blade Pitch Mechanism	Motor Gear box Slew ring bearing Integral brake Pinion gear Slip ring	-- -- **6 months - lubrication** -- -- --
Generator & Cooling	Generator Cooling system Power Converter / Drive Transformer "Wet" Connector	-- -- -- -- --
Buoyancy Control	Pumps Valves Compressed air tanks Salvage bags	-- -- -- --

-- not evaluated / non-limiting

NOTE: The red text highlights important lubrication maintenance schedule.

A modular bearing and seal package assembly was designed using commercially available standard components. Emphasis was placed on selecting components that would minimize maintenance and maximize bearing life. A modular bearing and seal package was proposed so that it could be assembled and tested separately from the balance of the assembly. Stock bearing and seal packages could be assembled and changed out as required thus minimizing turbine operational down time. The use of commercially available components, minimizing maintenance, and maximizing component availability would reduce this contribution to the system LCOE.

The resulting bearing design concept, illustrated in Figure 6-27, incorporates the use of Timken spherical roller bearings coupled with a Timken thrust bearing supporting thrust loads in one direction. The bearings are grease lubricated and, with the loads specified, have a predicted L10 life of 20 years. Power consumption for the bearings at the designated shaft speed is nominally 104 and 1841 Watts for the thrust and radial-combination bearings respectively. The design distance between the radial-combination bearings is 1.83 m.

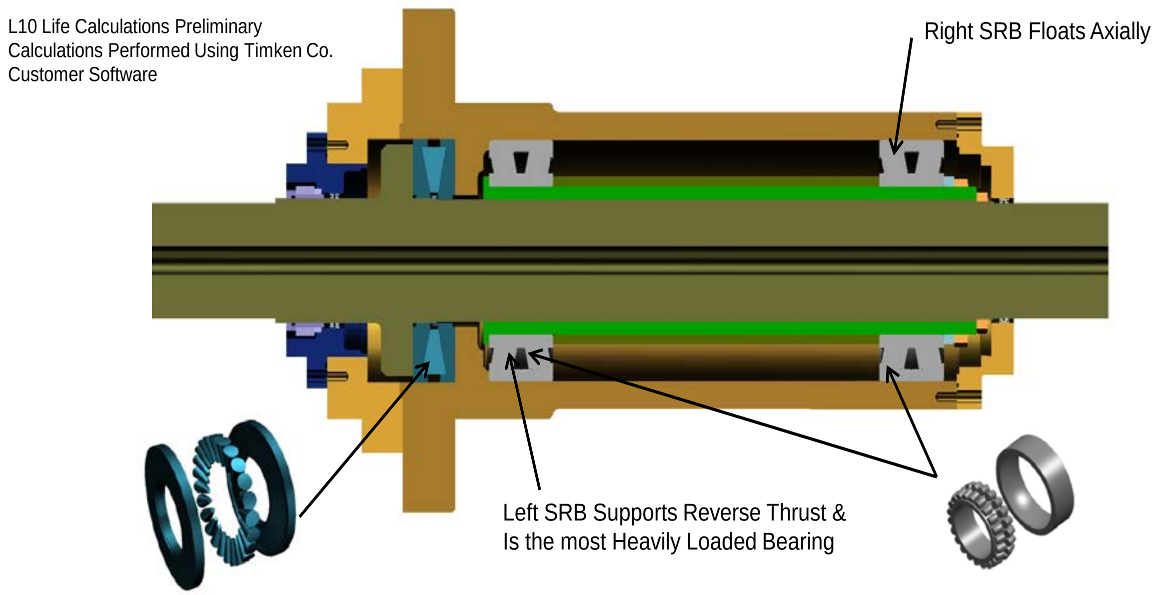

- Timken T20020 Thrust Bearing (supports thrust in one direction)
- 991 mm (39”) OD x 508mm(20”) ID x 197mm(7.75”)Thk
- Weight= 736 kg (1622 lbf)
- L10 life @ Normal Thrust = in excess of 20 years
- L10 life @ Max Gust= in excess of 20 years
- **APPROX** Power Consumption= 104 W (.2 HP) Scaled

- Timken 231/600TMB Spherical Roller (SRB) 2 Req’d
- Supports Radial and Thrust
- 981mm (39.6”) OD x 600 mm (23.6”) ID x 300mm (11.8”) Thk.
- Weight = 905 kg (1996 lbf.)
- L10 life @ Normal Operating Conditions=in excess of 20 years
- L10 life @ Worst Gust Condition = 14 years
- L10 Life @ Max Reverse Thrust Condition = 18 years
- **APPROX** Power Consumption= 1841 W (2.5 HP) Scaled

Figure 6-27. Bearing design.

6.3.1.4.4 Gearbox Design

The gearbox was specified as a commercial design from a manufacturer of gearboxes for wind and hydro-turbines. Unlike wind turbines, whose rotors spin at speeds from 10 rpm to 30 rpm, the reference hydro-turbine had a rotor rpm of ~7. The low rpm and high torque must be carefully considered in a gearbox selection. The gearbox is used to transmit torque from the rotor to a generator and is directly coupled to the drive train. Most commercial generators operate most efficiently at rotational speeds of hundreds of rpm. As a result, the gearbox, in this application, drives the generator as a speed increaser rather than a speed reducer. The gearbox contains sets of planetary gears and parallel shaft spur gears arranged in groups to develop the required gear ratio. A typical gearbox contains three sets of reduction gears. These gear sets can be arranged to have a common center for the input shaft and output shaft, or they can be arranged to have a horizontal offset of the output shaft from a centered input shaft. One advantage of the offset shafts is to have a pass-through for electrical cables or hydraulic lines used for blade pitch control from the generator side to the rotor side of the gearbox. This pass-through is located on the centerline of the drive train, in-line with the rotor shaft.

An Orbital 2 (W2000/D2000) gear box system was selected for each of the four turbines in the RM4 device design. This gearbox includes an integral internal lubrication system with a high rpm coupler and disc brake assembly.

6.3.1.4.5 Generator and Power Conditioning

The power conversion system greatly impacts the entire design of the power train delivery system, and the choice of using either an induction generator or a permanent magnet (PM) generator could lead to two very distinct designs. While induction generators are widely used and well understood, for the current RM4 device, a PM generator was selected for each turbine. As pointed out by Melfi et al. (2009), the PM generators are appealing because they are efficient, reliable, and have improved performance (i.e., high power density, low power factor, low rotor temperature) and flexibility (i.e., synchronous operation). The increased flexibility makes the operation frequency a degree of freedom in the system, which allows for operation at base frequencies other than 50 or 60 Hz. However, there is a price associated with this freedom—since the output frequency must be 50 or 60 Hz, an inverter must be added to the system. However, it was decided that the advantages of the PM generator outweighed the increase in complexity of the electric conditioning system.

The model of PM generator selected was ABB's model AMZ500LE10. One generator is placed in each turbine nacelle. Similarly, the remaining power conversion components (transformer, drive control, cables, and connectors) were primarily selected based on available information and were treated as off-the-shelf estimates for this conceptual design. Figure 6-28 lists the specifications for the ABB model AMZ500LE10.

Physical Properties	Electrical Properties
• 70" × 35" × 40"	• Permanent Magnet
• **Weight ≈ 3290 kg**	• Power Output = 1000 kW
• Efficiency = 96.9%	• Voltage = 690 V
• Max Speed = 600 rpm	• Frequency = Nominal 60 Hz
	• Heat rejection= ~50kw

Figure 6-28. ABB generator specification.

The power conditioning system will include four ABB ACS800-17-0790-7 power converter units, located in the central, power conditioning nacelle. The custom converters will transmit power to a 100 kV custom designed transformer (ABB is specified as the manufacturer). The converter/transformer footprint is of a sufficient size to fit in the power conditioning nacelle for all four turbines combined. Transmission line connections will be made at the power conditioning nacelle. To this end, waterproof 100 kV cable is readily available for undersea power transmission. However, wet-mate connectors rated for 100kV do not currently exist commercially and will require a development effort. It is proposed that a "dry" 100 kV connection be made inside the power conditioning nacelle and a flexible, dynamic seal be employed around the outside diameter of the waterproof cable at the nacelle penetration. Experience in the marine systems field suggests that this connection and seal arrangement could be achieved with reasonable reliability.

6.3.1.4.6 Blade Pitch Control Mechanism

The pitch control mechanism was designed and sized by MOOG Inc. This system, shown in Figure 6-29 and Figure 6-30, consists of the following components:

- Motor and drive unit
- Gear box speed reducer
- Slew ring and bearing to absorb rotor blade side loads
- Integral brake
- Pinion gear
- Slip ring
- Housing

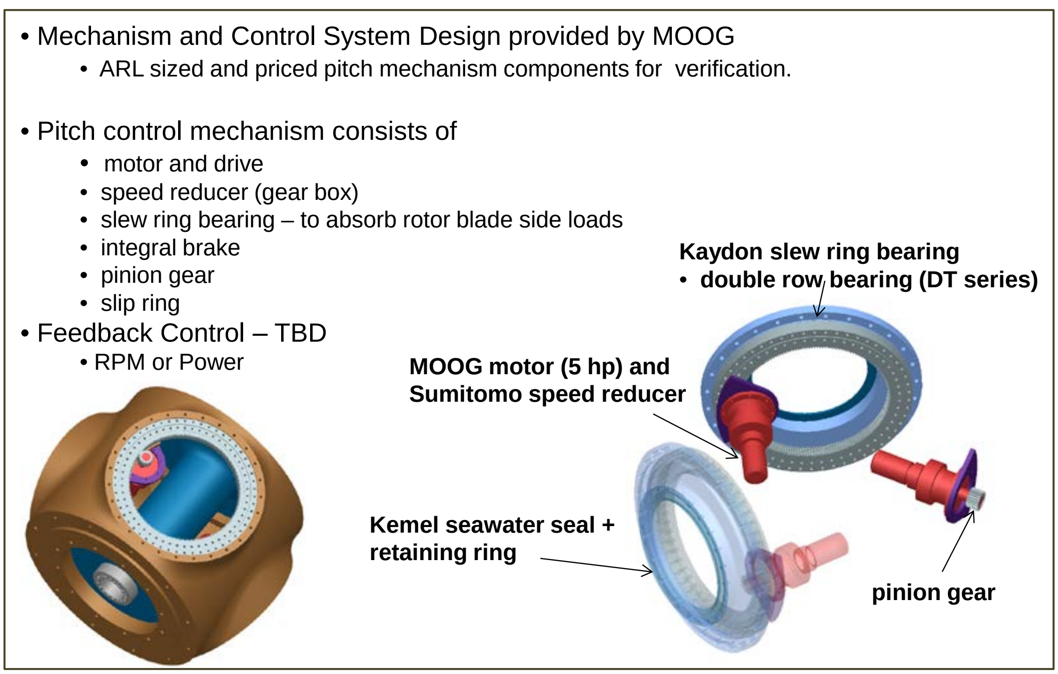

Figure 6-29. Pitch control mechanism.

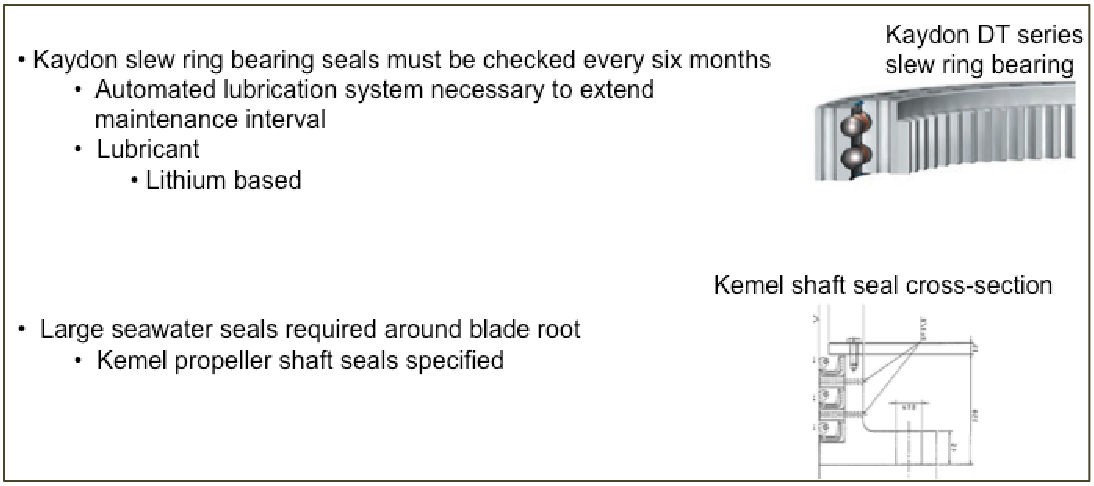

Figure 6-30. Pitch control mechanism bearing and seals.

The components are assembled around the bases of turbine blades, rotating with the turbine hub. The pitch feedback control system design has yet to be specified, but examples exist in the land-based wind turbine community. The feedback control can be based on rpm or power generation. Figure 6-30 shows the Kaydon DT slew ring bearing and Kemel shaft seals. The Kaydon slew ring bearing must be checked every six months. An automated lubrication system is recommended to extend this maintenance interval. The bearing lubricant is a lithium-based grease that should be environmentally acceptable for the Gulf Stream environment. The Kemel seawater seals were specified to seal the pitch-axis of the blade shafts.

6.3.1.5 Mooring Design

The mooring design consists of a thrust and buoyancy mooring line as shown in Figure 6-2. The buoyancy tank provides sufficient up-force to always keep the buoyancy mooring line in tension and provide an attachment point for the wing structure that will remain at a fixed water depth while the rotors induce a variable drag-force on the mooring system. This arrangement simplifies the depth-control of the submersed wing structure because it does not have to compensate for the variable downward force that otherwise would be exerted on the wing structure by the thrust mooring line.

Polyester was chosen as the main material for both mooring legs, because it is light-weight (reducing the buoyancy requirements of the buoyancy tank), has an extensive track-record in the offshore industry, and is relatively inexpensive. Near the seabed, a short section of chain was added to insure that the mooring leg is protected from abrasion near the seabed. The clump-weight of the up-stream mooring leg insures that the mooring line forces acting on the drag embedment anchor remain largely horizontal and hence there is no risk of the embedment anchor being dislodged. A Stevpris MK6 anchor is chosen to anchor the up-stream mooring line and a Suction Embedment Plate Anchor (SEPLA) is chosen to anchor the vertical buoyancy mooring leg (Figure 6-31). The advantage of a SEPLA anchor is that it provides for superior uplift capacity, with a minimum amount of mass and that it can be driven into the seabed using a suction pile, which can be done with relative ease in deep water.

In reality, these anchor choices are largely driven by the sedimentation type at the deployment site and these choices would have to be refined during a mooring design study phase of the project.

Figure 6-31. Suction embedment anchor (SEPLA) (top) and Stevpris MK6 Drag embedment anchor (bottom).

NOTE: The Suction Embedment Plate Anchor (SEPLA) is manufactured by SPT Offshore. The MK6 drag embedment anchor is manufactured by Stevpris; the photo is from Vryhof Anchors at http://www.vryhof.com/products/anchors/stevpris_mk6.html

The two anchors were sized using the holding capacity charts provided by the vendors. Because sediment conditions are largely unknown for the deployment site, a median value was chosen for the holding strength.

Simulations were performed with the commercial mooring analysis code OrcaFlex to determine if the mooring system design was statically and dynamically stable. Specifically, the mooring system was checked to determine if the device displacements with changing current directions were sufficiently small so that multiple devices in an array did not interact. Also, it was insured the mooring system would hold the device in place when there was zero and maximum current velocities, as well as when the gulfstream direction was abnormal (Lawson 2013, in preparation).

6.3.2 Manufacturing & Deployment (M&D) Strategy Module

6.3.2.1 Manufacturing Strategy and Costs

As described in Section 2.3.2.1, commercially available components (e.g., generators and anchors) and conventional materials (e.g., A36 steel, standard fasteners, mooring cables, etc.) were used where possible.

Manufacturing costs and PCC costs for RM4 at different array scales (1, 10, 50 and 100 units) are summarized in Figure 6-32 and Figure 6-33. The wing is the largest contributor to the cost of the device structure.

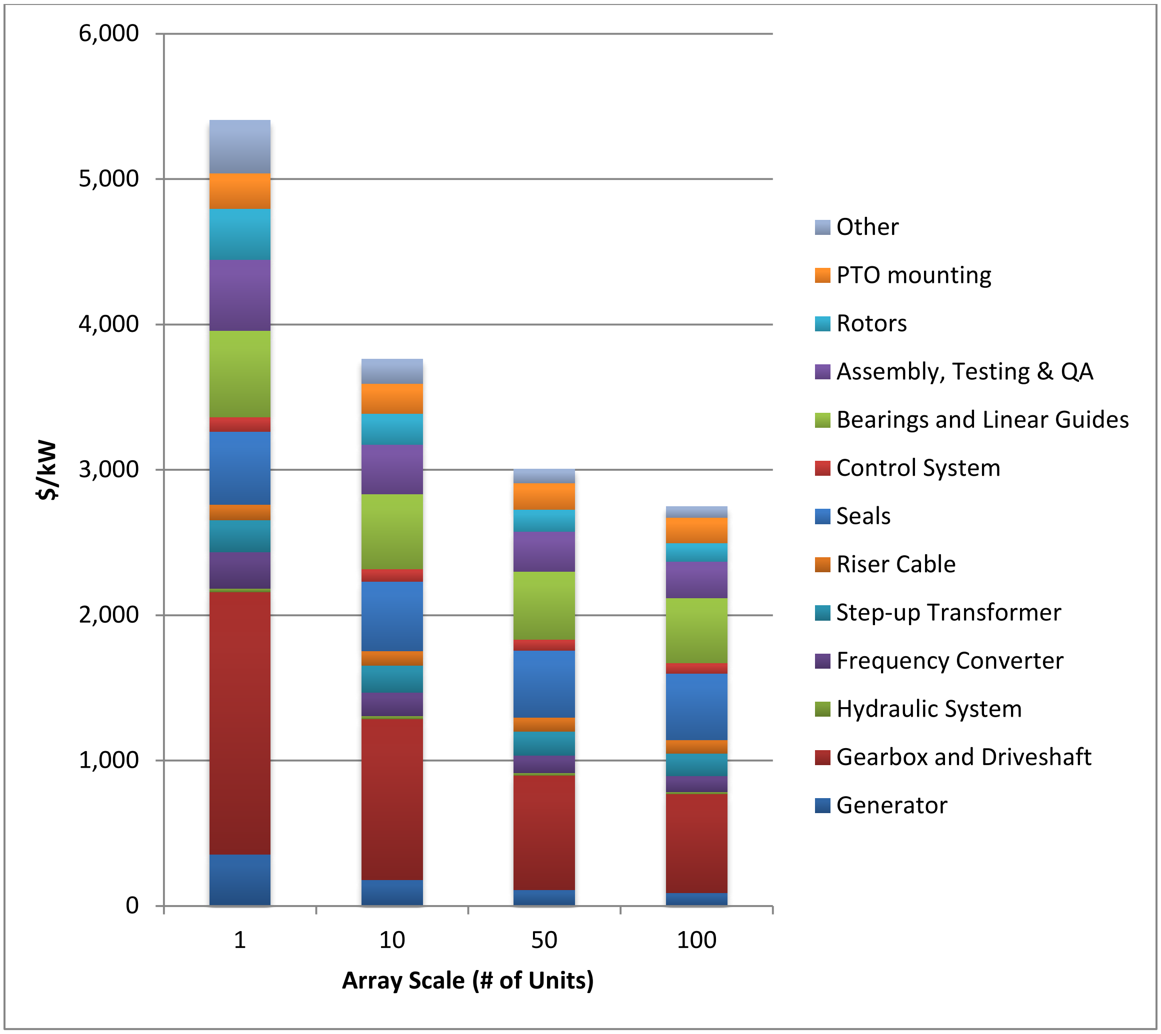

Figure 6-32. Cost breakdown ($/kW) for the energy capture and PCC components per deployment scale.

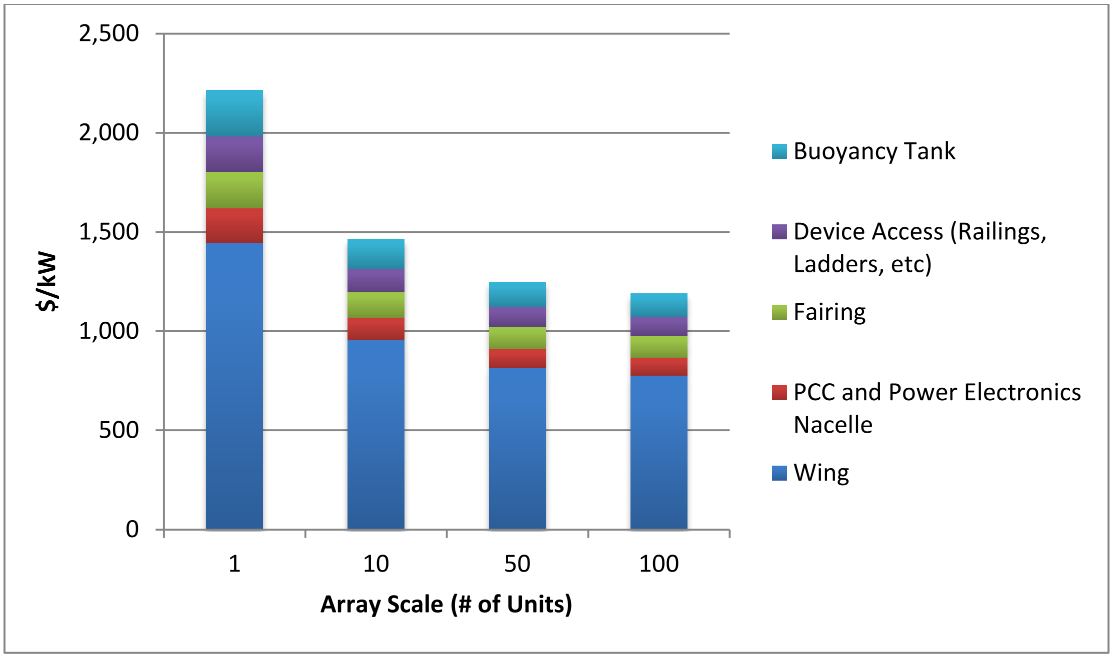

Figure 6-33. RM4 structural cost estimates ($/kW) per deployment scale.

The mooring system cost estimates are summarized in Table 6-12.

Table 6-12. Mooring component cost breakdown.

	Cost ($/kW) (1 unit deployment)	Cost ($/kW) (10-, 50-, or 100-unit deployments)
Mooring lines/chain	$362	$362
Anchors	$142	$55
Connecting Hardware (Shackles etc.)	$50	$42
Total	**$555**	**$459**

6.3.2.2 Deployment Strategy and Costs

The deployment strategy accounts for the installation of the: 1) subsea cable, 2) mooring system, and 3) the RM4 device itself. The following subsections provide an outline of considerations for these operations and describe the assumed installation procedures. Installation costs were estimated based on these procedures and the assumed installation durations and day rates for the required support vessels (Table 6-13).

Table 6-13. RM4 M&D Strategy Module cost assumptions.

Operational Detail	1 Unit			100 Units		
	No. Days	Vessel Day Rate	Cost	No. Days	Vessel Day Rate	Cost
Mooring Installation						
At Dock	10	$124,225	$1,242,250	208	$124,225	$25,838,800
Transit/Anchoring	5	$117,000	$526,500	54	$117,000	$6,318,000
Mooring Installation	3	$141,550	$455,366	322	$141,550	$45,531,964
Standby	2.6	$127,605	$335,346	88	$127,605	$11,171,818
Mobilization Charges			$242,200		$76,610	$242,200
Total	**20**		**$2,802,000**			**$89,103,000**
Cable Shore Landing						
Horizontal Directional Drilling (distance is 500 m)			$667,000			$2,301,600
Riser Cable Installation						
Mobilize Vessel	0.0	$68,741	$0			
Transit to Site	0.2	$81,025	$18,004			
Install Cable between two devices	0.1	$81,025	$5,623			
Splice Cables	1.0	$81,025	$81,025			
Transit to Home Port	0.2	$81,025	$18,004			
Operational Contingency (weather)	0.2	$77,345	$17,565			
Total	**1.7**		**$140,221**			
Cable Installation (using Cable Install Vessel)						
At Dock	14	$68,741	$962,374	14	$68,741	$962,374
Load Cable	2	$80,921	$138,237	6	$80,921	$512,497
Transit to Site	7	$79,156	$550,427	7	$79,156	$550,427
Install Cable	64	$81,025	$5,156,342	254	$81,025	$20,571,348
Standby	13	$77,345	$1,001,239	42	$77,345	$3,262,134
Mobilization Charges			$542,600			$542,600
Shore-end Cost			$300,000			$750,000
Total	**99**		**$8,651,219**			**$27,151,380**
Device Installation (using DP-2 Vessel for 100-units)						
Barge-in Device from GOM	5	$26,730	$133,650	500	$26,730	$13,365,000
Unload and Ready Device in Port	5	$26,730	$133,650	500	$26,730	$13,365,000
Tow-Out and Install Device	2	$26,730	$53,460	200	$26,730	$5,346,000
Commission Device	2	$26,730	$53,460	200	$26,730	$5,346,000
Contingency	3.5	$26,730	$93,555	350	$26,730	$9,355,500
Total	**9.0**		**$467,775**	**1750**		**$46,777,500**

The trunk cable installation is carried out from a DP-2 vessel, which is adequately equipped to carry-out the subsea cable installation. The subsea cable is to be buried 6 ft; this assumes that the seabed is adequate for burial without any major obstructions in the subsea cable route. The cable landing is accomplished using a short section of conduit that is placed using directional drilling from shore. Process timelines for up to four trunk-cables are shown in Table 6-14. Subsea cable installation is the largest cost-driver for a single unit deployment; however, the subsea cable's relative contribution to the cost of a 100-unit deployment is substantially less as shown in Figure 6-34.

Table 6-14. Subsea cable installation timelines (in days)

			1-Cable	2-Cables	3-Cables	4-Cables
1	Transit		7.0	7.0	7.0	7.0
2	Ft Laud to Job Site		0.2	0.2	0.2	0.2
3	Mobilization		8.0	8.0	8.0	8.0
4	Load Cable		1.7	3.3	4.8	6.3
5	Shore End Cable		1.0	2.0	3.0	4.0
6	Lay Trunk Cable		7.7	15.4	23.1	30.8
7	End for End Trunk Cable		0.5	1.0	1.5	2.0
8	Demobe		6.0	6.0	6.0	6.0
8	Contingency	15%	4.8	6.4	8.0	9.7
	Total		36.9	49.3	61.6	74.0

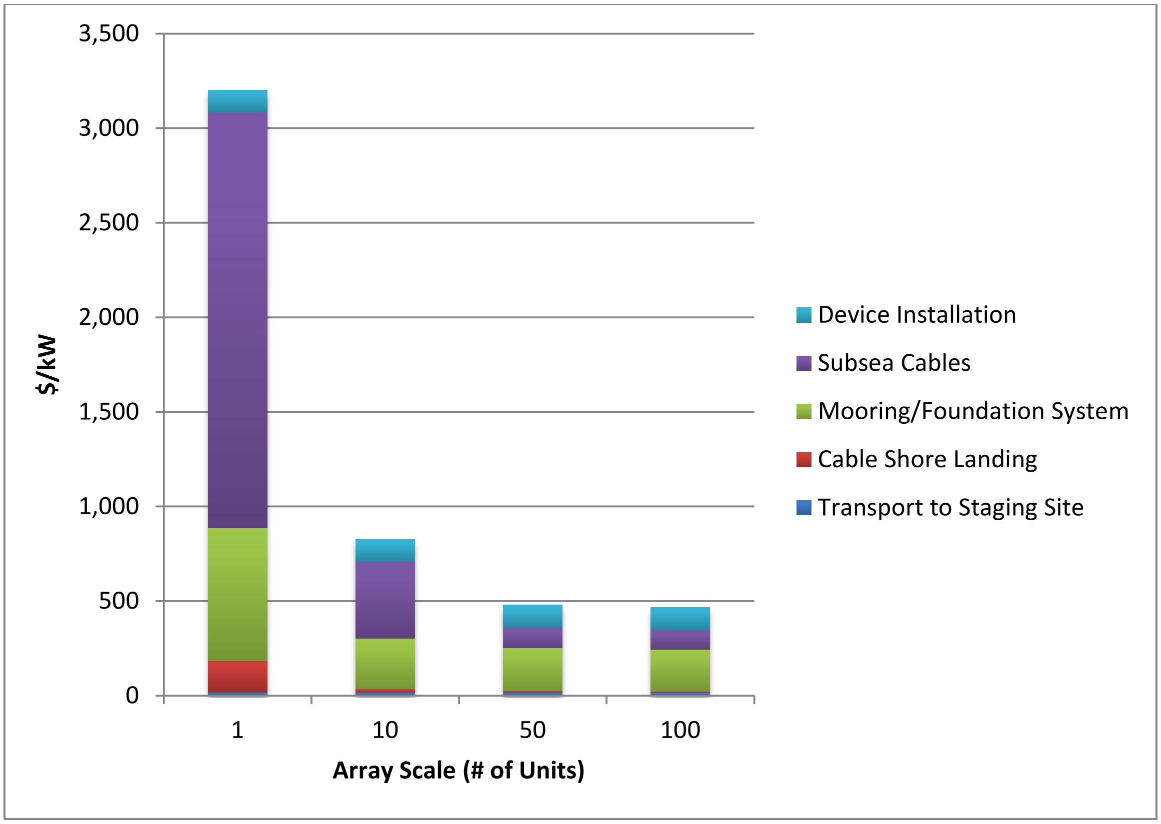

Figure 6-34. Installation cost breakdown ($/kW) per deployment scale.

While typically, marine operations in deep water are carried out from dynamic positioning (DP) capable vessels, the lifting and bollard-pull requirements for the mooring installation require very expensive vessel assets to be mobilized. In order to address this issue, Re Vision Consulting decided to utilize a Derrick barge with sufficient lifting capacity to handle all the mooring components similar to the one shown in Figure 6-35. The crane barge would be re-fitted with a suitable 4-point or 6-point mooring spread with sufficient scope for the 700-meter water-depth at the deployment site.

Figure 6-35. 400-foot crane barge with 400-tonne crane lift capacity.

In support of the primary crane-barge, an anchor handling tug (Figure 6-36), a DP-2 vessel, and a crew-boat would be required for the operation. The crane-barge would be loaded with all the required mooring components and towed to the deployment site using the DP-2 vessel. Once on station, the mooring-spread would be deployed using the anchor handling tug and actual installation activities can begin.

Figure 6-36. Anchor-handling vessel Atlantic Hawk (left); DP-2 vessel HOS Innovator (right).

Installation procedures were established and high-level timelines are shown in Table 6-15.

Table 6-15. Mooring installation timelines.

	Days			
	1 Unit	10 Units	50 Units	100 Units
Mobe Vessels	5.0	5.0	5.0	5.0
Transit from home port to Florida Port	4.0	4.0	4.0	4.0
Load Moorings	2.0	20.0	100.0	200.0
Transit to site	0.3	2.5	12.5	25.0
Setup 4-Point Moor	1.0	10.0	50.0	100.0
Install SEPLA mooring leg	0.3	3.0	15.0	30.0
Install Thrust Mooring	0.4	4.2	20.8	41.7
Pull-down buoyancy Tank	0.5	5.0	25.0	50.0
Final Rigging	1.0	10.0	50.0	100.0
Transit to home port	0.3	2.5	12.5	25.0
Demobe	3.0	3.0	3.0	3.0
Operational Contingency (15%)	2.7	10.4	44.7	87.6
Total Ops Days	20	80	343	671

The cost of the mooring installation is a significant cost driver for multi-unit deployments and the largest cost driver for the commercial scale deployment scenario (100 units).

The device installation itself can be carried out from a DP-2 vessel with specifications similar to the HOS Innovator (Figure 6-36). The process consists of towing the device to the deployment site, attaching all the mooring lines, and installing the riser cable system. Table 6-16 shows the number of days estimated device installation for 100 units.

Table 6-16. Device installation process for 100 units.

		# Days
1	Barge-in device from GOM	5
2	Unload and ready device in port	5
3	Tow-out and install device	2
4	Commission device	2
5	Contingency (25%)	3.5
	Total	17.5

6.3.3 Operations & Maintenance (O&M) Strategy Module

The O&M Strategy Module for RM4 was developed with cost efficiency in mind. Similar to the RM1 and RM2 concept designs, the RM4 concept design was developed to reduce O&M costs by deploying multiple rotors from a single platform and mounting the units on a subsurface wing that allows retrieval for shore-side PCC maintenance and repairs. The sub-surface wing is equipped with an active buoyancy system, which allows it to surface by itself. Once it is surfaced, repair activities can be carried out. However, in order to carry out repairs, the device would either need to be completely lifted out of the water and repaired onsite or towed to shore. A preliminary assessment showed that lifting the wing out of the water would be extremely difficult (and costly) given its weight and the strong surface currents at the deployment site. Therefore, the RM4 device will be towed to port for maintenance and repair. Assuming a towing speed of 6 knots, the transit time between the O&M port and the deployment site would be on the order of 3 hours, which would take 6 hours out of a 24-hour operational day.

6.3.3.1 Service Vessel Specifications

In order to efficiently carry out operational tasks, a purpose-built vessel was conceptualized that would be able to carry out all routine operation and maintenance activities, with the exception of mooring system repairs, which include: 1) towing the RM4 device wing at 6 knots, 2) riser-cable repairs, and 3) operation of ROV for subsea inspection activities. The vessel required for these activities falls well within the capability range of a typical offshore service vessel utilized in the Gulf of Mexico region. The vessel would be modified to meet the requirements of this application. A ship crew size of nine personnel and a deck-crew of 11 personnel were considered adequate for all operational activities.

A shore-side a crew of technicians and administrative personnel would be responsible for carrying out repairs and maintenance activities. Staffing cost was estimated based on data from the NREL WindPact data for a wind plant with similar installed capacity.

6.3.3.2 Failure Rates

Because the powertrain of an ocean-current turbine is similar to a wind-turbine, we used failure rates from a wind-turbine powertrain as an analogue (Poore and Lettenmaier 2003). While this data is somewhat outdated, it provides likely failure rate distributions for the components of a typical wind-power drive-train and is in the public domain. Given that the major components are very similar in this application, we re-used the same data. To simplify the analysis, we simply averaged the number of failures instead of following the more typical Weibull failure-rate distribution of many of the subsystems and components. We deemed this approach appropriate given the uncertainties in estimating failure rates for technologies with no operational experience.

Any repair carried out on the device requires the complete recovery of the powertrain, which is expected to be costly because of operational constraints. Hence reducing the number of failure events is a critical aspect of the powertrain design. Conceptually, such reductions in failure events that trigger a device recovery can be accomplished by introducing redundancy levels in sub-systems that are amenable to such measures. Examples may include items such as cooling system pumps, control systems, sensors, and other items that make a significant contribution to the total number of failures over the life of an array. Failed parts would still need to be replaced in such a ‘hardened’ system, but these replacements could take place during routine maintenance and hence would not trigger a device recovery procedure.

Table 6-17 shows the typical number of failure events in a typical 1MW wind-turbine powertrain. Highlighted in blue are items that are envisioned to be redundant systems.

Based on the above failure distribution, the wind-turbine requires an average of 3.9 repairs each year. To reduce the number of intervention, it was assumed that the powertrain could be hardened through introduction of redundant systems. While the total cost of the powertrain increases, this would result in a reduction of the number of repairs per powertrain and per year to 1.03. Given that each turbine assembly consists of four rotors, this would bring the average intervention cycles to 4.1 times per year for each quad-rotor machine. These intervention rates are conservative and newer wind-turbines have much lower failure rates overall, but this dataset was used because it was readily available in the public domain.

From a cost assessment perspective, there are two important factors that will drive O&M schedule and cost: 1) replacement part cost, and 2) number and type of operational interventions. To compute replacement part cost, it was assumed that failures were evenly distributed over the 20-year project life, and the replacement part cost was equal to the value of part/subsystem in the original device. The latter is a somewhat conservative assumption, because in reality, major components would be repaired instead of being replaced outright.

Table 6-17. Failure rates of a typical 1 MW wind turbine.

System	Component	Parts per turbine	Total Failures over 20 yrs / initial qty parts in fleet (%)	# Failures per Unit	Action	# Interventions per Unit
Rotor	Blade--struct. repair	3	5%	0.150	Recovery	0.150
	Blade--nonstruct. repair	3	100%	3.000	Redundancy	0.000
	Pitch bearing	3	5%	0.150	Recovery	0.150
	Pitch motor	3	123%	3.690	Recovery	3.690
	Pitch gear	3	143%	4.290	Recovery	4.290
	Pitch drive	3	117%	3.510	Recovery	3.510
Drivetrain	Main bearing	1	5%	0.050	Recovery	0.050
	High-speed coupling	1	39%	0.390	Recovery	0.390
Gearbox and Lube	Gearbox--gear & brgs	1	5%	0.050	Recovery	0.050
	Gearbox--brgs, all	1	67%	0.670	Recovery	0.670
	Gearbox--high speed only	1	67%	0.670	Recovery	0.670
	Lube pumps	3	147%	4.410	Redundancy	
	Cooling Fan, Gearbox Cooling	2	97%	1.940	Redundancy	
Generator and Cooling	Generator--rot. & brgs	1	5%	0.050	Recovery	0.050
	Generator--brgs only	2	92%	1.840	Recovery	1.840
	Motor, generator coolant fan	2	97%	1.940	Redundancy	
	Contactor, generator	3	78%	2.340	Recovery	2.340
Brakes & Hydraulics	Brake caliper	3	194%	5.810	Redundancy	
	Brake Pads	2	10%	0.200	Redundancy	
	Accumulator	1	340%	3.400	Redundancy	
	Hydraulic pump	1	146%	1.460	Redundancy	
	Hydraulic valve	4	148%	5.900	Redundancy	
Control System	Control board, Top	1	117%	1.170	Redundancy	
	Control board, Main	1	117%	1.170	Redundancy	
	Control Module	2	117%	2.340	Redundancy	
	Sensor, static	17	128%	21.830	Redundancy	
	Sensor, dynamic	2	156%	3.120	Redundancy	
Electrical and Grid	Main Contactor	1	77%	0.770	Recovery	0.770
	Main Circuit Breaker	1	37%	0.370	Recovery	0.370
	Frequency Converter	1	160%	1.600	Recovery	1.600
Misc. (All others)	Miscellaneous Parts	1	5%	0.050	Recovery	0.050
			Sum	78		20.64
			Failures per Unit-Year	3.9		1.03

NOTE: This table is adapted to a 100-unit project using four rotors for each unit. Shaded areas indicate redundant systems (hardened).

6.3.3.3 Annual O&M Costs

Marine operations include both scheduled and unscheduled maintenance. We assumed there would be four unscheduled interventions per year per device, and we assumed one scheduled maintenance activity per year per device, totaling five interventions per year per device. Thus, the annual marine operations cost is assumed to be approximately $115,000 for a one-off project, and approximately $11.5M per year for a 100-unit array.

The cost of replacement parts was assumed to equal the value of the part/subsystem of the original device. Annual replacement part costs were calculated from the part cost and the estimated replacement frequency; for example, a 10-year replacement cycle was assumed for the mooring system and riser cable.

Total annual shore-side operations were estimated to be approximately $675,000, which includes the cost of shore-side labor and the facilities lease ($60,000/year) and dockside rental ($60,000/year).

Based on the above number of interventions and replacement part values, the annual O&M cost was computed at different scales of deployment. Figure 6-37 shows the breakdown of the likely annual OpEx cost ($/kWh) as a function of the number of units in an array. See Section 2.3.3.4 for details on how insurance costs were estimated. Note that the post-installation monitoring is a part of environmental monitoring and regulatory compliance costed under the Environmental Compliance (EC) Module (see Section 6.3.4) and is included in the total OpEx costs shown in Figure 6-37. Initial environmental compliance and monitoring activities prior to start up would fall under CapEx as explained in the following section.

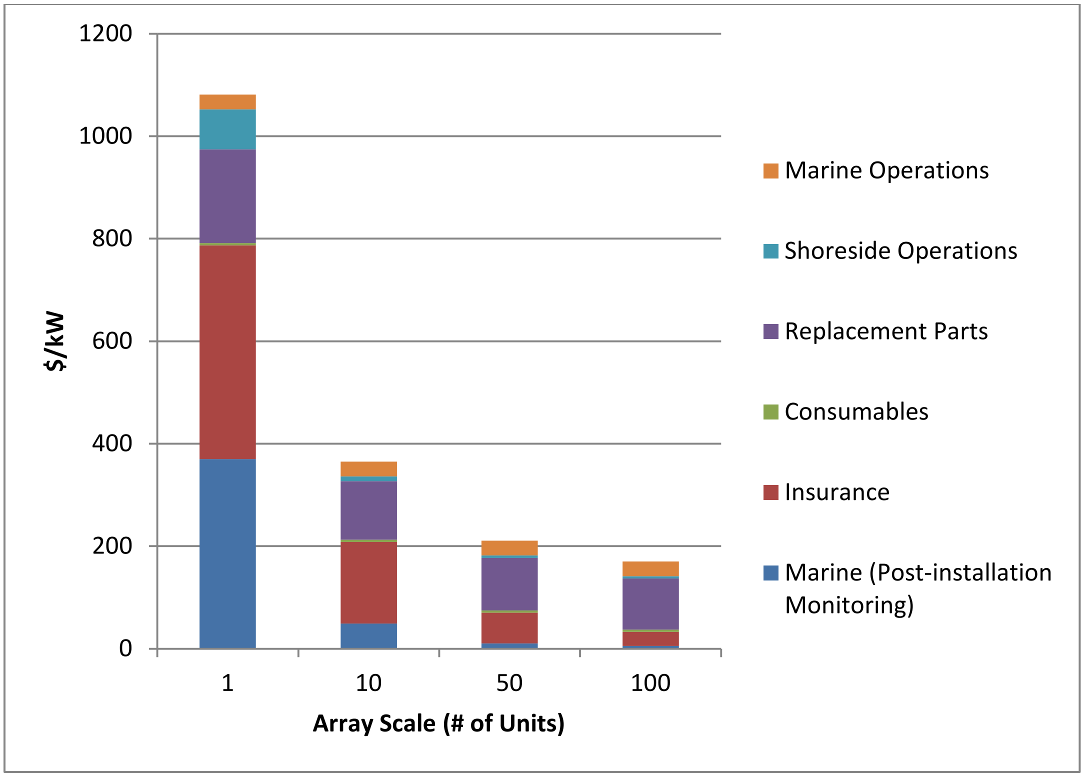

Figure 6-37. Annual OpEx cost ($/kW) per array size.

6.3.4 Environmental Compliance (EC) Module

The EC Compliance Module for RM4 was based on similar factors considered for RM1 through RM3. As provided for the first three Reference Models (tidal, riverine, and wave), Pacific Northwest National Laboratory (PNNL) undertook the task of determining the preliminary costs for the major categories of environmental and site specific studies that can be expected to be needed for RM4.

For the RM4 device, there are no similar configured projects in the water or in advanced stages of planning from which PNNL could begin the costing process. Therefore, the basis for costs of environmental studies and processes were developed for RM4 through extrapolation from the previous three models. While the RM4 device model differs considerably in the size and configuration of the device from RM1 (a dual-rotor axial-flow tidal turbine) (refer to Figure 1-1), there are commonalities between the potential interactions with animals (including blade strike) for the two devices. The impact of anchors and mooring lines on marine habitats in RM4 is somewhat analogous to the lines and anchors proposed for RM3 (wave point absorber). Although the ocean space occupied for RM4 differs greatly from the previous three proposed RM sites, the NEPA processes and study costs for RM4 can be extrapolated using PNNL staff knowledge of the oceanography of the Florida Current informed by published studies and modified by consultation with experts in the area (Polagye et al. 2011a).

The overall CapEx normalized by installed power for environmental studies and associated processes required for RM4 is summarized in Figure 6-38. Detailed spreadsheets, references, standardized protocols, and in-depth explanation of costing is available for all parts of the environmental costing process for RM4 in Copping et al. (2012).

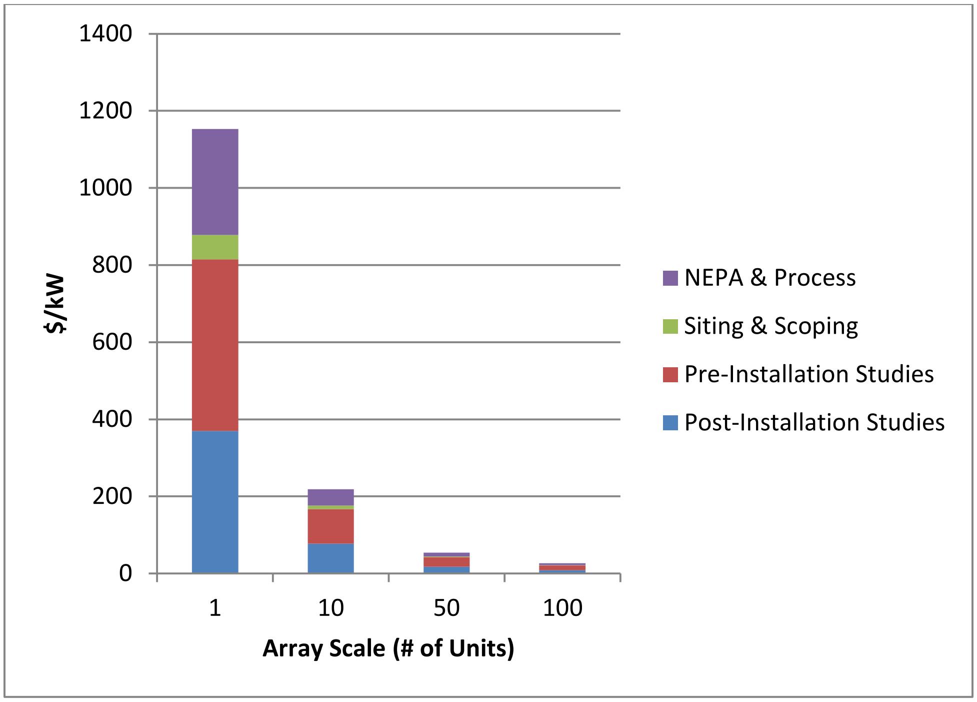

Figure 6-38. Total environmental CapEx estimate per deployment scale (1, 10, 50 or 100 units).

High and low bounds for the environmental compliance cost estimate were approximately +/- 20% relative to the mean value shown in Figure 6-38. Annually recurring costs for post-installation studies (OpEx) over the life of the project are shown on in Figure 6-39. As with the other RMs, normalized costs decrease with larger arrays.

.

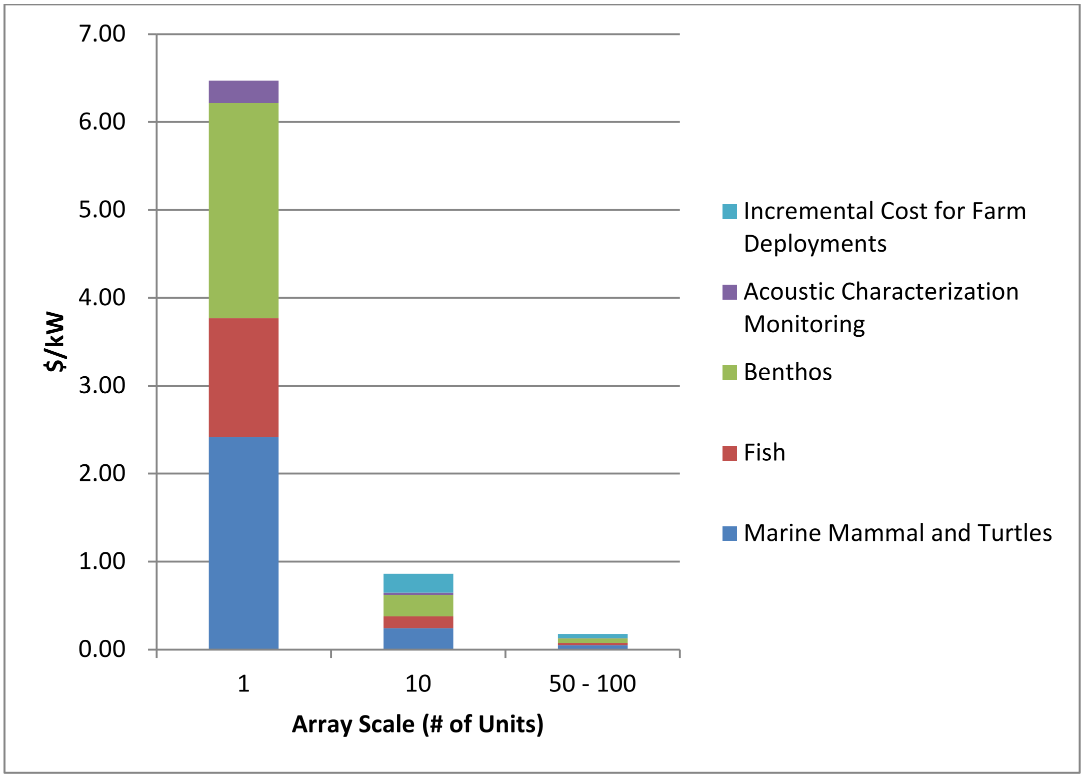

Figure 6-39. Annual cost of post-Installation monitoring per deployment scale.

6.4 LCOE Calculation

The LCOE estimate for or a 10-unit RM4 array is 25 cents/kWh based on the FCR, AEP, CapEx, and OpEx estimates described below. The estimated AEP for this array is 228,600 MWh per year. Table 6-18 gives a detailed breakdown of the LCOE estimate. The cost of M&D is the greatest LCOE driver for RM4, contributing 59% to the total LCOE, followed by O&M costs, which account for 26% of the LCOE. These findings indicate that the most critical area for targeting potential cost savings is M&D.

Table 6-18. RM4 LCOE breakdown by cost category (10-unit array).

	cents/kWh	% of total LCOE
Development	1.1	4.4%
M&D	14.6	59.2%
Subsystem Integration & Profit Margin	1.0	4.2%
Contingency	1.6	6.3%
O&M	6.4	25.9%
Total	24.7	100.0%

Figure 6-40 shows significant economies of scale at larger deployment scales.

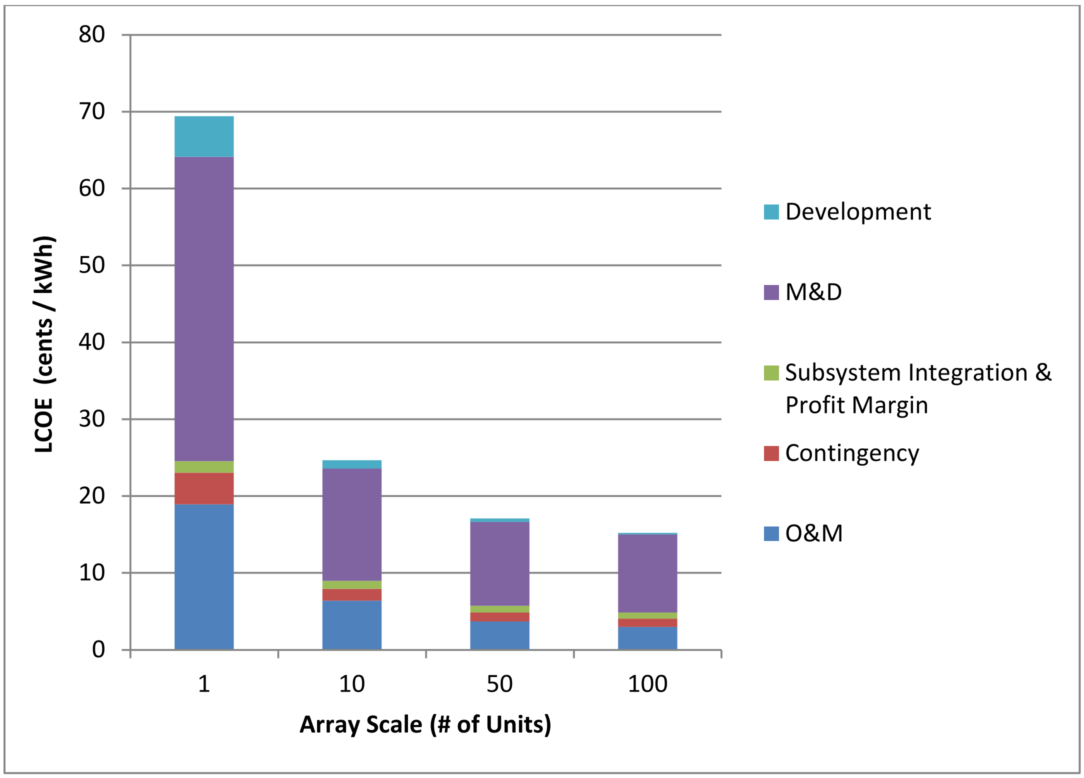

Figure 6-40. High-level LCOE (cents/kWh) breakdown per deployment scale for RM4.

The total CapEx for a single unit deployment was estimated to be approximately $25,641/kW, whereas the total CapEx per unit for a 100-unit array was estimated to be $6,220/kW. While there are some cost savings to be expected simply by increasing the manufacturing and fabrication volume from 1 to 100, major per-unit cost savings are expected to be realized within the installation cost category and the infrastructure cost category. Figure 6-41 shows the contribution of capital cost to LCOE.

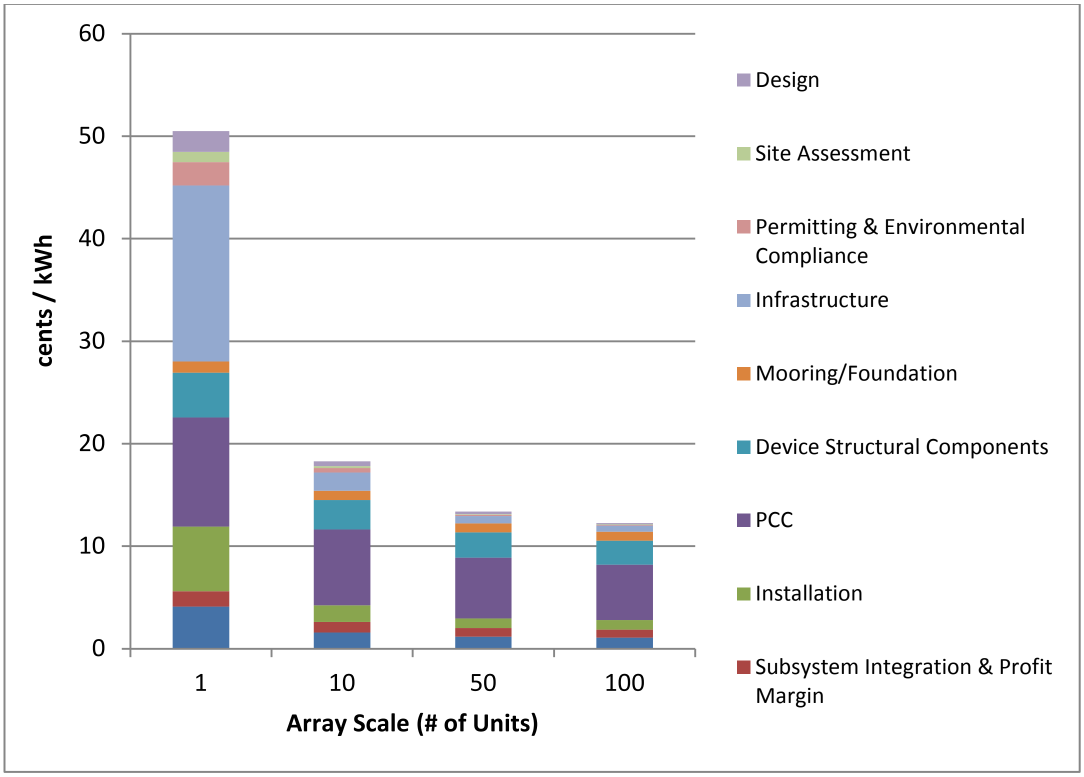

Figure 6-41. RM4 CapEx contributions to LCOE (cents/kWh) per deployment scale.

A detailed breakdown of major CapEx cost categories, in terms of LCOE, is provided in Table 6-19.

.

Table 6-19. Breakdown of RM4 CapEx contributions to LCOE (10-unit array).

	cents/kWh	% of total CapEx
Design	0.5	2.6%
Site Assessment	0.20	1.1%
Permitting & Environmental Compliance	0.4	2.4%
Infrastructure	1.8	9.7%
Mooring/Foundation	0.9	4.9%
Device Structural Components	2.9	15.8%
PCC	7.4	40.5%
Installation	1.6	8.9%
Subsystem Integration & Profit Margin	1.0	5.6%
Contingency	1.6	8.5%
Total	18.3	100.0%

Annual OpEx for a single unit deployment was estimated to be approximately $1,081/kW, whereas the annualized OpEx per unit for a 100-unit array was estimated to be $170/kW. Similarly to the capital cost (CapEx) contributions to LCOE, the operational cost (OpEx) contributions to LCOE are shown in Figure 6-42.

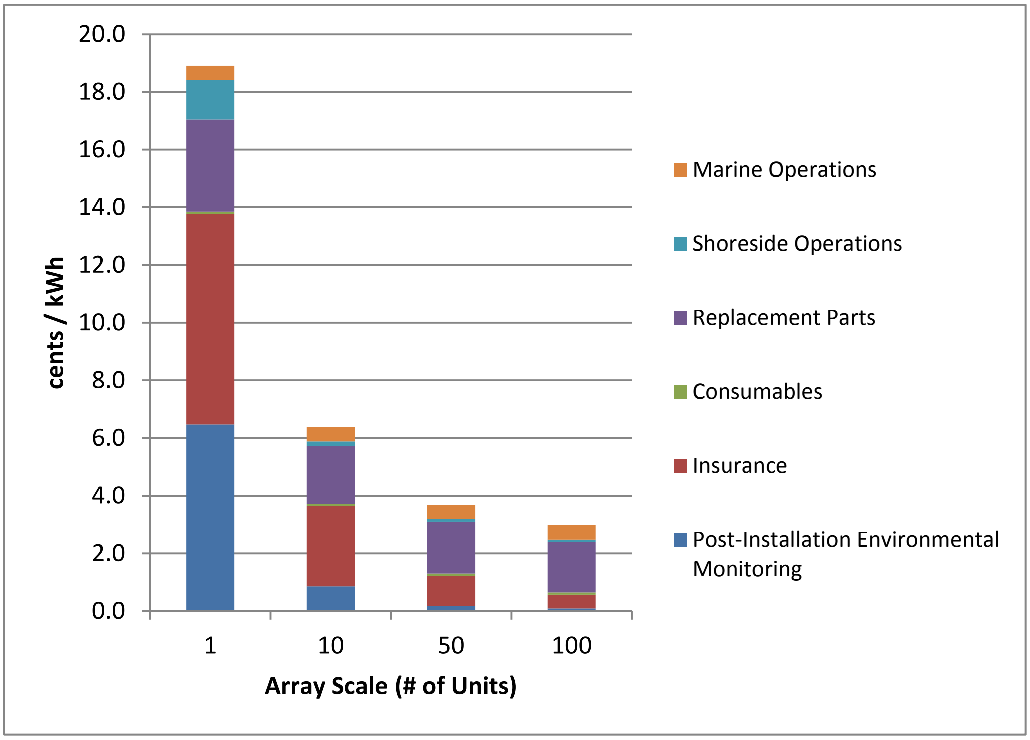

Figure 6-42. RM3 OpEx contributions to LCOE (cents/kWh) per deployment scale.

A detailed breakdown of major OpEx cost categories, in terms of levelized cost of energy, is provided in Table 6-20.

Table 6-20. Breakdown of RM4 OpEx contributions to LCOE (10-unit array).

	cents/kWh	% of total OpEx
Marine Operations	0.5	7.9%
Shoreside Operations	0.2	2.6%
Replacement Parts	2.0	31.4%
Consumables	0.1	1.2%
Insurance	2.8	43.5%
Post-Installation Environmental Monitoring	0.9	13.5%
Total	6.4	100.0%

7 Uncertainty

This chapter presents a more detailed description of the uncertainty present in the various performance, design, resource and environmental assessment, and economic analysis areas within the four reference models. The three tables presented under Section 7.1 assign the areas where there is low to very high uncertainty in the design for each reference model. Section 7.1.1 further illuminates the areas of uncertainty with a discussion of the specific topics needing further work and identifying areas with high cost uncertainty. The two tables in Section 7.2 categorize components of the Cost Breakdown Structure (CBS), respectively, the anticipated capital and operational expenditures (CapEx and OpEx), giving the reasons for the uncertainty associated with each major phase of development which includes the initial siting and scoping to the operations and decommissioning.

7.1 Uncertainty in Design and Economic Analysis

The uncertainty matrices presented in Tables 7-1 through 7-3 have six columns representing the various areas of uncertainty and four rows representing the qualitative assessment levels of uncertainty (low, medium, high, very high) and area shaded from blue to orange. The overall uncertainty is qualitatively estimated based on the type of data, if any, that has been generated or is available through engineering judgment or comparative analogy from similar technologies. For example, in a particular area such as Structural Design (second column of Tables 7-1 through 7-3), the structural analysis results were either derived from validated models (therefore low uncertainty) or less robust data based on engineering judgment alone (high uncertainty); or it may have been based on no data at all in that specific area, or the issue has not been addressed, in which case it would correlate to very high uncertainty. Consequently, for each row, the qualitative assessment of uncertainty moves from ‘Low’ (excellent data available) to ‘Very High’ (no data available). On each of these matrix tables for each specific RM device, the gray shaded areas indicate the type of data available in a particular column. The level of uncertainty associated with that data is shown by the row it resides within.

Table 7-1 provides a qualitative assessment of uncertainty for RM1 and RM4, which shared the same uncertainty characteristics Table 7-2 and Table 7-3 shows the uncertainty for RM2 and RM3, respectively. Within an area of design, multiple levels of risk/uncertainty for the various components (performance, design, compliance, economic analysis) illustrate how each RM has different levels of data quality to draw upon. Where applicable, the specific type of uncertainty is specified in blue font. For example, the results for Structural Design for RM1 and RM4 (Table 7-1, column 2) were derived from model simulation and is, therefore, assigned a level of medium uncertainty overall, while structural design areas of dynamic loads and fatigue were not addressed in the reference models and therefore add a component of very high uncertainty to the overall structural design.

Table 7-1. Uncertainty matrix for RM1 and RM4.

Uncertainty	Device Performance	Structural Design	PCC Design	Resource Assessment	Environmental Compliance	Economic*
Low	**Validated model *Turbine Performance***	Validated model	**Validated model or OEM parts**	**Actual data**	Actual data	Actual data
Medium	Model simulation, (no scaled test or field data)	**Model simulation, (no scaled test or field data)**	**Validated model simulation, no test data *Experience lacking submersed PCCs***	Validated model	Validated model	**Model simulation**
High	**Data from similar renewable energy technology – *Reliability***	Engineering judgment	Engineering judgment	Engineerin g judgment	**Engineering judgment**	**Data from similar renewable energy technology *M&D, O&M***
Very High	**Issue not addressed – *Array wake effects***	**Issue not addressed *– Dynamic loads & fatigue***	Issue not addressed	Issue not addressed	Issue not addressed	Issue not addressed

*NOTE: Economic assessment includes infrastructure, installation and operation and maintenance costs.

For RM1, RM3, and RM4 (Table 7-1 and Table 7-3, column 1) the turbine performance (or WEC performance in the case of RM3) was predicted using a validated model, and is, therefore, judged to have low uncertainty, while the RM2 turbine performance (Table 7-2) was judged to have medium uncertainty because the model used was not validated with scaled or field performance measurements. Device performance in arrays is highly uncertain because inflow conditions were assumed to be spatially uniform over the entire array layout and wake effects were assumed to be negligible. This assumption needs to be validated or refined. For the PCC design (third column) of RM1, RM2, and RM4, a validated model for the PCC design was used (low' uncertainty), whereas, for RM3, a non-validated model was used (medium uncertainty). Uncertainty levels for all other analyses are consistent between devices.

Table 7-2. Uncertainty matrix for RM2.

Uncertainty	Device Performance	Structural Design	PCC Design	Resource Assessment	Environmental Compliance	Economic*
Low	Validated model	Validated model	**Validated model or OEM parts**	**Actual data**	Actual data	Actual data
Medium	**Model simulation, no scaled test or field data-*Turbine Performance***	**Model simulation, no scaled test or field data**	**Validated model simulation, no test data *Experience lacking submersed PCCs***	Validated model	Validated model	**Model simulation**
High	**Data from similar renewable energy technology-*Reliability***	Engineering judgment	Engineering judgment	Engineering judgment	Engineering judgment	**Data from similar renewable energy technology *M&D, O&M***
Very High	**Issue not addressed – *Array wake effects***	**Issue not addressed *– Dynamic loads & fatigue***	Issue not addressed	Issue not addressed	Issue not addressed	Issue not addressed

*NOTE: Economic assessment includes infrastructure, installation and operation and maintenance costs.

Table 7-3. Uncertainty matrix for RM3.

Uncertainty	Device Performance	Structural Design	PCC Design	Resource Assessment	Environmental Compliance	Economic
Low	**Validated model –** ***WEC Performance***	Validated model	Validated model or OEM parts	**Actual data**	Actual data	Actual data
Medium	Model simulation, no scaled test or field data	**Model simulation, no scaled test or field data**	**Non-validated model simulation, no test data** ***Experience lacking submersed PCCs***	Validated model	Validated model	**Model simulation**
High	**Engineering judgment –** ***Reliability***	Engineering judgment	Engineering judgment	Engineering judgment	**Engineering judgment**	**Data from similar renewable energy technology** ***M&D, O&M***
Very High	**Issue not addressed –** ***Array Wake Effects***	**Issue not addressed** ***– dynamic loads and fatigue***	Issue not addressed	Issue not addressed	Issue not addressed	Issue not addressed

*NOTE: Economic assessment includes infrastructure, installation and operation and maintenance costs.

7.1.1 Knowledge Gaps and Key Areas Needing Further Work

Table 7-1, Table 7-2, and Table 7-3 identify knowledge gaps where more research, development and data collection could be focused to gain a better understanding of the power and cost performance of MEC devices and arrays. It is important to understand that while the economic uncertainty level here is ranked ’Medium’ or ‘High’ for the RMs, there may be compounding uncertainties from the other analyses performed that add to the economic uncertainty.

The following are key areas identified through the first iteration where more information is needed in order to improve the models.

- **Device Performance Characterization:** Model validation testing is critical to ensure accurate characterization of device performance and AEP estimates. To date, the only still outstanding performance testing needed for model validation is for the CACTUS model, which was used to predict turbine performance characteristics for the RM2 device.
- **Device Performance, Characterization of Performance Reductions:** Hydrodynamic interactions between devices in arrays (i.e., the effects of turbulence from upstream devices) are not presently modeled and such effects should be studied further to optimize spacing at each reference site.
- **Structural Design:** Unsteady dynamic loading or fatigue was not considered in the structural design analyses.
- **Power Conversion Chain (PCC) Design:** We have little experience with submersed PCCs. This technology is very sensitive to the number of times physical access is required to the device over the life-cycle of the project. The PCC drivetrain components and the hydraulic fluids and filters are housed within a watertight nacelle and must be scrupulously maintained. Increasing the robustness of the PCC design, thereby hardening the PCC by introducing redundancy in its subsystems is advocated to reduce the overall O&M costs. Therefore, we highly encourage future designers to thoroughly explore the feasibility of hardening the PCC and study alternate drivetrain configurations. Specific areas to investigate include the following:
  - Improving the stiffness of the frame may allow for a less robust PCC.
  - The PCC may need more study in terms of cost reduction with the number of units, which would correlate better with the cost of small scale wind plants.
  - Coupling multiple units with a gear box to one generator rather than the existing two generator design may reduce manufacturing and O&M costs.
- **Failure Rate Distributions and Failure Modes:** Component failure rates are critical cost drivers of O&M intervention cycles as well as the replacement cost for the entire device itself. The present analysis uses a simple average failure rate model, which need to be replaced with more accurate failure rate distributions. In addition, more recent work on the topic of failure rates should be leveraged from NREL and Sandia efforts in their wind energy programs.

- **RM3 Riser Cable:** The riser cable (which transmits electricity to a junction box) for a WEC device could be a critical failure point and requires further investigation. The potential damage to the riser cable includes the effects of water depth and currents along with the motion of the device which could cause significant stresses. These effects can be mitigated with a custom designed cable, but needs further examination..
- **Wet Mate-able Connector at High Voltage:** Wet mateable connecters for high voltage cables, such as needed for RM4, do not yet exist commercially and, therefore, require a custom-designed solution. There is great uncertainty estimating the cost of these components.
- **Device Recovery / Redeployment:** There are knowledge gaps in the device O&M costs stemming from recovery and redeployment of components and entire MEC devices. This includes medium to high uncertainty in deployment and maintenance methods, vessel requirements, and materials and equipment needed for PCC or MEC device recovery, redeployment, and umbilical cable handling. An initial concept design for recovering and redeploying the PCC powertrain for each device was developed during this study. However, there are a number of risk factors that would require further investigation as it relates to the procedure itself, the vessel's design, and umbilical cable handling.
- **Environmental Compliance:** There is considerable uncertainty associated with each environmental cost estimate, with the greatest uncertainties lying with post-installation environmental monitoring, including monitoring for negative or positive ecosystem effects on the pelagic and benthic marine life. As applicable, similar studies for river and tidal zones to include the land-water interface areas will be needed. The focus of environmental monitoring will certainly include, but not be limited to, protected marine mammals under the Marine Mammal Protection Act (MMPA), sea turtles, fish, birds, and a variety of benthic animals. There are a number of uncertainties in the cost estimates for pilot projects that cannot be quantified at this time. These are as follows:
    - **Monitoring Costs**. Costs for post-installation monitoring are less accurate than those for pre-installation studies because pre-installation studies that have been carried out at existing MEC pilot projects were used to inform the costs, thus providing a reasonably accurate level of confidence in the information that would be needed for RM1 through RM3 monitoring. However, the ocean current device, RM4, being proposed is unlike any other tidal or wave project with respect to its design and projected deployment area. To date, no monitoring programs have even been proposed for such a project and there are no existing technologies to act as surrogates for environmental baseline monitoring. Costs were estimated based on professional and engineering judgment and a few published studies. The yearly monitoring costs were estimated and extended to the proposed 5-year term of a FERC pilot license.

- **Mitigation Costs.** Although mitigation for impacts to marine animals, habitats, or ecosystem processes may or may not be required for most MHK projects, these types of costs have not been factored into the cost estimates. These costs could be added to post-installation monitoring costs, but we cannot reasonably estimate their range in magnitude at this time.
- **Uncertainty of Costs for Regulatory Requirements.** There is considerable uncertainty associated with the costs for complying with NEPA and other federal and state regulatory mandates with respect to protecting the environment. Meeting these mandates will require concentrated effort and close coordination with stakeholders at each stage of a MEC project. The magnitude of these costs will be dependent on the length of time these regulatory processes require. Each project and location will be unique in meeting the environmental protection laws. While some applicable laws and regulations have established timelines for processing permits, adhering to set timelines (which often exceed the initial schedule) may not be possible. The outcome for a MEC project will ultimately depend on achieving not only regulatory acceptance and alignment but also will depend on many areas of agreement between all of the parties involved.
- **Scaling Pilot Project Costs.** There is also considerable uncertainty in scaling the pilot project costs to commercial developments for post-installation environmental monitoring. Some of the post-installation studies carried out at the pilot-scale are likely to continue for some time. However, information collected during environmental monitoring of pilot-scale devices may satisfy a number of regulatory questions, particularly the risk of direct mechanical effects of the devices on animals (such as blade strike). As with pre-installation studies, increases in post-installation monitoring costs may be related to additional studies to understand far-field or ecosystem effects resulting from large arrays of MEC devices.

7.2 Uncertainty in CapEx and OpEx Costs

Project costs are categorized under OpEx and CapEx correlating primarily to pre-operational design and deployment type costs and costs incurred after the MEC array comes online. Table 7-4 shows the uncertainties assigned to each category of CapEx. Table 7-5 shows the uncertainties for each OpEx topic.

Environmental Compliance has medium to high uncertainty for a variety of reasons, as described in detail above.

Design and engineering has high uncertainty, as the reference models in this report are at a conceptual level (TRL 3-4) and, therefore, have not been optimized to a level needed for commercialization.

The **LCOE estimates** are based on relatively simple device designs that use commercial-off-the-shelf (COTS) components that prevent performance optimization. However, this conservatism is likely offset by not accounting for any reduction to AEP for devices in arrays. Subsystem integration and profit margin is very difficult to estimate given the level of design of the RMs, and therefore has high uncertainty.

Contingency can be considered a buffer in cost estimates for any type of commercial project, and will always have high uncertainty.

For **OpEx**, marine and shoreside operation costs are highly uncertain because there is no water power failure rate data to base it on. Instead, failure rates for onshore wind turbines are used to estimate schedule and costs of interventions making the cost estimates less certain. For most cost categories, uncertainty levels will go down over time as further studies and actual deployments are completed.

Table 7-4. Assessment of CapEx cost uncertainty categories.

Cost Breakdown Structure (CBS) Category	Topic (If Applicable)	Result Maturity / Fidelity	Uncertainty
Development	✓ Siting & Scoping, ✓ Pre-Installation Environmental Studies ✓ Post-Installation Environmental Studies ✓ NEPA & Process ✓ Site Assessment	Based on data from similar studies and/or engineering judgment and/or data from PNNL study	**Medium to High**
	✓ MEC Design and Engineering	TRL 3-4 design and analysis	**High**
Infrastructure	Cables and Connectors	Conceptual layout, generic hardware ID and estimates	**Medium**
	Dockside and Vessel	Generic for dockside and specific vessel ID	**Medium**
Foundation/ Mooring	NA	Design with combination of specific and conceptual hardware	**Low to Medium**
Device Structural Components	All	CAD designs, conceptual designs, and steel cost models	**Low to Medium**
PCC	All Components	CAD design and specific hardware ID with cost	**Low**
Installation	N/A	Time and materials estimated for defined resource location with labor and materials costs included	**Medium**
Subsystem Integration & Profit Margin	N/A	Assumed to 10% of machine cost	**High**
Contingency	N/A	Assumed as 10% of project cost	**High**
Decommissioning	N/A	Assumed to be same as Installation cost	**Medium**

Table 7-5. Assessment of OpEx cost uncertainty categories.

Cost Breakdown Structure (CBS) Category	Topic (If applicable)	Result Maturity / Fidelity	Uncertainty
Marine Operations	N/A	Large uncertainties with respect to maintenance and a simplified O&M model	**High**
Shoreside Operations	N/A	Large uncertainties in failure rates, maintenance and repair costs	**High**
Replacement Parts	N/A	Limited failure rate data. Based on original parts cost and reliability from Windpact Study.	**Medium**
Consumables	N/A	Assumed 10% of replacement	**High**
Insurance	N/A	Based on oil and gas and other renewable project experience	**Low**
Post-installation Environmental Monitoring	N/A	Based on data from PNNL and similar studies	**Low to Medium**

8 Conclusions

The primary purpose of this report was to:

- Present a methodology for the design and economic analysis of four Marine Energy Conversion (MEC) technology point designs. Each RM design was inspired by existing MEC concepts from the MEC industry. Design and analysis was achieved using existing and newly developed open-source design tools (numerical models), physical scale modeling to test performance and validate open-source tools, and leveraging a wide range of resources and knowledge from academia, industry, and the MEC community in all areas.
- Present four MEC technology Reference Models. Each Reference Model is a "point design," a term used to emphasize that it is a unique device designed for a reference resource site modeled after an actual site in the United States; it is not intended to be a device that is a general representation of a specific MEC technology archetype.
- Demonstrate our methodology for the four MEC technology Reference Models, referred to herein as Reference Models (RM) 1, 2, 3, and 4.

While the Reference Model technologies were only designed at the conceptual level (DOE Technology Readiness Level 3-4), we assumed—for the purpose of estimating AEP and the costs to design, develop, deploy, and maintain an RM device/array—our designs are mature and commercially viable; our goal here was to reflect a mature MEC industry.

We encourage MEC developers to apply our methodology, with the appropriate reference resource sites, to design and estimate LCOEs for their technologies. Of course, such a comparison is only possible if developers use the same methodology, reference resource sites, as well as our basic assumptions and approximations, which we attempt to articulate clearly in this report.

For the purpose of facilitating open-source MEC research and development (R&D), we have archived all supporting documentation on Sandia's web site: http://energy.sandia.gov/rmp. Here one can find reports detailing the design and analysis of each RM, physical modeling studies used for model validation (with corresponding experimental data sets), reference resource site development work, and Excel spreadsheets that detail the cost breakdown structure (CBS). We also show our calculations for AEP, capital expenditure costs (CapEx), operational expenditure costs (OpEx), and estimates for LCOE.

8.1 LCOE Estimates

Figure 8-1 shows our LCOE estimates for 10- and 100-unit arrays for all four RM point designs. The blue bars represent the cost range for projects with 10-units; we believe smaller arrays with 10-units are more likely to be deployed in the early stages of MEC commercialization. LCOE estimate ranges for arrays of 100 units, as shown by the red bars, illustrate the significant cost reductions expected with larger MEC deployments.

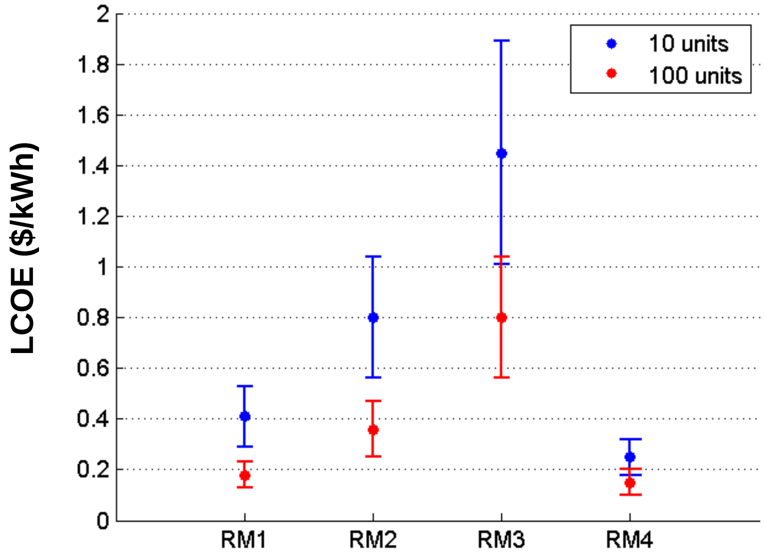

Figure 8-1. LCOE estimates ($/kWh) for four reference MEC technology point designs.

A summary of our LCOE estimates for 10-unit arrays, in order of increasing cost, is summarized in Table 8-1. We recognize that some of the costs used in the LCOE estimates may be perceived as optimistic by experienced MEC developers in a nascent industry; especially those costs benefiting from cost reductions as the number of units in an array increases; however, the MEC developer community, whom will continue to evolve this technology, are encouraged to adjust these costs based on their judgment and experiences. For the *current* energy conversion (CEC) devices devices—RM1, RM2 and RM4—we believe our LCOE estimates (based on 10-unit arrays) are in reasonable agreement with other published LCOE estimates. However, we acknowledge that the LCOE estimate for the WEC device, RM3, may be overly pessimistic due to the aforementioned lack of DOE laboratory experience and investments.

Installed capacity and capacity factor were key drivers that affected the LCOE estimates. For 10-unit arrays, the low LCOE for the ocean current turbine, RM4 ($0.25/kWh), is due to the high installed capacity for each device (4 MW) and the high capacity factor (CF=0.7) due to the constancy of the Gulf Current in the Florida Strait. The capacity factors for all the other RMs were 0.3, less than half the value for RM4. The LCOE for the tidal current turbine, RM1 ($0.41/kWh), is slightly more than values reported for offshore wind turbines. For the river current turbine, RM2, the high LCOE ($0.80/kWh) is due to the low installed capacity and the spatial constraints inherent at a river site. The LCOE estimate for the WEC device, RM3 ($1.45/kWh), is comparatively much higher, but this largely reflects the lack of experience and tools available for designing this technology at the time of this study. Unlike the turbine-based Current Energy Conversion (CEC) RM designs, which benefited from decades of DOE laboratory R&D experience and investments in wind turbine technologies, there was relatively little design experience and developed tools that could be leveraged to design the RM3 device.

Table 8-1. Summary of LCOE average estimates based on a 10-unit Array.

	LCOE Based on 10-Unit Array
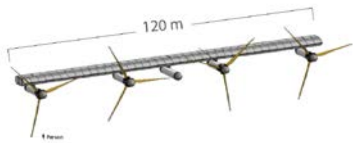	**RM4, Ocean Current Turbine** This design has the lowest average LCOE at **$0.25/kWh**. This is primarily due to the high installed capacity for each four-turbine device (4 MW). It also has a low LCOE because of the high reliability and consistency of the Gulf Current in the Florida Strait which gives it a high capacity factor of CF=0.7.
	**RM1, Tidal Current Turbine** The LCOE for the tidal current turbine is **$0.41/kWh**. This is slightly more than the values reported for offshore wind turbines.
	**RM2, River Current Turbine** RM2 has the third highest LCOE at **$0.80/kWh.** This is due to its low installed capacity as well as increased inefficiency in energy capture due to the spatial constraints inherent at a river site.
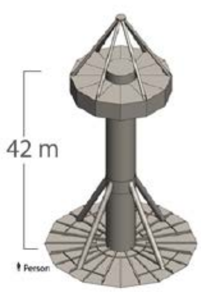	**RM3, Wave Energy Conversion (WEC)** The WEC device has the highest LCOE at **$1.45/kWh**. This is largely a consequence of the sparsity of developed WEC tools and models available at the time of its development as well as the general inexperience with WEC designs—there were no analogues to draw upon during the RM3 design. As a comparison, the turbine-based designs for RM1 and RM4 drew upon wind turbine technology, which has benefited from decades of DOE laboratory R&D experience and investments. With new critical innovations in development by WEC researchers, including the development of advanced controls to increase the energy capture efficiency, we believe the costs for wave absorption technology will come down. Further, if these design innovations had been applied to RM3 for this effort, we believe the LCOE cost would be significantly less.

As a caveat, we advise caution when comparing the LCOEs among these four Reference Models for the following reasons:

1. The LCOE for each RM was estimated for a specific reference resource site. Therefore, the theoretical hydrokinetic power densities and environmental constraints varied considerably between sites.

2. Knowledge gaps and uncertainties are greater in some RMs as compared to others. WECs, for example, are more nascent technologies than CECs. Also, unlike CECs, WECs do not have analogue technologies such as wind turbine plants from which design, M&D, and O&M experience can be used to more accurately extrapolate the expected design, M&D, and O&M strategies and their costs.

3. Varying levels of design optimization were performed for the different RMs.

8.2 Key Cost Drivers

One of the main purposes of this study was to identify key cost drivers and cost reduction pathways to direct future R&D efforts. As illustrated in Figure 8-2, the CBS contributions to LCOE for each of the four RMs identify common trends; these trends remain similar between the four RMs and are also consistent between 10-unit and 100-unit arrays. In particular, for all RMs, CapEx contributions, which include costs for design and development, manufacturing and deployment, environmental studies and permitting, subsystem integration (e.g., grid connections), and profit margin and contingency, are about three to four time greater than all OpEx contributions. As shown in the figure, M&D is by far the dominant CapEx contributor for all RMs, representing about 50% of the total LCOE. O&M contributions are the next most significant contributor, representing about 30% of the total LCOE, with insurance and post-installation (environmental) monitoring generally being the main O&M cost drivers. The exception to this generalization for the O&M costs (for each RM) is RM4, where the cost of replacement parts is the second highest cost driver, behind insurance, contributing over 30% to its O&M costs.

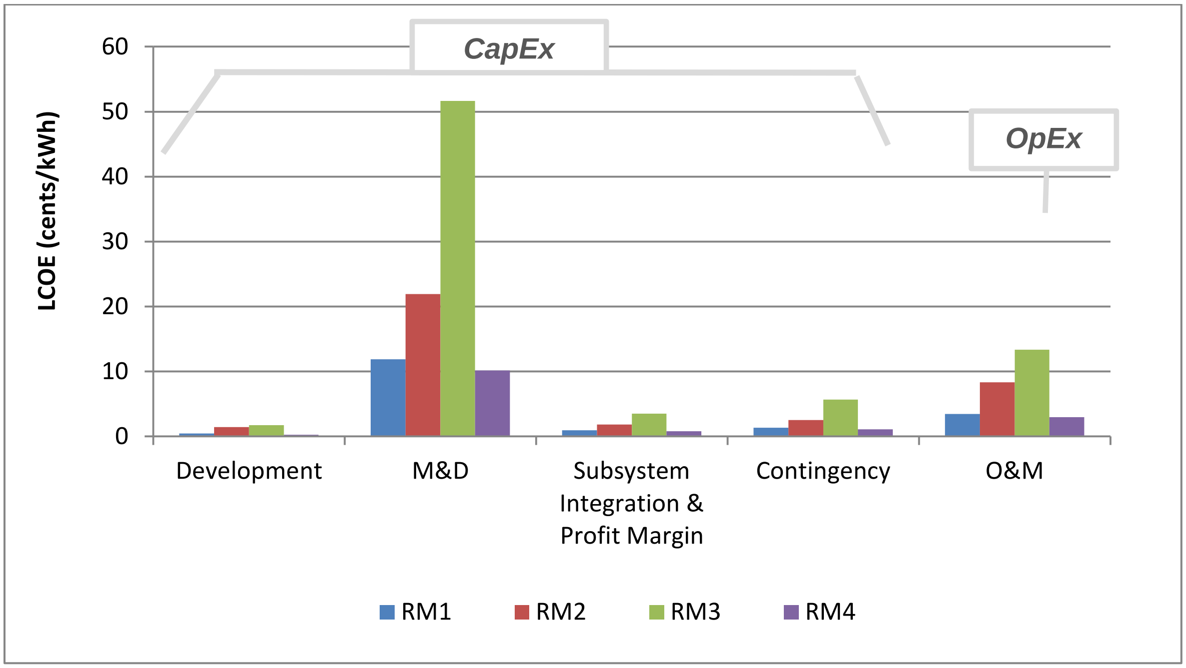

Figure 8-2. Comparison of CBS contributions to LCOE (based on 100-unit array).

The CBS contributions to CapEx are shown in Figure 8-3. For RM1, RM2 and RM4, the PCC and device structural components are the highest cost drivers. For the RM3 device, the device structural components are significantly higher than any other contributor due to the high cost of the float, vertical column, and reaction plate; this is mainly due to the high volume and cost of steel. Also, costs for the mooring system, installation, and contingency costs are comparable to the PCC cost.

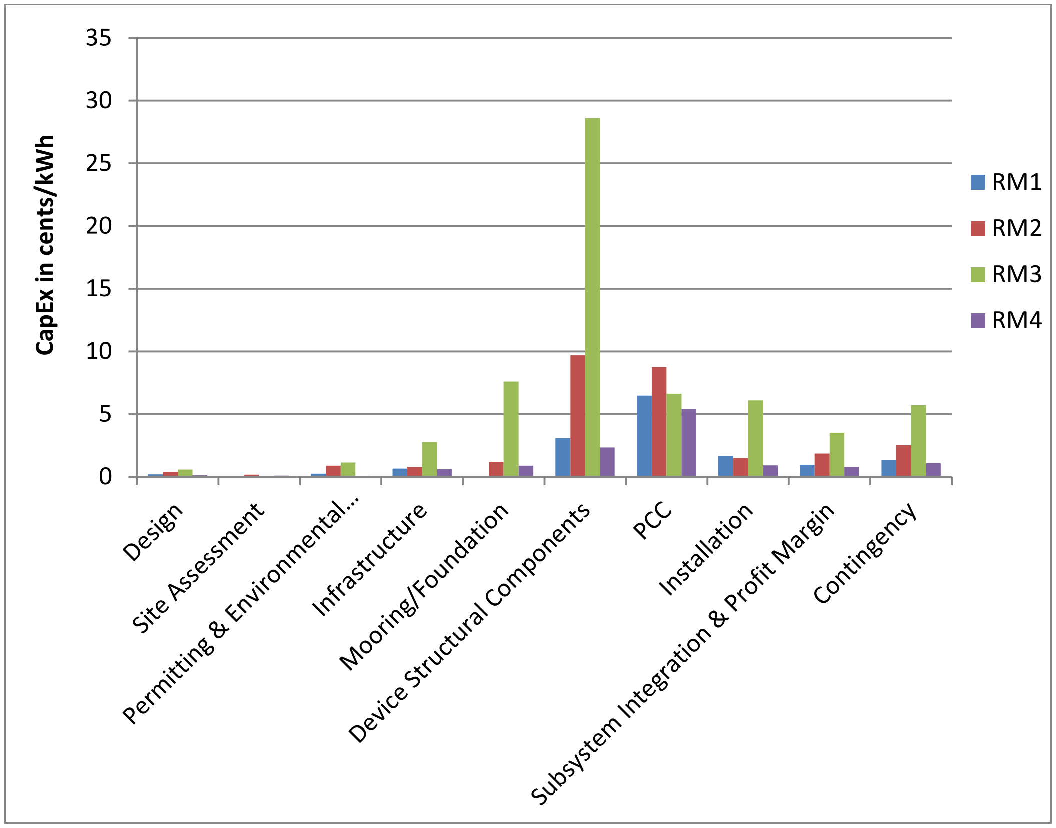

Figure 8-3. Comparison of CBS contributions to CapEx (based on 100-unit array).

8.3 Recommendations

We recognize that our methodology requires improvements and we encourage the MEC industry and the R&D community to further its development. The following subsections summarize what we perceive as important weaknesses in design, analysis, performance, and cost modeling. We provide recommendations for:

1. Closing knowledge gaps to reduce uncertainty bands on performance and costs; and
2. Improving technology and economic performance based on identified key cost drivers by employing improved design optimization modeling and implementing advanced control systems.

8.3.1 Improve Power Performance and AEP Estimates

Continued scaled model testing of MEC devices and new scaled model testing for arrays is critical to narrow uncertainties and increase confidence in power performance predictions and AEP estimates. Performance predictions for RM1, RM2, and RM4 were based on applied models that were developed for wind turbine design and analysis, including WT_Perf and CACTUS. These models have undergone extensive validation for wind turbines in atmospheric boundary layer flows; however, more work is needed to validate these codes for modeling hydrokinetic turbines in water current environments. For this study, only the CACTUS model, which was used to predict power performance for the RM2 device, was not validated with experimental data from a scaled model test. Scaled model testing of the entire dual-rotor RM1 and RM2 devices is planned at the University of Minnesota, St. Anthony Falls Laboratory (Neary et al. 2013c). These experiments will allow rigorous validation of the models used to predict the device performance detailed in this report. No scaled model testing is planned for the RM4 device due to resource limitations, but since it is an axial flow turbine, like the RM1 device, and performance predictions were based on the same model as the RM1 device, we do not believe this testing is as critical. In order to facilitate further physical model testing and model validation, SolidWorks (CAD software) files of all RM device geometries are available for download from the Sandia National Laboratories Energy, Climate, and Infrastructure Security website: http://energy.sandia.gov/rmp.

8.3.2 Leverage More Operational Experience from Technology Analogues

Estimated CapEx and OpEx costs in our study relied heavily on design, M&D, and O&M experience from land-based wind power turbines and farms. For example, data for component failure rates is based on the WindPACT study (Poore and Lettenmaier 2003) and does not reflect gains in reliability of wind power technologies. To estimate RM device and array operational availability to calculate the actual AEP used in the LCOE estimate we applied an availability level of 95%, which is similar to the availability of 95.5% reported by Graves et al. (2008) and Peters et al. (2012) for land-based wind plants surveyed in the United States (i.e., a downtime of 5%).

We recognize that land-based wind plant analogues do not reflect the added cost of working in the marine environment. For this reason, our RM device designs incorporate considerable mechanical and electrical redundancy for components that have higher failure rates. This is expected to considerably improve operational availability by reducing the number of necessary service trips. In our O&M Strategy Module, we also planned for one reserve device (unit) to be available in storage at dockside to reduce operational downtime for all array sizes. Finally, high operational availability can be better ensured by adopting design standards and insurance costs from offshore oil and gas exploration and shipping industries.

Until commercial MEC project operational experience is available, we believe additional efforts should be made to leverage more information from various marine infrastructure industries. Uncertainties in CapEx and OpEx costs can be narrowed further for CEC RMs by incorporating empirical data from other more mature analogue renewable energy technologies used to delineate M&D and O&M strategies and costs, specifically, using more empirical data from more current land-based wind power projects and offshore wind projects. OpEx costs for offshore wind, for example, are approximately three times those of land-based wind plants and are well understood (Paish 2012).

8.3.3 Refine Operations Modeling with Use of Weather Windows

As demonstrated by Teillant et al. (2012), estimates for operational costs and device availability can be improved by applying more rigorous operational models (based on O&M experience with wind energy farms and oil and gas exploration). In particular, Teillant et al. (2012) apply weather windows to determine when conditions are suitable for operation of vessels and equipment required for preventative and corrective O&M tasks, e.g., installation, repair, inspection, and removal. While distance to shore and service vessel speed affect the transit time for O&M, weather windows affect, not only the timing of when O&M activities can be conducted, but also the total period of time a vessel needs to “wait on weather” before completing a particular task. Weather windows, which vary among different resource types (e.g. wave environments compared to tidal current environments) and specific sites, were not considered in our O&M Strategy Module.

8.3.4 Continue Optimizing RM CEC Designs and Advance WEC R&D

The RM device designs were developed primarily to estimate their LCOE. As such, they are simple, robust, conceptual (TRL 3-4) designs. Technical and economic performance are, therefore, not optimal. Optimization of the performance of RM devices was minimal. For CEC RM devices, this can be improved using well developed optimization methods used for wind turbines.

For WEC RM devices, however, more fundamental R&D is needed in the area of real-time-forecasting and advanced controls. Recent research shows that advanced controls can provide substantial improvements to energy capture efficiency. Kara (2010) showed that latching control can result in absorbed power increases of 168% over the standard resistive controls. Hals (2011) showed that three distinct nonlinear reactive control techniques can result in absorbed power increases of 230% to 330% over the standard resistive controls. The same work also shows absorbed power increases of 100% to 200% for four distinct nonlinear control strategies utilizing latching and clutching. Li et al. (2012) showed that nonlinear reactive controls, with perfect forecasting, result in an absorbed power increase of 200%.

8.3.5 Conduct Performance Analyses of MEC Arrays

No models were applied to optimize the design of arrays because these models are in early stages of development (Hassan 2013, Weywada et al. 2012). As a result, the device spacing and array footprint was conservatively large so that inflows could be reasonably assumed to be unaffected by the wakes caused by upstream devices (velocity deficits and increased turbulence). While we expect the assumption that the inflow characteristics are spatially invariant for individual devices in an array can result in a significant overestimation of AEP that lowers our LCOE estimates, the assumption of sparsely packed devices in an array also raises a number of costs covered under the M&D, O&M and EC Modules described above. The cost of transmission cables, for example, is therefore overestimated. Trip durations for service vessels would increase as well, increasing OpEx costs; but the current O&M Strategy Module (and sub-modules) is currently not of high enough fidelity to predict cost reductions that would be achieved by denser device spacing in arrays. The same is true for environmental cost estimates (EC Module), which currently do not have the fidelity to account for the increased CapEx resulting from conducting environmental studies over a larger footprint, as well as the increased OpEx costs for environmental monitoring. In addition, the application of array design models would account for feedback and optimization between the environmental analysis and operational conditions analysis sub-modules.

8.3.6 Environmental Compliance Costs

We assigned no costs for long-term mitigation activities that will be required for environmental risks. Until knowledge gaps, including the potential impacts from MEC devices and projects on the physical and biological environment (e.g., animal strike, noise, and electromagnetic frequencies [EMF]) can be closed, it will not be possible to determine mitigation requirements and their costs. Many studies are ongoing or are planned to continue characterizing the potential impacts to marine life and habitats (e.g., marine mammals, sea turtles, benthic organisms, and zooplankton) from deployed MEC devices. NEPA compliance activities and effectively addressing stakeholder concerns will direct a large part of the MEC planning process.

The process PNNL used to estimate costs of environmental studies and permitting relied heavily on information from developers, researchers, and consultants involved in facilitating deployment of MEC devices in the U.S. The variability of cost estimates shown for environmental studies and permitting are large, as reflected by the cost ranges shown, and represent preliminary answers that require more investigation before they can be seen as reliable contributors to the LCOE. Each major study has been costed independently, but there may be considerable cost savings if baseline and monitoring studies for various organisms are combined. For example, combining boat-based observer assessments of marine mammals and sea turtles along an open coastline will reduce days of ship time; similarly, acoustic monitoring for aquatic mammals and fish can be conducted during the same cruise, using an array of acoustic imaging devices and hydrophones. Where possible, these potential efficiencies were captured in low cost estimates and described in the assumptions; however, considerable variability in the effectiveness and, therefore, the requirements for conducting combined environmental studies can still be expected.

With a limited number of U.S. MEC projects approaching deployment (and none of them planned for capturing energy from ocean currents), there have been limited sources of cost data available during this study. Future iterations of this process will help hone the costs of studies and permitting, as well as determine the proportionate contributions to the LCOE.

The cost ranges shown for the RM4 ocean current technology reflect choices among the studies, as indicated by the logic models. As we learn more about the conditions found at proposed MEC sites, the potential effects of these devices on marine animals, habitats, and ecosystem processes, and the studies required to understand and address these effects, the logic models could be revisited, with further refinement of the list of studies and associated costs for each stage of development. Similarly, the scaling rules (refer to Table 2-5) could be further refined and applied to commercial scale studies. Once sufficient study and costing data become available at the commercial scale, the scaling rules should become unnecessary and could be replaced with estimates of realistic costs.

Bibliography

ABB. "Brochure: ABB Wind turbine generators: reliable technology for all turbine applications." ABB, 2009.

—. *Setting new efficiency records.* Apr 5, 2013. http://www.abb.us/product/ap/seitp322/40ffb400507a8f09c1257b43002ea769.aspx (accessed Nov 2013).

Abernethy, Robert. *The New Weibull Handbook Fifth Edition, Reliability and Statistical Analysis for Predicting Life, Safety, Supportability, Risk, Cost and Warranty Claims.* Unknown, 2006.

Alger, Mark S. M. *Polymer Science Dictionary.* Springer Publishing, 1997.

Anchor Marine and Industrial Supply. *Online Catalog.* Nov 2011. ttp://www.anchormarinehouston.com/.

Babarit, Aurélien. "A Review of the Park Effect in Arrays of Wave Energy Converters." *International Conference on Ocean Energy, Oct 19* . Dublin, Ireland: ICOE , 2012.

Baccarini, D. "Estimating project cost contingency - a model and exploration of research." *20th Annual ARCOM Conference (Sep 1-3).* Heriot-Watt University, Edinburgh: Association of Researchers in Construction Management, 2004. pp. 105-113.

Banchant, P., and M. Wosnik. "Performance and Wake Measurements for a Cross-Flow Axis Turbine at Moderate Reynolds Number." *Proceedings of ASME Fluids Engineering Division Summer Meeting 2013, Paper FED2013-0000, July 7-13.* Incline Village, NV, 2013.

Barone, M., T. Griffith, and J. Berg. *Reference Model 2: Rev 0 Rotor Design.* Technical Report: SAND2011-9306, Albuquerque, New Mexico: Sandia National Laboratories, 2011.

Beam, M. J., et al. "Marine Hydrokinetic Turbine Power-Take-Off Design for Optimal Performance and Low Impact on Cost-of-Energy." *31st International Conference on Ocean, Offshore, and Arctic Engineering (OMAE) June 10-15.* Rio de Janeiro, Brazil: National Renewable Energy Laboratory, Conference Paper NREL/CP-5000-54410, 2012.

—. "Power-Take-Off Design NREL Reference Turbine 1." *Presented to Sandia National Laboratories and U.S. Department of Energy.* National Renewable Energy Laboratory, January 14, 2011a.

—. "Power-Take-Off Design SNL Reference Turbine 2." *Presented to Sandia National Laboratories and U.S. Department of Energy.* National Renewable Energy Laboratory, January 14, 2011b.

Bedard, Roger, et al. "North American Ocean Energy Status -- March 2007." *7th European Wave and Tidal Energy Conference, Sep 11-13.* Porto, Portugal, 2007. 1-8.

Berg, J. C. *Extreme Ocean Wave Conditions for Northern California Wave Energy Conversion Device.* Technical Report: SAND2011-9304, Albuquerque, NM: Sandia National Laboratories, Nov 2011.

Bir, G., M.J. Lawson, and Y. Li. "Structural Design of a Horizontal-axis Tidal Current Turbine Composite Blade." *30th International Conference on Ocean, Offshore, and Arctic Engineering, June 19-24.* Rotterdam, The Netherlands: American Society of Mechanical Engineers, 2011.

Bir, Gunjit. *National Renewable Energy Laboratory, National Wind Technology Center (NWTC) Design Code: PreComp.* 2013. http://wind.nrel.gov/designcodes/preprocessors/precomp/ (accessed March 26, 2007).

Boehlert, George, Gregory McMurray, and Catheryn Tortorici. "Ecological Effects of Wave Energy Development in the Pacific Northwest: A Scientific Workshop, October 11-12, 2007." *NOAA Technical Memorandum NMFS-F/SPO-92.* Oregon State University, Newport, OR: NOAA, National Marine Fisheries Service, 2008.

Budar, K., and J. Falnes. "A resonant point absorber of ocean-wave power." *Nature* (Institutt for eksperimentalfysikk, N-7034 Trondheim—NTH, Norway) 256 (August 1975): 478–479.

BVG Assoc. *Wave and Tidal Energy in the Pentland Firth and Orkney Waters: How the Projects Could Be Built.* Technical Report available at: http://www.thecrownestate.co.uk/media/71431/pentland_firth_how_the_projects_could_be_built.pdf, United Kingdom: BVG Associates - Report commissioned by the Crown Estate, 2011.

Carbon Trust. *Accelerating Marine Energy: The Potential for Cost Reduction -- Insights from the Carbon Trust Marine Energy Accelerator.* Technical Report, available at: http://www.carbontrust.com/media/5675/ctc797.pdf, London, UK: Carbon Trust, 2011.

Carbon Trust. *Future Marine Energy Results of the Marine Energy Challenge: Cost Competitiveness and Growth of Wave and Tidal Stream Energy.* Technical Report, London, UK: Carbon Trust, prepared by John Callaghan, Jan 2006.

Cargo, C. J., A. R. Plummer, A. J. Hillis, and M. Schlotter. "Determination of Optimal Parameters for a Hydraulic Power Take-off Unit of a Wave Energy Converter in Regular Waves: Proceedings of the Institution of Mechanical Engineers, Part A." *Journal of Power and Energy* 226, no. 1 (2011): 98-111.

Chamorro, L. P., V. S. Neary, C. Hill, B. Gunawan, R.E.A. Arndt, and F. Sotiropoulos. "Effects of Energetic Coherent Motions on the Power and Wake of an Axial-flow Turbine." *Fluid Mechanics*, 2013: Submitted.

Child, B. F. M., J. Cruz, and M. Livingstone. "The Development of a Tool for Optimising Arrays of Wave Energy Converters." *Proceedings of the 9th European Wave and Tidal Conference.* Southampton, UK: EWTEC, 2011.

Churchfield, M. J., Y. Li, and P. J. Moriarty. "A large-eddy simulation study of wake propagation and power production in an array of tidal-current turbines." *Philosophical Transactions of the Royal Society A: Mathematical, Physical and Engineering Science* 371, no. 1985 (January 2013).

Clare, R., and R. C. Mays. "The Musgrove Variable Geometry Vertical-axis Wind Turbine." *Modern Power Systems* Vol. ? (1982): 35-38.

Copping, A. E., and S. H. Geerlofs. "The Contribution of Environmental Siting and Permitting Requirements to the Cost of Energy for Marine and Hydrokenetic Devices: Reference Models #1, #2, and #3." *Proceedings of the 9th European Wave and Tidal Conference, Sep 5-9.* South Hampton, UK: Pacific Northwest Laboratory, 2011.

Copping, A.E., L. A. Hanna, and S.H. Geerlofs. "The Contribution of Environmental Siting and Permitting Requirements to the Cost of Energy for Marine and Hydrokenetic Devices: Reference Model #4." Richland, WA: Pacific Northwest Laboratory, 2012.

Cruz, J., R. Sykes, P. Siddom, and R. Eatock Taylor. "Estimating Loads and Energy Yield of Arrays of Wave Energy Converters under Realistic Seas." *IET Journal of Renewable Power Generation* Vol 4, no. 6 (2010): 488-494.

Dehlsen Associates. *Final Report: Siting Study for a Hydrokinetic Energy Project Located Offshore Southeastern Florida: Protocols for Survey Methodology for Offshore Marine Hydrokinetic Energy Projects.* DOE Grant Award Number:DE-EE0002655.000, Dehlsen Associates, 2012.

Department of Trade & Industry. *Impact of Banding the Renewable Obligation--Costs of Electricity Production.* Technical Report: URN 07/948, UK: ERNST & YOUNG LLP, 2007.

Det Norske Veritas (DVN). "Design of Offshore Steel Structures, General (LRFD Method)." *DVN Service Specifications, Standards, and Recommended Practices.* April 2011. http://exchange.dnv.com/publishing/Codes/ToC_edition.asp (accessed 2013).

DOE. *Progress Alert News, Jan. 18, 2012: DOE Reports Show Major Potential for Wave and Tidal Energy Production Near U.S. Coasts.* DOE Office of Energy Efficiency and Renewable Energy. 2012. http://apps1.eere.energy.gov/news/progress_alerts.cfm/pa_id%3D664 (accessed Mar 1, 2013).

DOE. *Report to Congress on the Potential Environmental Effects of Marine and Hydrokinetic Energy Technologies.* Wind and Hydropower Technologies Program: DOE/GO-102009-2955, Washington D.C.: U.S. Department of Energy, Wind and Hydropower Technologies Program, Dec 2009.

Duerr, A. E. S., and M. R. Dhanak. "Hydrokinetic Power Resource Assessment of the Florida Current." Published in OCEANS, Retrieved from http://ieeexplore.ieee.org/xpls/abs_all.jsp?arnumber=5664377, 2010.

Eder, J., J. Bretl, and K. Edwards. "Empirical Demonstration of Advanced Control Strategies for Wave Energy Converters." *32nd International Conference on Ocean, Offshore, and Arctic Engineering, Jun 9-14.* Nantes, France: Ocean Offshore and Artic Engineering, 2013.

EPA. *Phase I Final Rule and Technical Development Document of Uniform National Discharge -- Underwater Ship Husbandry: Nature of Discharge (in Appendix A).* EPA Report: EPA-842-R-99-001, Washinton DC: Environmental Protection Agency, April 1999.

Falnes, Johannes. *Ocean Waves and Oscillating Systems.* Cambridge, UK: Cambridge University Press, 2002.

Federal Energy Regulatory Commission (FERC). *White Paper on Licensing Hydrokenetic Pilot Projects.* Washington D.C.: FERC, 2008.

Fisher, Cameron, and Michael Slater. *Electromagnetic Field Study, Effects of electromagnetic field on marine species: A literature review* . Oregon Wave Energy Trust (OWET), Sep 2010.

Folley, M., and T. Whittaker. "The Adequacy of Phase-averaged Models for Modelling Wave Farms." *ASME 2011 30th International Conference on Ocean, Offshore, and Arctic Engineering, Jun 19-24.* Rotterdam, The Netherlands: OMAE, 2011.

Garrett, Chris, and Patrick Cummins. "The Efficiency of a Turbine in a Tidal Channel." *Journal of Fluid Mechanics* (Cambridge University Press) Vol. 588 (2007): 243-251.

Gerstein, Edmund R., Laura Gerstein, Josiah Greenewald, and Steven E. Forsythe. "Parametric Projectors Protecting Marine Mammals from Vessel Collisions." *157th ASA Meeting.* Portland, OR: Accoustial Society of America (ASA), 2009.

Gill, Andrew. "Offshore Renewable Energy: Ecological Implications of Generating Electricity in the Coastal Zone." *Journal of Applied Ecology* Vol. 42, Issue 4 (2005): 605-615.

Ginter, Vince, and Clayton Bear. *Development and Application of a Water Current Turbine.* Technical Report, New Energy Corporation, Inc., 2009.

Graves, A., K. Harman, M. Wilkinson, and R. Walker. "Understanding Availability Trends of Operating Wind Farms." *Poster Presentation at the AWEA Windpower Conference, June.* Houston, TX: American Wind Energy Association (AWEA), 2008.

Haas, Kevin, Hermann Fritz, Steven French, Brennan Smith, and Vincent Neary. *Assessment of Energy Production Potential from Tidal Streams in the United States.* Funded by U.S. DOE Wind & Water Power Program, Atlanta, GA: Georgia Tech Research Corporation, June 2011.

Hagerman, G., G. Scott, and P. Jacobson. *Mapping and Assessment of the United States Ocean Wave Energy.* EPRI Tech. Report: 1024637, Palo Alto, CA: Electric Power Research Institute (EPRI), Dec 2011.

Hals, J., J. Falnes, and M. Trogeir. "A Comparison of Selected Strategies for Adaptive Control of Wave Energy Converters." *Journal of Offshore Mechanics and Arctic Engineering* 133, no. 3 (Mar 2011): 031101.

Hanson, H. P., S. H.Skemp, G. M. Alsenas, and C. E. Coley. "Power from the Florida Current: A New Perspective on an Old Vision." *American Meteorological Society* 91, no. 7 (2010): 861–866.

Hassan, Garrad. "Renewable Energy Consultants." *Wave and Tidal Service Brochure.* Oct 2012. http://www.gl-garradhassan.com/assets/downloads/ GL_Garrad_Hassan_Wave_and_Tidal_Services.pdf (accessed Jun 8, 2013).

Inger, Richard, et al. "Marine renewable energy: potential benefits to biodiversity." *Journal of Applied Ecology* 46, no. 6 (Dec 2009): pp 1145-1153.

International Electrotechnial Commission (IEC). *Efficient Electrical Energy Transmission and Distribution.* 2007. http://www.iec.ch/about/brochures/pdf/technology/transmission.pdf (accessed Nov 2013).

Javaherchi, T. A., N. Stelzenmuller, and A. Aliseda. "Experimental and numerical analysis of the DOE Reference Model 1 horizontal axis hydrokinetic turbine." *Proceedings of the 1st Marine Energy Technology Symposium, GMREC-‐METS13, April 10-11.* Washington, D.C., 2013.

Jensen, A. S., and G. K. Silber. *Large Whale Ship Strike Database.* NOAA Technical Memorandum NMFS-OPR, Silver Spring, Maryland: National Oceanic and Atmospheric Administration (NOAA) Nation Marine Fisheries Service, 2003.

Johnson, E., J. Barco, S. James, and J. Roberts. *Reference Model MHK Turbine Array Optimization Study within a Generic River System.* Technical Report: SAND2011-9305, Albuquerque, New Mexico: Sandia National Laboratories, 2011.

Kara, F. "Time Domain Prediction of Power Absorption from Ocean Waves with Latching Control." *Journal of Renewable Energy* 35, no. 2 (Feb 2010): 423-434.

Knik Arm Bridge and Toll Authority. *Knik Arm Crossing: Pile-Driving Noise Attenuation Measures.* Technical Report, Anchorage, AK: Knik Arm Bridge and Toll Authority, Nov 2005.

Koncoski, J. J., E. G. Paterson, and W. C. Zierke. *A Blade-Element Model of Propeller Unsteady Forces for Computational Fluid Dynamics Simulations.* Developments in Marine CFD (March 22-23, 2011), London, UK,: The Royal Institute of Naval Architects, 2011.

LaBonte, A., P. O'Conner, C. Fitzpatrick, K. Hallett, and Y. Li. "Standardized Cost and Performance Reporting for Marine and Hydrokenetic Technologies." *Proceedings of the 1st Marine Energy Technology Symposium (April 10-11).* Washington, D.C.: METS13, 2013.

Larsen, J., and T. Sanford. "Florida Current Volume Transports from Voltage Measurements." *Science*, 1985: Retrieved from ftp://kakapo.ucsd.edu/pub/sio_220/b02 - Florida Current Transport/Larsen_Sanford.sci_85.pdf.

Lawson, M. J., G. Bir, Y. Li, and R.W. Thresher. *The Development of a Preliminary Design for a Horizontal Axis Tidal Current Turbine.* Technical Report, National Renewable Energy Laboratory, 2013 [in preparation].

Lawson, M. J., Y. Li, and D.C. Sale. "Development and Verification of a Computational Fluid Dynamics Model of a Horizontal-axis Tidal Current Turbine." *Proceedings of the 30th International Conference on Ocean, Offshore, and Arctic Engineering.* 2011.

Leishmann, J. G. *Principles of Helicopter Aerodynamics, 2nd Edition.* New York, NY: Cambridge University Press, 2006.

Leishmann, J. G. "Challenges in Modeling the Unsteady Aerodynamics of Wind Turbines ." *21st ASME Wind Energy Symposium & 40th AIAA Aerospace Sciences Meeting, Jan 14-17.* Reno, NV: AIAA Paper 2002-0037, 2002.

Li, G., G. Weiss, M. Mueller, S. Townley, and M. R. Belmont. "Wave energy converter control by wave prediction and dynamic programming." *Journal of Renewable Energy* 48 (2012b): 392–403.

Li, Ye, and Yi-Hsiang Yu. "A Synthesis of Numerical Methods for Modeling Wave Energy Converter-Point Absorbers." *Renewable and Sustainable Energy Reviews* 16, no. 6 (2012): 4352–4364.

Li, Ye, Yi-Hsiang Yu, Jeff Epler, and Mirko Previsic. "Experimental Investigation on the Power Generation Performance of Floating Point Absorber Wave Energy Systems." *27th International Workshop on Water Waves and Floating Bodies (IWWWFB).* Copenhagen, Denmark: IWWWFB, 2012.

Luznik, L, K. A. Flack, E. E. Lust, and D. P. Baxter. "Hydrodynamic performance of a horizontal axis tidal turbine under steady flow conditions." *Proceedings of Oceans 2012 (October 16).* Hampton Road, VA, 2012.

Mackay, E. B. L., P. G. Challenor, and A. S. Bahaj. "On the Use of Discrete Seasonal and Directional Models for the Estimation of Extreme Wave Conditions." *Ocean Engineering* 37, no. 5-6 (2010): 425–442.

Mays, I. D., C. A. Morgan, M. B. Anderson, and S. R. Powles. "Experience with the VAWT 850 Demonstration Project." *Proceedings of the European Community Wind Energy Conference, 10-14 Sep.* Madrid, Spain, 1990.

McGuinn, J. *Gear Technology: "Wind Turbines: Clean Energy, but Energy Efficiency?".* June/July 2011. http://www.geartechnology.com/issues/0611x/gt0611.pdf (accessed 2013).

Melfi, M., S. Evon, and R. McElveen. "Induction versus permanent magnet motors." *Industry Applications Magazine* (IEEE) 15, no. 6 (2009): 28-35.

Michelen, C., J. Murray, and V. S. Neary. *Model Performance Evaluation of CACTUS.* Internal Technical Memorandum, Water Power Technologies, Albuquerque, NM: Sandia National Laboratories, Nov. 15, 2013.

Murray, J., and M. Barone. "The Development of CACTUS, a Wind and Marine Turbine Performance Simulation Code." *49th AIAA Aerospace Sciences Meeting including the New Horizons Forum and Aerospace Exposition (January 4-7).* Orlando, FL: Sandia National Laboratories (Doc # AIAA 2011-147), 2011.

Neary, V. S. *Reference Inflow Characterization for River Resource Reference Model (RM2).* Technical Report: ORNL/TM-2011, Oak Ridge, Tennessee: Oak Ridge National Laboratory, 2011.

Neary, V. S., B. Gunawan, and A. S. Ryou. *Performance Evaluation of HYCOM-GOM for Hydrokinetic Resource Assessment in the Florida Strait.* Technical Report: ORNL/TM-2012/221 Available at: https://wiki.ornl.gov/sites/publications/Files/Pub36784.pdf, Oak Ridge, TN: Oak Ridge National Laboratory, 2012a.

Neary, V. S., B. Gunawan, and D.C. Sale. "Turbulent Inflow Characteristics for Hydrokinetic Energy Conversion in Rivers." *Renewable and Sustainable Energy Reviews* 26 (2013a): 437-445.

Neary, V. S., B. Gunawan, C. Hill, and L.P. Chamorro. "Near and far field flow disturbances induced by model hydrokinetic turbine: ADV and ADP comparison." *Renewable Energy* 60 (2013b): 1-6.

Neary, V. S., et al. "U.S. Department of Energy National Lab Activities in Marine Hydrokinetics: Scaled Model Testing of DOE Reference Turbines." *10th European Wave and Tidal Energy Conference (EWTEC) (September 2-5).* Aalborg, Denmark: EWTEC, 2013c.

Neary, V. S., L. P. Chamorro, and B. Gunawan C. Hill. *Experimental test plan – DOE tidal and river reference turbines.* Technical Report ORNL/TM-2012/301. Available at: http://wiki.ornl.gov/sites/publications/Files/Pub37919.pdf, Oak Ridge, TN: Oak Ridge National Laboratory, 2012b.

Nelessen, A. *CFD Analysis of Viscous Effects on Wave Energy Devices.* Golden, CO: National Renewable Energy Laboratory, 2012.

NEPA. "National Environmental Policy Act, as amended." 1970.

New Energy Corporation. *25 kW Power Generation System.* n.d. http://www.newenergycorp.ca/Products/PowerGeneration/25kWPowerGenerationSystem (accessed 2013).

O'Sullivan, D., D. Mollaghan, A. Blavette, and R. Alcorn. *Dynamic Characteristics of Wave and Tidal Energy Converters and a Recommended Structure for Development of a Generic Model for Grid Connection.* OES-IA Doc # T0321 (available at http://www.iea-oceans.org/), HMRC-UCC for OES-IA, 2010.

Paish, M. "Can 1 MW Tidal Systems Compete with Off-shore Wind? An analysis of the Opportunities and Challenges Associated with Scaling Up." *4th International Conference on Ocean Energy, 17-19 October.* Dublin, Ireland: ICOE, 2012.

Peters, Valerie, Alistair Ogilvie, and Cody Bond. *Continuous Reliability Enhancement of Wind Database (CREW): Wind Plant Reliability Benchmark.* Technical Report: SAND2012-7328 (Available online http://energy.sandia.gov/crewbenchmark), Albuquerque, NM: Sandia National Laboratories, 2012.

Polagye, B., and J. Thomson. "Tidal Energy Resource Characterization: Methodology and Field Study in Admiralty Inlet, Puget Sound, WA (USA)." *Proceedings of the Institution of Mechanical Engineers, Part A: Journal of Power and Energy* 227, no. 3 (2013): 352-367.

Polagye, Brian. *Reference Model #1 – Tidal Energy: Resource.* Technical Report: UW-2011-02, Seattle, WA: University of Washington, Northwest National Marine Renewable Energy Center, 2011b.

Polagye, Brian, et al. "Summary of Environmental Effects of Tidal Energy Development: A Scientific Workshop (Mar 22-24)." *NOAA Technical Memorandum NMFS F/SPO-116.* Seattle, WA: University of Washington, 2011a.

Poore, R., and T. Lettenmaier. *Alternative Design Study Report: WindPACT Advanced Wind Turbine Drive Train Designs Study, Nov. 1, 2000 — Feb 28, 2002.* Accession Number 33196, Report Number SR-500-33196, Kirkland, WA: Prepared for the National Renewable Energy Laboratory by Global Energy Concepts, LLC, 2003.

Previsic, M., J. Epler, M. Hand, D. Heimiller, W. Short, and K. Eurek. *The Future Potential of Wave Power in the United States.* Prepared for U.S. DOE, Wind & Water Power Technologies Program, Sacramento, CA: RE Vision Consulting, LLC, Aug 2012.

Previsic, Mirko. *100 kW Wave Power Hydraulic System.* Sacramento, CA: Re Vision Consulting, LLT, 2011a.

Previsic, Mirko. *Economic Methodology for the Evaluation of Emerging Renewable Technologies.* Prepared for U.S. DOE, Sacramento, CA: RE Vision Consulting, LLC, 2011b.

Previsic, Mirko. *Wave Energy Resource and Site Characterization.* Sacramento, California: Re Vision Consulting, LLC, 2011c.

Previsic, Mirko, Roger Bedard, George Hagerman, and Omar Siddiqui. *System Level Design, Performance, and Costs--Oregon State Offshore Wave Power Plant.* Technical Report: E21 EPRI Global-WP-006-OR, Rev. 1, EPRI Global, 2004.

Raye, R. E. *Characterization Study of the Florida Current at 26.11 North Latitude, 79.50 West Longitude for Ocean Current Power Generation.* Boca Raton, FL: Florida Atlantic University, 2002.

Re Vision Consulting, LLC. *Reference Model 1 – Structural Design Supplement Tidal Turbine.* . Sacramento, California: Re Vision Consulting, LLC , Sep 2011a.

Re Vision Consulting, LLC. *Reference Model 2 – Structural and Mooring Design Supplement.* Sacramento, California: Re Vision Consulting, LLC, Sep 2011b.

Reed, M. C., A. Moreno, T. Ramsey, R. Bagbey, and J. Rieks. "Accelerating U.S. Marine and Hydrokinetic Technology Development Through the Application of Technology Readiness Levels (TRLs)." *7th Annual Energy Ocean International Conference, June 8-10.* Ft. Lauderdale, FL: Energy Ocean, 2010.

RenewableUK. *Channelling the Energy: A Way Forward for the UK Wave & Tidal Industry Towards 2020.* London, UK: RenewableUK, 2010.

Shields, M.A., L.J. Dillon, D.K. Woolf, and A.T. Ford. "Strategic Priorities for Assessing Ecological Impacts of Marine Renewable Energy Devices in Pentland Firth." *Journal of Marine Policy* Vol. 33, no. 4 (2009): 635-642.

Short, Walter, Daniel J. Packey, and Thomas Holt. *A Manual for the Economic Evaluation of Energy Efficiency and Renewable Energy Technologies.* Tech. Report: NREL/TP-462-5173, Golden, CO: National Renewable Energy Laboratory, March 1995.

Siemens. *Seagen-Technology.* 2013. http://www.marineturbines.com/Seagen-Technology (accessed June 23, 2013).

TECO Westinghouse. *Wind Turbine Generators.* n.d. http://www.tecowestinghouse.com/site/DefaultSite/filesystem/documents/wind_turbine_generators.pdf (accessed Nov 2013).

Teillant, B., R. Costello, J. Weber, and and J. V. Ringwood. "Productivity and economic assessment of wave energy projects through operational simulations."." *Renewable Energy* 48 (2012): 220-230.

TM4 Electrodynamic Systems. *Generators for Gen-Sets.* n.d. http://www.tm4.com/en/generators_gent-sets.aspx (accessed Nov 2013).

U.S. Department of Defense (DoD). "Unified Facilities Criteria (UFC) 4-159-03 Design: Moorings." October 3, 2005. http://www.hnsa.org/doc/pdf/ufc_4_159_03.pdf (accessed 2013).

University of Massachusetts. *Community Wind Power Fact Sheet #2a -- Wind Power: Capacity Factor, Intermittancy and what happens when the wind doesn't blow.* n.d. http://www.umass.edu/windenergy/publications/published/communityWindFactSheets/RERL_Fact_Sheet_2a_Capacity_Factor.pdf (accessed July 20, 2013).

—. *The Coastal Systems Group; Technology Related Environmental Impacts, an overview of DOE-funded projects in marine renewable energy.* n.d. http://www.smast.umassd.edu/Coastal/research/energy/Technology.html (accessed Dec 2013).

USGS LAWSC. *Louisiana Water Science Center (LAWSC), Gage # 07374000.* n.d. http://la.water.usgs.gov/ (accessed Jan 2013).

USGS. *USGS Water Data for Louisiana. U.S. Department of the Interior, U.S. Geological Survey, National Water Information System.* 2013. http://www.waterdata.usgs.gov/la/nwis (accessed 2013).

Weywada, Pauline L., Benjamin Child, and Joao Cruz. "Implementation of a Spectral Wave Model for Wave Energy Converter Arrays." *4th International Conference on Ocean Energy, Oct 17-19.* Dublin, Ireland: ICOE, 2012.

Wilson, Ben, and Caroline Carter. *The Use of Acoustic Devices to Warn Marine Mammals of Tidal-Stream Energy Devices.* Scottish Government Report, Scotland.gov.uk, Oban, Argyll Scotland: Scottish Association of Marine Science, 2013.

Yu, Y.-H., R. Thresher, Y. Li, E. Nelson, and M. Lawson. *Design and Performance Analysis of a Floating-Point Absorber Wave Energy Converter.* Technical Report (in preparation), Golden, CO: National Renewable Energy Laboratory, 2013.

Yu, Yi-Hsiang, and Ye Li. "RANS Simulation of the Heave Performance of a Two-Body Floating-Point Absorber Wave Energy System." *Journal of Computers & Fluids* 73 (2013): 104-114.

Distribution

External

2 Alison LaBonte
Wind and Water Power Program
U.S. Department of Energy
1000 Independence Ave, SW
Washington, DC 20585

1 Jeff Rieks
Cardinal Engineering LLC
735 8th Street SE
Suite 200
Washington, DC 20003

1 Mirko Previsic
Re Vision Consulting, LLC
1100 Corporate Way
Sacramento, CA 95831

1 Michael J. Lawson
National Renewable Energy Laboratory
Wind and Water Power Program
15013 Denver West Parkway
Golden, CO 80401

1 Yi-Hsiang Yu
National Renewable Energy Laboratory
Wind and Water Power Program
15013 Denver West Parkway
Golden, CO 80401

1 Kathleen C. Hallett
National Renewable Energy Laboratory
Wind and Water Power Program
15013 Denver West Parkway
Golden, CO 80401

1 Andrea E. Copping
Pacific Northwest National Laboratory
P.O. Box 999
Richland, WA 99352

1	Arnold A. Fontaine Pennsylvania State University, Applied Research Laboratory P.O. Box 3-0 State College, PA 16804-0030		

Internal

1	MS1124	Daniel Laird	6122
1	MS1124	Vincent Neary	6122
1	MS1135	Richard A. Jepsen	1534
1	MS0899	Technical Library	9536 (electronic copy)

Sandia National Laboratories